The Physiology and Morphology of Thoracic Interneurones Following Spinal Cord Injury

Claire Francesca Meehan

Institute of Neurology

University College London

Submitted for the degree of Doctor of Philosophy (PhD)

December 2004

Supervisor : Dr P. A. Kirkwood

ProQuest LLC
789 East Eisenhower Parkway
P.O. Box 1346
Ann Arbor, MI 48106-1346

Abstract

The physiology and morphology of thoracic spinal neurones has previously been described. This thesis now examines plasticity with respect to this population of cells in the segment rostral to a partial spinal cord injury.

Intracellular penetrations were made of ventral horn interneurones, one segment rostral to an ipsilateral spinal hemisection. This was done in conjunction with extracellular recordings of expiratory bulbospinal neurones in the medulla. Spike-triggered averaging was performed to reveal new connection to the interneurones from sprouting EBSNs. The yield however, was too low to draw any valid conclusions

Intracellularly penetrated interneurones were iontophoretically labelled with neurobiotin. The axons and dendritic trees were completely reconstructed. No significant difference was found overall between the control and the lesion populations in terms of numbers of collateral branches from the first 3mm of axon, although this parameter was affected by distance of the soma from the lesion and survival time. Axon collaterals terminated in a significantly larger proportion of the ventral horn/intermediate zone than in controls. This effect was significantly affected by distance from the lesion and survival time and was most prominent in the intermediate zone. These observations are taken as being indicative of axonal sprouting, although alternative hypothesis are discussed.

The dendritic trees of the interneurones showed unusual features indicative of sprouting. These included tangled structures, twisted dendrites, commissural dendrites, unusually thick proximal dendrites, a lack of normal dendritic tapering, right angle branching and an overall asymmetry of the dendritic tree. Distal branches of an interneurone labelled for the cytoskeletal dendritic protein, MAP2a/b lacked immuno-labelling for this protein. Overall, MAP 2a/b labelling was noted to be less dense on the lesion side compared to the non-lesioned side of the spinal cord.

Thus new forms of plasticity have been demonstrated in uninjured interneurones in the injured spinal cord.

Acknowledgements

During the course of this PhD I have been fortunate to have the support of a wonderful department. The Sobell department has been my surrogate family for the past 5 years and there have been numerous people who have helped and supported me during the course of this PhD.

Dr Chris Seers, not only for constant IT support throughout the PhD but for his friendship and good advice, an excellent shoulder to moan on and chocolate.

Deborah Hadley, Kully Sunner and Molly Cureton for organising me.

Tony Pullen for his advice and encouragement.

The Greensmith laboratory, especially Jo Decker for the introduction to immuno-labelling and Jim Dick for the use of and help (with considerable patience) with the lab microscope.

The Lemon laboratory for their friendship and support especially Rachel Spinks

I must also acknowledge and thank my current boss Dr Ken Rose, without whose support, the completion of this thesis would not have been possible. Ken not only had considerable patience, allowing me time to finish the never-ending thesis, but also provided me with a wonderful environment in which to finish writing up with all the facilities I needed to finish. I also wish to acknowledge the incredible support I received from my new laboratory during this time, Monica Neuber-Hess, Stacey Armstrong, John Grande, Keith Fenrich, Tuan Bui and Diane Bedrossian.

I wish to acknowledge the constant support from my parents who haven't seen much of me over the past 10 years yet have always been there for me.

Finally and most importantly I wish to acknowledge and thank my PhD supervisor, Dr Peter Kirkwood. Peter has been both a supervisor and a best friend to me over the past 4 years. Peter is an incredible man and an inspiration to me and can only hope that in my future career I will be able to do him justice as one of the "Science daughters of Kirkwood".

Abbreviations

Böt-C : Bötzinger Complex

cVRG : Caudal Ventral Respiratory Group

CST: Corticospinal Tract

DRG : Dorsal respiratory Group

EBSN: Expiratory Bulbospinal Neurones

FSP : Focal Synaptic Potential

IML: Intermedio-lateral column

LPNs : Long Propriospinal Neurones

Pre-Böt C : Pre-Botzinger Complex

rVRG : Rostral Ventral Respiratory Group

SPG: Sympathetic Preganglionic

SPNs : Short Propriospinal Neurones

STA : Spike Triggered Averaging

TP : Terminal Potential

VRG : Ventral Respiratory Group

Contents

Title page.....1

Abstract.....2

Acknowledgements.....3

Abbreviations.....4

Contents.....5

List of figures.....8

List of tables.....11

Chapter 1: Introduction.....12

1.1 The respiratory Apparatus.....14

1.2 Respiratory Rhythm Generation: The Pre-Botzinger Complex.....18

1.3 Respiratory Output Neurones of the Medulla.....26

1.4 Specific bulbospinal connections.....31

1.4.1 Connections to the Cervical motoneurones.....32

1.4.2 Connections to the Cervical interneurones.....34

1.4.3 Connections to the Thoracic motoneurones.....36

1.4.4 Connections to the Thoracic Motoneurones.....39

1.5 Plasticity following spinal cord injury 41

Chapter2: Methods.....58

2.1 Spinal Lesions.....58

2.2 Terminal Physiological Experiment.....59

2.2.1 Preparation.....59

2.2.2 Stimulation and recording /experimental protocol.....62

2.2.3 Identification of EBSNs.....62

2.2.4 Intracellular recording from interneurones.....62

2.2.5 Data Acquisition.....65

2.2.6 Analysis.....65

2.2.6 Intracellular Labelling.....66

2.3 Histological processing.....67

2.4 Reconstruction of cells.....70

Chapter 3: General & Physiological Properties of interneurones.....72

3.2 Spike-Triggered Averaging.....73

3.3 Physiological Characteristics of labelled interneurones.....78

3.4 lesions.....83

Chapter 4: Results: Axons and Collateral Branches.....85

4.1 Collateral Branches.....120

4.11 Survival time.....122

4.12 Distance from lesion.....123

4.13 Survival times and distance from lesion.....123

4.14 Axon Trajectory.....123

4.2 Reconstructions of collaterals.....128

4.3 Terminal areas of axon collaterals.....143

4.31 Survival time.....146

4.32 Distance from lesion.....146

4.33 Axon Trajectory.....146

4.4 Zones of termination.....151

Chapter 5: Results: Dendritic Trees.....156

5.1 Rostro-caudal Extent of dendrites.....156

5.2 Qualitative analysis of the Dendritic tree of the control population.....160

5.3 The 6-8 week survival time interneurones.....168

5.4 The 16-18 Week survival time interneurones.....175

5.5 Map2a/b immunohistochemistry.....188

5.6 Motoneurone dendrites.....193

Chapter 6: Discussion.....197

6.1 Summary of results.....197

6.2 Alternative explanations.....199

6.21 Axons.....199

6.22 Dendrites.....203

6.3 Methodological issues.....206

6.4 Relationship of findings to other work.....208

6.5 Implications.....217

6.6 Suggestions for future work.....222

6.7 General conclusions.....223

References

List of Illustrations

Figure 1.1: Hypothesized methods of sprouting with respect to thoracic interneurones.....57

Figure 2.1: Experimental setup.....71

Figure 3.1: Spike-triggered averages of thoracic interneurone recordings 76

Figure 3.2: Spike-triggered average of intracellular recording from a thoracic interneurone, using spikes from an EBSN as the trigger for the averages.77

Figure 3.3: Approximate locations of labelled interneurones in the control population (Saywell et al. 2000) and those of the lesioned population of this study...81

Figure 3.4: Cell B73J with a physiologically confirmed contralateral descending axon.....82

Figure 3.5: Lesions 84

Figure 4.1: Trajectories of main stem axons of interneurones in control and lesioned groups.....86

Figures 4.2: A-P: Axon trajectories for labelled interneurones from the control population with axon collateral branches and the extent of these collateral branches in the rostro-caudal axis. 88-104

Figure 4.3: A-M: Axon trajectories for labelled interneurones from the lesioned population with axon collateral branches and the extent of these collateral branches in the rostro-caudal axis.....105-118

Figure 4.4: Lesions and ipsilateral axons..... 119

Figure 4.5: Percentage of those axons possessing at least 2 collateral branches which have collaterals which overlap along the rostral caudal axis.....121

Figure 4.6: Number of collateral branches in the first 3mm of labelled axon of interneurones from the control and the lesion population.....124

Figure 4.7: Survival time post lesion and number of collateral branches in the first 3mm of labelled axon.....125

Figure 4.8: Number of collaterals and distance from lesion.....126

Figure 4.9: Number of collaterals and axon trajectory.....127

Figure 4.10: Reconstructions of axon collateral branches of interneurone B68F.....129

Figure 4.11: Reconstructions of axon collateral branches of interneurone B73J.....130

Figure 4.12: Axon collateral branches of interneurone B74D.....131

Figure 4.13: Axon collateral branches of interneurone B79I.....132

Figure 4.14a: Axon collateral branches from the rostral branch of the axon from cell B88F. 133

Figure 4.14b: Axon collateral branches from the caudal branch of the axon from interneurone B88F.....134

Figure 4.15: Axon collateral branches from interneurone B89D.....135

Figure 4.16: Examples of axon collateral branches of B95A.....136

Figure 4.17: Axon collateral branches of interneurone B96A.....137

Figure 4.18: Axon collateral branches of interneurone B96F.....138

Figure 4.19: Axon collateral branches from interneurone B99N.....139

Figure 4.20: Axon collateral branches of interneurone C1E.....140

Figure 4.21a: Axon collateral branches from interneurone C4A.....141

Figure 4.21b: Axon collateral branches of interneurone C4A continued.....142

Figure 4.22: Areas of termination of axon collaterals for each cell in the control and lesion populations.....144

Figure 4.23: Terminal areas of axon collateral branches of cells from control and lesion populations, expressed as the percentage of the total area of the ventral horn/intermediate zone.....145

Figure 4.24: Survival time post injury and the terminal area of axon collaterals expressed as a percentage of the total area of the ventral horn and the intermediate zone.....147

Figure 4.25: Distance of the interneurone soma from the start of the lesion area and the terminal areas of the axon collateral branches, expressed as the percentage of the total area of the ventral horn/intermediate zone.....148

Figure 4.26: Terminal area and ipsilateral/contralateral axons.....149

Figure 4.27: Terminal area and axon trajectory.....150

Figure 4.28: Grid used to divide the ventral horn and intermediate zone into 12 zones.....153

Figure 4.29: Mean number of regions from a possible twelve with the presence of an axon collateral from interneurones in the lesioned and the control spinal cords.....153

Figure 4.30: Mean numbers of zones with the presence of collaterals.....154

Figure 4.31: Percentage of cells from the control and lesion population which have collaterals branches with terminations or en-passant boutons in each of the 12 zones illustrated in figure 4.28.....154

Figure 5.1: Total extent of the dendritic trees of interneurones in the rostro-caudal axis.....158

Figure 5.2: Rostro-caudal extent of dendritic trees of the interneurones.....159

Figure 5.3: Reconstructions of the interneurones from the control population..161-167

Figure 5.4: Reconstruction of thoracic interneurone B96F.....172

Figure 5.5: Reconstruction of thoracic interneurone B99N.....173

Figure 5.6: Reconstruction of thoracic interneurone C4-A.....174

Figure 5.7: Reconstruction of a thoracic interneurone B73J.....179

Figure 5.8: Reconstruction of a thoracic interneurone B77.....180

Figure 5.9: Reconstruction of a thoracic interneurone B88F 181

Figure 5.10: Reconstruction of thoracic interneurone B95C 182

Figure 5.11: Reconstruction of thoracic interneurone B95C.....183

Figure 5.12: Reconstruction of thoracic interneurone C1E.....184

Figure 5.13: Commissural dendrites from interneurone B68F.....185

Figure 5.14: Example of asymmetry of an interneurone from the lesion population.....186

Figure 5.15: Reconstructions of Cell C4A with immunohistochemical data for MAP2a/b labelling 191

Figure 5.16: Map2a/b labelling in control and lesioned preparations using mouse anti-MAP2a/b antibody and a secondary conjugated to Texas Red 192

Figure 5.17: Motoneurone with commissural dendrites 195

Figure 5.18: MAP2a/b positive commissural dendrites from motoneurone B91D...196

List of Tables

Table 5.1: Unusual features on dendritic trees of thoracic interneurones from the lesion population.....187

Chapter 1

Introduction.

"Pathologists consider it an unimpeachable dogma that there is no regeneration of the central paths, and therefore that there is no restoration of the normal physiology of the interrupted conductors in the spinal cord. A vast series of anatomico-pathological experiments in animals and an enormous number of clinical cases that have been methodologically followed by an autopsy serve as a foundation for this doctrine which is universally accepted today. Nevertheless, some neurologists setting on one side the incontestable disturbing fact that functional damage is irreparable, have made known histological observations of the partial regeneration of neurones and nerve fibres."

Cajal (1928)

"Even though this be exceptional we must admit that in certain conditions the axons as well as the dendrites and the soma of spinal neurones that have been shaken by traumatic violence are able to emit ramified sprouts. We can say nothing concerning their fate."

Cajal (1928)

It is now clear that the damaged spinal cord is indeed capable of considerable plasticity and, in the case of partial spinal cord injury, considerable functional recovery although to date, there is still no cure for complete spinal cord injury. Further understanding of the fate and regenerative abilities of spinal neurones in the injured spinal cord may help explain the functional recovery, as well as help explain

the development of maladaptive symptoms such as neurogenic pain, spasticity, tremor and autonomic dysreflexia that can occur following spinal injury. It may also aid in the development of potential attempts to regenerate complete spinal injuries if one can find ways to enhance this intrinsic ability of a neurone to regenerate.

The study of plasticity requires an adequate animal model of spinal cord injury with a defined, known pattern of connectivity that can be observed prior to injury, post injury and following experimental regeneration. One possible candidate is the pathway transmitting the expiratory commands from the brainstem to the respiratory musculature of the thorax.

The respiratory rhythm of alternating inspiration and expiration is generated in the medulla and transmitted to the cervical, thoracic and lumbar cord as an excitation and/or and inhibition of neurones innervating the respiratory muscles. A considerable amount is now known about the specific connections made by respiratory neurones in the medulla with specific classes of spinal interneurones in the cervical and thoracic cord. This, combined with the fact that such pathways are still active in the anaesthetised, paralysed animal makes them an ideal model for the study of plasticity following spinal cord injury and with which to compare connections formed following future spinal cord regeneration experiments.

It is within this system that plasticity related to spinal interneurones in a model of partial spinal cord injury will be studied. A brief overview of the neural control of respiration is therefore required.

1.1 The respiratory apparatus

Ventilation (inspiration and expiration) occurs as result of changes in the volume of the thoracic cavity causing an inward and outward displacement of gases. This is largely due to the coordinated actions of the upper airway muscles and two systems which Monteau and Hilaire (1991) distinguish as the axial and the radial pumps.

The major muscle of the axial pump is the diaphragm, contraction of which results in a downward displacement of the chest, decreasing intra-thoracic pressure causing air to enter the lungs (inspiration). Relaxation of this muscle reverses this, leading to expiration. The relative contribution of this muscle to overall ventilation varies with species, contributing more in animals than in man, and across different situations.

The main muscles of the radial pump are those of the rib cage and abdominal wall. Contraction of some of these lift the ribcage, increasing thoracic circumference promoting inspiration and others act to decrease it by lowering the ribcage promoting expiration. Again the relative contribution of this pump to overall ventilation varies across species (D'Angelo and Bellemare 1990) and across different circumstances.

The two pumps cooperate together to produce the pattern of inspiration and expiration that we observe, receiving commands from central respiratory centres, muscle afferents, other non respiratory cortical/sub cortical areas and modulated by spinal interneurones.

The diaphragm is a dome shaped sheet of muscle attached to the lower ribs, the sternum and the vertebrae separating the abdominal and thoracic cavities. Contraction of this muscle causes a downward displacement of the chest wall resulting in an inflow of air to the lungs

The diaphragm is innervated exclusively by the phrenic nerves exiting the spinal cord via the C4 – C6 roots (Sant'Ambrogio et al 1963). In the cat the costal region is innervated mainly by C5 but also by C4 and the vertebral region mainly by C6 but also C5. The discharge patterns of the phrenic nerve in the cat are typically characterised by an increasing ramp at the beginning of inspiration reaching a plateau then decreasing at the end of inspiration (Hilaire et al 1972).

The phrenic motoneurone pool itself is a narrow column extending from C4 to C6 in the cat (Keswoni et al 1955, Webber et al 1979). It was generally concluded that there was no evidence of crossed phrenic axons in the cord (Webber et al 1979). The mean soma size was estimated at 40μm (Rose et al 1984, Cameron et al 1983) with extensive dendritic trees extending over 2-3 mm. The phrenic motoneurones are depolarised during inspiration then repolarised during expiration (a result of a combination of inhibition and withdrawal of inspiratory excitation).

The main muscles of the radial pump are the intercostals, levator costae and the abdomen. The intercostal muscles are arranged in 2 layers between the ribs. The outer layer, the external intercostals muscle consists of fibres running diagonally from the top part of one rib to the bottom of the next most caudal rib. The fibres of the lower layer, the internal intercostal muscle also run diagonally but in the opposite direction.

This causes contraction of the external intercostal muscle to elevate the ribs and expand the rib cage and contraction of the internal intercostals muscle to lower the rib cage. The external intercostal muscle is generally considered to have an inspiratory function and the internal intercostals muscle an expiratory function. The two are not necessarily always antagonistic. In the dog it was demonstrated that these muscles show topographic differences. The external intercostal muscle in the dorsal third of the rostral interspaces had large inspiratory effects which decreased rapidly towards the rostro-caudal junctions and the base of the ribcage, so that in the ventral portion of the caudal interspaces they actually had an expiratory effect. The internal intercostals in the dorsal portion of the caudal interspaces had large expiratory effects which decreased ventrally and cranially such that in the most rostral interspaces it was reversed into an inspiratory effect (DeTroyer et al 1999). Such topographic differences have also been demonstrated in humans (Wilson et al 2001). During breathing however, inspiratory activity in the external intercostals is only seen with an inspiratory effect and similarly expiratory activity in the internal intercostals, with an expiratory effect. The distribution of the activity of the external intercostals corresponds to the distribution of the inspiratory effect (De Troyer et al 2003). DeTroyer (2002) therefore concludes that the external intercostal muscles have a clear cut inspiratory action and the internal intercostal, an expiratory function during breathing.

The intercostal muscles are innervated by 2 branches of the spinal ventral ramus from thoracic segments T1-T12 (Eccles et al 1962; Sears 1964a). The thicker of the two branches, the internal intercostal nerve runs beneath the internal intercostal muscle giving off branches along its course innervating this muscle (Sears 1964a,b). This

branch contains axons of both expiratory and inspiratory motoneurones (Sears 1964a). The second branch, the external intercostal nerve lies between the internal and external intercostal muscle layers, giving off branches innervating the external intercostal muscle and contains only axons of inspiratory motoneurones (Sears 1964a).

During quiet breathing external intercostal motoneurones are depolarized during inspiration and internal intercostal motoneurones are depolarized during expiration (Sears 1964d, Saywell 2000). These depolarisations could be suppressed by a rostral spinal transection and hence were termed "Central Respiratory Drive Potentials" (CRDPs).

The patterns of discharge of intercostal motoneurones vary, with some firing at specific phases of the inspiration/expiration cycle and some firing tonically with respiratory modulation. Depolarisation involves the active excitation of cells (Sears 1964d, Kirkwood and Sears 1978). The drive potential for both internal and external intercostal motoneurones is provided by alternating excitatory and inhibitory synaptic drives which respectively depolarise and hyperpolarise the motoneurones (Sears 1964d).

Another muscle forming part of the radial pump is the levator costae muscle. This is located at the most proximal regions of each intercostal space running from the transverse process of each vertebrae to the next most caudal rib. This muscle is innervated by a small branch of the spinal dorsal ramus. The levator costae

motoneurones are located near the ventral tip of the ventral horn more deeply and medially than the intercostal pools.

Levator costae motoneurones show strongly phasic inspiratory activity terminating abruptly at the onset of expiration with no tonic activity during expiration (Hilaire et al 1983), although tonic activity has been observed in the dog (DeTroyer 1999). Levator costae is more active in caudal segments. This is suggested to have a role in counterbalancing the tendency to inward displacement of the caudal ribs due to diaphragmatic contraction and the weak inspiratory activity of external intercostals muscles of the caudal segments (Monteau and Hilaire 1991).

The abdominal muscles consist of four muscles, the external abdominal oblique, the internal abdominal oblique, the transversus abdominis and the rectus abdominis. Contraction of these muscles increases pressure in the abdominal cavity and provides the compressive force required for activities such as defaecation, urination, childbirth and vomiting and are thought to push up the slack diaphragm into the thoracic cavity during forced expiration but its role in quiet breathing is questioned and appears to depend on experimental setup, postural and interspecies differences (Monteau and Hilaire 1991). These muscles have been reported to be inactive in humans during quiet breathing (DeTroyer 1983) and only active during forced expiration (Floyd and Silver 1950).

Motoneurones innervating abdominal muscles are located from T4 to L3 (Holstege et al 1987), rectus abdominis from T4 to L3, internal oblique from T13 to L3,

transversus abdominis from T9 to L3 and external oblique from T6 to L3 (Miller 1987).

Effective respiration requires the rhythmically coordinated contractions of all the respiratory muscles and consequently much work has focussed on the origin of this rhythm with the concept of a respiratory centre where this rhythm may be generated.

1.2 Respiratory Rhythm Generation: The Pre-Botzinger Complex

In 1812 Legallois showed in the medulla oblongata there is a region "dans lequel le reside le premier mobile de la respiration". This area was subsequently loosely termed the respiratory centre (cited from Sears 1964c). In 1964 Sears (in agreement with Liljestrand 1953) argued that such terminology neglects the importance of the motoneuronal integration of excitatory and inhibitory synaptic input and suggests that "the term 'respiratory centre' must be regarded as not particularly meaningful ... that its use should be disregarded."

Forty years on, an area in the ventrolateral medulla is still viewed as a "respiratory centre"

Here different groups of cells can be found each firing with different phases of the respiratory cycle. One particular area in the ventrolateral medulla, the pre-Bötzinger complex (pre-Böt C) contains pre-inspiratory neurones that fire before onset of inspiratory activity, early inspiration and post inspiratory neurones – all classes of cells proposed to be involved in respiratory phase transitions. (Bianchi 1995, Rybak et al 1997).

Unlike the other groups of respiratory related neurones in the ventrolateral medulla the pre-Böt C contains very few bulbospinal neurones, the majority of its neurones being propriobulbar (Smith et al 1991, Ellenbereger 1990, Dobbins and Feldman 1994). It is thus here in the pre-Böt C that the rhythm generator has been hypothesised to reside.

The pre-Böt C lies ventral to the compact division of the Nucleus Ambiguus, midway between the facial nucleus and obex, caudal to the Bötzinger Complex (Böt-C). Local cooling or injection of procaine (a reversible Na+ channel blocker) into the medial area of the retrofacial nucleus located proximal to the pre-Böt complex at its rostral boundary abolishes respiration (Budzinska et al. 1985 Zhang et al. 1991). Similarly, injection of muscimol (a $GABA_A$ agonist) into the pre-Böt C of the rat eliminates respiratory activity (Koshiya and Guyenet 1996) as does the blockade of synaptic transmission by unilateral injection of ω-conotoxin GVI_A into adult rat pre-Böt C (Ramirez et al 1994).

Developments of *in-vitro* preparations have allowed manipulations which can be used to evaluate the necessity of this region to respiratory rhythm generation which are not possible in the *in-vivo* models. In the enbloc brainstem spinal cord preparation (Suzue 1984), short rhythmic burst of activity, representing respiratory motor outflow can be recorded from spinal ventral roots and cranial nerves synchronous with the activity of the still attached thorax (Smith and Feldman 1987). Transverse brainstem slice preparations have also been used where the rhythm-generating circuits appear to

remain intact and an endogenous respiratory related motor output can be recorded from the roots of the hypoglossal nerves.

Using the newborn rat *in-vitro* enbloc preparation on a vibrotome, Smith et al (1991) demonstrated how careful serial microsectioning caudal to rostral, rostral to caudal and dorsal to ventral section did not abolish respiratory rhythm until sectioning reached the area of the pre-Böt C, where further sectioning abolished the respiratory rhythm. So, a brainstem slice containing this region continued to generate a respiratory-related rhythmic motor output on the hypoglossal roots. Injection of CNQX (a non-NMDA receptor agonist) into the pre-Böt C in this slice completely abolished the respiratory rhythm (Smith et al 1991, Funk et al 1993).

Despite their obvious advantages, the *in-vitro* models have been questioned as to the extent to which the respiratory rhythm seen there represents that of real respiration. The rhythm differs from that seen in the intact animal in that it is slower, partly explained by removal of afferents and the low temperature at which preparations are kept. The pattern is also different, with a decrementing pattern in vitro compared with the incrementing pattern seen *in-vivo*.

The discharge of motor nerves during gasping is also decrementing at a low frequency so it has been suggested that the respiratory rhythm observed *in-vitro* could represent gasping (St John 1996). In defence of *in-vitro* models Recklin and Feldman (1998) cite lesion studies suggesting that the pre-Böt C is essential for respiratory rhythm but not for gasping and the existence of distinct area producing more gasp-like response

(Ramirez 1998). They explain the differences in firing patterns between *in-vitro* and *in-vivo* preparations as a consequence of deafferentation.

The suggested role of the pre-Böt C in rhythm generation received further support with the discovery of neurones with apparent pacemaker properties there (Smith et al 1991).This lead to the suggestion of a pacemaker model where intrinsic properties of bursting pacemakers are capable of producing the respiratory rhythm. Pacemaker cells, however, are also found in Bötzinger complex (Arata et al. 1990). If this hypothesis is true then the rhythm should be unaffected by blocking synaptic transmission, which was done in the adult rat preparation and it did not interfere with the respiratory rhythm. (Hayashi & Lipski 1992, Paton et al. 1994) where as in the neonatal rat preparation it modulated but did not abolish the rhythm (Feldman et al 1991, Onimaru et al 1990, Paton 1997).

Hence it has been suggested that the rhythm generator undergoes a developmental change from a pacemaker driven system at the foetal/neonatal stage to a network requiring postsynaptic inhibition in the mature brain or that rhythm occurs from a hybrid of pacemaker and network properties with pacemaker predominating at the foetal stage and synaptic networks dominant in the mature brain (Richter et al 1992) This is consistent with the finding that in rat brain the inhibitory GABA-ergic systems are not fully mature at birth (Hayashi and Lipski 1992).

Gray et al (1999) suggested that pacemaker cells in the pre-Böt C may be identified by a marker for the neurokinin receptor NK1R, a receptor for substance P and opiods. Using this marker Guyenet and Wang (2001) in the anaesthetised adult rat confirmed

that pre-inspiratory firing neurones in the pre-Böt C expressed the NK1R receptors but those firing in other phases of the respiration did not.

By conjugating a toxin to substance P (specific to NK1R receptors) and injecting this into the pre-Böt C normal breathing rhythm was severely disrupted (Gray et al 2001). Knock-out neonatal mice lacking the NK1R receptor however, still breathe (Defelipe et al 1998) as do animals lacking substance-P (Ptak and Hilaire 1999, Telgkamp et al 2002).

It is argued however, that it may not be the specific receptor that is important, more the particular cell that happens to express them that is important and so this may still be a good marker of pacemaker neurones in the pre-Böt C. It is also possible that there exist other important pacemaker neurones in the pre-Böt C without these receptors.

There is also now evidence that cells with pacemaker properties may exist in other areas of the ventrolateral medulla and that other areas may also be involved in the generation of the rhythm. Just because a slice containing the pre-Böt C is capable of producing a respiratory rhythm *in-vitro* it does not necessary prove that this is the sole generator of the real respiratory rhythm *in-vitro.*

A novel optical imaging system developed by Tominaga et al (2000) allows the acquisitions of optical signals from a certain given trigger point in the respiratory cycle. Onimaru and Homma (2003) used this system with the brainstem-spinal cord preparation to visualise the time course of activity of respiratory related regions across

all of the ventral medulla, stained with a voltage sensitive dye. Neuronal activity first appeared in a limited region ventro lateral to the facial nucleus and close to the ventral surface which preceded inspiratory activity by approximately 500ms. Electrophysiological recording from this area suggested the signal reflected pre-inspiratory neuronal activity in this area which they called the para-facial respiratory group (pFRG).

A bilateral lesion of this area significantly reduced respiratory frequency leading the authors to conclude that the pFRG may be involved in primary rhythm generation. However in the earlier transection studies of Smith et al (1991) after removal of this region the respiratory rhythm persisted. So just because this area has been demonstrated to be active it cannot be directly assumed that it is necessary for rhythm generation.

Onimaru and Homma (2003) suggest that the pre-inspiratory neurones of the pFRG interact with the neurones of the pre-Böt C as a coupled oscillator system to regulate rhythm.

Feldman and colleagues go further to suggest that the pre-Böt C oscillator drives the inspiratory activity while the pre-inspiratory network drives expiratory activity. (Jancezewski et al. 2002, Jancezewski and Feldman 2002, Feldman et al 2003).

Ramirez et al (2002) raises an important issue when considering models based on the various preparations in that what actually constitutes "normal breathing". Much of the critique surrounding the *in-vitro* models has concerned the different pattern observed

as compared to those observed in the *in-vivo* models. Respiratory activity can vary significantly depending on the species of animal, the age, the state of the preparation and experimental conditions. For example, Richter and Spyer (2001) question the extent to which *in-vivo* studies describe the real physiology of the respiratory network because central respiratory neurones are sensitive to commonly used solvent narcotic agents. In particular barbiturates potentiate inhibitory synaptic processes. It is entirely plausible that indeed respiratory rhythm generation may be operating differently in the different preparations.

Such issues surrounding the use of the *in-vivo* preparation used in respiratory neurophysiology however, are not really relevant for the study contained within this thesis. It is more concerned with the transmission of the respiratory generation (however generated) via the bulbospinal axons to the spinal cord and the specific connections made by these axons to spinal motoneurones/interneurones in the anaesthetised paralysed *in-vivo* preparation. There exists a large number of respiratory interneurones in the thoracic spinal cord (Kirkwood et al 1988) which may suggest a possible recapitulation of networks similar to those in the medulla. This thesis will use such a system to examine changes formed following a spinal cord injury causing disruption to the bulbospinal axons in the same preparation under the same experimental conditions as a model for studying plasticity of circuitry following spinal cord injury.

1.3 Respiratory output neurones of the medulla

In addition to those of the pre-Böt C other respiratory related neurones of the medulla are grouped in distinct places. One group lies in the ventral nucleus of the solitary tract, this group being referred to as the dorsal respiratory group (DRG) The other group, in the ventrolateral medulla, is referred to as the ventral respiratory group (VRG). This extends from its caudal part in the nucleus retroambiguus (cVRG) to its rostral part close to the retrofacial nucleus (rVRG) then rostral to this group (and rostral to the pre-Böt C) lays the Bötzinger complex, although to Bianchi et al (1995) this should be considered an extension of the VRG.

The DRG is a relatively discrete region extending from 0-2 mm rostrally to the obex from 1.7-2.5 mm laterally and 2.5 ventrally to the medullary surface in the cat. It contains inspiratory neurones of the augmenting type (Bianchi 1979). These are predominantly late peak neurones showing maximum discharge frequency in the late stages in inspiration (Bianchi et al 1971, 1974, Hilaire and Monteau 1975, 1976) and almost all are bulbospinal (Bianchi 1979 Hilaire and Monteau 1976).

The DRG contains two types of inspiratory neurone (Baumgarten & Kanzow 1958), the Rα neurones which are inhibited by lung inflation and the Rβ neurones which are excited by lung inflation (Fedorko et al 1983). Another group of inspiratory cells called P-cells fire synchronously with lung inflation but do not receive an inspiratory drive of central origin. In an anaesthetised paralysed ventilated animal their discharge is phasic with pump and is suppressed when inflation is withheld).

The inspiratory bulbospinal neurones of the DRG are a source of input to the phrenic motoneurones. Axons leave the soma and travel either dorsally or ventrally then always proceed ventrally, turn medially and cross midline of medulla rostrally to the soma (Berger et al 1984). There is also axonal branching within the ipsilateral medulla, confirmed by Otake et al. (1989) who found ipsilateral collateral branches in 6/28 neurones with a variety of patterns including distributions of terminal boutons in the ipsilateral VRG and in the DRG.

The VRG contains both bulbospinal neurones, firing simultaneous with inspiration and those with expiration (Merrill 1972). Inspiratory neurones are located in an area mainly rostral to the obex, referred to by Merrill 1972 as the rVRG (rostral ventral respiratory group). Expiratory neurones are located more caudally, from the obex to the 1st cervical root in an area referred to as the cVRG (caudal ventral respiratory group), although there is some overlap between the two populations at the level of the obex (Bianchi 1974).

The firing rates of the expiratory neurones of the cVRG start at a low initial rate gradually increasing to a plateau or late peak in the expiratory peak. Termination occurs synchronously thoughout the expiratory population, 150ms before the onset of inspiration.

The inspiratory population of the rVRG can be divided into subgroups by firing patterns.

Early burst inspiratory neurones form a uniform population which start firing when expiration stops (150ms before inspiration). Their frequency peaks then declines with

firing ceasing mid-inspiration. Late inspiratory neurones make up 80% of the inspiratory population of the rVRG. Their frequencies peak near the peak of inspiratory effort (late in inspiration) and sometimes overlap with the next expiratory phase. They form two groups, one involved with peak inspiratory effort and the other, with the whole of inspiration (with an earlier onset and later termination), (Merrill 1972).

Using the technique of antidromic mapping Merrill (1972) traced the paths of the axons from the rVRG and cVRG neurones. The axons of expiratory neurones in the cVRG took uniform courses with one axon per cell that crossed the midline near the central canal slightly rostral to the level of its soma. The axons turned abruptly ventral as they course laterally, descending into the spinal cord ventro-lateral to the ventral horn. Nearly all of the axons descended in the spinal cord forming a discrete tract at C3 which was more diffuse by T7. They remained on the side contralateral to soma where they arborized extensively between T1 and L3.

The maps for the axons of inspiratory cells of the rVRG were more varied. All inspiratory cells with peak firing late inspiration appeared to have spinal axons, most had crossed axons and some had medullary collaterals. Inspiratory axons crossed medulla rostral to obex at many dorsoventral levels before they turned caudal and descend into the spinal cord. Early burst inspiratory cells of the rVRG do not have extensive spinal projections but did have very rich medullary axon arborizations among both inspiratory and expiratory cells in the caudal NRA.

The axons of the bulbospinal inspiratory neurones travel in the ventrolateral white matter, the dorsal part of the lateral funiculus and also the medial part of ventral column. 5-10% are uncrossed. They do not form a discrete tract at any level. 25 % were identified as having collaterals which arborize in the phrenic nucleus (C4-C6). Some arborizations crossed the midline but most often were confined to the contralateral cord. All inspiratory axons with a phrenic arborisation had a thoracic arborisation (Merrill 1972).

In a series of lesion experiments, Merrill (1972) created a sagittal hemisection from C1 to 1mm caudal to the obex, selectively cutting the descending expiratory axons then stimulated the expiratory medullary neurones and recorded the discharges of the internal and external intercostal nerve branches. After the lesion all spontaneous expiratory activity stopped but tidal volume and inspiratory duration remained unchanged.

If a hemisection at C4 was made on the side contralateral to the intercostal recording electrodes then stimulation of expiratory medullary neurones produced activation of the expiratory internal intercostal nerve. This brief excitation was followed by a period of 50 msec or so of inhibition of expiratory motoneurone firing. Also at a period of about 50 msec following this inhibition the inspiratory motoneurones were excited, even during expiration when they are usually silent so this was probably a disinhibition. This was eliminated by a sagittal hemisection. Merrill concludes that this suggests a segmental mechanism for reciprocally influencing inspiratory contraction.

The latency of soma spikes for antidromic stimulation was not constant in a particular respiratory neurone but varied slightly with the respiratory cycle which appeared to be due to variations in membrane potential resulting from variations in synaptic input. Due to their small size, lack of spinal projection, extensive medullary arborizations and distinctive firing pattern Merrill concluded that the early burst inspiratory cell of the VRG were probably the interneurones which supply the inhibitory input to the expiratory bulbospinal population of the NRA.

The last region to mention is the Bötzinger Complex. This region extends from the pre-Böt C to the retrofacial nucleus (see figure 1.1). Various classes of neurone are present here including both inspiratory and expiratory, although they are predominately expiratory (Lispki and Merrill 1980). Of the expiratory neurones some are motoneurones, some are bulbospinal.

The somata of the expiratory neurones are close to the ventromedial boundary of the retrofacial nucleus (Otake et al 1987). The inspiratory cells are more caudal and more ventral. The stem axon of the expiratory cell courses dorsomedially then gives rise to a crossing axon and a descending ipsilateral one. The crossing axon crosses the midline rostral to or at the level of the soma and travels caudally to the phrenic motoneurones of the cervical cord. The ipsilateral axon courses in an area ventromedial to the retrofacial nucleus and the nucleus ambiguous and gives off several collaterals that distribute synaptic boutons in the rostral medulla (in the Böt-C), retrofacial nucleus and NA (Otake et al 1987). No collaterals were seen from contralateral axons (Otake et al 1987).The contralateral projections were to the contralateral DRG (Kalia et al 1979) and the spinal cord (Merrill and Fedorko 1984).

Intracellular recordings of the expiratory neurones of the Botzinger complex reveal they have an increasing depolarisation present throughout expiration (Otake et al 1987). A step increase in depolarisation occurs at onset of expiration then progressive depolarisation during expiration and peak depolarisation and maximum firing just before onset of inspiration, then all are hyperpolarised at onset of inspiration (Bianchi et al 1988). Recordings from inspiratory cells reveal augmenting or early burst decrementing inspiratory discharges (Bianchi et al 1988).

Thus the respiratory rhythm may be thought to be generated in the pre-Böt-C in the medulla and then projected to the spinal cord by the bulbospinal neurones of the DRG, rVRG, cVRG and the Böt-C. The specific nature of the connections made by the bulbospinals with spinal motoneurones differs between groups in terms of specificity and strength.

1.4 Specific bulbospinal connections

Two main methods have been used to establish the nature of the connections to neurones. These are the techniques of cross-correlations and spike triggered averaging (STA). In the first the timing of the spike discharge of one unit is correlated with that of another unit with which it is presumed to connect, to show the probability of the second unit firing following a spike in the first. A peak in the correlogram would indicate an excitatory connection to the second unit from the first or a common input to both units. A trough indicates inhibition of the second unit by the first. In STA intracellular synaptic activity of one cell is averaged using the extracellular spike from

the neurone presumed to contact the cells as a trigger. This allows the visualisation of small postsynaptic potentials otherwise masked by noise. (Kirkwood and Sears 1980). An extracellular recording can be averaged as alternative to reveal an extracellular synaptic field potential without identifying a specific target cell (Munson and Sypert 1979).

1.4.1Connections to the cervical motoneurones

Using cross correlations Cohen et al (1974) showed that two thirds of inspiratory DRG neurones gave rise to positive cross correlograms, suggesting the projections from the DRG to phrenic motoneurones are monosynaptic because of the short latency of the waves and the sharp rise to a maximum. Hilaire and Monteau (1976) obtained similar results from 80% of bulbospinal cells.

Experiments using STA have confirmed a strong excitatory monosynaptic connection from a large percentage of DRG neurones to contralateral phrenic motoneurones (Lipski et al 1983, Fedorko et al 1983, Monteau et al 1985). Interestingly, monosynaptic connections were more frequently found to exist between neurones and motoneurones having similar recruitments times suggesting the bulbospinal connections are not randomly distributed and that order of recruitment of phrenic motoneurones is partly determined by the synaptic inputs from the bulbospinal axons (Monteau et al 1976).

Not all the DRG bulbospinal neurones have monosynaptic connections with motoneurones and Davies et al (1985ab) claim that the monosynaptic connections

were responsible for only about 22% of the total depolarization on the motoneurones and suggest that the majority of input to phrenic motoneurones may come via cervical interneurones.

An excitatory drive also appears to come from the rVRG. Using cross correlations Hilaire and Monteau (1976) demonstrated monosynaptic connections exist between the rVRG and phrenic motoneurones in 59% of pairs. Such connections were also found by Feldman and Speck (1983). In other studies this percentage was found to be lower (Fedorko et al 1983) and early STA suggested monosynaptic connections were rare (Fedorko et al 1983), although a later study found 35% of VRG neurones selected because they possessed an axon collateral in the phrenic nucleus where found to generate an EPSP in at least one motoneurone (Fedorko 1989).

So it would appear that there is a monosynaptic connection from the rVRG but that it is smaller than from the DRG, although anterograde tracers injected into rVRG and retrograde labelling of phrenic motoneurones revealed no terminal field of bulbospinal rVRG neurones labelled outside of the phrenic nucleus. Terminals were only around soma or dendrites of labelled motoneurones (Ellenberger and Feldman 1990). The authors argue that as there are no interneurones in the phrenic nucleus the VRG neurones are likely to project monosynaptically to phrenic motoneurones. Ultrastructural data indicated that rVRG bulbospinal inspiratory neurones make direct synaptic connections on phrenic motoneurones. Ellenberger et al (1990). There also appears to be some evidence for polysynaptic pathways (Pallisses et al 1988, Bellingham and Lipski 1990).

There is evidence that phrenic motoneurones are strongly inhibited during expiration (Berger 1979). This is unlikely to be from the expiratory bulbospinal neurones of the cVRG as they do not appear to have any axonal arborizations around the phrenic nucleus (Merrill 1974) and are excitatory (Kirkwood et al 1995). Unsurprisingly STAs between cVRG and phrenic nucleus have all been negative (Merrill and Fedorko 1984).

Inhibitory monosynaptic connections have been demonstrated between descending neurones from the Böt-C and phrenic motoneurones but these are not extensive and only seem to apply to a subgroup of Böt-C bulbospinal expiratory neurones (Merrill 1972, Merrill & Fedorko 1984).

1.4.2 Connections to cervical cord interneurones

The interneurones of the cervical cord are best discussed divided into two distinct groups. Those of the upper cervical cord (C1-C3) and those of the lower cervical cord (C4-C5).

Upper cervical cord interneurones were first reported by Aoki et al (1978, 1980) in cats following complete spinal transections at the rostral boundary of C1. Spontaneous respiratory activity could, after a period, re-establish itself which was taken to suggest a site for rhythm generation in the spinal cord and interneurones were proposed as the likely originators of this rhythm (although it is possible that medullary respiratory neurones may still exist in C1).

The upper cervical respiratory interneurones form a discrete column from C1 to rostral half of C3 with soma located in the intermediate zone of grey matter near the lateral border of lamina VII (Lipski and Duffin 1986, Aoki et al 1980). They exhibit an inspiratory augmenting firing frequency similar to medullary late peak inspiratory neurones (Duffin and Lipski 1987).

Aoki et al (1983) demonstrated orthodromic activation of these neurones by stimulation of medullary respiratory nuclei, which was observed more frequently with contralateral than ipsilateral activation (72% V 45% in DRG 93% V 54% in VRG).

The axons of upper cervical interneurones are nearly all ipsilateral, 94% were antidromically activated by stimuli delivered to the ipsilateral ventral funiculus at C5-C6 (Aoki et al 1982, 1983, 1984). HRP injections to the phrenic nucleus labelled neurones detected in C1-C2 segments but it was not established whether these were the same population.

Using antidromic mapping, Lipski and Duffin (1986) showed that these upper cervical ipsilateral neurones also send axons into the ipsilateral thoracic segments (85%) where collateral branches were found too occur within up to 3 thoracic levels in the region of the intercostal motor nuclei although there is no clear evidence for monosynaptic connections to the motoneurones. Hoskin et al (1988) found most upper cervical neurones send their axons to the T9 –T10 level and some to L3 although STA showed no monosynaptic connections with motoneurones at these levels.

So there is probably a propriospinal system involved in the control of motoneurones pools via segmental interneurones (Monteau and Hilaire 1991)

Baumgarten et al 1963 produced the first report of existence of neurones within the phrenic pool (C4-C6) which were not antidromically activated by stimulation of the phrenic nerve. The activity of interneurones is likely to be strongly depressed by the deep barbiturate anaesthesia used for many experiments which could explain why their activity has not always been observed.

Using non-anaesthetised decerebrate rabbits, Palisses et al (1989) studied the activity of respiratory related neurones not activated antidromically from phrenic nerve. They observed patterns of discharge in all phases of inspiration (all, late and tonic) and expiration (all, late and tonic).

The lower cervical interneurones are located from 500μm dorsal to the phrenic nuclei down to the nucleus, extending more laterally than the motoneurone pool (Bellingham and Lipski 1990). Approximately half have been identified as having ipsilateral axons with collaterals in the phrenic nucleus and there is some evidence using STA for connections between interneurones and phrenic motoneurones (Douse and Duffin 1993).

1.4.3 Connections to the thoracic cord intercostal motoneurones

Davies et al (1985ab) found 20/41 of inspiratory bulbospinal neurones of the rVRG formed monosynaptic connections with thoracic motoneurones but argued that such

inputs were only responsible for a reduced fraction of the depolarization on the inspiratory motoneurones, implying that much of the depolarization is due to thoracic interneurones. Feldman et al (1985) however using an autoradiographic study looking for spinal projections of rVRG neurones found spinal labelling to be confined to ventral horn regions containing motoneurones (T1-T12) and so authors argued that monosynaptic connections must be important.

Merrill and Lipski (1987) using STA concluded that connections from rVRG were infrequent. Also cross-correlations between spike trains and the firing of external (inspiratory) nerve suggested that monosynaptic connection of inspiratory bulbospinal neurones from the medulla with thoracic motoneurones were less frequent than those with phrenic motoneurones.

Despite the strong monosynaptic connections made by DRG neurones in the phrenic nucleus there appears to be few or no monosynaptic connection from the inspiratory DRG to inspiratory intercostal motoneurones using cross correlations (Hilaire and Monteau 1976, Davies et al 1985) and STA (Duffin and Lipski, 1987). Monosynaptic connections do exist but are less common than those from the same bulbospinal neurones with the phrenic nucleus.

Expiratory bulbospinal neurones from the VRG do appear to make monosynaptic connections with intercostal motoneurones as was first demonstrated by Kirkwood and Sears (1973) using STA. Later studies from Merrill and Lipski (1987) using STA with cVRG bulbospinal neurones having arborizations in thoracic cord concluded that these monosynaptic connections were rare. During the course of the experiment

expiratory discharges attributable to interneurones were recorded close to the motor nuclei so they concluded that most of the drive from the cVRG is transmitted via segmental interneurones.

Using cross-correlations Cohen et al (1985) however found 17/42 cVRG neurones gave rise to monosynaptic excitation of internal intercostal motoneurones. Kirkwood (1995) also found stronger connections than Lipski and Merrill. Projections of expiratory bulbospinal neurones were found to be stronger in the rostral part of a segment than in the caudal part of a segment. (Kirkwood 1995, Ford et al 2000).

In a comprehensive STA study of 170 expiratory bulbospinal cVRG neurone - motoneurone pairs Saywell et al (2000 Thesis, unpublished) most motoneurones showed a CDRP which could be classified as expiratory, inspiratory or expiratory decrementing.
EPSPs were found in all groups of motoneurones but connections were strongest to expiratory motoneurones with axons in the internal intercostal nerve.

The amplitude of EPSPs positively correlated with the amplitude of the CRDP of the motoneurones. Unpublished calculations suggest that this input alone is sufficient to account for all the expiratory depolarization seen on the recorded motoneurones. However an extra source of input or amplification of this one is likely to be necessary to produce a useful motoneurone output.

Focal synaptic potentioals from EBSNs were discovered to have an uneven distribution within a thoracic segment, being stronger rostrally than caudally

(Kirkwood et al 1995, Ford et al 2000). Uniformly strong connections, however, were demonstrated to individual motoneurones in rostral and caudal parts of the segment (Annisimova et al 2001). This has been partly explained by an uneven distribution of the motoneurones themselves, being more common in the rostral part than in the caudal part of a segment (Meehan et al 2004). This is all consistent with the theory that motoneurones are the prime targets of the expiratory bulbospinal neurones (EBSNs). As yet there is no certain explanation for the differences between the Lipski/Merrill and Kirkwood laboratories.

There are unlikely to be any monosynaptic connections from the expiratory neurones of the Böt-C given that their axons generally terminate at the cervical level and are inhibitory.

1.4.4 Connections to the thoracic cord interneurones.

Kirkwood et al (1988) reported the existence of thoracic interneurones with respiratory-phased firing patterns. These interneurones were classified as inspiratory, expiratory or post-inspiratory units.

Schmid et al (1993) used extracellular iontophoretic injection of HRP at the location of neurones projecting to thoracic horn of cat where multi unit respiratory discharges were recorded. A concentration of labelled neurones was seen in the contralateral medial ventral horn of the immediately opposite rostro-caudal position. Single units whose firing patterns were related to the central respiratory cycle were recorded extracellularly in one ventral horn. These were used as triggers for recordings of

spike-triggered average field potentials in the contralateral ventral horn thus revealing axonal terminal potentials (TPs) and focal synaptic potentials (FSPs) for 34/55 units. This gave a similar number as those electrophysiologically classified as have a contralateral projection by Kirkwood et al (1988). This predominantly contralateral projection to the immediately opposite rostro-caudal position was confirmed by intracellular labelling of thoracic interneurones by Saywell (2000).

Kirkwood et al (1993) examined the nature and function of the projections by looking at the sign and location of FSPs. They found 2 types of FSP, negative-going and positive-going. Negative-going FSPs were interpreted as representing inward currents of synaptic excitation with latencies being generally monosynaptic and positive-going FSPs as representing inhibition. The phasic, most strongly respiratory-modulated units were mostly inhibitory in function. Those with a tonic discharge only partly modulated by respiration were mostly excitatory.

For inspiratory interneurones the sites of maximum positive-going FSPs were ventrolateral, within the motor nucleus of the internal intercostal nerve (among the expiratory motoneurones). Negative going FSPs were found more dorsomedially and so could represent synapses on interneurones or motoneurone dendrites. A role was suggested for the phasic inspiratory interneurones of phasic inhibition of expiratory motoneurones. Tonic excitation could contribute to the strong respiratory modulation in the activity of other interneurones in the thoracic cord, corresponding with Sears (1964) observation of that thoracic motoneurones were inhibited during inspiration. (Kirkwood et al 1993). Similar but less marked differences were found for the expiratory interneurones.

Given the relatively large proportion of respiratory modulated interneurones estimated by Kirkwood et al (1988) compared to amount of bulbospinal neurones this was taken to indicate their functional importance by the authors

STA was performed for intracellular recordings from 2 tonic inspiratory, 5 phasic inspiratory, 11 expiratory, 14 non respiratory and 1 unclassified interneurones using extracellular spikes for EBSNs as triggers. No EPSPs were unequivocally identified despite the observations of terminal potentials from some of the averages indicating bulbospinal collaterals in the region of the interneurones (Saywell 2000).

So it would appear that the expiratory bulbospinal axons from the cVRG makes strong/ abundant monosynaptic connection with expiratory intercostal motoneurones of the thoracic cord innervating the internal intercostal and abdominal muscles but do not appear to make such connections to the thoracic interneurones of the same level recorded from thus far.

Hence it is these neurones and their known connections which will be used as a model in this thesis to examine plasticity expressed in the adult spinal cord following lesions axotomising the long descending bulbospinal axons.

1.5 Plasticity following spinal cord injury

Partial spinal cord injury results in an immediate period of flaccid paralysis which is followed, over a variable period of time, by a gradually recovery of function.

Understanding the factors underlying this intrinsic ability of the spinal cord to recover may provide insight into how to stimulate recovery following total spinal transections where little functional recovery is seen. It is also crucial to help explain the formation of the maladaptive features seen in spinal patients such as spasticity, tremor, hypereflexia and dysreflexia. Such explanations then may also lead to clinical interventions aimed at prevention or therapy for such problems in the future or to ensure that such maladaptive plasticity is not accentuated by regeneration attempts.

It is important to understand the changes that occur rostral and caudal to an injury when considering experimental strategies aimed at repairing the spinal cord. A naïve view that simply bridging the gap between the rostral and caudal stump by regenerating fibres past the lesion to make connections in the distal stump will restore function by restoring normal connectivity ignores the plasticity that will have already occurred above and below the lesion.

A number of hypotheses have been put forward to explain the recovery of function seen following partial spinal cord injury. The resolution of temporary factors leading to a restoration of conduction though spared fibre tracts is one such way via which recovery of function can occur, for example, following the reduction of oedema which causes compression, maximal in the first days after injury. There is also evidence that demyelination constitutes a significant component of the pathology of experimental spinal cord injury (Waxman 1989). Following partial spinal cord injury, demyelination of spared axons starts within the first 24 hours following the injury and increases during a 2 week period, during which time some fibres degenerate. Evidence of remyelination, however, has been observed at 3 weeks post injury

(Harrison and McDonald 1977, Gledhill and McDonald 1977). Schwann cells have been implicated in physiological recovery after compression injury in the cat by remyelinating axons in the dorsal funiculus (Blight and Young 1989).

Another mechanism of functional recovery may be the unmasking of redundant systems that are capable of the function of the damaged systems which but which are normally inhibited from doing so. The removal of this inhibition by injury may therefore allow the previously redundant pathway to now replace the damaged one. Latent pathways certain do appear to exist in the adult cat. For example, neurones in the dorsal columns that normally respond to stimulation of the cat foot respond to stimulation of the abdomen instead when the cat is under anaesthesia, a feature which disappears as the anaesthetic wears off (Finger and Stein 1982).

Such unmasking however, might only really explain recovery occurring at very short time intervals following the injury and could not account for the delayed onset of some recovery of function seen. The removal of supraspinal inhibition of spinal reflexes has also been offered as an explanation of spasticity. Again, however, the time course in the evolution of this condition suggests this may not be the case (Sheean 2002).

Functional recovery may also result from sprouting from the lesioned descending axons. Adult spinal and supra-spinal neurones not only survive axotomy but can sprout. Ramon y Cajal (1928) first described how axotomy of descending tracts resulted in an initial period of dieback followed by abortive attempts at sprouting and regeneration.

Following electrolytic lesions in the corticospinal tract Li and Raisman (1995) demonstrated the ability of the damaged corticospinal tract to sprout. Cut ends of labelled axons not only survived but greatly expanded and gave rise to extensive arborisations of sprouts directed towards the lesion even in the presence of a dense astrocytic scar (They also saw evidence of collateral sprouting of uncut corticospinal axons). Following a thoracic lesion, Fouad et al (2001) also witnessed a strong sprouting response of the corticospinal tract 2.5 cm rostral to the injury. Many of the sprouts arborized in the intermediate laminae of the grey matter and seemed to innervate spinal interneurones.

Significant sprouting rostral to spinal hemisection of labelled hypothalamic axons after 3-12 weeks has also been observed (van den Pol and Collins 1994). There was a significant increase in the numbers of branches per axon and at all times post lesion structures suggestive of growth cones and lateral filopedia and lamellipodia were present.

Sprouting from lesioned tracts may be limited and may not reach the distances required for functional reconnectivity. Also their original pathway may be barred to the regenerating axon by the inhibitory nature of the scar. In such a case it would be advantageous for sprouting fibres to form new connections with local networks that do pass a partial lesion, such as local interneurones.

This has been observed by Bareyre et al (2004) following a mid thoracic dorsal hemisection in adult rats which transected the corticospinal tract (CST). The CST was anterogradely labelled by injection of BDA into the left and right motor cortices and long and short propriospinal neurones (LPNs and SPNs) were retrogradely labelled by pressure injection of a tracer into each side of the spinal cord, at C8 for short propriospinal neurones (CSNs) and T12 for long propriospinal neurones (LPNs).

At survival times of 3 weeks post injury the number of contacts (bouton-like structures) onto LPNs from the CST had increased 5-7 fold compared to controls and there was a four-fold increase in the number of collaterals from the lesioned CST fibres. By 12 weeks this had decreased but was still significant compared to controls. Despite an initial increase in contacts for the SPNs at 3 weeks post injury by 12 weeks the number of contacts on SPNs had decreased. Thus the lesioned fibres had sprouted to local propriospinal neurones, maintaining connection with those that bypassed the lesion. Thus local funicular neurones may provide a way of maximising the limited short-range sprouting potential of lesioned fibres.

Such sprouting may also have occurred within the system used in this thesis, which involved a spinal lesion of one side of the thoracic spinal cord, designed to sever the axons of expiratory bulbospinal neurones in the cVRG.

Using such a lateral mid-thoracic hemisection, Ford et al (2000) looked at changes in focal synaptic potentials (FSPs) from expiratory bulbospinal neurones. 2-16 weeks after the lesion a large number of the expiratory bulbospinal neurones appeared to

survive (hypothesised as being due to trophic support from surviving terminals above the lesion), with similar firing patterns to normal.

An increase of functional connections was shown as larger than normal FSPs, particularly at more lateral sites than medial ones, suggesting that proximity to lesion maybe a factor. The authors interpreted this as evidence of short term sprouting of the bulbospinal axons. This was seen at 16 but not 2 weeks and so is consistent with the idea that this is not a release effect but an effect that develops slowly, over a time scale that could be expected by sprouting (Bernstein and Bernstein 1973).

In the same model, STA of intracellular recording from motoneurones one segment rostral to the lesion, using spikes from extracellular recordings of the lesioned expiratory bulbospinal units as triggers, revealed no increases in the number of monosynaptic connections above that seen in normal animals, suggesting a hypothesis that the spinal interneurones maybe the new targets of sprouting lesioned bulbospinal axons (Annisimova et al 2001).

Given that the majority of the thoracic interneurones are commissural (Kirkwood et al 1988), the interneurones whose soma lie on the side ipsilateral to the lesion would not only be in the range of the short range sprouting of the EBSNs but would be the most attractive target for sprouting neurones given that the commissural axons would bypass the lesions.

This constitutes the first hypothesised mode of sprouting that was studied in this thesis. Intracellular recordings of thoracic interneurones rostral to an injury similar to

that described were averaged, using the extracellular spikes of lesioned EBSNs as triggers to test the first hypothesis:

Hypothesis 1

Following a mid-thoracic lesion, cutting the axons of EBSNs, lesioned fibres will sprout, so as to make monosynaptic connections with local interneurones one segment rostral to the injury.

Given the hypothesis of sprouting to these cells it is equally plausible that the axons of the inteneuones themselves may sprout, as was the case for the long propriospinal neurones of Bareyre et al (2004).

It is possible for sprouting to occur from cells/axons close to an injury even if they have not themselves been damaged by the injury. The phenomenon of collateral spouting whereby undamaged local pathways sprout to compensate for the loss of the damaged pathway has been well documented for dorsal root afferents. Following injury to primary afferents neighbouring uninjured afferent fibres sprout collaterals occupying the newly vacated synaptic sites in the dorsal horn (Liu and Chambers 1958, Goldberger and Murray1974, Mannion et al 1996, Doubell et al 1997, Mannion et al 1998, Ondarza et al 2003). Although the somatotopic reorganization appears to be limited to the dorso-ventral plane in the adult (Doubell et al 1997). Such sprouting may therefore result in the abnormal somatosensory processing or central sensitisation explaining the clinical symptoms of Allodynia and Hyperalgesia (Ondarza et al 2003).

35-38 months after a spinal hemisection of the lower thoracic or upper lumbar cord of the monkey HRP was injected unilaterally in hemisected side caudal to the lesion retrogradely labelled a significantly increased number of corticospinal neurones on the ipsilateral precentral motor cortex suggesting that new corticospinal connections to lumbosacral motoneurones are formed on the side of the lesion, which the authors suggest may be due to collateral sprouting of intact corticospinal fibres (Aoki et al 1986).

Lesioning of the dorsal corticospinal tract in adult rats produced spontaneous sprouting from the intact ventral corticospinal tract which paralleled the functional recovery observed in these animals (Weidner et al 2001).

In the model of Bareyre et al (2004), where lesioned corticospinal fibres sprouted to make new connections with LPNs, the number of contacts from the LPNs on lumbar motor neurones labelled with Cholera Toxin B increased. Given that the thoracic interneurones in this thesis are also a hypothesised target for sprouting axotomised tracts, then it may be plausible to hypothesise that the axons of the interneurones themselves may show similar plasticity to the LPNs of Bareyre et al (2004).

Intracellular penetrations of the interneurones can allow these cells to be labelled intracellularly and this allows examination of possible plasticity expressed by the interneurones themselves rostral to the hemisection. Of particular interest is the possible collateral sprouting from the axons of these cells, especially because the majority possess a contralateral axon that may by-pass the ipsilateral lesion.

Thus the second hypothesised mode of sprouting to be studied in this thesis was the sprouting of non-injured local thoracic interneurones one segment rostral to the injury, studied by intracellular labelling with neurobiotin and subsequent analysis and reconstructions of the axon collaterals.

Hypothesis 2

Following a mid thoracic lesion, cutting the axons of the EBSNs, non injured local interneurones in the segment rostral to the lesion will show collateral sprouting.

i) **The axons will possess more collateral branches than controls.**

ii) **The axon collateral branches will terminate over a larger area than those from control axons.**

iii) **The axon collateral branches will terminate in different regions than those from control axons.**

Intracellular labelling also allowed reconstructions of the dendritic trees of the cells. Most spinal cord injury research focuses on the plasticity of damaged or undamaged axons following injury or experimental regeneration attempts. The target of such sprouting however would be dendrites of local spinal neurones, hence the integrity of the dendritic trees of such cells must also be considered to be of importance. They themselves may be just as likely to exhibit morphological plasticity. Most of the research on plasticity of dendrites of adult spinal neurones following injury has concerned peripheral axotomies of spinal motoneurones rather than actual spinal cord injury. However insight can be gained from this work which shows that dendrites are also capable of sprouting and that in some cases even the conventional neuronal

polarity of a neurone can be altered with the growth of supernumerary axons from dendrites (for a review see Rose et al 2001). The assumptions from such work have been that axotomy is necessary to produce such changes. Very few studies have used non-injured controls from an injured environment so it is not known the extent to which some of the observed changes may also be induced by an injured environment or deafferentation. It is therefore plausible to hypothesise that there may be changes in the dendrites of the thoracic interneurones a local injury.

One of the earliest descriptions of the sprouting of dendrites in response to an injury is from Cajal (1928). He cites work from Rossi (1908) who recognized sprouting of short and fine expansions of dendrites of some spinal neurones following spinal cord injury. Cajal himself acknowledges having seen such cases in his own work.

"In precocious phase we have also seen dendritic sproutings and even new dendrites but this was only after contusions, triturations and rough shakings of the grey matter" (Cajal 1928).

In a young cat days after an attempt to graft a nerve in a spinal cord caused grave contusions and lacerations a short distance away from the necrotic zone the neurones were "furnished with expansions" displaying signs of a "fresh neoformation". Cajal claimed that one could see sprouting from the dendrites as well as the in the axon. New dendrites were preferentially seen from larger sized funicular cells in the anterior horn. They radiated what Cajal called "filoform expansions" ending in "grumes" or "reticulated thickenings of variable configuration and size" (Cajal 1928).

Rather than growth, Sumner and Watson (1971), following application of botulinum toxin and axotomy, observed a retraction of dendrites of hypoglossal motoneurones. This dendritic loss was therefore partly attributed to a consequence of a failure of synaptic transmission. This retraction was reversible upon reinnervation or on regaining of functional transmission. This observation of retraction, however, was based on golgi-stained dendritic branches that were contained in only a single histological section however which would exclude most distal branches.

Using complete reconstructions of intracellularly labelled dendritic trees, Brännström et al (1992) confirmed shrinkage of the dendritic trees of hind limb spinal motoneurones in the adult cat at 12 weeks following a permanent axotomy close to the muscle. A few dendrites however showed signs of expansion. Unusual features of the dendrites took 2 forms: either a tangled short preterminal and terminal dendritic segments or a long meandering, usually thick process that ended simply, with no branches.

Linda et al (1985) axotomised spinal motoneurones, cutting more proximal to the soma using a longitudinal incision in left ventral funiculus of the spinal cord at L7. Cells in 3 different cats had dendritic branches within the lesion area with a highly abnormal appearance. In normal cat α-motoneurones the axon originated from soma 95% of the time or proximally in proximal dendrites 3% of the time but never distal to the first branching point in a dendritic tree. In the axotomised cells axon type processes were observed to arise distal to the first branching point of dendrites. These processes were axon-like in that they had constant diameters and were myelinated. It was proposed these hybrids be called dendraxons.

Havton and Kellerth (1987) described axon-like processes from axotomised MG α motoneurones in the cat which originated from the cell body region. There was only one such process per axotomised motoneurone and they had a fairly uniform diameter along their length and were myelinated (although this was patchy and irregular).All of these processes gave off collateral branches which formed bouton like specializations of both en passant and terminal types. They had different projections to normal and were never seen to extend into the ventral roots or to cross to the contralateral side. Electron microscopy of these processes revealed that they contacted neuronal profiles and contained mitochondria as well as numerous dense core spheroid vesicles of 35-65nm diameter and the presence of synaptic clefts with post-synaptic dense material.

Rose and Odlozinski (1998) using intracellular labelling and complete reconstructions showed that axotomy caused an expansion of the dendritic tree of neck motoneurones of the adult cat spinal cord. It must be noted that the axotomy of the neck motoneurones results in a more proximal axotomy than that of the hind limb motoneurone axotomy of Brännström et al (1992). In the neck motoneurone model two unusual of dendritic features were observed. One was complex arborisations with a tangled appearance and twisting paths where web-like expansions and irregular varicosities were common. The other main feature was branches that did not taper and had unusually large diameters. These followed meandering paths including reversing directions with some entering the lateral or ventral funiculi where they turned to follow a rostral or caudal trajectory. Rose and Neuber-Hess (1997) discovered that these axon-like processes were myelinated and contained dense collections of neurofilaments, primary cytoskeletal elements of axons and a low incidence of microtubules, the main cytoskeletal components of dendrites.

MacDermid et al (2002) examines the specific distribution of cytoskeletal proteins across the entire dendritic tree of these axotomised neck motoneurones. Map2a/b is a cytoskeletal protein normally confined to dendrites. GAP-43 however is an axonal growth protein only found in growing axons (Mattson 1999). The distribution of MAP2a/b in proximal dendrites was not affected by axotomy, however there was an absence of MAP2a/b labelling in the abnormal (and some normal appearing) distal processes of axotomised neck motoneurones. In contrast GAP-43 was found in unusual distal processes (and some normal distal processes).

The relevance of such changes may be questioned by observations that axon type processes seen to emerge from axotomised lamprey neurones retract over time (Hall and Cohen, 1988). Studies of the time course of the changes in the axotomised neck motoneurone model suggest that this is not the case for these cells (MacDermid et al 2004). At shorter time periods 92-4 weeks all of the unusual distal processes (UDPs) were arboreal. By 8-12 weeks the axon-like processes had appeared, by 35 weeks 60 % of UDPs were described as axon-like. The dendrites giving rise to UDPs have fewer biforcations over time. At 2-4 weeks 10 % of UDPs were immunoreactive for GAP-43, at 8-12 weeks 88% and none at 20 weeks or 35 weeks. None of the UDPs tested were map positive at any time intervals.

Axotomy proximal to the soma has been shown to cause both morphological and cytoskeletal changes in spinal motoneurones. This has led some investigators to assume that axotomy is necessary to see these changes. There is however evidence

that cytoskeletal changes may occur as a result of deafferentation making this body of work more relevant in the context of spinal cord injuries.

Gazula et al (2004) used a complete spinal cord transection of rats (23 day post natal) T5-T6. 5 day later motoneurones rostral to the lesion were labelled using a viral vector (HSV-LacZ) injected in to the sciatic nerve. Dendritic trees from individual neurones were reconstructed from single tissue sections. Following the injury motoneurones had statistically significantly less primary dendrites, less branching, lower average arbour per dendrite and shorter longest dendrites than controls. For animals that underwent a daily exercise programme actively moving paralyzed limbs however, levels were comparable to controls. Dendritic trees were only labelled at 5 days post-injury and clearly much plasticity may occur at time spans longer than this, indeed if connections to cells from lesioned fibres can change at later times (as discussed earlier) it is plausible to argue that changes in the dendritic tree on which sprouting axons make contact may also continue to change simultaneous with this.

Hamori (1990) describes the reduction of size of the dendritic tree following dennervation as adaptive, leading to a relative increase in the density of surviving axon terminals. Hamori also points out that the deafferentation can also cause the formation of presynaptic specializations along their otherwise classical post synaptic membrane (the axonization of dendrites) resulting in the formation of new dendritic synapses (Hamori et al 1997).

Caceres and Dotti (1985) following destruction of the inferior olive in adult rats creating partial dennervations in the cerebellum. After 1 day the MAP2a/b staining

was similar to controls. After 3 days however there were clear decreases in MAP2a/b staining both in proximal and distal portions of thick secondary and tertiary dendritic trunks. There was a considerable decrease in the intensity of the reaction product in fine dendrites ramifications of the purkinje cells. At 8 days MAP2a/b immunoreactivity began to increase but only in climbing fibre deprived dendrites (ie. thick trunks) and only light staining was observed in the fine dendritic ramifications both in the inner and outer layers. By 11 days immunoreactivity had increased considerably with patterns similar to that of controls, by day 20 it was indistinguishable from controls.

Shaw et al (1988) showed that both axotomy rat superior ganglion neurone and dennervation of these cells by preganglionic section caused similar changes in each model with phosphorylated epitopes normally seen in axons being visible in cell bodies and dendrites. The changes occurred more slowly following dennervation than axotomy and in both cases were reversible.

Thus it may be hypothesised that the dendrites of the interneurones under study in this thesis despite not themselves being axotomised by the lesion may still show changes in response to a local lesion either in terms of a retraction or by sprouting or disruption to their cytoskeleton.

Hypothesis 3

The dendrites of interneurones one segment rostral to a partial hemisection which have not been axotomised by the lesion will show, retraction, sprouting and/or disruption to their cytoskeleton protein distribution.

Thus we hypothesise sprouting to the interneurones from lesioned bulbospinal axon and by the interneurones from their axons and from their dendrites (figure 1.1).

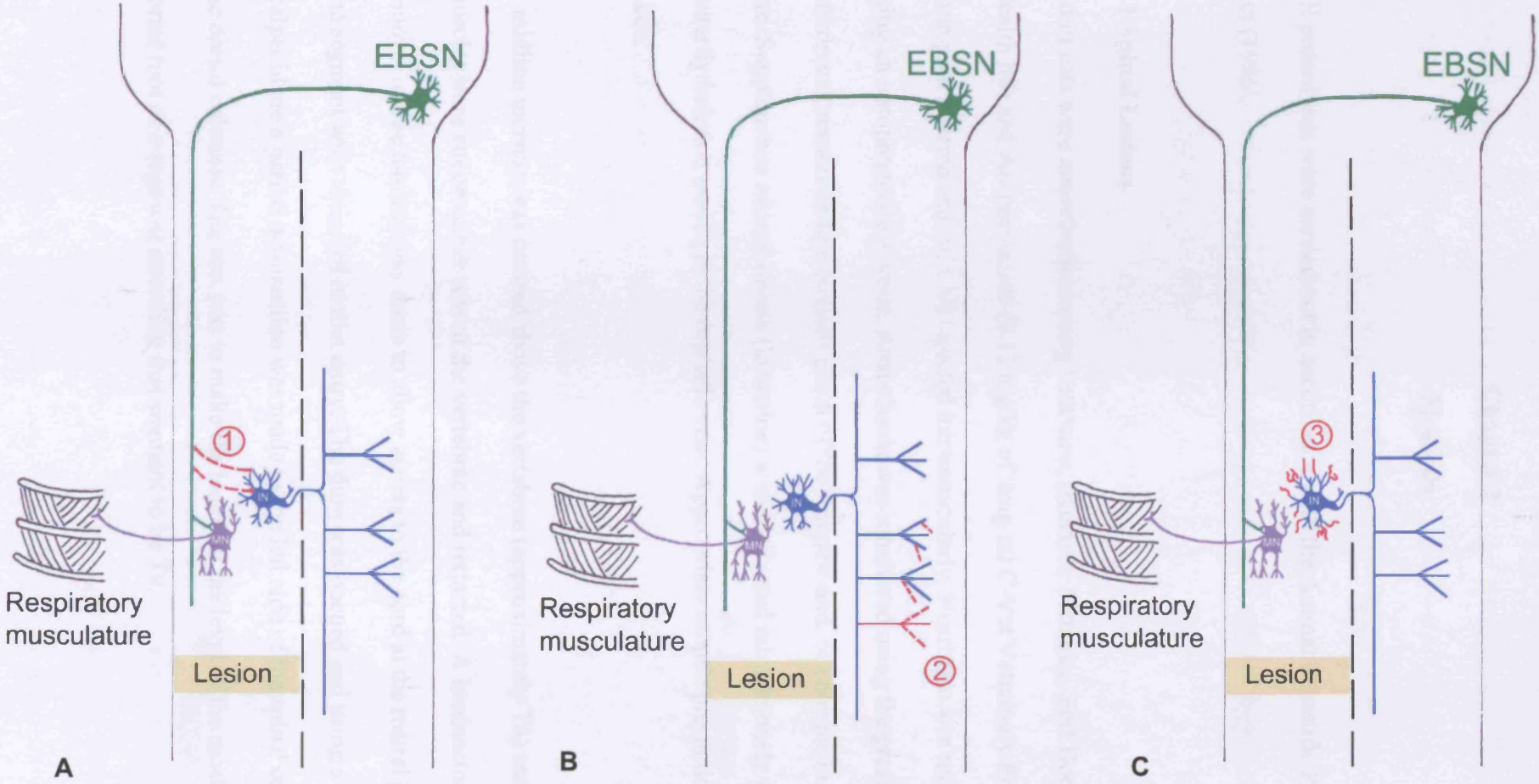

Figure 1.1 Hypothesised methods of sprouting with respect to thoracic interneurones (IN) following a lesion interrupting the expiratory bulbospinal neurones (EBSN) which normally make strong monosynaptic connections to thoracic motoneurones (MN)
A) from lesioned EBSN axons (1)
B) from the axons of the interneurones (2)
C) from the dendrites of the interneurones (3)

Chapter 2

Methods

All procedures were carried out in accordance with the Animal Scientific Procedures Act (1986).

2.1 Spinal Lesions

Adult cats were anaesthetised using ketamine, (Ketaset, 36mg/kg, Fort Dodge Animal Health ltd) and Acepromazine (0.12 mg/kg of 2mg/ml C-Vet Veterinary Products, Grampian Pharmaceutical Ltd) injected intramuscularly. Heart rate was monitored using an oesophageal electrode. Anaesthesia was monitored using the presence of withdrawal responses to a noxious pinch of the forepaw and, or changes in the heart rate. Supplements of anaesthesia (ketamine) were delivered intravenously via a butterfly infusion needle in the cephalic vein. Appropriate aseptic precautions were taken.

A midline incision was centred above the vertebrae (approximately T8) and the muscles were cut on either side of the vertebrae and retracted. A laminectomy (partial removal of one lamina) was made to allow access to the cord at the rostral part of the one segment with vision of rootlet entry. The dura was opened and using a small scalpel blade a partial hemisection was made to the left side of the spinal cord, sparing the dorsal columns. The aim was to make the lesion at the level of the most rostral dorsal root of a segment intending that segment to be T9.

The dura was folded back over the lesioned cord and the muscles closed in layers, applying Cicatrin (Glaxo Welcome) antibiotic between layers.
The skin was closed with absorbable suture and spray dressing (Opsite, Smith and Nephew, UK) and a spray dressing and Amoxicillin (1ml, make) was applied. Antibiotic (Amoxicillin 1ml, make) and an anti inflammatory (Rimadyl) was administered intramuscularly.

The animal was monitored constantly until it regained consciousness. Functional recovery was monitored carefully thereafter, especially for the first few days day following the operation. 2-3 days were allowed for recovery of bowel, bladder and limb function. Two animals which did not show sufficient signs of recovery within 3 days were painlessly euthanised in accordance with the project licence. Animals had been specifically selected that were of a friendly disposition to make it easier to be able to monitor distress, additional analgesia requirements, the wound status, bowel and bladder functions and locomotion.

Terminal physiological experiments were carried out between 7 and 32 months following the lesion.

2.2 Terminal Physiological Experiment

2.2.1 Preparation

Experiments were carried out under terminal anaesthesia using sodium pentobarbital (Sagatal) with an initial dose of 37.5 mg/kg given intraperitoneally, subsequently supplemented intravenously as required. The level of anaesthesia was assessed by the presence of a withdrawal response to a noxious pinch of the forepaw and/or changes

in blood pressure (measured by an arterial cannula). The temperature of the animal was monitored throughout with a rectal thermometer and maintained at 37 °C by a Thermostatically controlled heating blanket under the animal. The bladder was emptied manually when necessary.

The femoral vein was cannulated, allowing intravenous administration of substances and the femoral artery cannulated to monitor arterial blood pressure. A tracheostomy was made allowing the insertion of a Y-shaped cannula for artificial ventilation.

A midline incision was made, approximately 7 cm in length. Lattisimus dorsi was separated from the midline and tied with the skin so that both could be retracted to make an oil pool.

Superficial muscles were removed either side of the cord around the segments of interest. Branches of the dorsal ramus one segment rostral to the lesion on the side ipsilateral to the lesion were prepared for stimulation (as Kirkwood et al 1988) for the segment above the lesion. The external and internal intercostal nerves were also prepared for stimulation for this segment and the external nerve 3 segments rostral to the lesion prepared for recordings of efferent discharges. These dissections were as described in Sears 1964 and Saywell 2000.

The animal was supported by vertebral clamps, placed on vertebra rostral and caudal to the segments of interest, and a clamp on the iliac crest. The head was held ventro-flexed by a plate screwed to the skull.

A laminectomy was performed to expose the spinal cord from a length reaching three segments rostral to the lesion and one to two segments caudal to the lesion. The dura was then opened and a 1-3 small patches of pia removed in the segment rostral to the lesion to enable recordings to be made. A pressure plate was gently applied.

Animals were paralysed with gallamine triethodide (Flaxedil/dosage) and artificially ventilated with CO_2 enriched air to give a brisk respiratory drive. Whilst paralysed anaesthesia was monitored using possible changes in the blood pressure to a noxious pinch of the forepaw as an indicator of depth of anaesthesia. Changes in discharges of the most rostrally dissected external nerve were also observed.

The spinal cord and dissected nerves were submerged together in one pool of paraffin oil formed by the retracted skin and the nerves were mounted onto bipolar platinum electrodes. A bilateral pneumothorax was performed to reduce movement of the cord related to the ventilator to help mechanically stabilize the cord.

A pair of stimulating electrodes was placed in each side of the cord below the lesion and in some experiments a pair of fine tungsten electrodes were also placed immediately rostral to the lesion. A recording electrode was placed at the dorsal root entry to record incoming volleys from stimulation of the dissected nerves.

Extracellular recordings of expiratory bulbospinal units in the medulla were performed and for these experiments an occipital craniotomy was performed to expose the medulla. The dura was opened and the pia removed from the area of interest and a pressure plate applied.

2.2.2 Stimulation and Recording/ Experimental protocol.

Electrical thresholds for the dissected nerves were obtained from volleys recorded by the cord dorsum electrode. To antidromically activate the cells with axons running in these nerves the nerves were stimulated at five times this threshold when characterising cells in the spinal cord..

Inspiratory discharges recorded from the more rostral of the two dissected external and intercostal nerves were used to define the respiratory cycle and used to monitor for possible signs of EMG activity indicating a need to administer more Flaxedil.

A glass microelectrode with an external tip diameter of 3.0-3.2 μm, filled with sodium chloride was slowly inserted in to the medulla (at around 2-3 mm caudal to obex on the right side) manually until expiratory units could be identified extracellularly in the nucleus retrombiguus (as in Merrill 1972). In some experiments two units were recorded separately with two independent microelectrodes.

2.2.3 Identification of EBSNs

Expiratory units were identified by the phasing of their discharges with the respiratory cycle as defined by the inspiratory discharge of the external nerve. Units were selected for use in STA if they were identified to be axotomised bulbospinal units by invasion of an antidromic potential elicited by stimulation of the thoracic cord above the lesion but not from stimulation of the cord below the lesion (Ford et al 2000).

The antidromic nature of the responses were also confirmed using the collision test (Paintal 1959) where a stimulus is applied after a spontaneous orthodromic spike at an interval shorter than the critical interval (the relative refractory period of the axon + the orthodromic latency) of that cell. This will cause the orthodromic and antidromic spikes to collide and so result in the failure of the antidromic spike to invade the soma. A double stimulus was used to confirm that the failure of the antidromic spike to invade the soma was a result of collision and not due to the soma being in a refractory state.

The collision test was used to obtain the antidromic latency of the unit which was used to estimate the conduction velocity of the unit (Davies et al 1985; Kirkwood 1995)

2.2.4 Intracellular Recording from interneurones.

For recording in the cord the first few tracks a glass microelectrode with an external tip diameter of approximately 1.2-1.6 μm with resistances of between about 2-5 mΩ filled with 3M potassium acetate was used, suitable for intracellular recording of motoneurones. It was inserted into the cord at an angle of between 10 and 15 degrees through the dorsal columns. This was used to locate antidromic field potentials from stimulation of the 3 dissected peripheral nerves and so identify suitable entry points for electrodes which would lead to areas expected to contain the thoracic interneurones of interest given their known location relative to that of the motoneurones.

Once a suitable entry point for the interneurones was identified the electrode was replaced with a higher resistance glass electrode with a tip diameter between 0 μm and 1.2 μm, this being more suitable for intracellular penetrations of interneurones. For tracks where the sole aim of penetrating the interneurones was to record from them for STA the electrode was filled with 3M potassium acetate. For those tracks where cells were to be labelled, the electrode containing solution of 2-4% Neurobiotin (Vector laboratories) in 0.1m Tris buffer in 3M potassium acetate.

Interneurones were identified by different criteria, as in Kirkwood et al (1988). The most unequivocal identification was the ability to antidromically stimulate the cell from one of the caudal spinal stimulating electrodes, but not from the dissected peripheral nerves. Failing this (as would be the case with interneurones with very short or ascending axons) identification of cells as interneurones could be made by their more dorsa-ventral location, being dorsal to the motoneurones. Given the angle of entry of the microelectrode the ideal position for the interneurones should be ventral to Clarke's Column cells which were used as another guide to depth.

The interneurones also often had a distinctive injury discharge on initial penetration which further helped in their identification

Intracellular recording were made from interneurones for a duration long enough to allow STA (see analysis), simultaneous with the extracellular recoding of an EBSN. Upon exit of the interneurone an extracellular record was taken to be used as a control for averaging if necessary (see analysis)

2.2.5 Data Acquisition.

Signals from the medulla microelectrode, the spinal glass microelectrode (AC and DC) and from the rostral external nerve were fed into the 1401 analogue to digital converter from (Cambridge Electronic Design) coupled to a computer running the Spike-2 data acquisition program (CED). The data were also recorded on a magnetic tape using a pulse-code modulated interface unit and a conventional video recorder and including a voice channel. This allowed data to be reacquired again offline at a later date where necessary.

2.2.6 Analysis

The selection of intracellular interneurone recordings for STA was made using the following criteria

i. Positive identification of the cell as an interneurone

ii. A membrane potential of below - 20mv which was verified on exiting the cell.

iii. Averages would contain more than 1000 sweeps

iv. The presence of postsynaptic potentials resulting from stimulation of the peripheral nerves or spinal cord confirming that penetrations were somatic or close to the soma for axonal penetrations.

v. the unitary nature of the extracellular recording of the EBSN made simultaneously with the interneurone could be confirmed by an interval histogram or auto-correlation

Spike triggered averaging was performed for each intracellular interneurone recording meeting this criteria (using the high gain record), triggered by the extracellular EBSN unit recorded simultaneously with that particular interneurone recording. The

averages were analysed for EPSP-like waveforms. To test the reproducibility of any waveforms produced by the averages the recordings were split up into 3 equal time intervals and separate averages carried out on each interval. The timing of any EPSPs were checked for consistency with the appropriate latency for a direct connection calculated for that EBSN unit (as Kirkwood et al 1985; Ford et al 2000).

If consistent waveforms were apparent in the intracellular averages, STA was also performed between the medulla units and the extracellular recordings close to the interneurone as an additional control.

2.2.6. Intracellular labelling

When electrodes contained neurobiotin, intracellularly penetrated identified interneurones with stable membrane potentials could be filled with neurobiotin by passing positive current through the electrode (600ms cycle duration). Filling periods ranged from 6 to 60 nA. minutes. In some experiments motoneurones were also labelled, in which case they were identified by antidromic stimulation of their peripheral axons.

At approximately 2 hours after the intracellular injection of neurobiotin the preparation was given 5000 units of heparin (i.v.) and a supplementary dose of Sagatal. Immediately following the overdose the preparation was perfused via the left ventricle with saline until the perfusate ran clear, followed by a solution of 4% paraformaldehyde and 5% sucrose for approximately 20 minutes. The segments of the spinal cord of interest (including the lesion) were removed and prepared for histological processing.

2.3 Histological Processing.

The removed segments of spinal cord were post-fixed in 4% paraformaldehyde + 30% sucrose overnight. If the perfusion had resulted in extremely well fixed tissue it was stored in phosphate buffer with 30% sucrose. Postmortem checks were made to confirm the integrity of the ventral root at the segment of interest. This was important to confirm that any labelled motoneurones had not been axotomised. Checks were made for shrinkage of the cord using measurement taken during the terminal experiments. Any shrinkage was usually minimal. Final distances could therefore be calculated by counting numbers of sections of known thickness.

50 μm thick transverse sections were cut frozen on a freezing microtome and kept in serial order in 0.1m phosphate buffered saline (PBS).

Sections were washed 3 times in 0.01m PBS before being immersed, for one hour, in a blocking solution of 10% ethanol, 10% hydrogen peroxide in 0.1M PBS, to reduce background staining by blocking endogenous peroxidase activity.

After 3 rinses in PBS, sections were incubated overnight in ABC Elite (Vector, 8 drops A plus 8 drops B in 80 ml 0.1M PBS) plus 0.3% Triton-X. Next day, after 3 rinses in 0.01M PBS and 3 rinses in Tris buffer, sections were incubated in a solution of 10 mg diaminobenzidine (DAB) and 0.5 mg nickel ammonium sulphate in 50 ml Tris buffer for 20 minutes after which time 0.8ml of 0.003% hydrogen peroxide (diluted from 30% using Tris buffer) was added and the reaction observed under a microscope.

The reaction was stopped once the cell or it processes had appeared and before the background started to become dark, by rinsing in cold Tris buffer. Sections received 5 rinses and then were mounted on gelatine-subbed slides and left to air dry for 2 days. The dried sections were counterstained with 1% Neutral Red, dehydrated through increasing concentrations of acetone, defatted in xylene and then cover slipped using DePeX mounting medium (BDH).
Cells were then reconstructed by hand using a drawing tube attached to a Zeiss Axioscope microscope.

In some of the later experiments an aim was to label dendrites with an antibody to recognise the dendritic protein MAP-2a/b and demonstrate co-localization of these labelled processes with the neurobiotin.

For these experiments alternate sections were placed in 2 different sets of wells (so they remained in series). Both series went through the same blocking phases as for the previous experiments. Only the first of the two alternate series of sections were incubated in the ABC solution and reacted with DAB (as previously described).Reacted sections were temporarily mounted and cover-slipped using glycerol. This allowed the sections containing the labelled soma to be identified together with the rostral and caudal extent of the dendrites. The un-reacted alternate sections falling within this range could then be selected for fluorescent labelling. The remaining unreacted sections that were not selected for fluorescent labelling were incubated in the ABC solution and reacted with DAB (as previously described) using the appearance of the axon of the labelled cell as a sign of a successful reaction.

Those sections to be fluorescently labelled were immersed in a blocking solution of 1% sodium borohydride in 0.1 M PBS for 15 minutes to reduce background staining by blocking aldehyde groups. After sufficient rinses in 0.001M PBS the sections were then immersed overnight in a solution consisting of 10% normal horse serum (NHS, Vector laboratories), 3% triton X (sigma laboratories) and dried milk fat in 0.1M PBS to prevent non-specific binding of the primary antibody. After 3 rinses in PBS with 2% NHS and 0.3% triton-X, each lasting 10 minutes, sections were incubated overnight in a solution containing the primary antibody, mouse anti-MAP 2a/b, (1:10,000 Chemicon).

After 3 rinses in PBS (with 2% NHS and 0.3% triton-X) sections were immersed in the secondary antibody, anti-mouse with Texas red (1:100, Vector laboratories) for 3 hours and then 3 times (15 minutes each) in PBS without NHS. Finally, sections were immersed in PBS with avidin-fluoroscein (1:100 Vector laboratories) for 3 hours to fluorescently label the neurobiotin in the filled cell.

Each section was rinsed 3 times in PBS before being mounted on plain glass slides and coverslipped using Vectorshield (Vector Laboratories) and stored in the fridge.

Co-localization of the fluoroscein with the Texas red was analysed using a Zeiss Axioscope microscope or using a confocal microscope. Further analysis used Adobe Photoshop software. Once analysed, sections were then incubated in the ABC solution for 3 hours and reacted with DAB (as previously described) and permanently mounted in their correct serial order with all of the other sections on gelatine subbed slide as previously described.

2.4 Reconstructions of Cells

Using the Axioscop microscope and a drawing tube, labelled neurones were reconstructed. For those experiments where fluorescent labelling had been used it was found that those sections that underwent he processes of fluorescent labelling had shrunk compared to the other sections. For these cells each section was drawn separately and a composite drawing traced using a light box. The locations of processes on the non-shrunken sections rostral and caudal to shrunk sections were taking to be correct and correction for the shrinkage in the intermediate shrunken section was made such as to allow labelled processes on each section to join with the appropriate processes on the rostral and caudal sections.

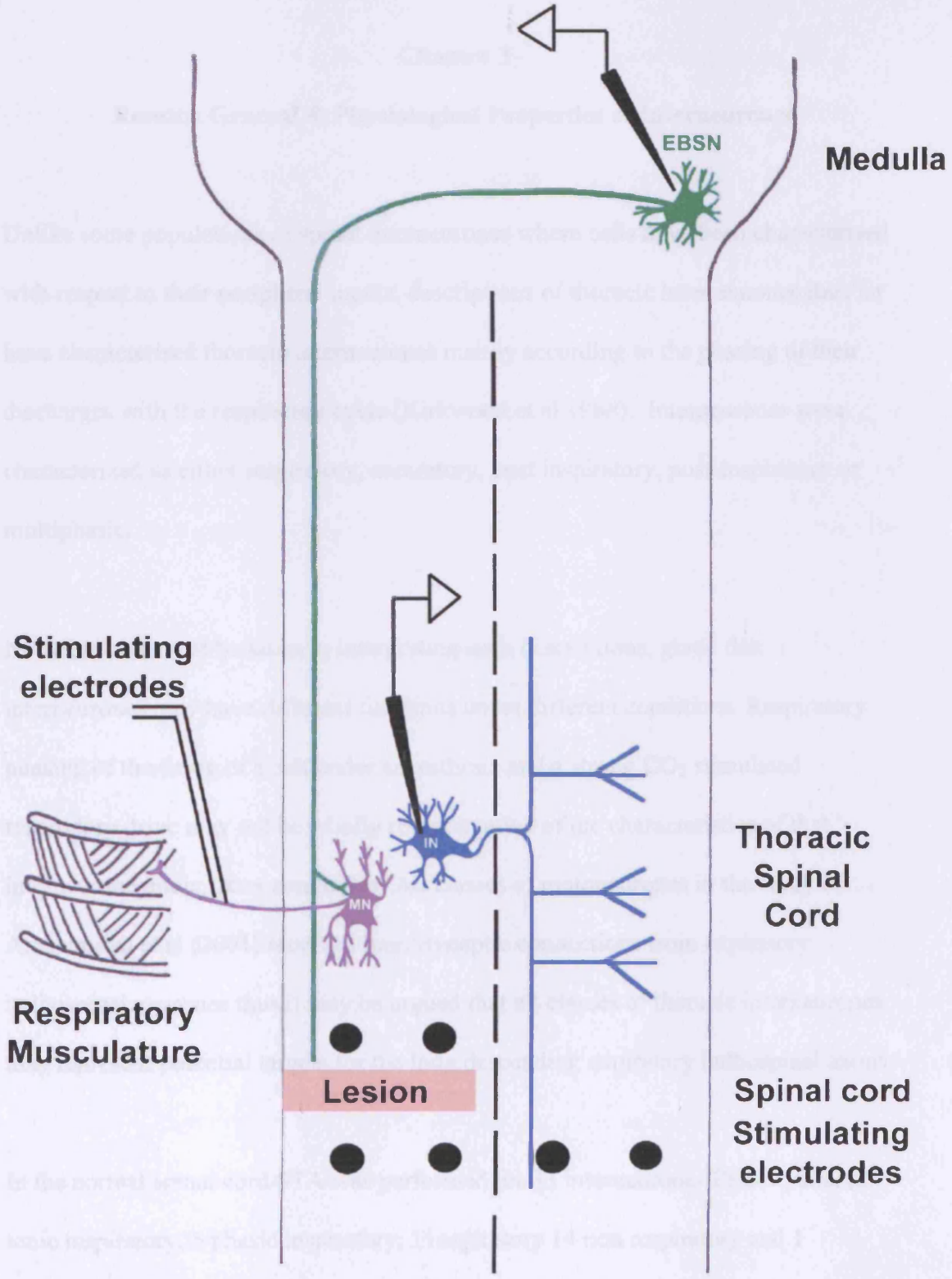

Figure 2.1 : Experimental Setup.
Extracellular recording from EBSNs in the medulla and intracellular recordings of thoracic interneurones (IN). The location of the interneurones obtained using, as guides, antidromic field potentials from thoracic motoneurones (MN) following stimulation of peripheral nerves. Spinal cord electrodes antidromically activate thoracic interneurones aiding in their identification.

Chapter 3

Results: General & Physiological Properties of Interneurones

Unlike some populations of spinal interneurones where cells have been characterised with respect to their peripheral inputs, descriptions of thoracic interneurones thus far have characterised thoracic interneurones mainly according to the phasing of their discharges with the respiratory cycle (Kirkwood et al 1988). Interneurones were characterized as either inspiratory, expiratory, post inspiratory, post-inspiratory or multiphasic.

Note that care must be taken in interpreting such descriptions, given that interneurones may have different functions under different conditions. Respiratory phasing of the firing of a cell under anaesthesia and a strong CO_2 stimulated respiratory drive may not be wholly representative of the characteristics of that interneurone under other conditions. All classes of motoneurones in the study of Annisimova et al (2001) received monosynaptic connections from expiratory bulbospinal neurones thus it may be argued that all classes of thoracic interneurones may represent potential targets for the long descending expiratory bulbospinal axons.

In the normal spinal cord STA was performed for 33 interneurone- EBSN pairs. (2 tonic inspiratory, 5 phasic inspiratory, 11expiratory 14 non respiratory and 1 unclassified). No EPSPs were unequivocally identified from these averages. (Saywell 2000)

This indicates an absence of a strong descending monosynaptic connection from expiratory bulbospinal neurones to the sample of interneurones in contrast to their strong monosynaptic drive to thoracic motoneurones (Annissimova et al 2001).

In the lesioned spinal cord extracellular recordings of terminal potentials suggest sprouting by these bulbospinal fibres one segment rostral to the lesion (Ford et al 2000). This combined with the apparent absence of any increases in the monosynaptic input to motoneurones in the lesion model using STA (Annisimova et al 2001) makes the interneurones good candidates as targets for the sprouting EBSNs. Given the lack of any ESPS in the interneurones in the control population any EPSPs seen in the new lesion population of this study would therefore be consistent with this hypothesis.

3.2 Spike Triggered Averaging

In the lesioned populations cells were selected for STA which had been identified as interneurones by the ability to antidromically stimulate them from caudal spinal stimulating electrodes (n=5). Failing this, their characteristic high frequency injury discharge on penetration and depth (n=1) or depth only (n=2) were used for identification. Penetrations were confirmed to be somatic (or axonal but close to the soma) if the recordings showed synaptic noise, or if postsynaptic potentials could be seen from stimulation of the peripheral nerves or the spinal cord.

Obtaining good intracellular recordings of interneurones one segment rostral to a lesion simultaneously with recordings of EBSNS proved to be extremely difficult in the lesioned preparation as compared with controls. Only 11 pairs of

interneurone/EBSN pairs (9 cells, 2 with 2 medulla units) suitable for STA were recorded before it was decided on both practical and ethical grounds to discontinue this part of the project due to the low yield per animal. Of these cells only 1 demonstrated a detectable respiratory modulation.

The criteria used by Saywell for identifying EPSPs in the averages was a positive potential with a fast rise time beginning at an appropriate latency, as calculated from the conduction velocity of the bulbospinal unit and that could repeatedly identified. The same criteria were used in this study.

For all but one pair spike triggered averages of the intracellular recordings using spikes from the EBSN revealed nothing of appropriate latency to represent monosynaptic EPSPs. 2 Examples of these averages are illustrated in figure 3.1

One exception is cell B54E which, when averaged using spikes from the extracellularly recorded lesioned EBSN (R2) as the trigger, revealed a small EPSP-like waveform, approximately 10 μV in amplitude (figure 3.2). The latency for this is 3.45ms, consistent with it being monosynaptic for this EBSN. The predicted axonal conduction time was estimated as 2.2 ms for this unit. 0.5ms could be allowed for synaptic delay and 0.75 ms for slowed conduction in collateral branches (Ford et al 2000). The repeatability of this possible EPSP was confirmed by splitting the total time of recording into 3 roughly equal time intervals and performing separate averages on each. The EPSP was consistent across all 3 averages.

This cell, however, was only identified as an interneurone by injury discharge on initial penetration and on its depth, this being 2.35mm. With motoneurones being recorded at 2.4, 2.5 and 2.6mm in this animal, it cannot be regarded as 100% conclusive that this cell is an interneurone and so one must exercise caution when drawing conclusion from this one EPSP seen with this cell.

Due to the extremely low yield of pairs of recordings however the inability to demonstrate any unequivocal monosynaptic connections does not negate the hypothesis and the interneurones remain a likely target for sprouting expiratory bulbospinal axons.

It had been hoped to carry out both STA and intracellular labelling on the same neurones but although this was attempted, successful combinations of the techniques was not achieved. Obtaining single penetrations of the interneurones alone, stable enough to allow iontophoretic injections of neurobiotin, although also difficult in this preparation, was more successful. Removal of the need for good simultaneous recordings in the medulla allowed more time for tracking in the spinal cord. Thus the majority of this thesis is devoted to the analysis of the morphology of these cells.

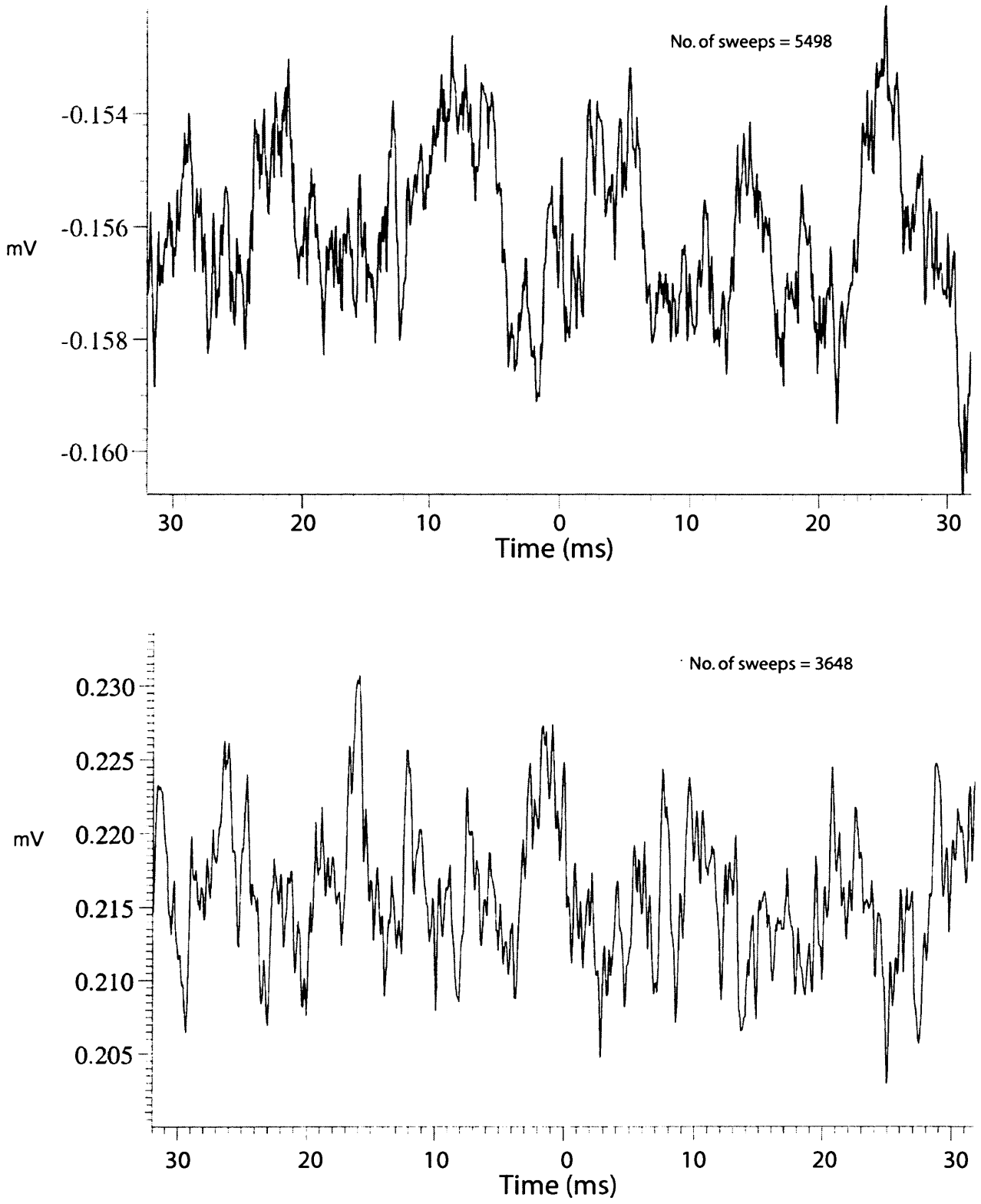

Figure 3.1 Spike -triggered averages of thoracic interneurone recordings.
Examples of spike-triggered averages for intracellular recordings from 2 thoracic interneurones one segment rostral to a spinal hemisection, using spikes from an EBSN as the trigger for the averages.
These interneurones were activated antidromically from the cord and yielded a sufficient number of sweeps.
From these averages no clear EPSPs can be seen .
Zero time represents the time of the EBSN spikes.

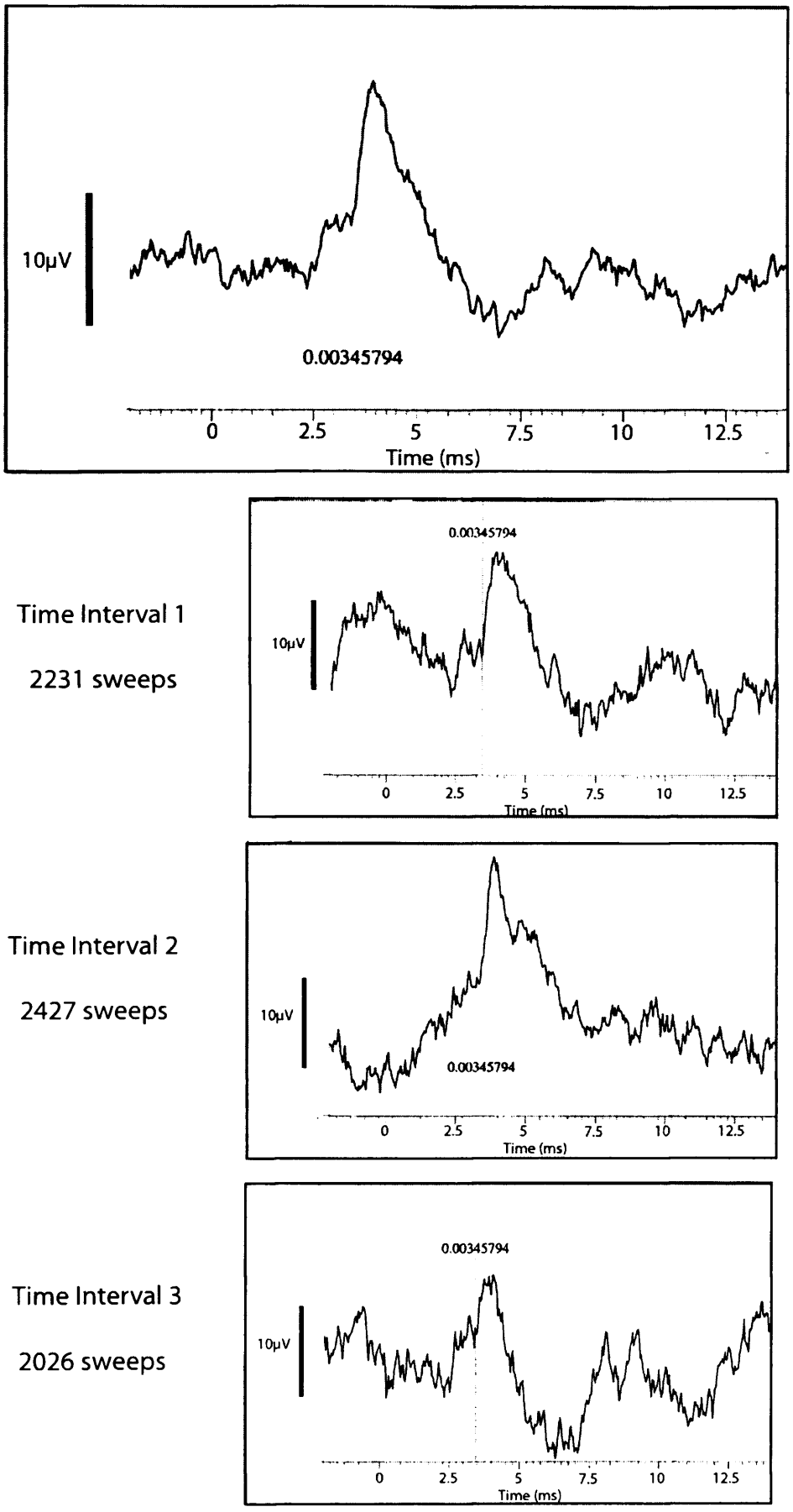

Figure 3.2
Top: spike-triggered average of intracellular recording from a thoracic interneurone , using spikes from an EBSN as the trigger for the averages. A small EPSP-like waveform is apparent, approximately 10 μV in amplitude at a latency of 3.45ms, consistent with this being monosynaptic for this EBSN (see text). Zero time represents the time of the EBSN spikes. Splitting the total time of recording into 3 roughly equal time intervals and performing separate averages on each confirms the repeatability of this EPSP (3 lower waveforms).

3.3 Physiological characteristics of labelled interneurones.

A total of 17 interneurones in the lesioned cord were iontophorectically injected with neurobiotin. All had been identified as interneurones by at least one of the criteria discussed in the methods chapter. In fact a number of these were only identified by the characteristic high-frequency injury discharge. 14 of the cells were recovered. All of these were subsequently found to be interneurones, by virtue of their axonal trajectories.

Interneurones were labelled at various survival times post lesion: 6 weeks (n=1); 7 weeks (n=2); 8 weeks (n=1); 16 weeks (n=6); 17 weeks (n=2); and 18 weeks (n=2).

In order to ensure that only the selected neurone was stained, a continuous check on the condition of the penetration was maintained during the passage of current. Either an antidromic spike or a synaptic potential from one of the nerves or from the spinal cord was evoked between each of the depolarising pulses. If there was a decline in membrane potential during the injection period, then the amplitude of the evoked potential also decreased, but the evoked potential was used as the prime indicator of the quality of the recording, rather than the membrane potential itself. A maximum amplitude of around 5 nA was used and current pulses passed for as long as the neurone was judged to be in reasonable condition (typically an evoked potential of around 50% of its initial amplitude). For the cells recovered, the integral of injected currents ranged from 6-60 nA minutes.

One clue as to the depth of the recordings were penetrations of Clarke's column neurones. In early experiments one or two of these cells were filled. These were not required because they did not fit the original criteria of interneurones within the normal projection area of EBSN collaterals (Kirkwood et al 1999). Moreover they are very difficult to reconstruct from transverse sections because their dendrites are restricted to tight bundles running almost exclusively rostrocaudally. We learnt to recognise their typical recording characteristics, with relatively large monosynaptic EPSPs from one or more of the peripheral nerves and their showing a greater ease of penetration and stability of recordings than most of the other interneurones. They were typically found at a depth of around 2.0 - 2.1 mm. Subsequently, we did not start searching for interneurones until a depth of at least 0.2 mm greater than their location.

For 9 of the interneurones, the soma and dendrites were labelled sufficiently well to allow reconstruction of the soma and its dendritic tree. Of the reconstructed cells 3 of these also had dendritic processes on sections that had been labelled for MAP 2a/b.

Axons for 14 interneurones could be followed and, for 12, their axon collaterals reconstructed. There were 2 interneurones where despite a strongly labelled axon no soma was recovered. The circumstance of strongly labelled axon with no labelled soma is consistent with the experience of Saywell (2000) in the control experiments where this was the case for 3 of the 20 labelled interneurones.

The labelled interneurones were all found in the segment rostral to the lesion (as expected), this ranging from T4 to T9 (T4, n= 1; T5. n= 2; T6, n=1; T7, n=5; T8, n=2; T9, n=3) at distances from the lesion ranging from 4mm to 13mm. Those from the

control population were located in T5 (n=3), T6 (n=3), T7 (n=2), and T8 (n=7). All had funicular axons and thus can be considered to be propriospinal or possibly ascending tract cells. 12 had crossed axons and can therefore be classed as commissural.

The interneurones were located in laminae VII, VIII and IX, their precise positions as compared to those of the control population are illustrated in figure 3.3. This range of locations in the transverse plane is not so different from the control population, the control group perhaps being more ventral.

This may be relevant given the observation of Saywell (2000) that the interneurones with the strongest respiratory modulation were located more ventrally than less strongly modulated interneurones. Of the labelled cells from the control group 6 had expiratory modulation, 3 inspiratory and 6 had no respiratory modulation. From the lesioned population only 4 showed respiratory modulation. An example of an intracellular recording from a respiratory modulated interneurone from the lesioned population is illustrated in figure 3.4 along with inspiratory discharges from the external nerve defining the respiratory cycle. The cell shows a high frequency discharge in early expiration and silence in post inspiration. Also illustrated is an example of the antidromic spike recorded in this cell following stimulation of the spinal cord, contralateral to the lesion below the lesion, confirmed the descending contralateral non-lesioned projection of this cell. This was also confirmed histologically (see chapter 4).

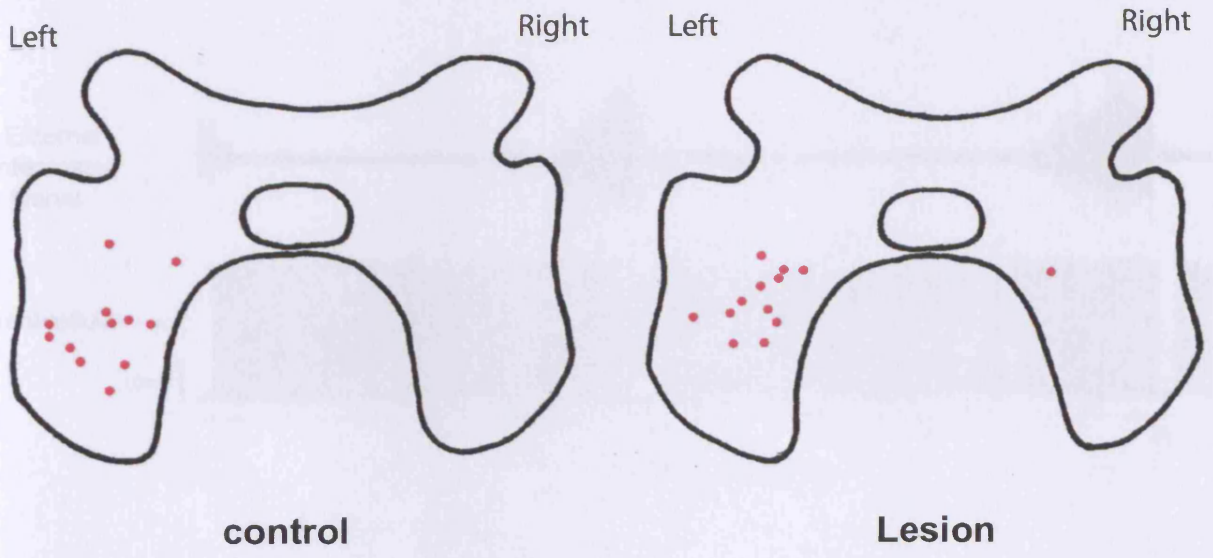

Figure 3.3 : Approximate locations of labelled internueurones in the control population (Saywell et al. 2000) and those of the lesioned population of this study. Locations are represented as red circles on a standardised outline of a thoracic ventral horn in the transverse plane. The lesion was on the left side of the spinal cord.

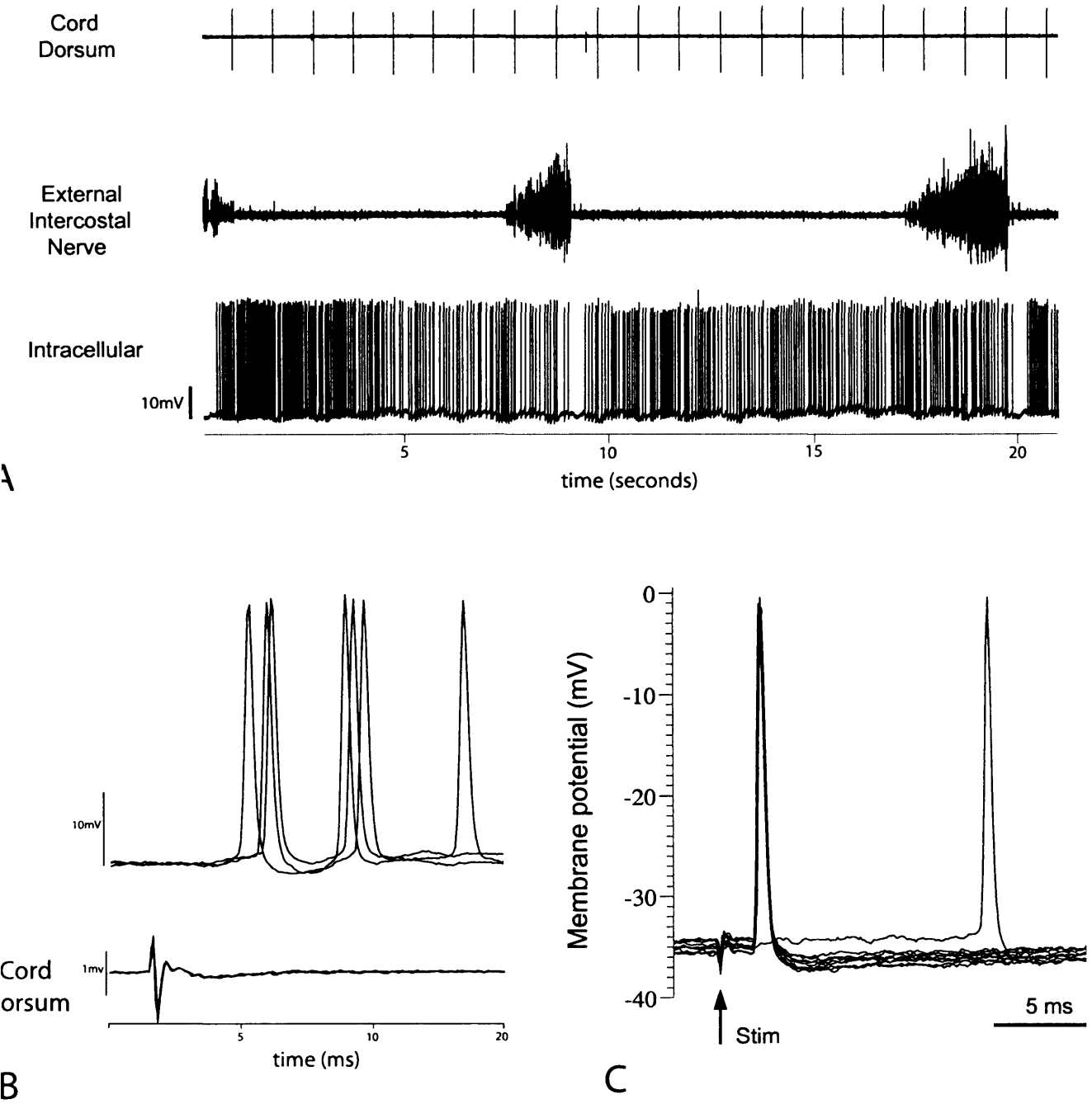

Figure 3.4 : Cell B73J with a physiologically confirmed contralateral descending axon

A. Typical recording from an interneurone soon after penetation, before starting to inject Neurobiotin. During this period, the internal intercostal nerve was stimulated at 5x threshold. Afferent volleys shown in cord dorsum record (upper trace). The recording was almost certainly axonal: note that there is relatively strong respiratory drive represented by the high frequency discharge in early expiration, compared to silence in immediate post-inspiration, but this drive not apparent as a respiratory drive potential. Nevertheless, the recording must have been close the soma, because small polysynaptic EPSPs (amplitude of about 1mV) are apparent in B (upper trace) at a latency of 2.2 ms from the cord dorsum volley (lower trace). These EPSPs fire the cell, and are presumably attenuated in this recording.

B. Records representing 3 superimposed traces from the middle of A. Injury effects may have contributed to the spontaneous discharges in A.

C. Antidromic spike from stimulation of the contralateral spinal cord in caudal T10. The recording was in rostral T8, the lesion in ipsilateral T9.

3.4 Lesions

Following histological processing, the lesions were reconstructed for each experiment in which labelling occurred. These lesions were classified using the system of Ford et al (1995). From this figure it can be observed that in 4 animals a large cyst formed (B74, B77, B88 and C1). Surprisingly, the post-operative notes showed that these 4 animals neither recovered slower than the others nor showed any later deterioration in motor performance. In fact, to the contrary, all 4 recovered well, with B77 recovering very quickly, using all 4 limbs for locomotion next day. At 16 weeks post-lesion B74 is described as being "in very good shape", B77 being "very healthy looking", B88 "in great condition: walks and jumps well" and C1 "a fit friendly cat – walks runs jumps well". The extent of the lesions did not appear to correlate with the recovery rates of the animals. The most influential factor appeared to be the individual personalities of each animal.

Comparison of the lesioned population of labelled cells with the control population will be dealt with in two separate chapters, one concerned with the axons and their collateral branches and the other with the dendritic trees of the neurones.

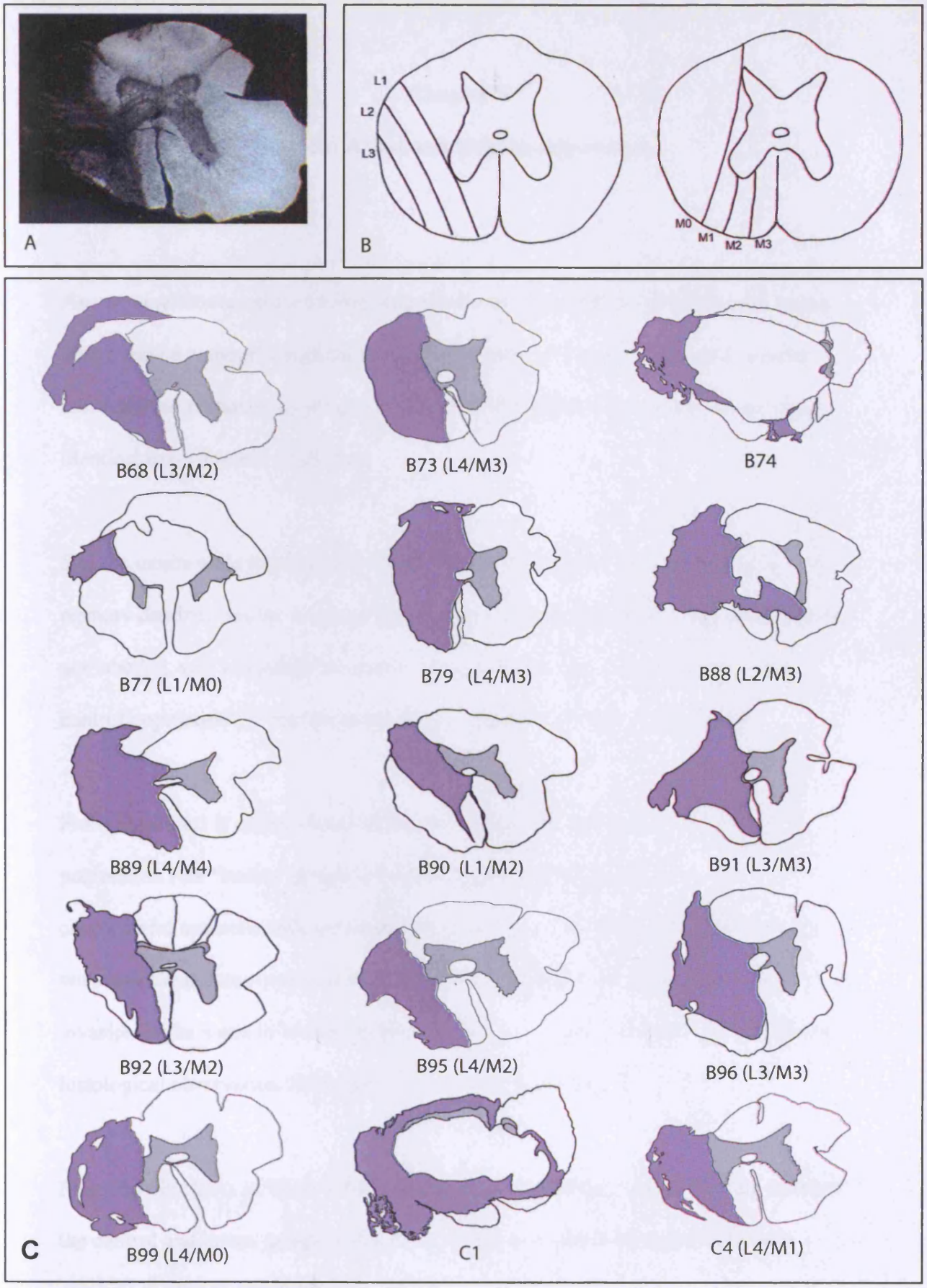

Figure 3.5 : Lesions

A: Photomicrograph taken using darkfield illumination to show the extent of a lesion (experiment B69)

B: Scheme for classifying lateral and medial borders of the lesion as used in Ford et al (1995)

C: Reconstructions of the extent of lesions for each experiment in which cells were labelled, with their classification in brackets. Note the presence of cysts in B74, B77, B88 and C1.

Chapter 4

Results: Axons and Collateral branches.

Axons were recovered for 14 interneurones from 12 animals 6-18 weeks post lesion. These can be compared with the control population of 17 cells obtained in similar non-lesioned preparations obtained by Saywell (2000) in the same laboratory under identical experimental conditions

5 of the axons were found to arise directly from the soma, 4 from the base of a primary dendrite and the origin of 5 were impossible to identify because the soma was not labelled, was too faintly labelled or was damaged. This is comparable with the control population (7 from the soma, 4 from dendrites and 4 undetermined)

From Figure 4.1 it can be observed that the sample obtained in the lesioned preparation (the "lesion" group) contained similar proportions of cells with contralateral and cells with ipsilateral axons as the control group. None of the cells with ipsilateral axons had been axotomised as confirmed by either antidromic invasion of the soma following stimulation of the axon below the lesion or by direct histological observation of the axon running past the lesion.

From the pie charts in figure 4.1b it can be observed that the main difference between the control and lesion groups is that there were fewer cells with descending only axons in the lesion population.

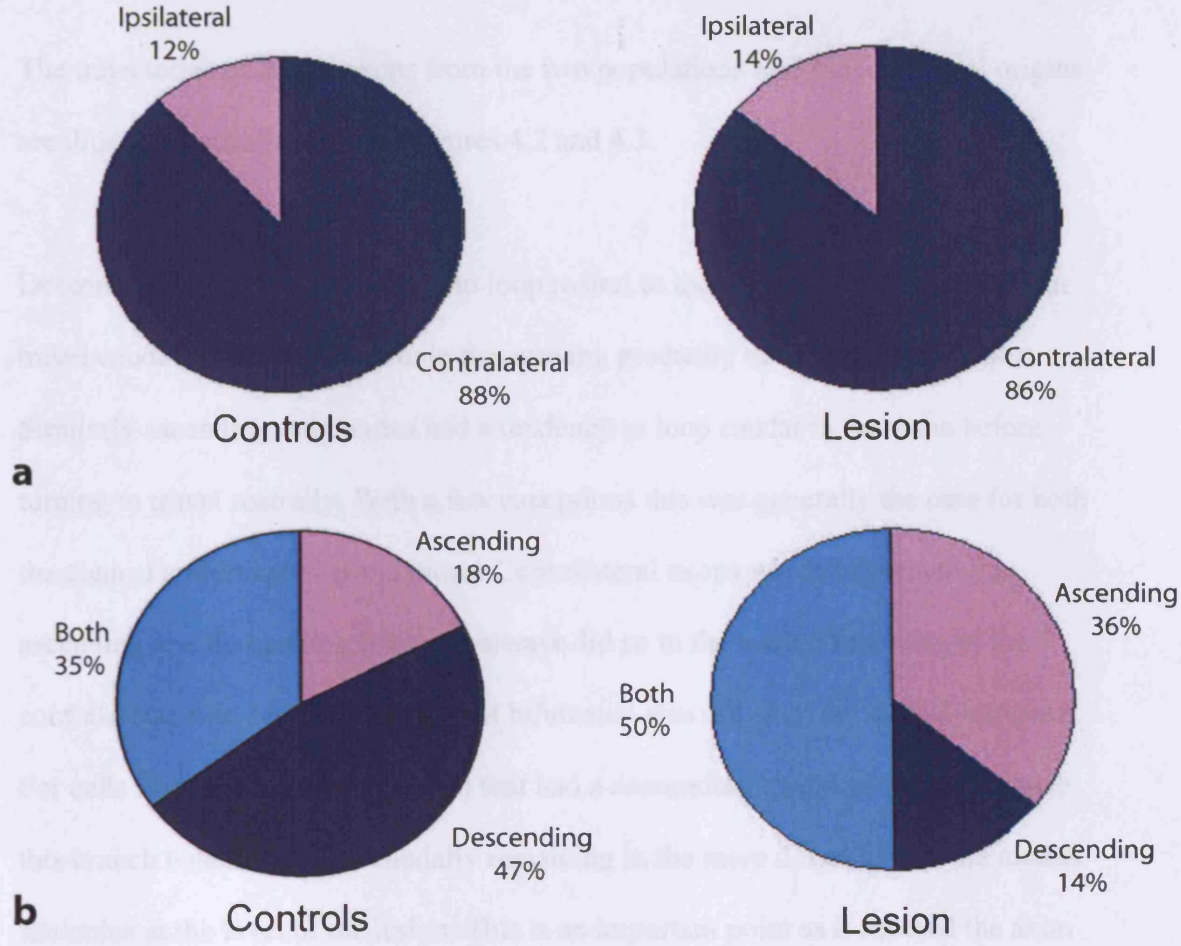

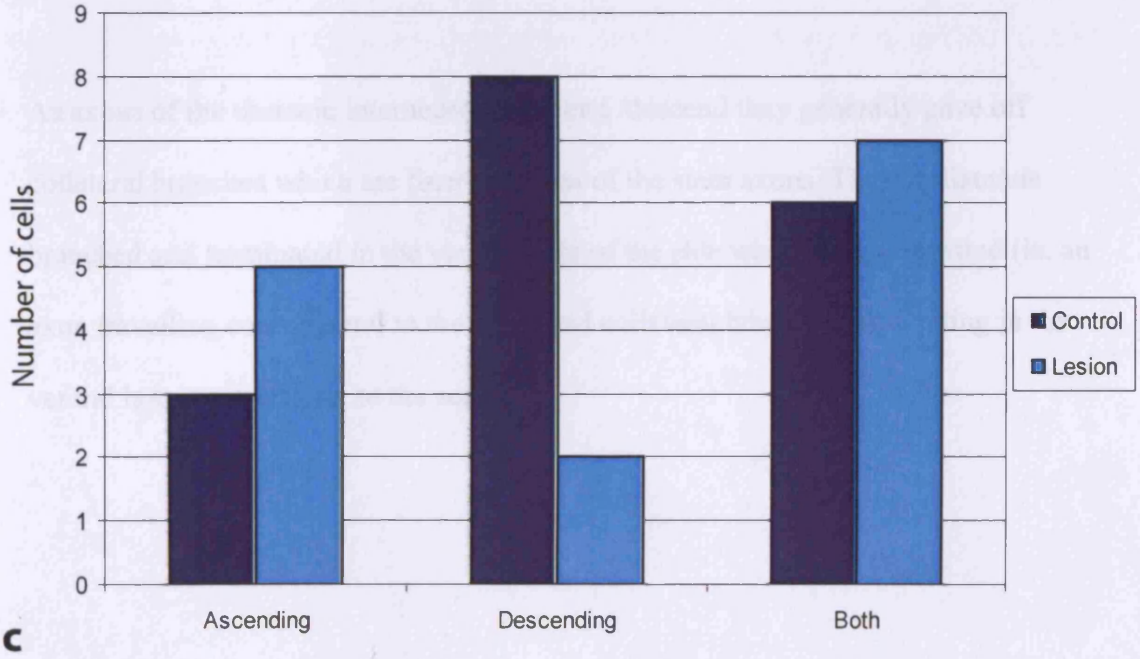

Figure 4.1
Trajectories of main stem axons of interneurones in control and lesion groups.
a) contralateral or ipsilateral with respect to soma
b and c) Ascending, descending or both an ascending and descending branch

The trajectories of all the axons from the two populations and their collateral origins are illustrated schematically in figures 4.2 and 4.3.

Descending axons had a tendency to loop rostral to the soma before turning to then travel caudally in the medial funiculus moving gradually to the ventral funiculus. Similarly ascending only axons had a tendency to loop caudal to the soma before turning to travel rostrally. With a few exceptions this was generally the case for both the control and lesioned populations. Contralateral axons which bifurcated into ascending and descending branches always did so in the medial funiculus of the contralateral side. Ipsilateral cells that bifurcated also did so in the medial funiculus. For cells from the lesion population that had a descending ipsilateral axonal branch this branch tended to travel caudally remaining in the more dorsal half of the medial funiculus at the level of the lesion. This is an important point as it ensured the axon had not been cut by the more lateral lesions in these cases (figure 4.4).

As axons of the thoracic interneurones ascend /descend they generally gave off collateral branches which are finer than that of the stem axons. These collaterals branched and terminated in the ventral horn of the side which they originated (ie. an axon travelling contralateral to the soma had collateral branches terminating in the ventral horn contralateral to the soma).

Figures 4.2 A – P

Axon trajectories for labelled interneurones from the control population with axon collateral branches and the extent of these collateral branches in the rostro-caudal axis.

Note:

Trajectories are to scale in the rostro-caudal axis.

NP = Rostral-caudal extent of collateral not possible to ascertain (this was usually due to either faint labelling of the collateral, damage to a section or the end of the series of sections that were cut).

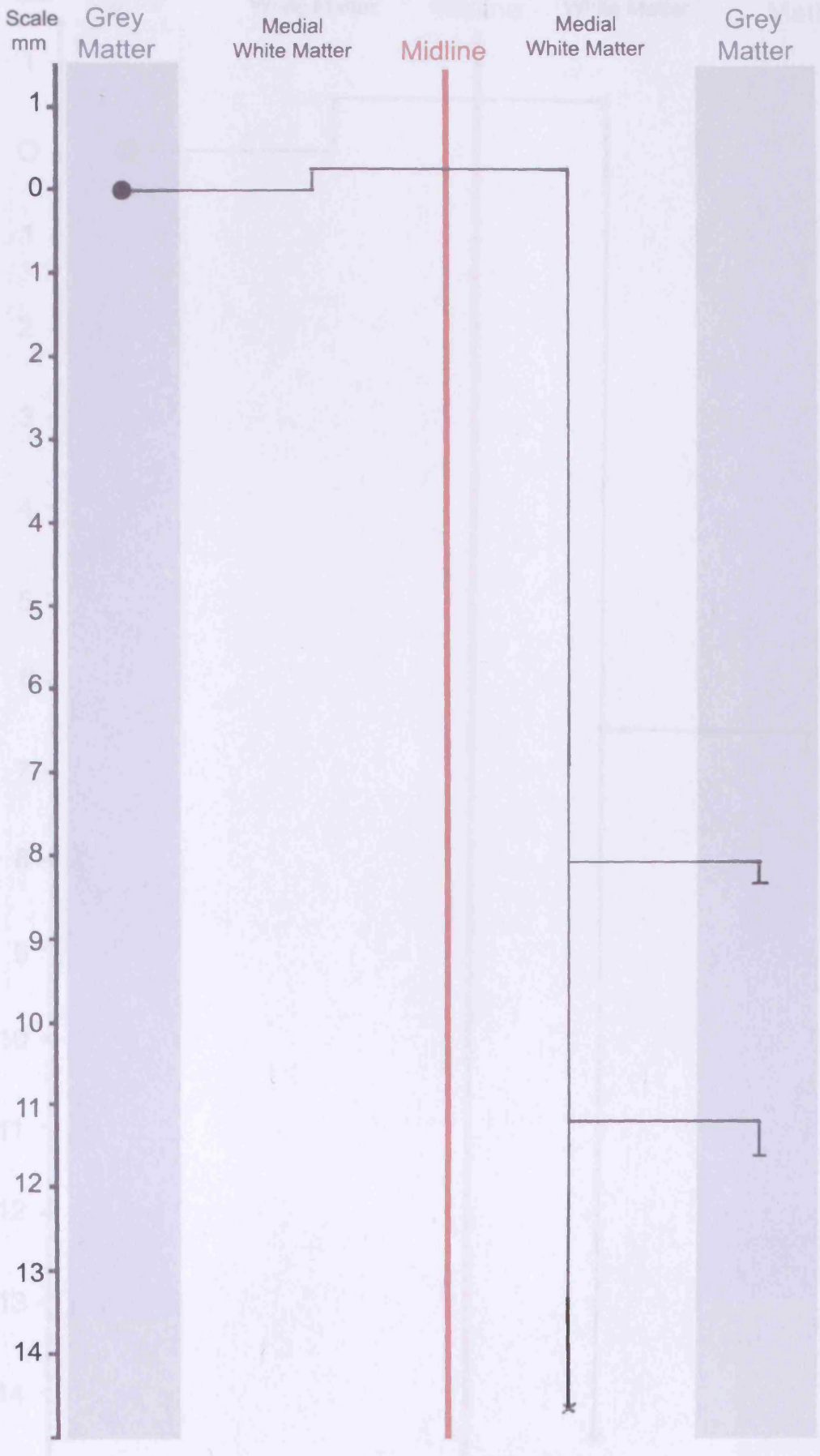
Scale mm
Grey Matter
Medial White Matter
Midline
Medial White Matter
Grey Matter
1
0
1
2
3
4
5
6
7
8
9
10
11
12
13
14

A: Cell B16-6

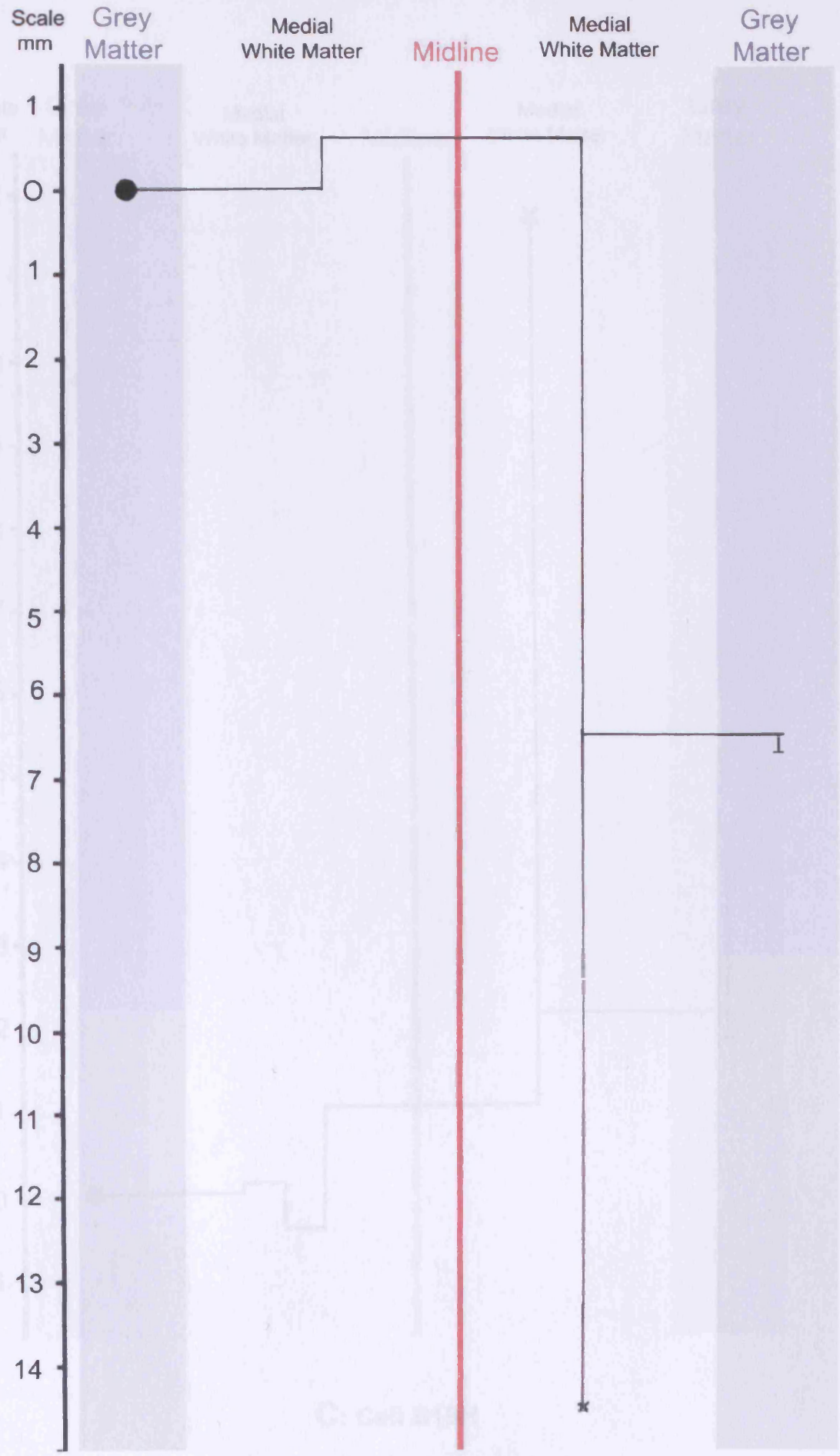
Scale
mm
Grey
Matter
Medial
White Matter
Midline
Medial
White Matter
Grey
Matter
1
0
1
2
3
4
5
6
7
8
9
10
11
12
13
14

B: Cell B16-7

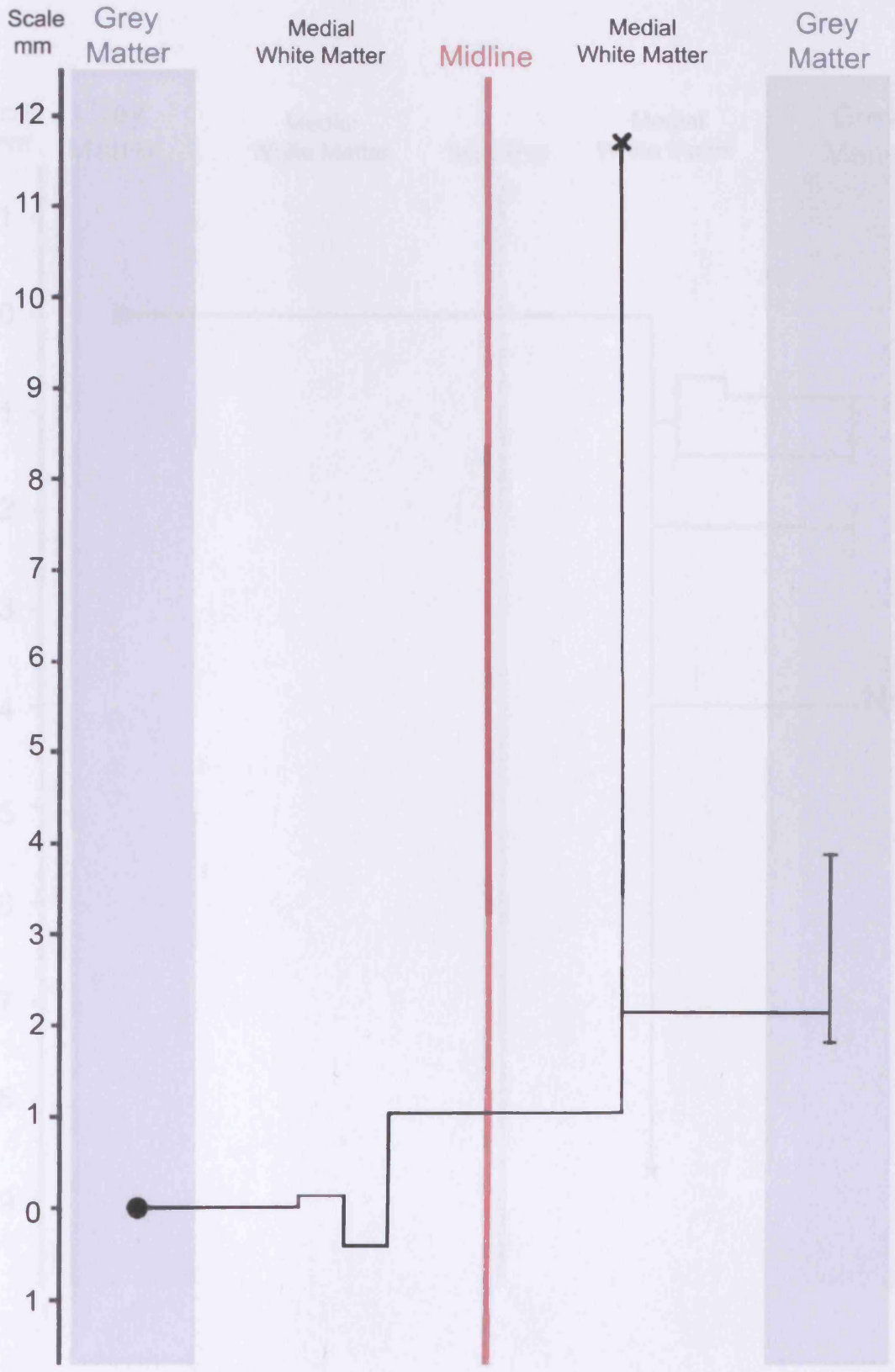
Scale mm
Grey Matter
Medial White Matter
Midline
Medial White Matter
Grey Matter
12
11
10
9
8
7
6
5
4
3
2
1
0
1

C: Cell B18H

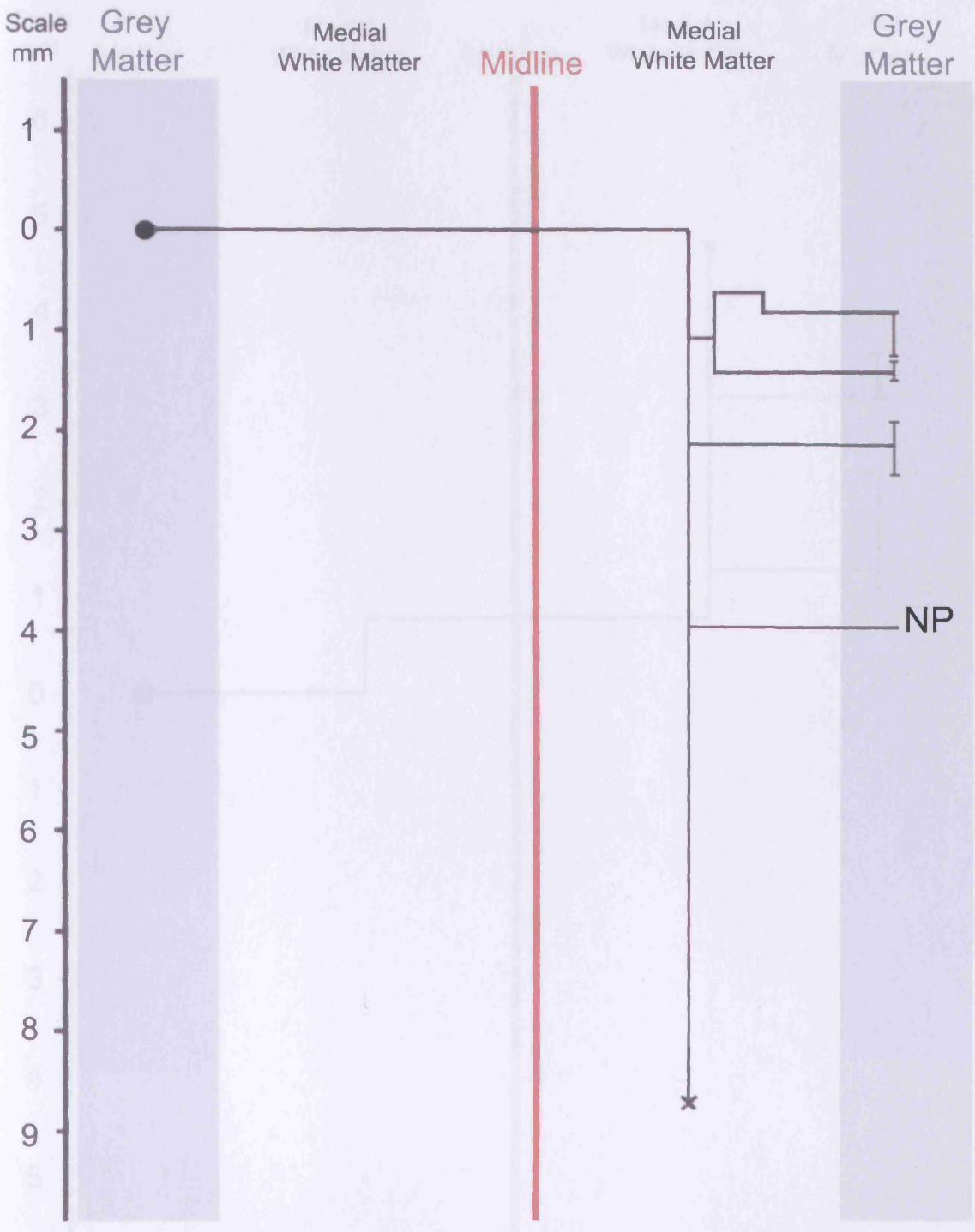
Scale
mm
Grey
Matter
Medial
White Matter
Midline
Medial
White Matter
Grey
Matter
1
0
1
2
3
4
5
6
7
8
9
NP

D: Cell B18l

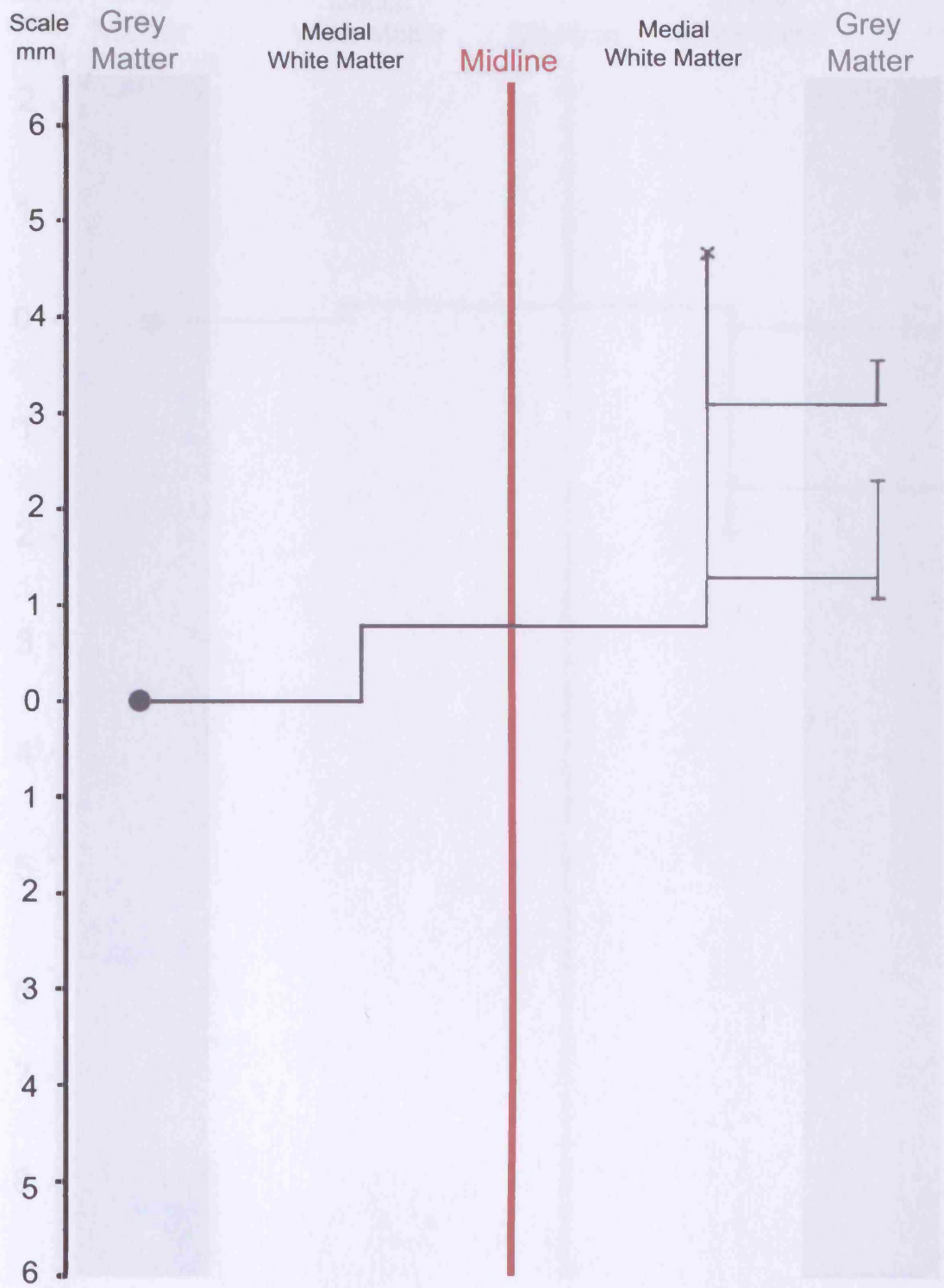
Scale
mm
Grey
Matter
Medial
White Matter
Midline
Medial
White Matter
Grey
Matter
6
5
4
3
2
1
0
1
2
3
4
5
6

E: Cell B20D

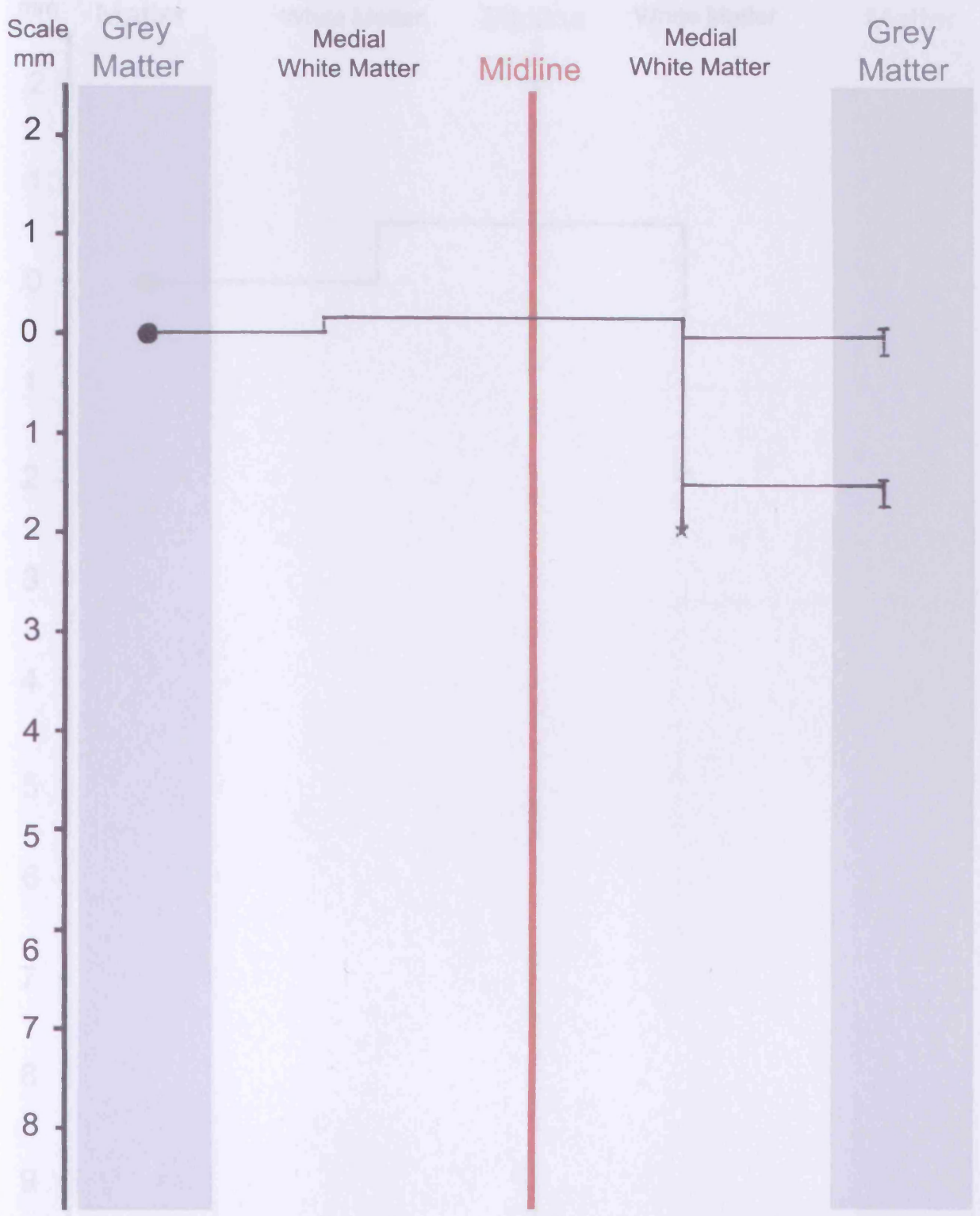
Scale
mm
Grey
Matter
Medial
White Matter
Midline
Medial
White Matter
Grey
Matter
2
1
0
1
2
3
4
5
6
7
8

F: Cell B20l

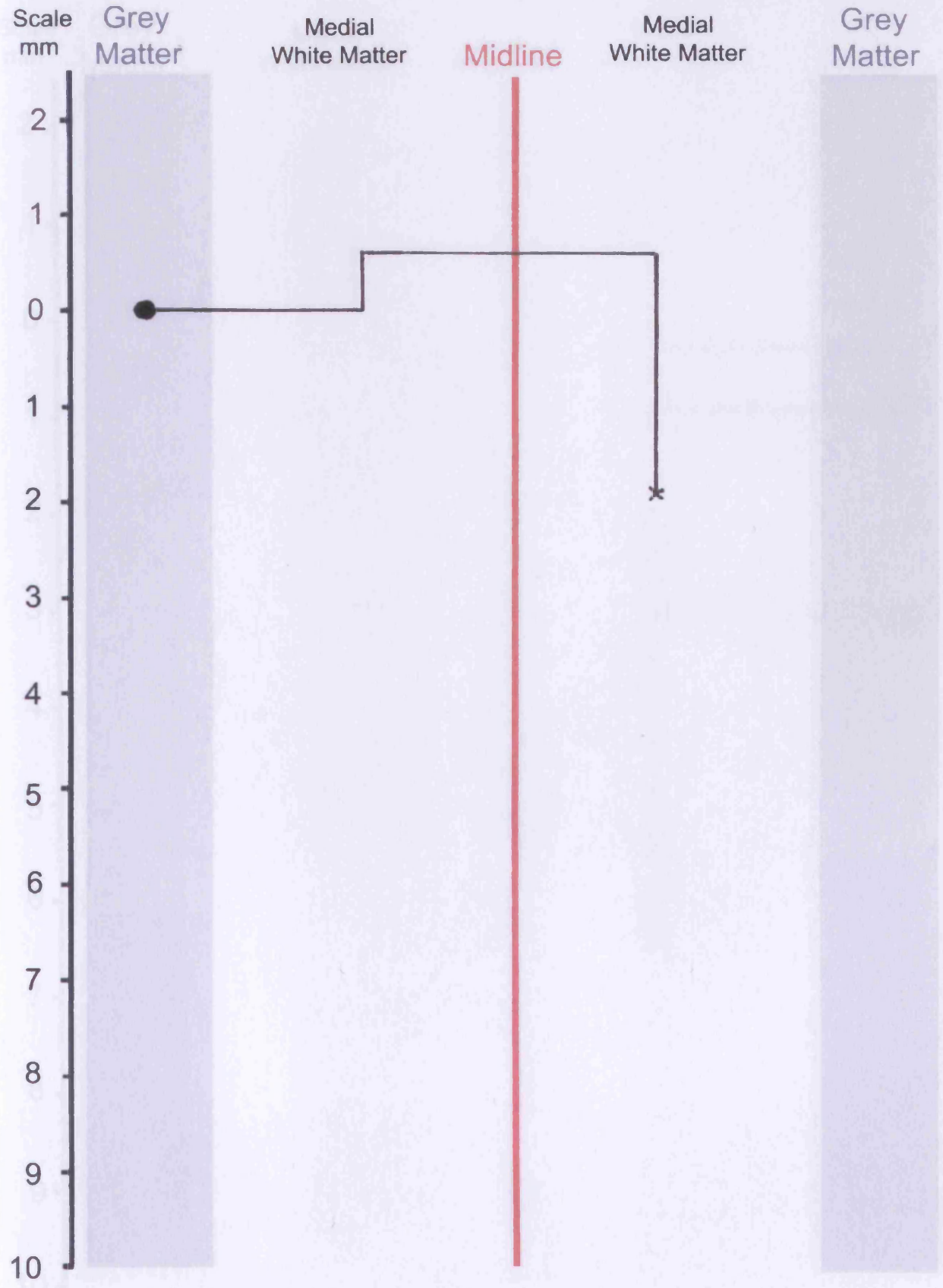
Scale mm
Grey Matter
Medial White Matter
Midline
Medial White Matter
Grey Matter
2
1
0
1
2
3
4
5
6
7
8
9
10

G: Cell B24N

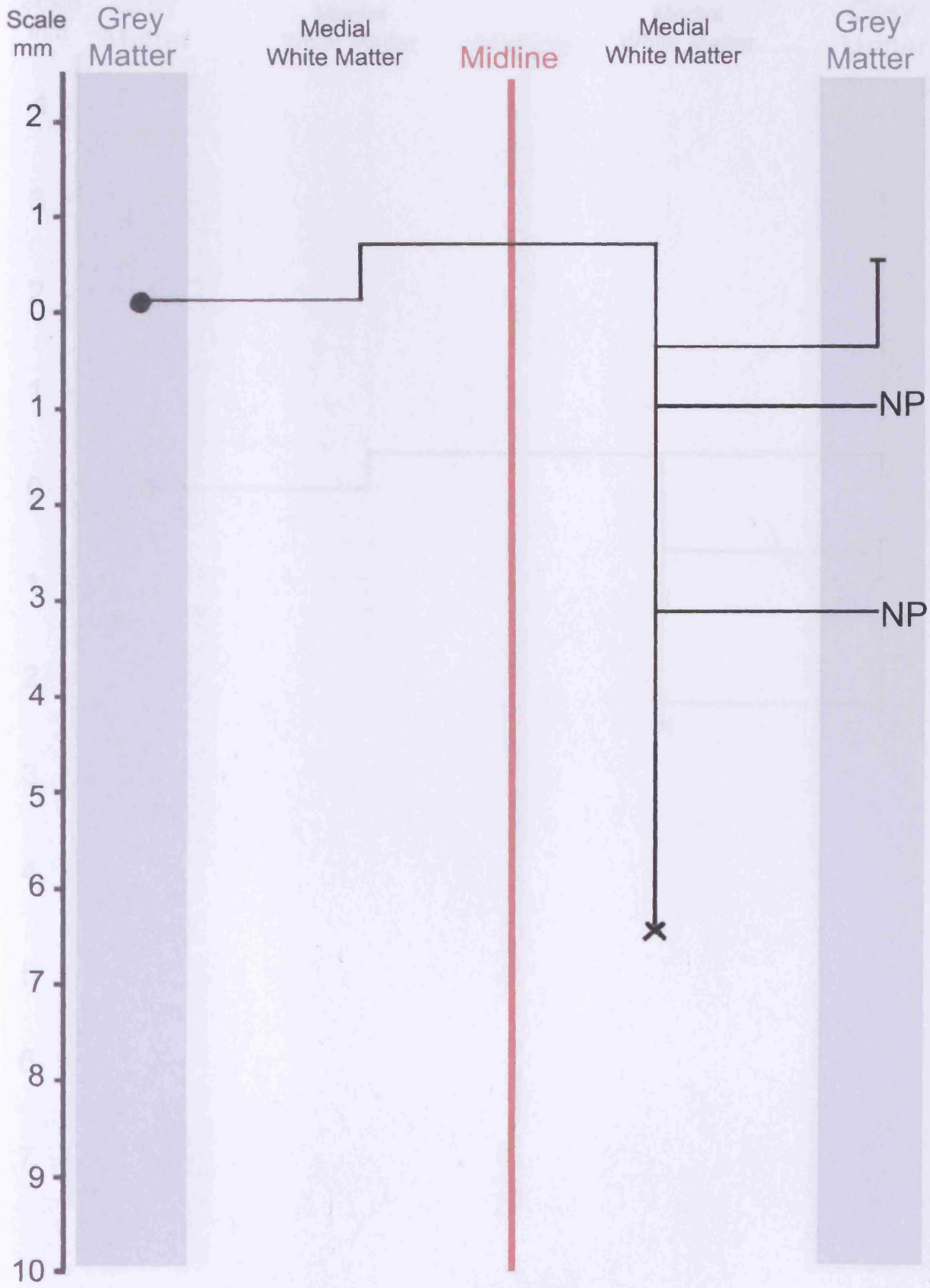
Scale mm
Grey Matter
Medial White Matter
Midline
Medial White Matter
Grey Matter
2
1
0
1
2
3
4
5
6
7
8
9
10
NP
NP

H: Cell B25J

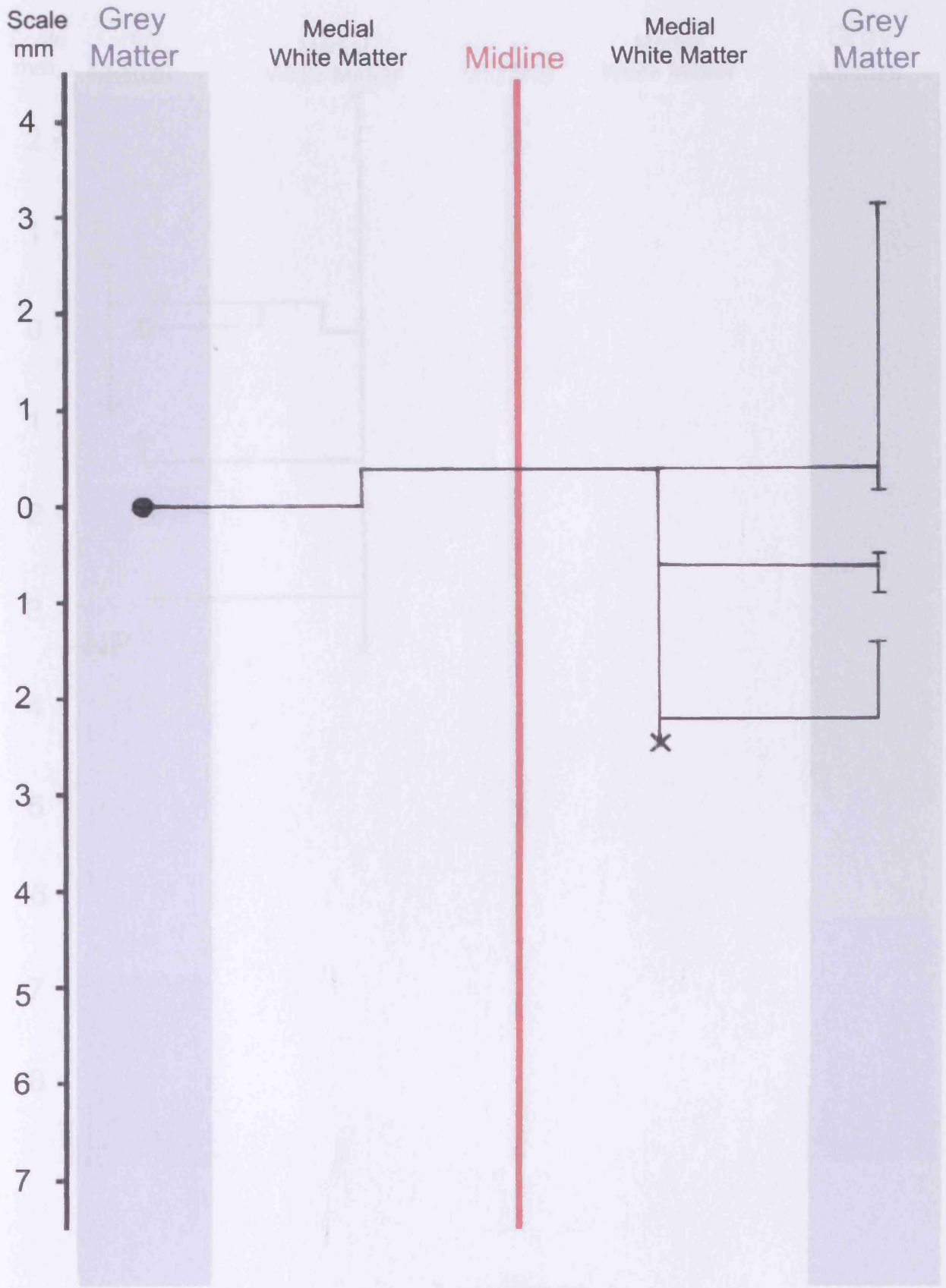
Scale
mm
Grey
Matter
Medial
White Matter
Midline
Medial
White Matter
Grey
Matter
4
3
2
1
0
1
2
3
4
5
6
7

I: Cell B25N

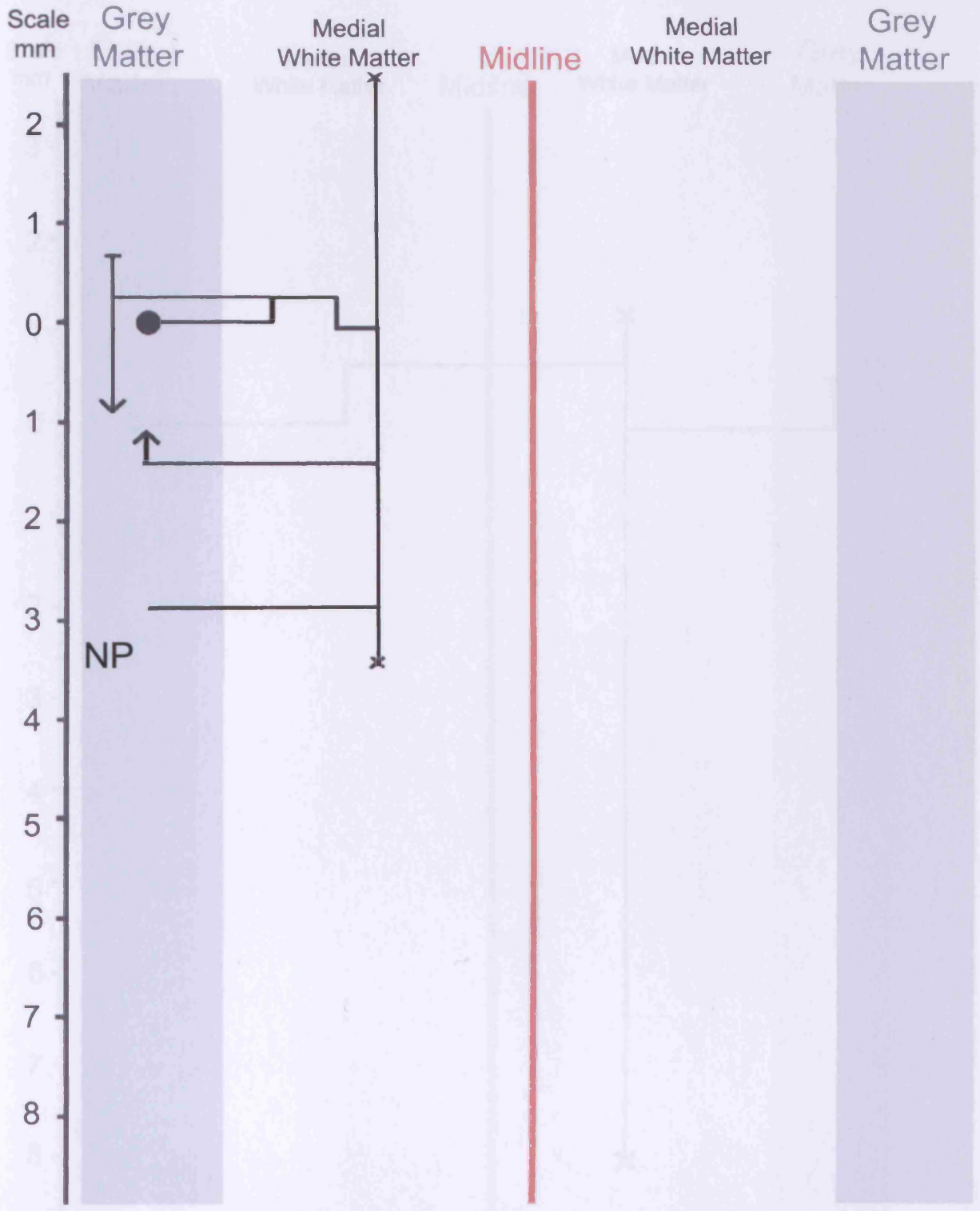

J: Cell B28E

Note that two axon collaterals overlap in the rostro-caudal axis, although the full extent of their overlap is unclear (represented by arrows)

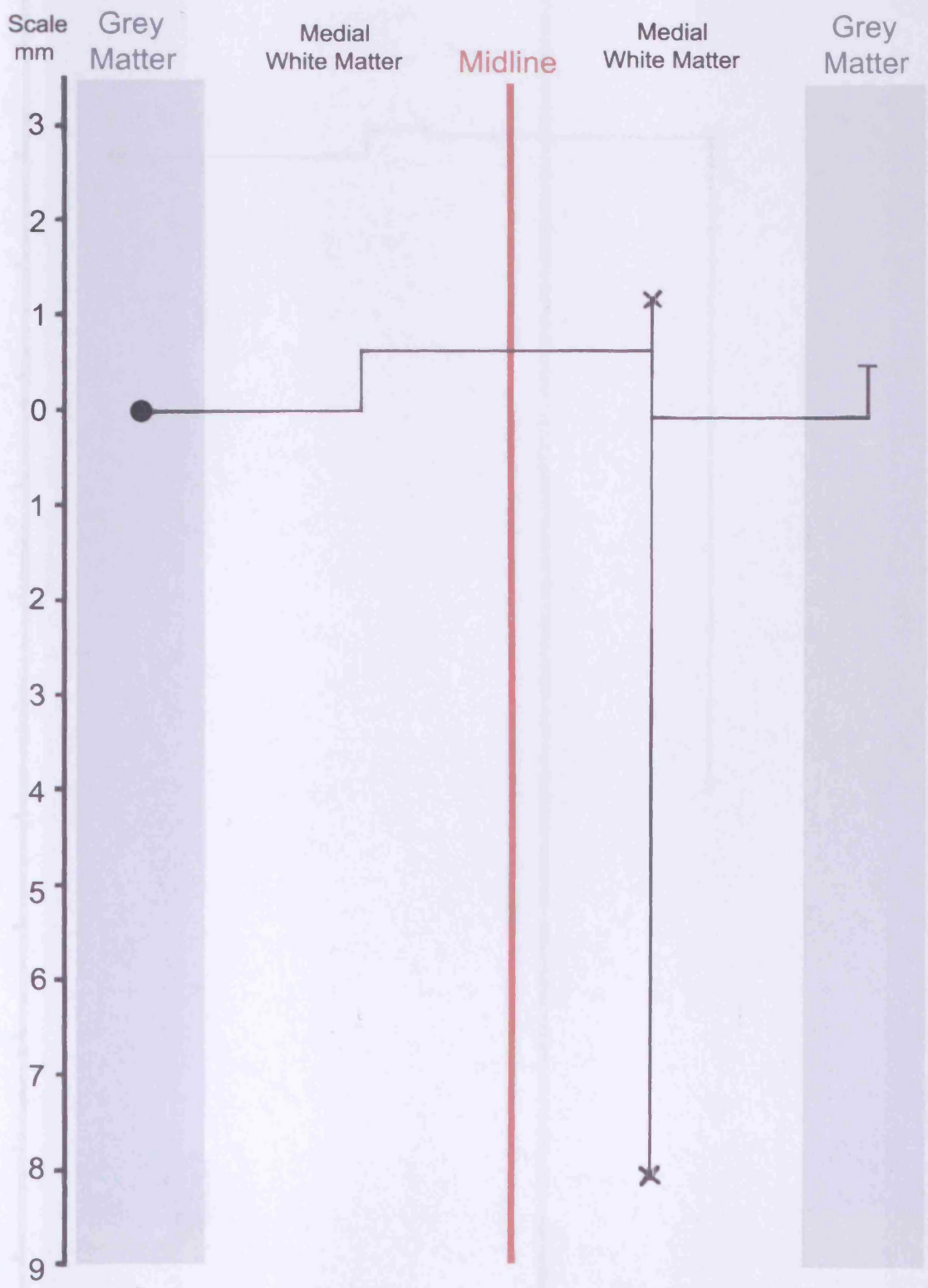
Scale
mm
Grey
Matter
Medial
White Matter
Midline
Medial
White Matter
Grey
Matter
3
2
1
0
1
2
3
4
5
6
7
8
9

K: Cell B29D

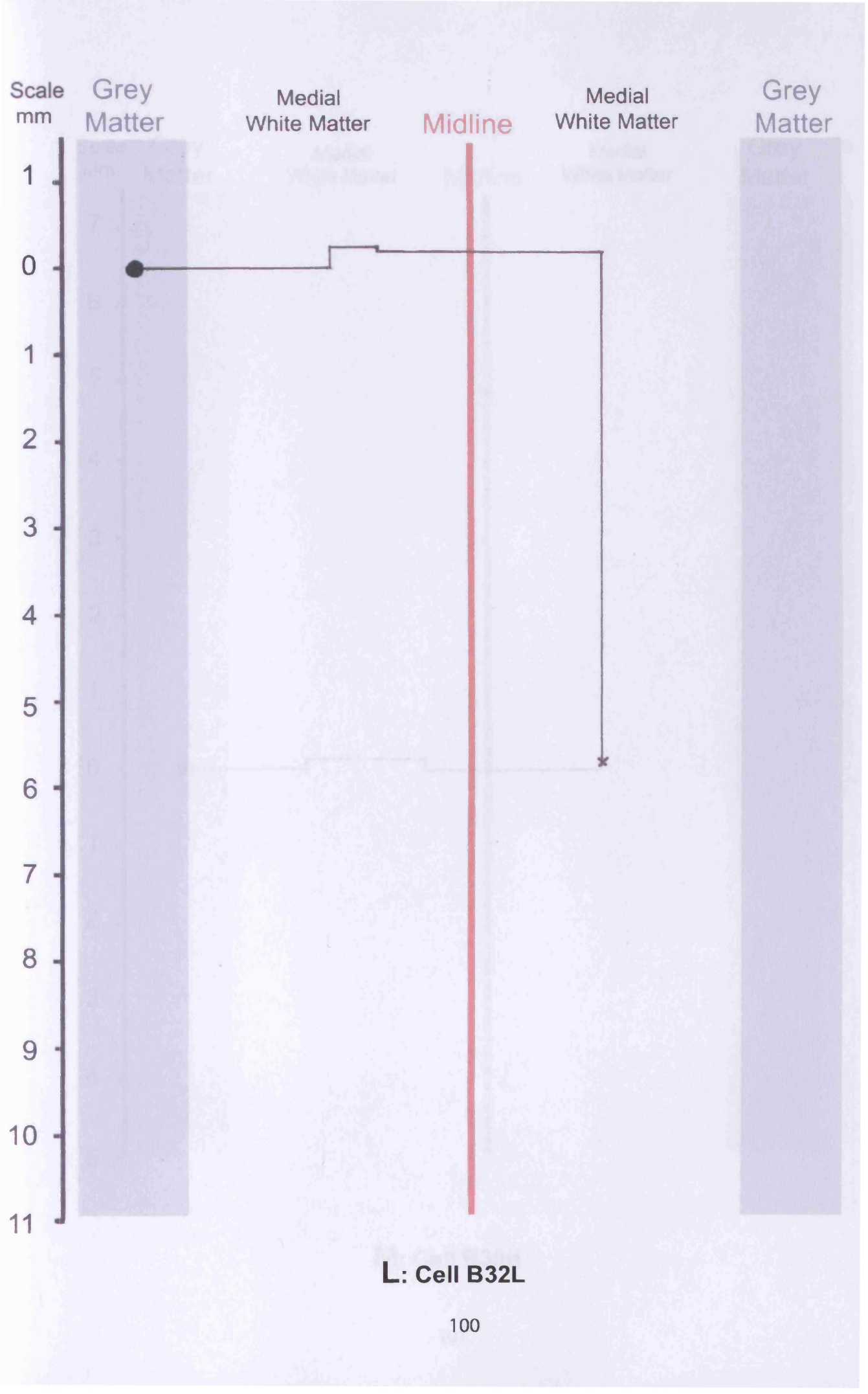
Scale
mm
Grey
Matter
Medial
White Matter
Midline
Medial
White Matter
Grey
Matter
1
0
1
2
3
4
5
6
7
8
9
10
11

L: Cell B32L

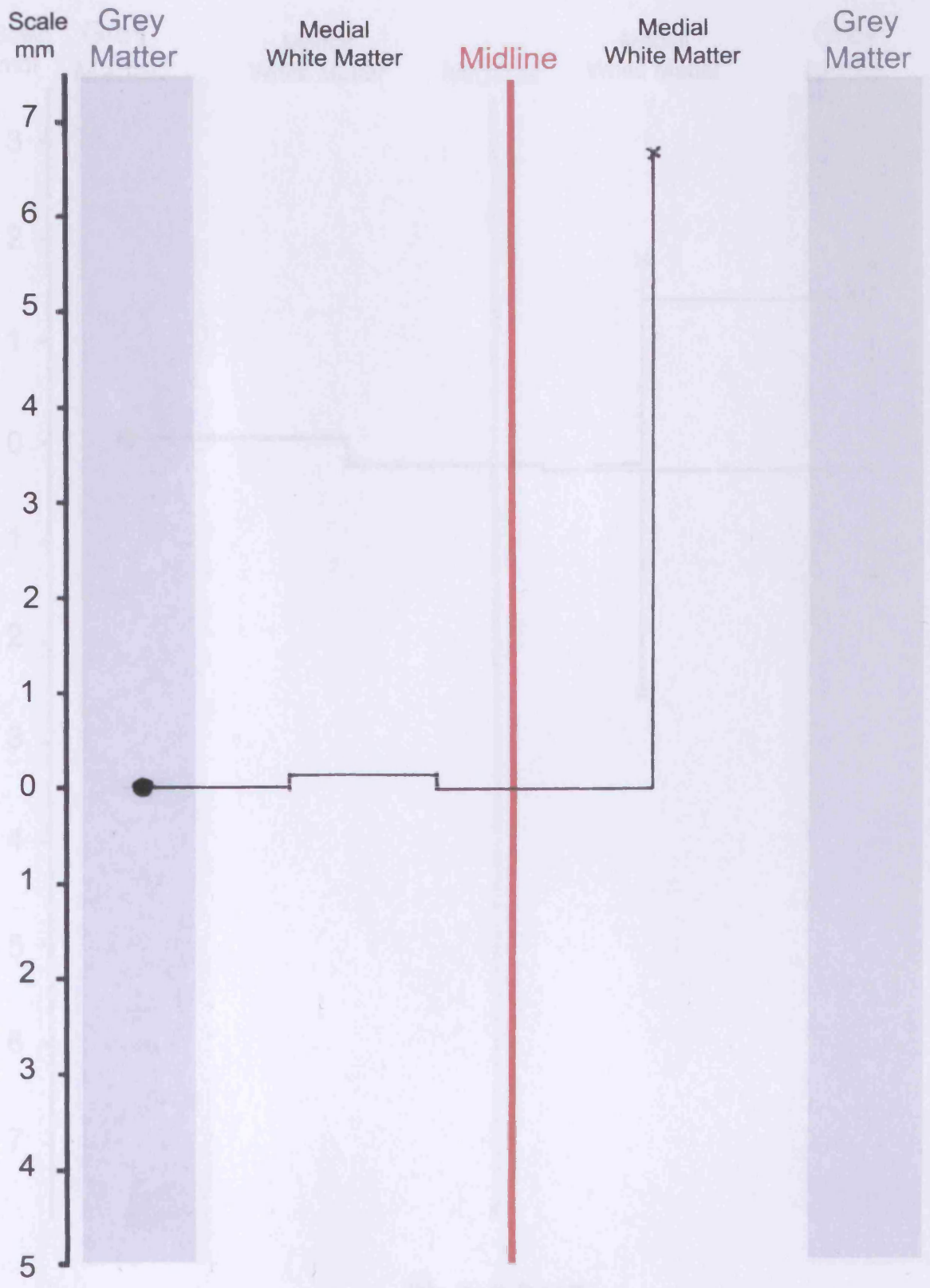
Scale
mm
Grey
Matter
Medial
White Matter
Midline
Medial
White Matter
Grey
Matter
7
6
5
4
3
2
1
0
1
2
3
4
5

M: Cell B39H

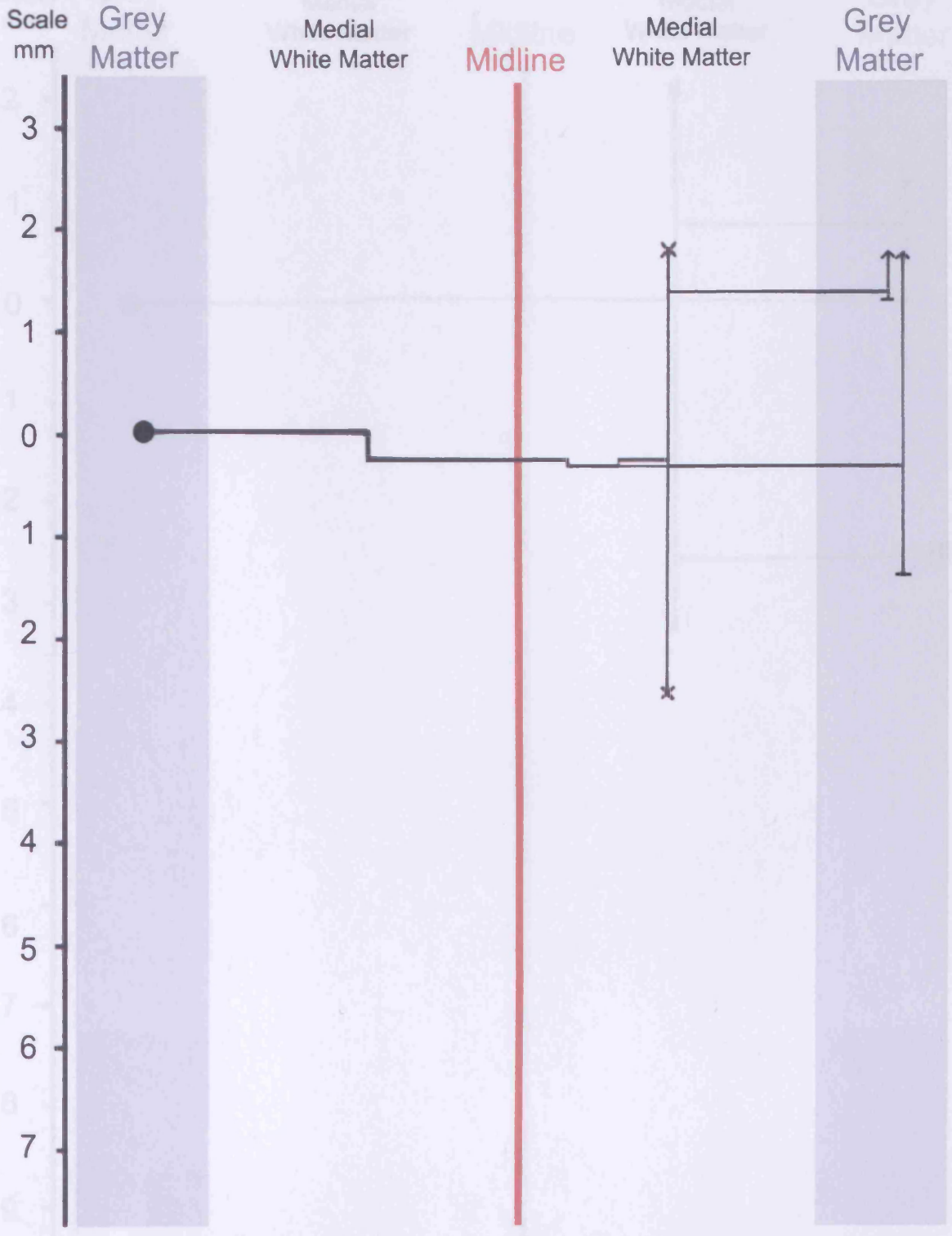

N: Cell B41Z

Note that the two collaterals overlap although their total extent rostrally is unknown (due to the end of the block of spinal cord cut).

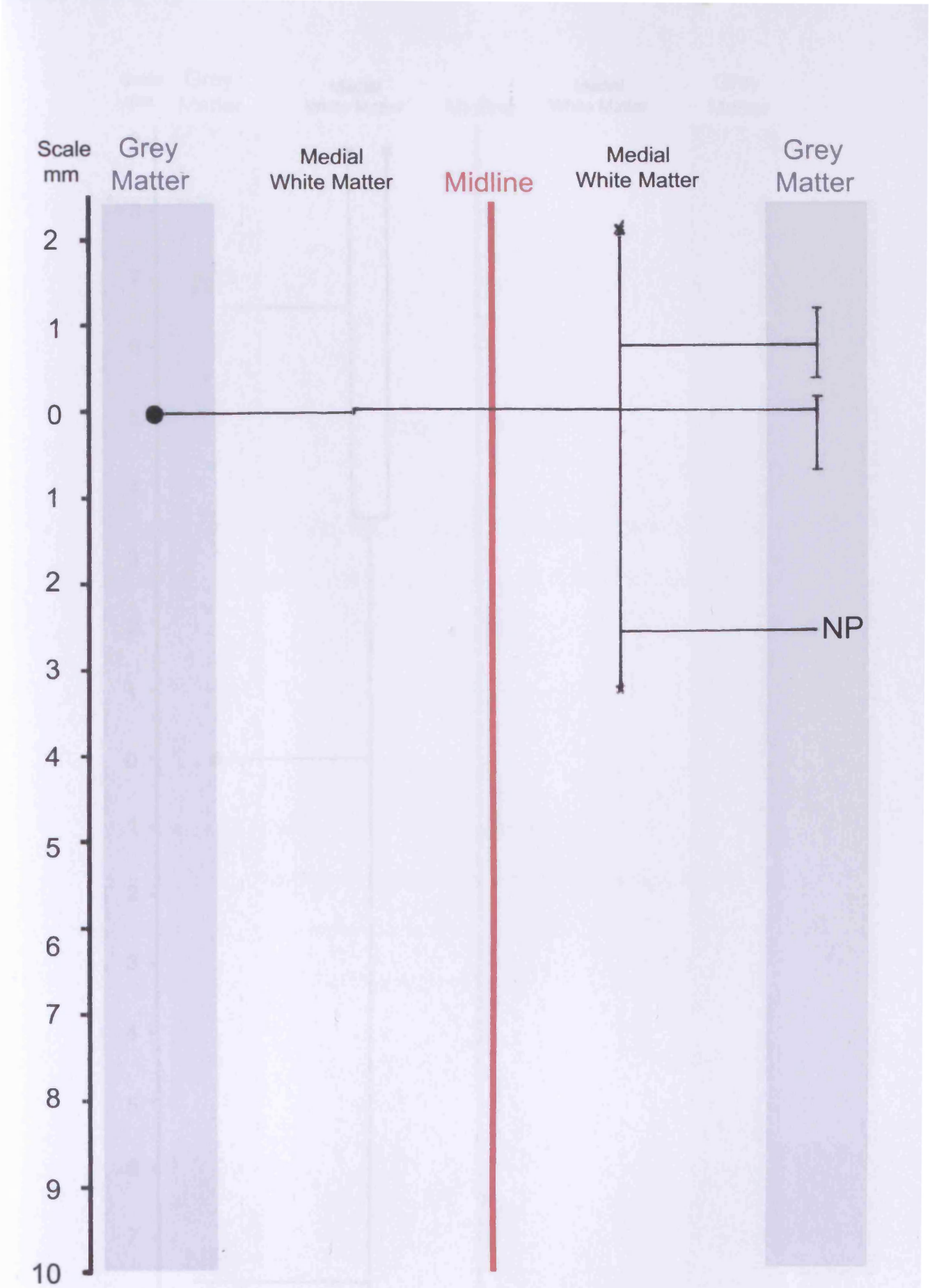
Scale
mm
Grey
Matter
Medial
White Matter
Midline
Medial
White Matter
Grey
Matter
2
1
0
1
2
3
4
5
6
7
8
9
10
NP

O: Cell B42N

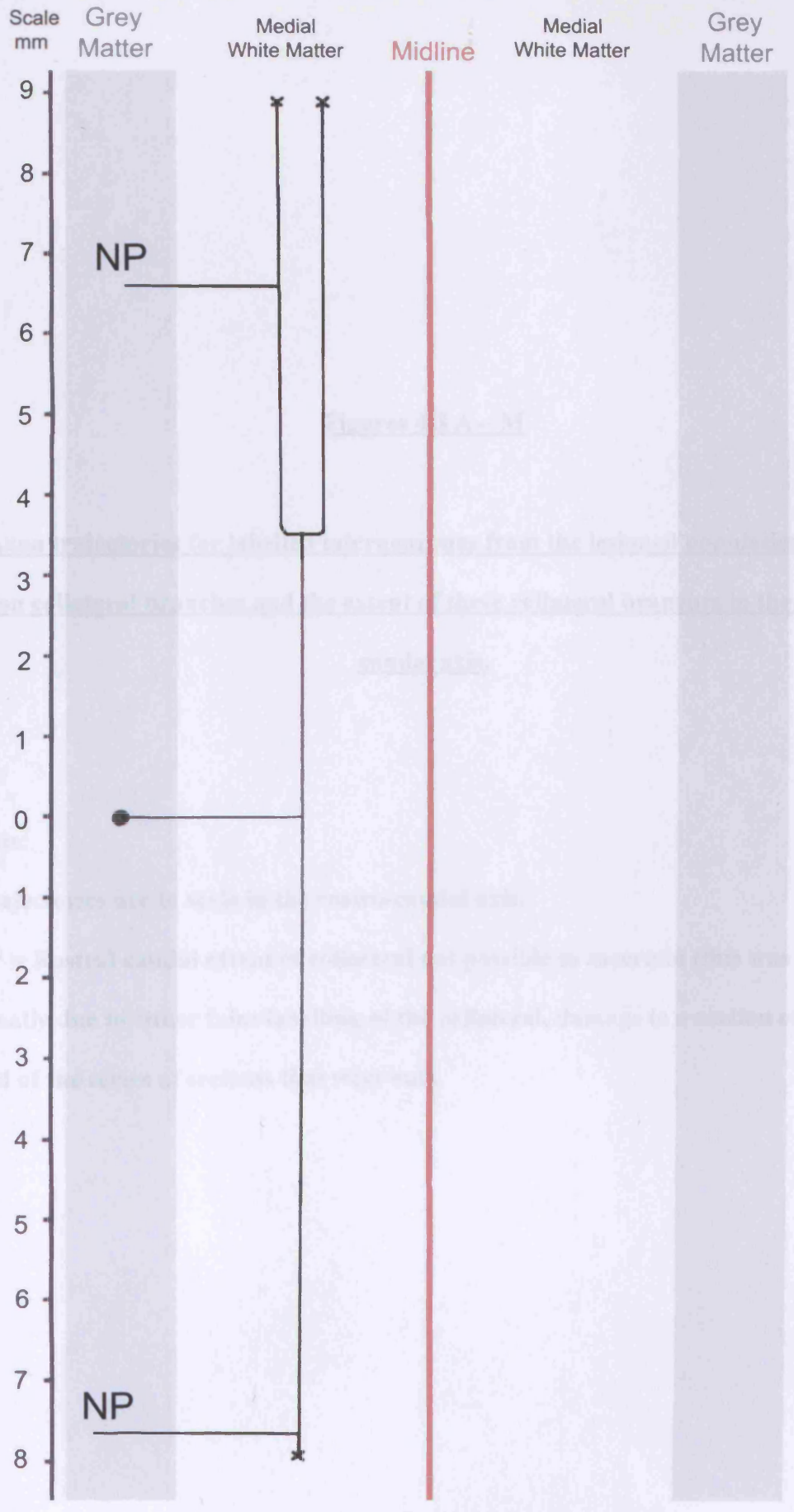
Scale mm
Grey Matter
Medial White Matter
Midline
Medial White Matter
Grey Matter
9
8
7
6
5
4
3
2
1
0
1
2
3
4
5
6
7
8
NP
NP

P: Cell B48H

Figures 4.3 A – M

Axon trajectories for labelled interneurones from the lesioned population with axon collateral branches and the extent of these collateral branches in the rostro-caudal axis.

Note:

Trajectories are to scale in the rostro-caudal axis.

NP = Rostral caudal extent of collateral not possible to ascertain (this was usually due to either faint labelling of the collateral, damage to a section or the end of the series of sections that were cut).

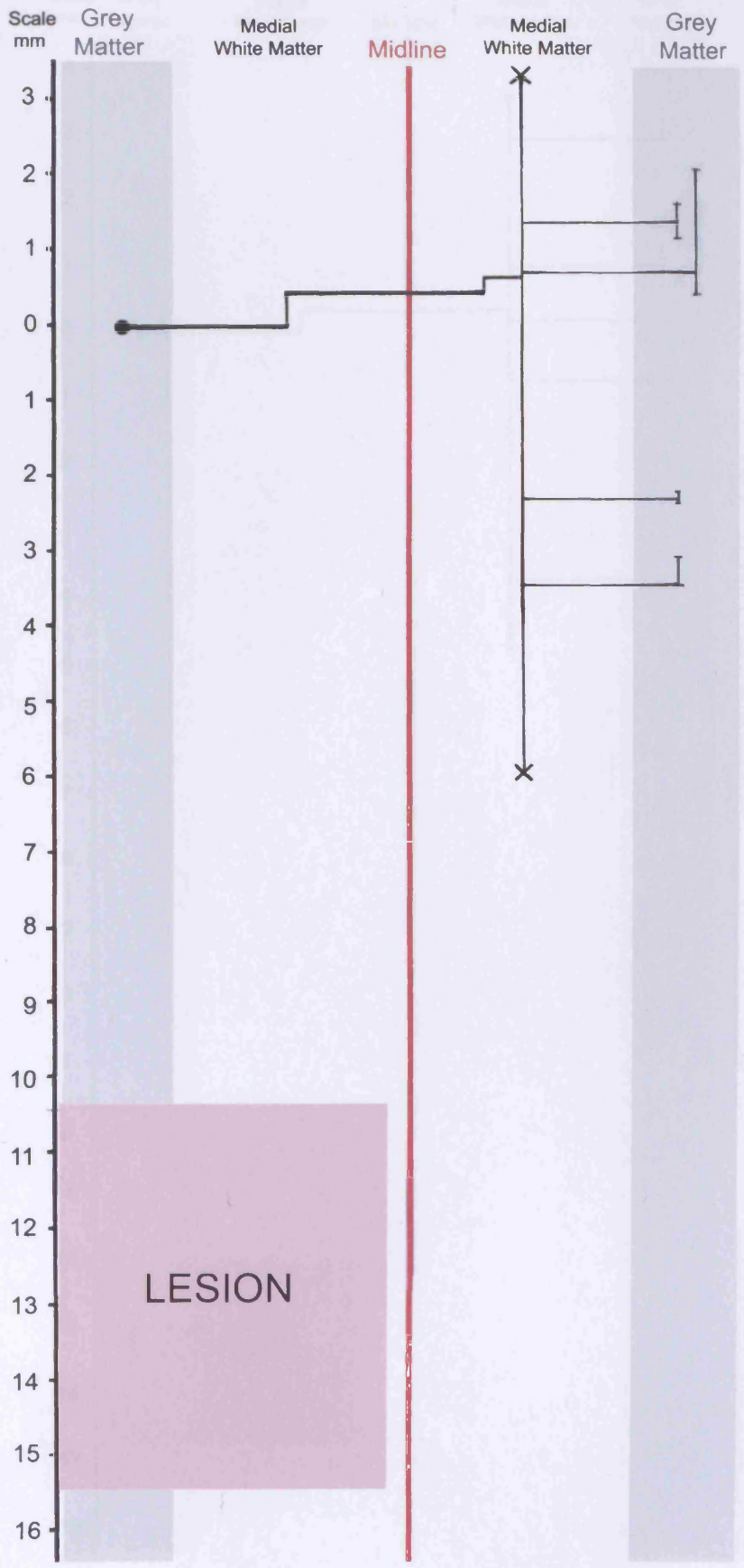
Scale mm
Grey Matter
Medial White Matter
Midline
Medial White Matter
Grey Matter
3
2
1
0
1
2
3
4
5
6
7
8
9
10
11
12
13
14
15
16
LESION

A: Cell B68F

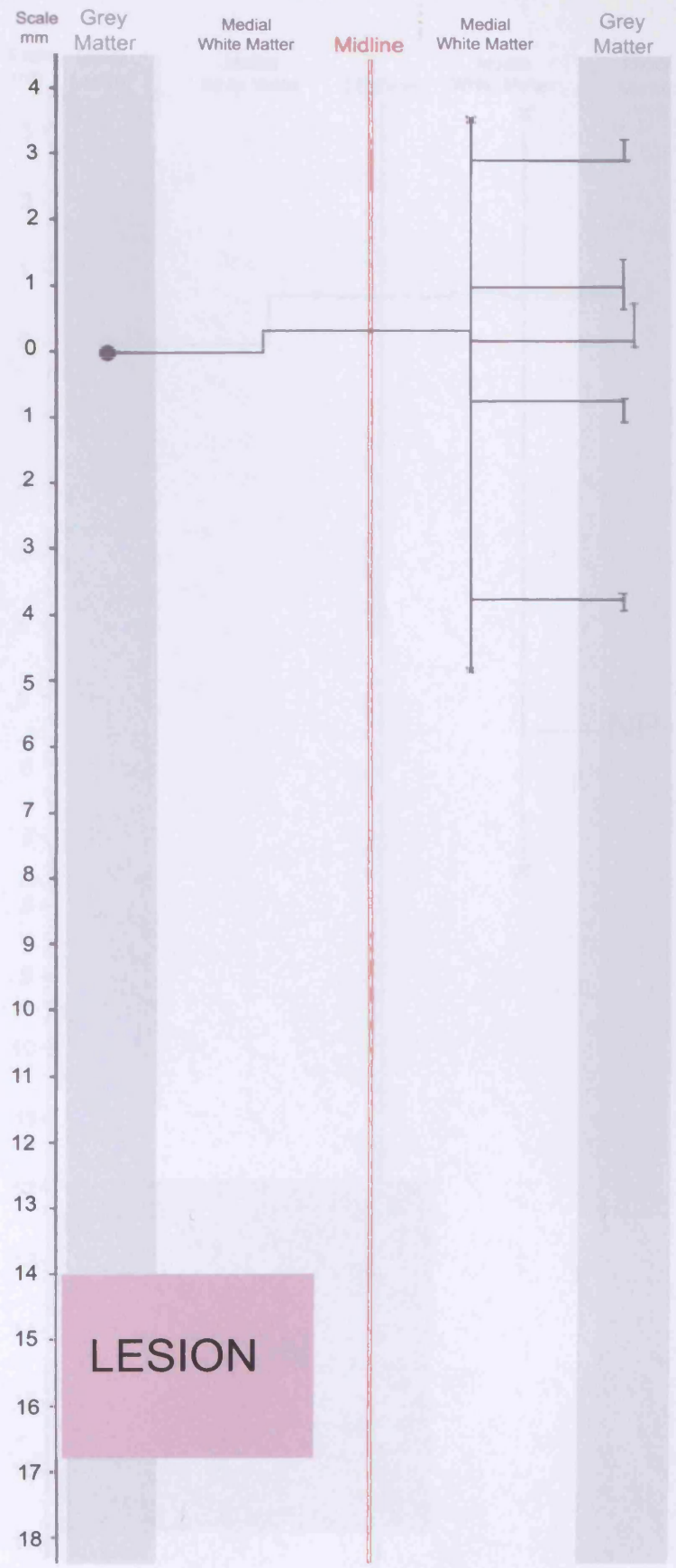
Scale mm
Grey Matter
Medial White Matter
Midline
Medial White Matter
Grey Matter
4
3
2
1
0
1
2
3
4
5
6
7
8
9
10
11
12
13
14
15
16
17
18
LESION

B: Cell B73J

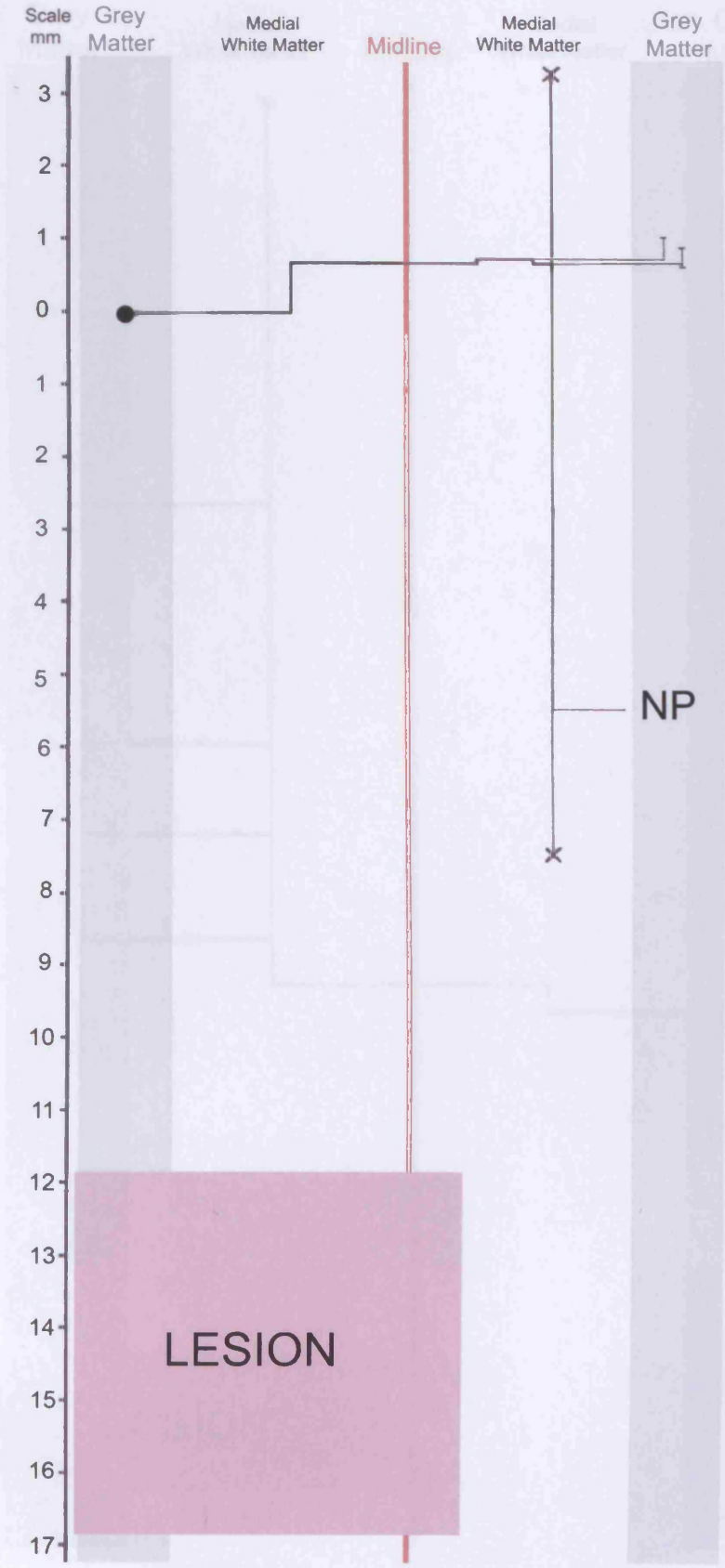
Scale mm
Grey Matter
Medial White Matter
Midline
Medial White Matter
Grey Matter
3
2
1
0
1
2
3
4
5
6
7
8
9
10
11
12
13
14
15
16
17
NP
LESION

C: Cell B74D

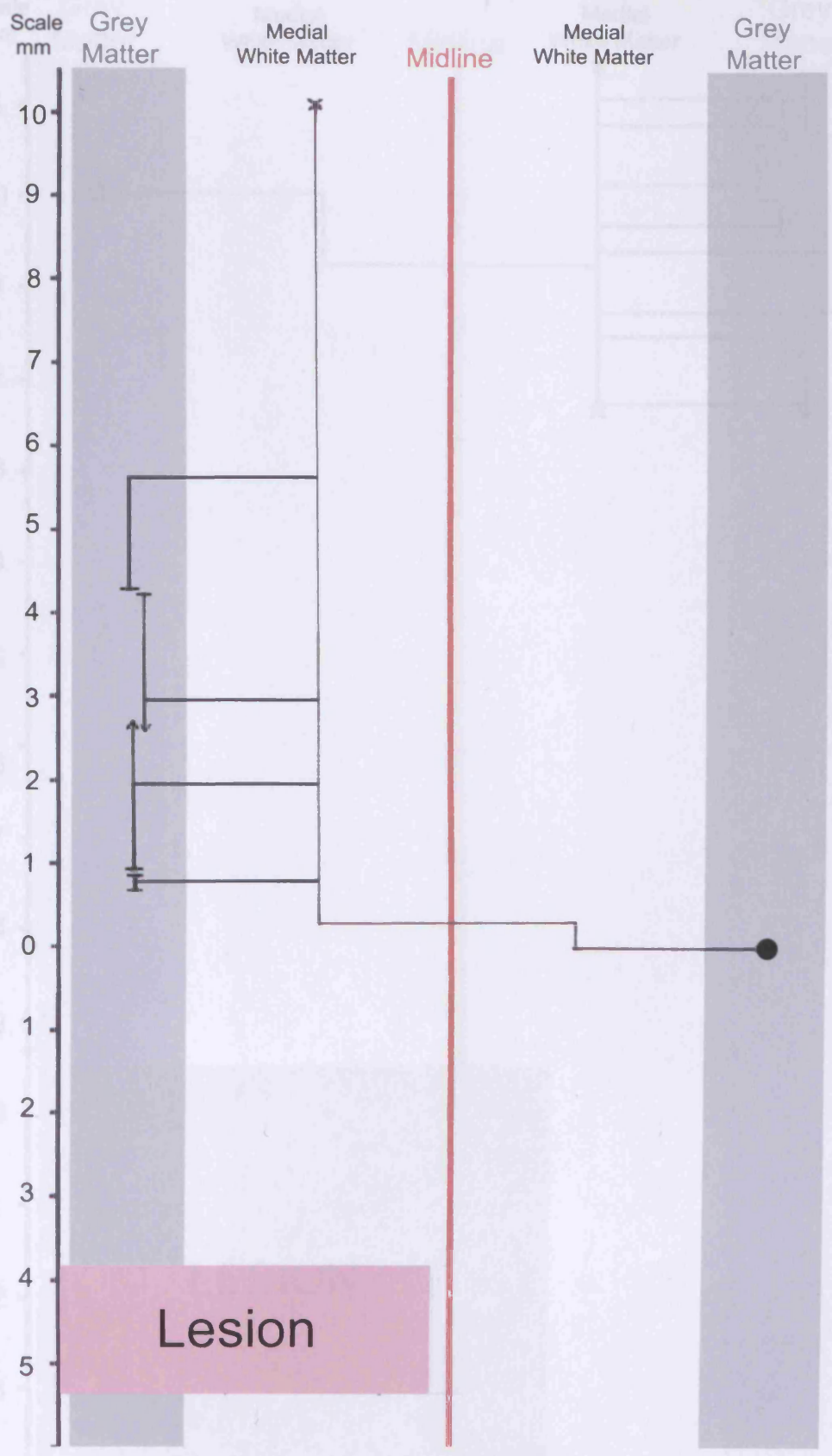

D: Cell B79l

Rostro-caudal extent of two collaterals hard to confirm due to overlapping of the collaterals with each other.

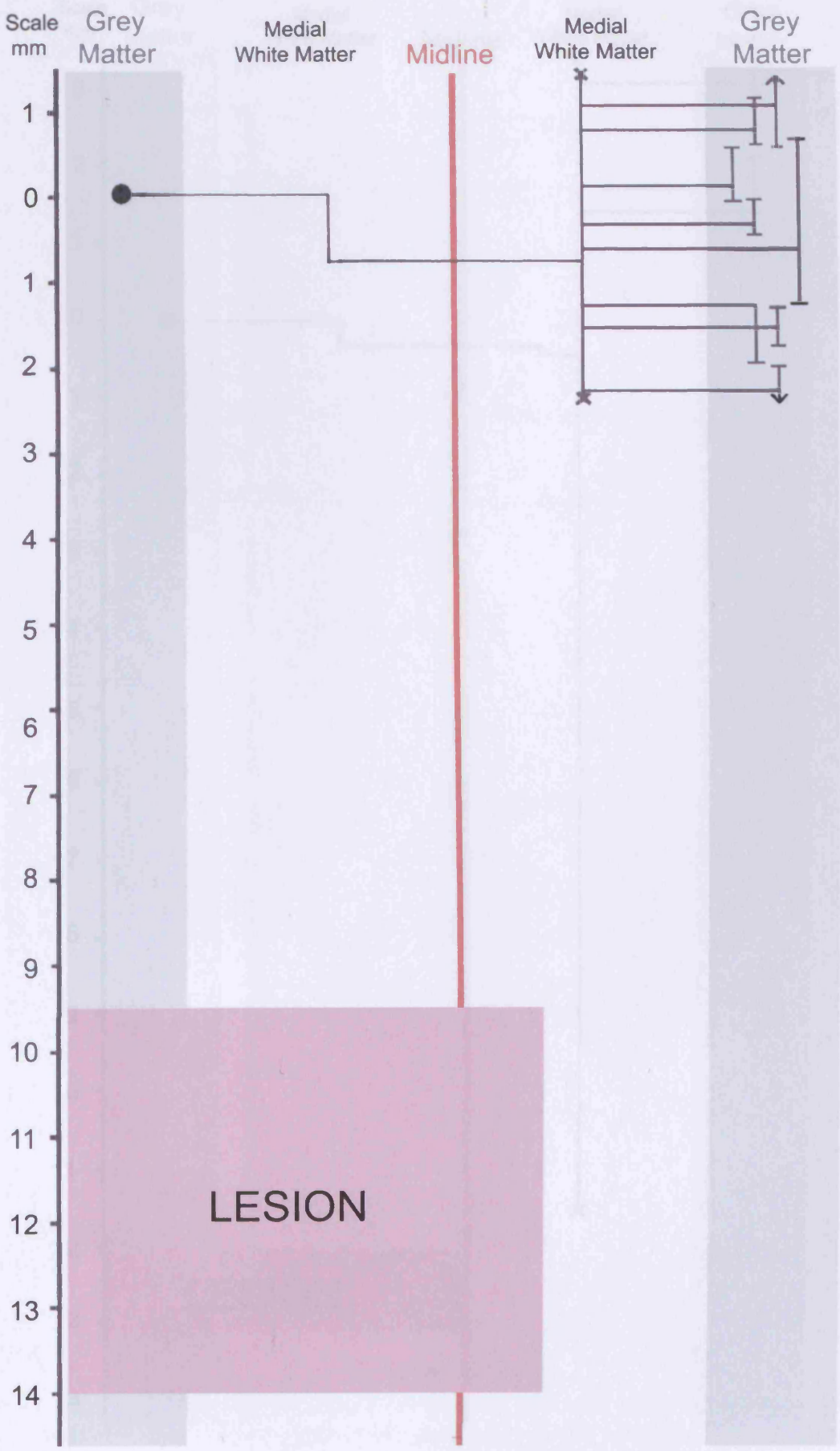
Scale mm
Grey Matter
Medial White Matter
Midline
Medial White Matter
Grey Matter
1
0
1
2
3
4
5
6
7
8
9
10
11
12
13
14
LESION

E: Cell B88F

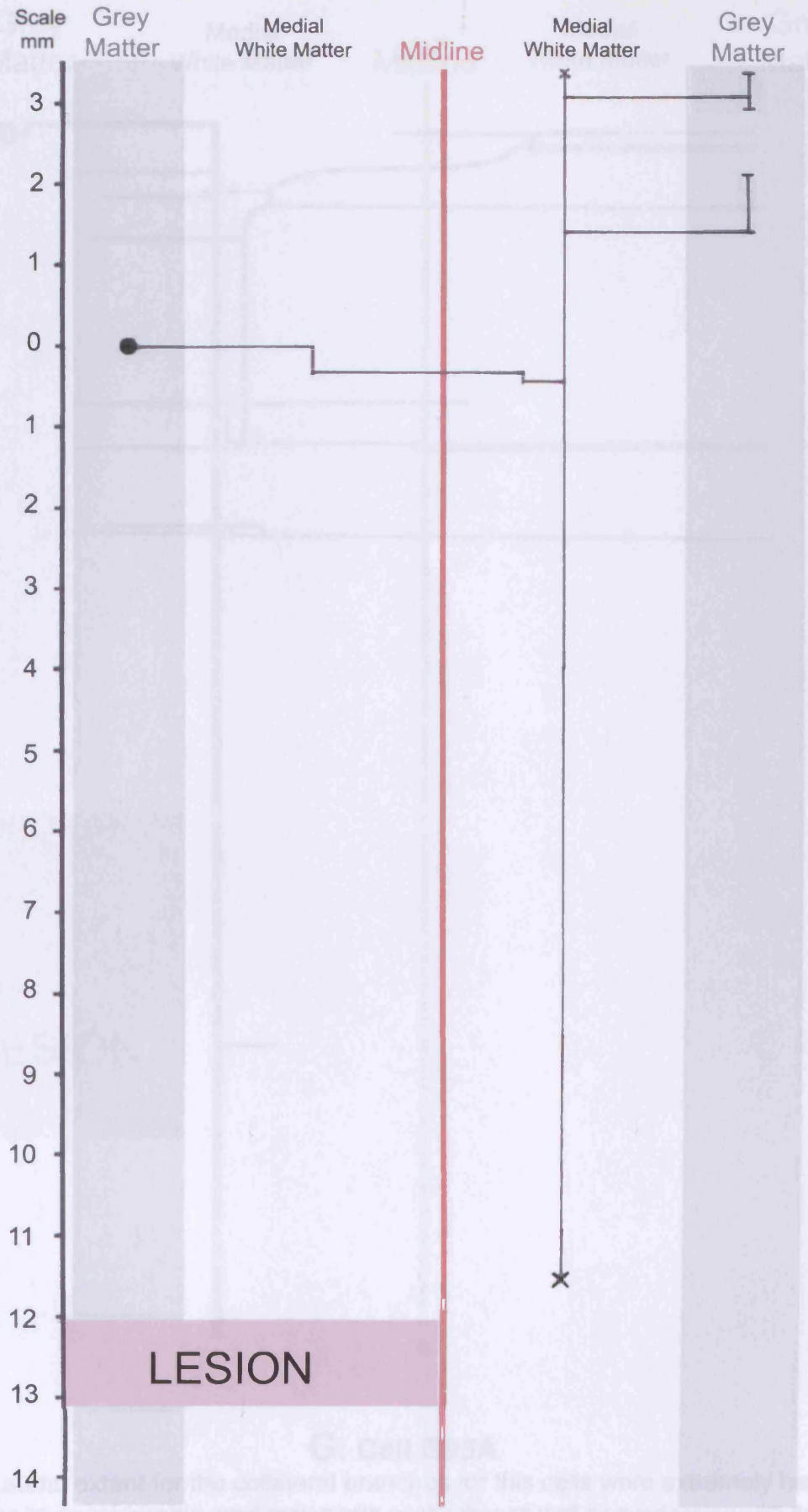
Scale mm
Grey Matter
Medial White Matter
Midline
Medial White Matter
Grey Matter
3
2
1
0
1
2
3
4
5
6
7
8
9
10
11
12
13
14
LESION

F: Cell B89D

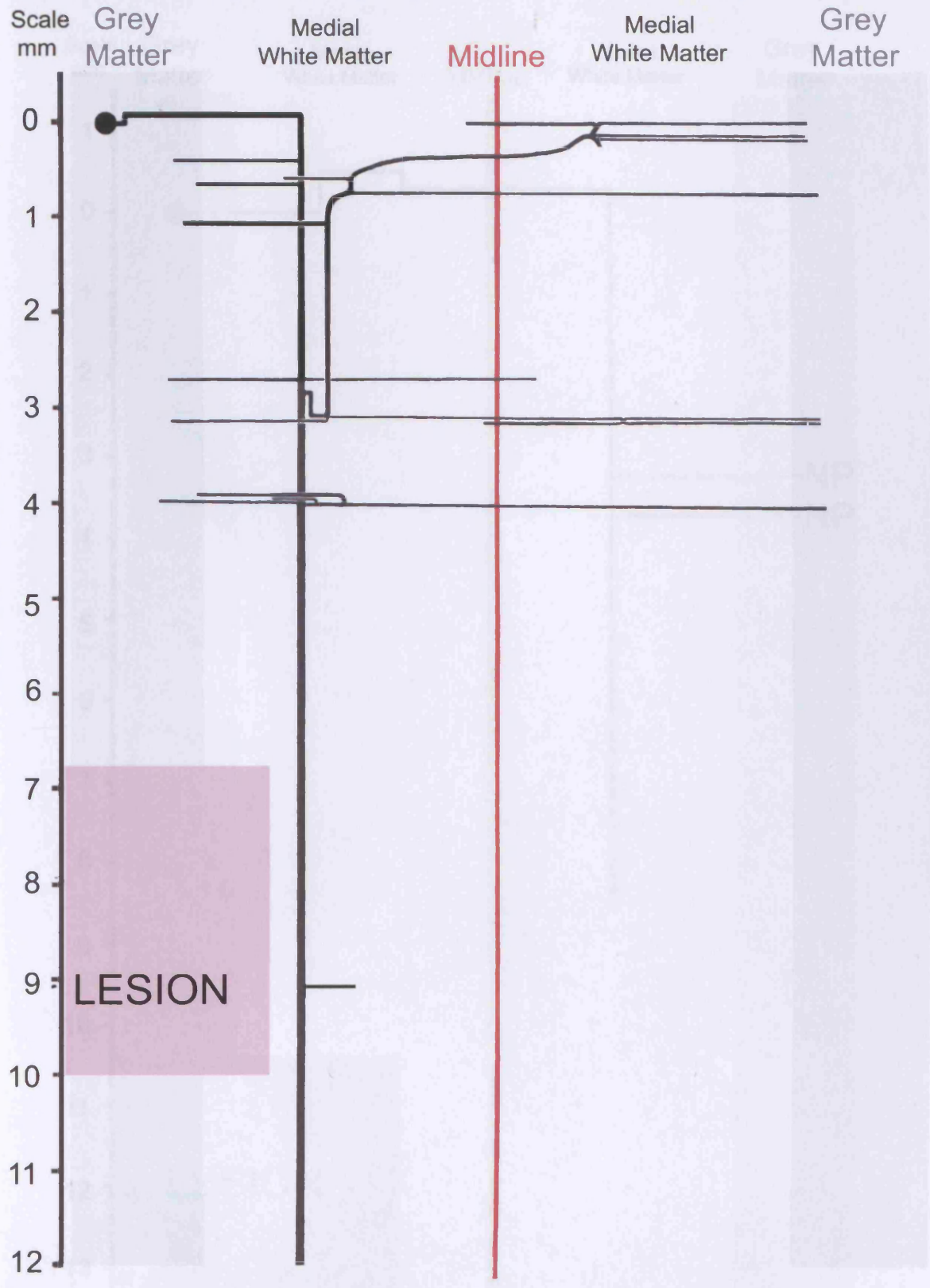

G: Cell B95A

The rostro-caudal extent for the collateral branches for this cells were extremely hard to ascertain due to considerable overlapping with each other as well as overlapping with its complex dendritic tree. Also some collaterals branches occured where the peice of spinal cord was cut into 2 peices prior to sectioning.

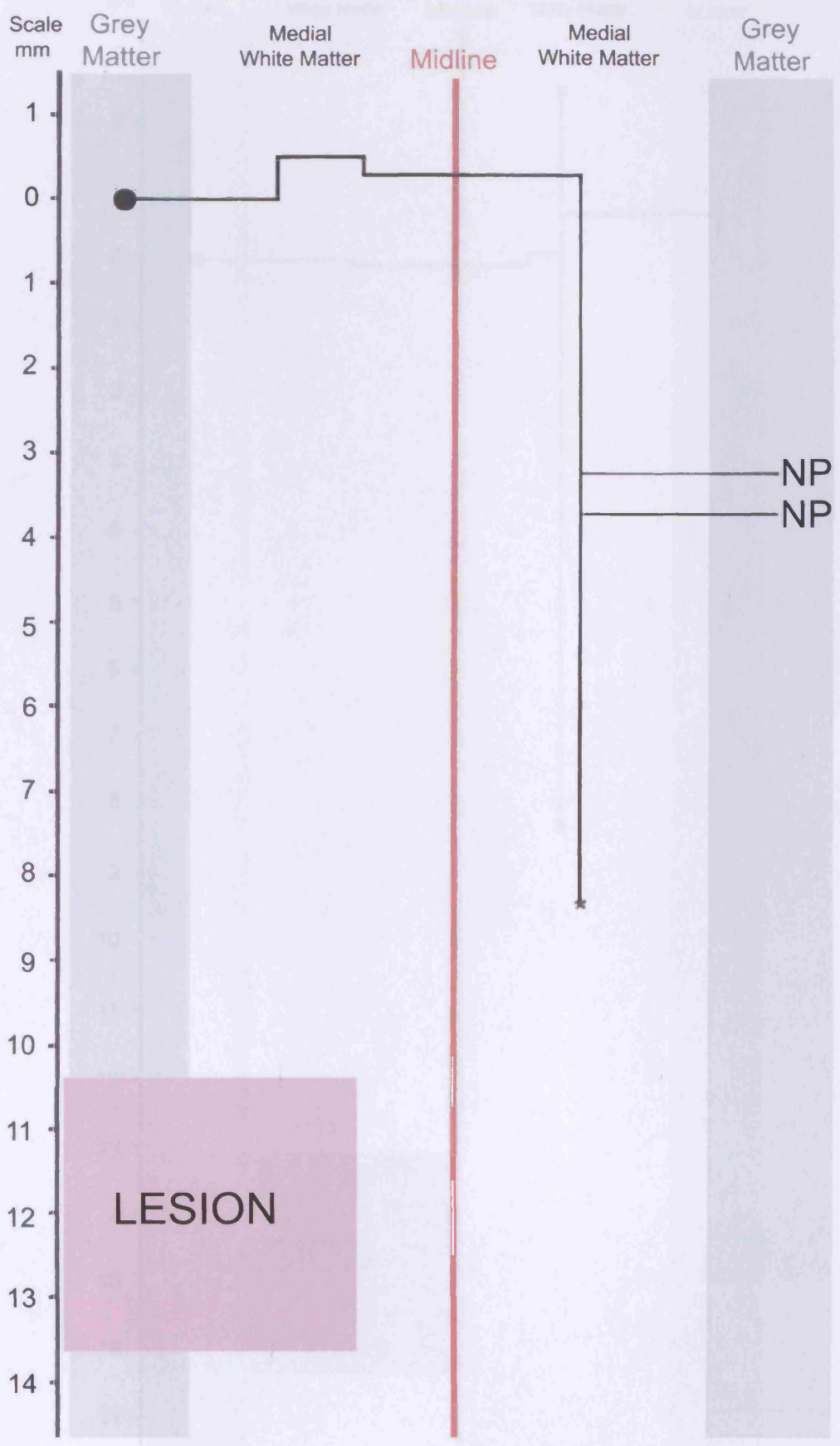
Scale mm
Grey Matter
Medial White Matter
Midline
Medial White Matter
Grey Matter
1
0
1
2
3
4
5
6
7
8
9
10
11
12
13
14
NP
NP
LESION

H: Cell B95C

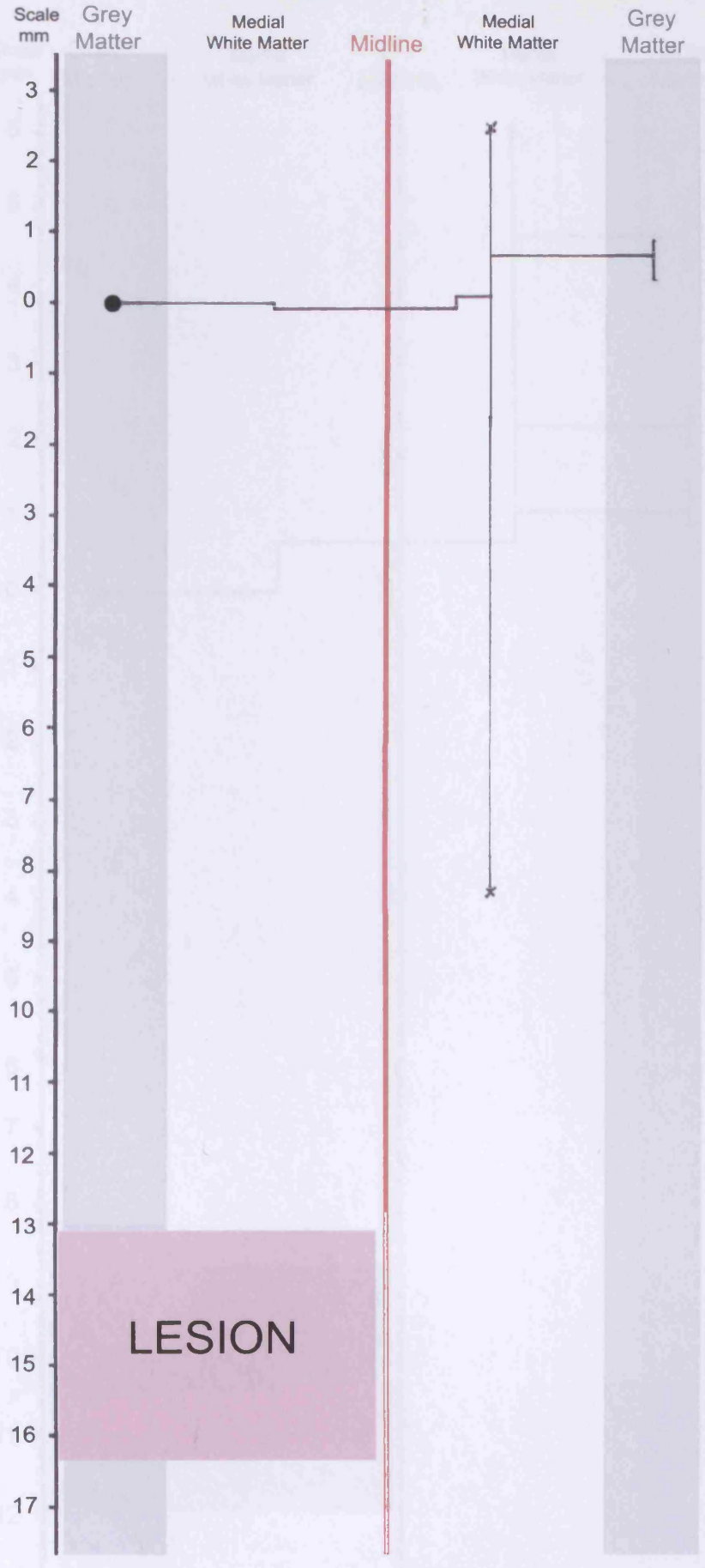
Scale mm
Grey Matter
Medial White Matter
Midline
Medial White Matter
Grey Matter
3
2
1
0
1
2
3
4
5
6
7
8
9
10
11
12
13
14
15
16
17
LESION

I: Cell B96A

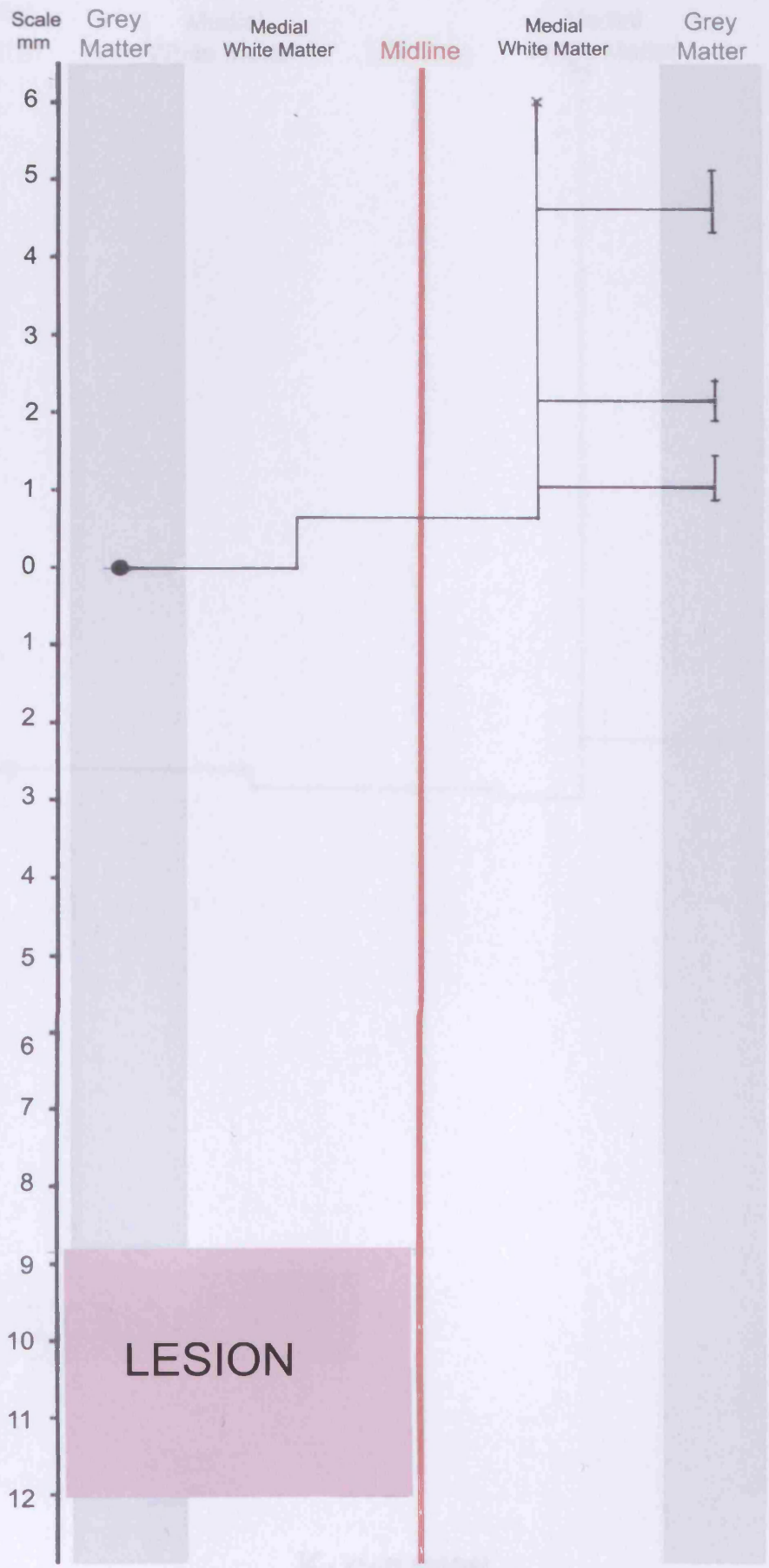
Scale mm
Grey Matter
Medial White Matter
Midline
Medial White Matter
Grey Matter
6
5
4
3
2
1
0
1
2
3
4
5
6
7
8
9
10
11
12
LESION

J: Cell B96F

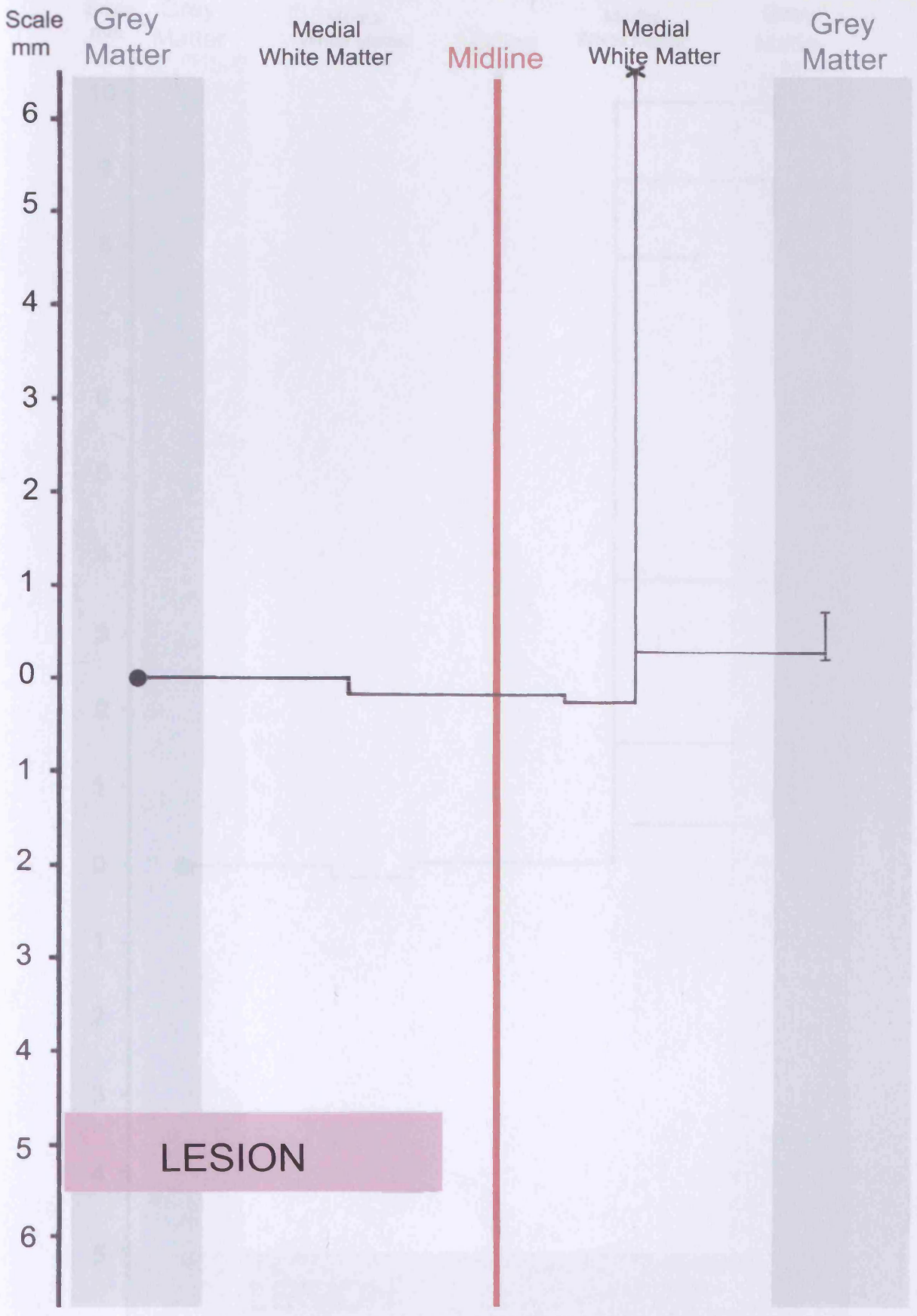
Scale mm
Grey Matter
Medial White Matter
Midline
Medial White Matter
Grey Matter
6
5
4
3
2
1
0
1
2
3
4
5
6
LESION

K: Cell B99N

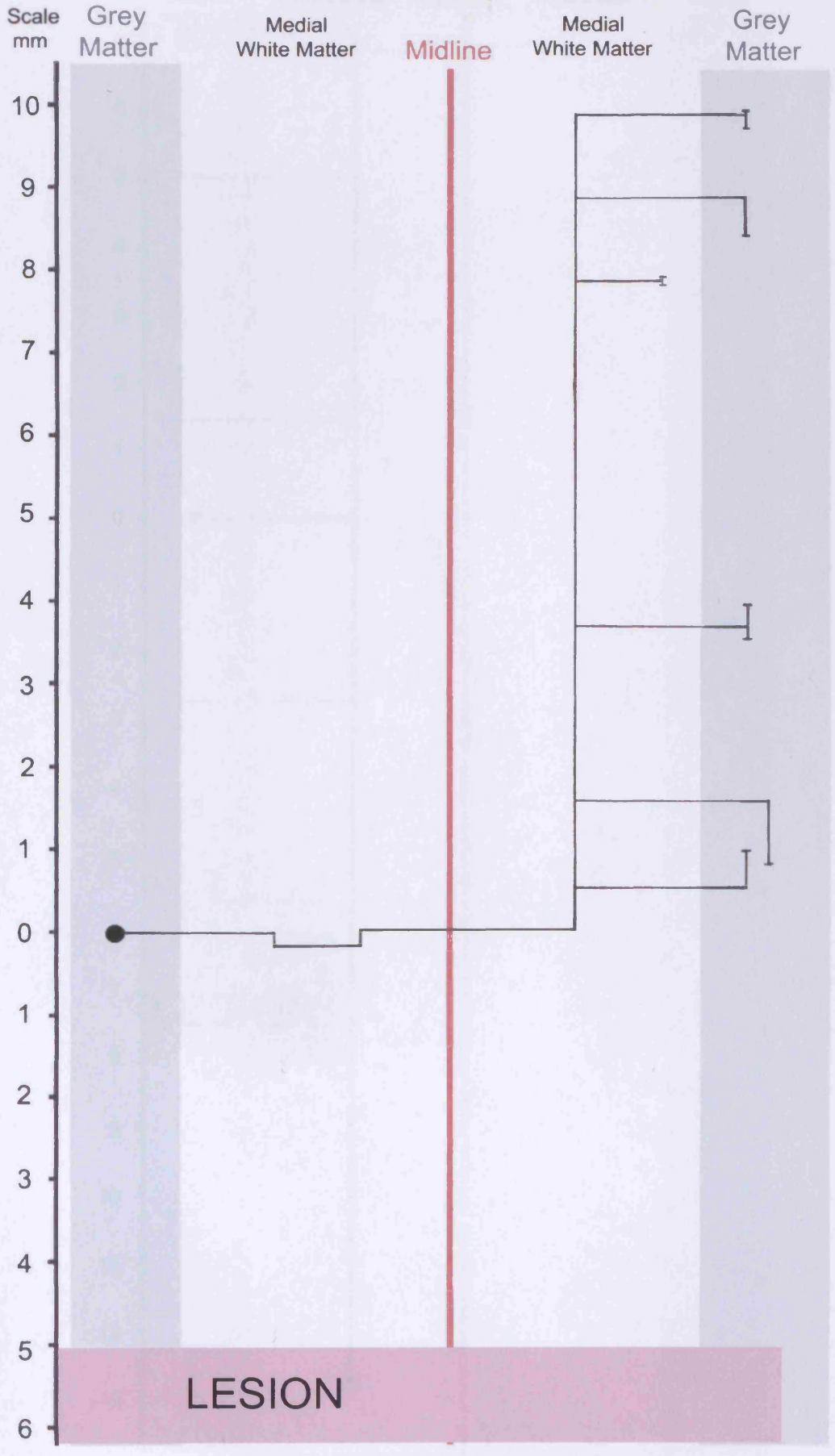
Scale mm
Grey Matter
Medial White Matter
Midline
Medial White Matter
Grey Matter
10
9
8
7
6
5
4
3
2
1
0
1
2
3
4
5
6
LESION

L: Cell C1E

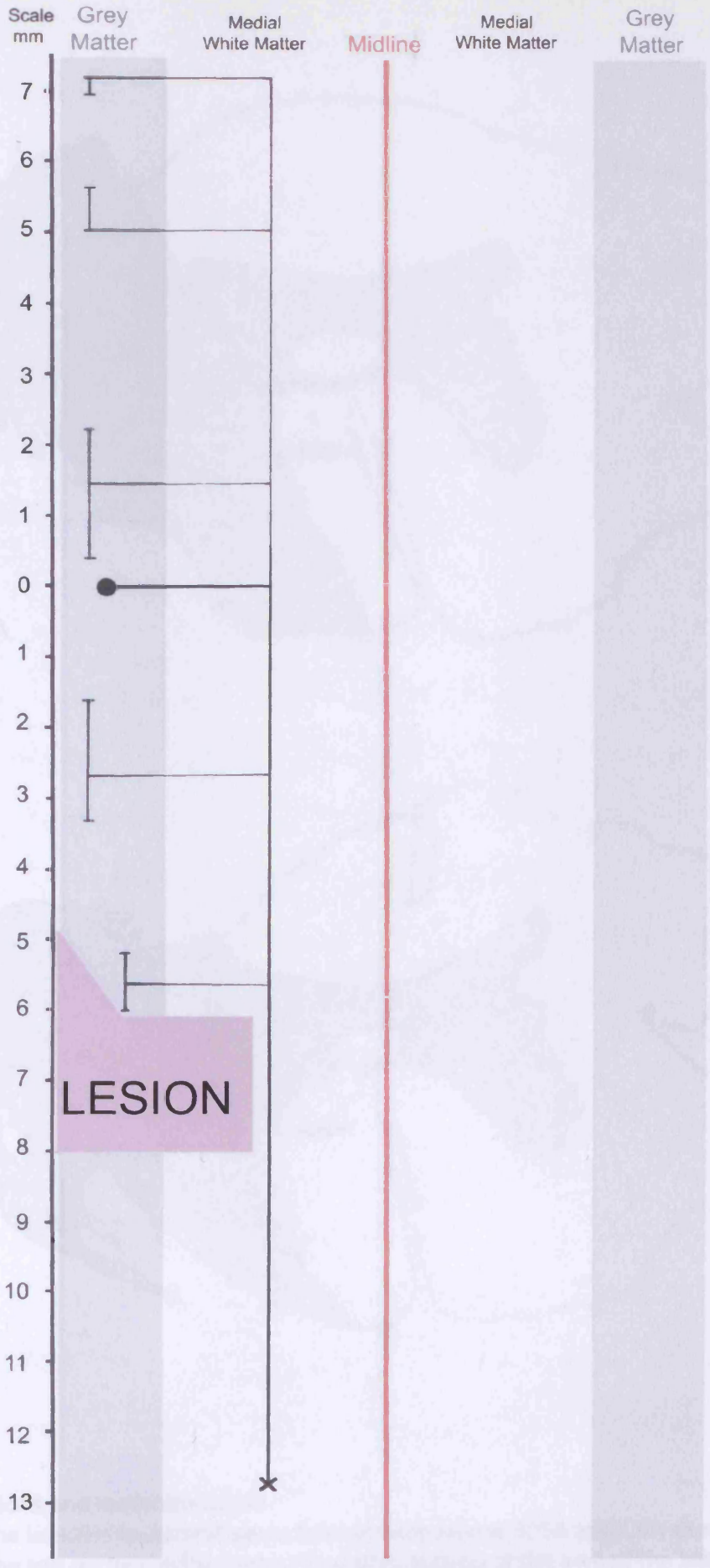
Scale mm
Grey Matter
Medial White Matter
Midline
Medial White Matter
Grey Matter
7
6
5
4
3
2
1
0
1
2
3
4
5
6
7
8
9
10
11
12
13
LESION

M: Cell C4A

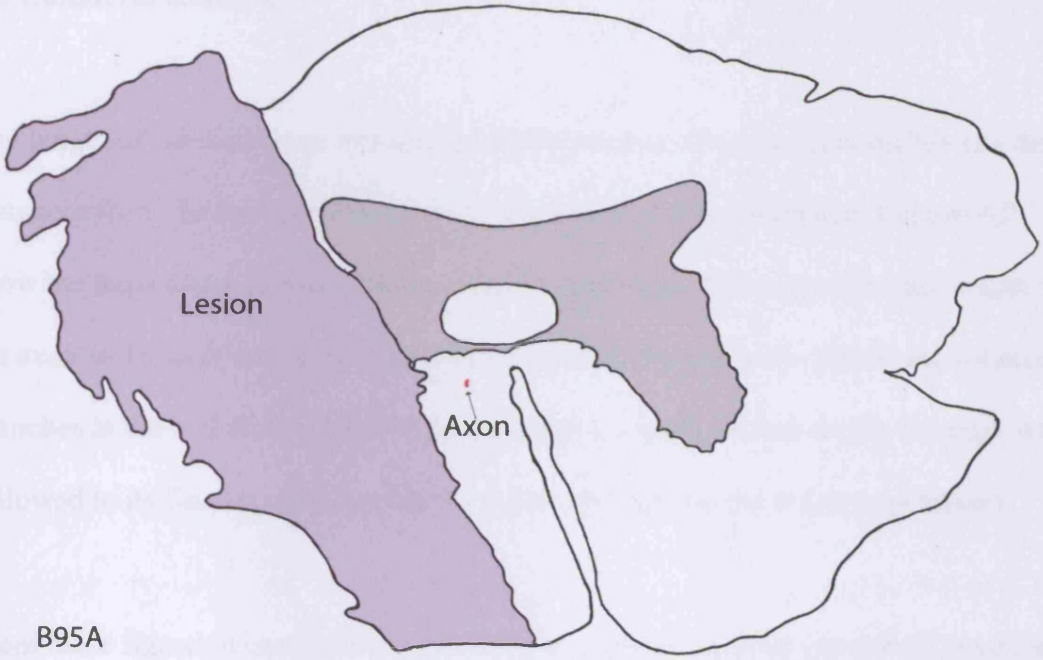

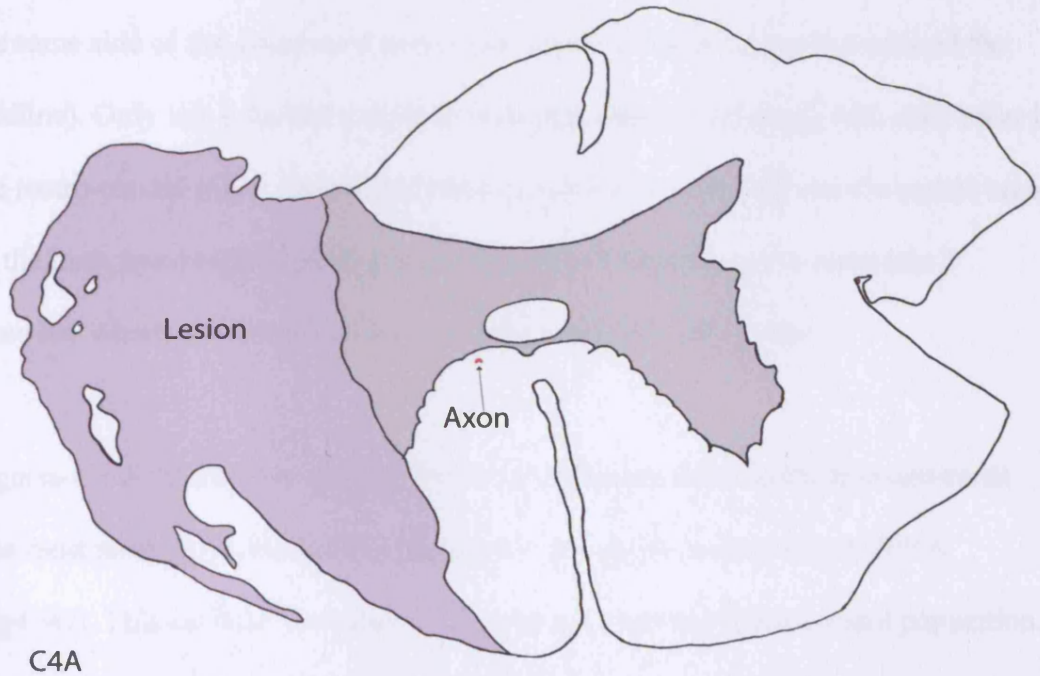

Figure 4.4 Lesions and ipsilateral axons
These show the labelled ipsliateral axons from interneurones B95A and C4A showing the axon travelling in the top of the medial ventral funiculus outside of the area of the lesion. This confirms that these cells were not axotomised.

4.1 Collateral Branches

The length of labelled axon was noted and the number of collateral branches and their distances from the soma so that the two populations can be compared. Figures 4.2 show the trajectories of axons in the control population. These represent the length of the axon as far as it was considered stained reliably enough to be able to see collateral branches at the end of the pieces of cord sampled (represented as an X). No axon was followed to its final termination (this was also the case for the lesion population).

From these figures it can be observed that cells from the control population possessed either one contralateral axon or one ipsilateral axon, for which up to 4 collateral branches were identified. These collateral branches terminated in the grey matter on the same side of the spinal cord as it arose (i.e. no collateral branches crossed the midline). Only two cells had collateral branches which overlapped with each other in the rostro-caudal plane. One usual feature observed on cell B48 was the rostral branch of the axon apparently branching approximately 3.5mm from the soma into 2 branches which continued to travel rostrally alongside one another.

Figures 4.3 A-M illustrate the trajectories of the axons filled in the lesioned cords. The most striking deviation from the normal group was shown by cell B95A (fig4.3G). This cell had a number of features not observed in the control population. The first of these is the presence of a thick axonal branch arising just under 3 mm from the soma. This branch is thicker in diameter than the finer collaterals, being similar to the main stem axon. It ran rostrally alongside the main axon for some distance giving off collateral branches of its own, terminating in the contralateral grey

matter including boutons, before it finally crossed the midline itself where it terminated. Thus a second unusual feature is the presence of collateral branches crossing the midline to the ventral horn contralateral to their origin. No cells in the control population had axons with both ipsilateral and contralateral collateral branches. A third unusual feature of the collaterals of B95A is the overlapping of the areas of termination of collateral branches along the rostro-caudal axis. This was observed in 7/13 of the lesioned population. In contrast this was observed only 2/17 in the control population (n =17). Taking only cells possessing at least 2 collateral branches and using Chi-Square test this difference was significant at the $p<0.05$ level.

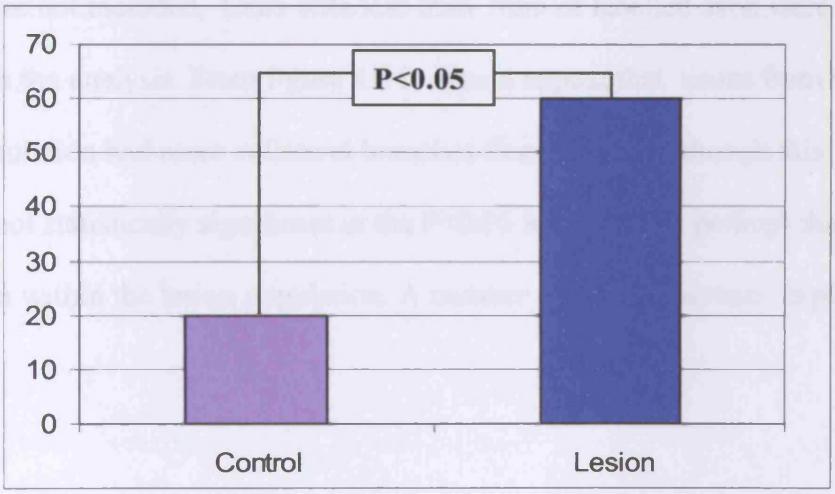

Figure 4.5 Percentage of those axons possessing at least 2 collateral branches which have collaterals which overlap along the rostral caudal axis

Also observed on B95A and C4A are what shall be referred to as micro-collaterals. These were extremely short branches of emanating from the main axon (figure 4.20b). These were not observed on axons of cells from the control population suggesting that that may represent sprouting. They may perhaps represent the beginning of new axon

collaterals, although these spikes do not appear to terminate as growth cone-like structures so they may represent aborted sprouts.

Obviously the axon of B95A had more collateral branches than usual. This would also appear to be the case for some of the other cells from the lesion condition, although not so immediately obvious. One possibility is that these cells from the lesioned cord may have been more successfully labelled than those in the control population and so the axons labelled for longer. To control for this the number of collaterals was calculated for the first 3 mm of labelled axon only. For those with both ascending and descending branches the first 1.5 mm of each was used (figure 4.6). The micro-collaterals were not included. Cells with less than 3mm of labelled axon were excluded from the analysis. From figure 4.6 it would appear that axons from cells of the lesion population had more collateral branches than controls although this difference is not statistically significant at the $P<0.05$ level. This is perhaps due to the large variation within the lesion population. A number of key factors may explain this variance.

4.11 Survival time

The lesion population compromised two groups with respect to the survival time post-injury at which the cell was labelled, 6-8 weeks and 16-18 weeks. If we distinguish between these groups then a relationship appears with respect to survival time and the number of collateral branches in the first 3mm of axon. There is a slight increase in the number of collaterals at 6-8 weeks (although this is not statistically significant). At 16-18 weeks a clear difference can be observed which is statistically significant at the $P<0.05$ level. Thus survival time appears to be a significant factor.

4.12 Distance from lesion.

Cells from the lesioned population also fall into two categories based on their distance from the start of the lesion, these being more than 10 mm from the start of the lesion and less than 10mm. Separating the lesion group in this way reveals a statistically significant difference between the groups with respect to the number of axon collateral branches in the first 3mm of axon (figure 4.8). Those cells with somas located within 10 mm of the start of the lesion had significantly more axon collateral branches in the first 3mm of labelled axon than both those cells with soma more than 10mm away ($P<0.05$) and those of the control population ($P<0.05$).

4.13 Survival times and distance from lesion.

It would appear that the variation within the groups distinguished with respect to these two factor individually may be partly explained a combination of the factors. Thus if we separate the cells according to both criteria the pattern is as expected (figure 4.8b)

4.14 Axon trajectory

If one distinguishes between ascending axons/axonal branches (ie. travelling away from the lesioned environment) and descending axons/axonal branches (ie. travelling toward the lesioned environment) then this difference increase in collaterals appears to consistent across all 3 trajectory groups although the numbers in each group being to small to allow any statistical analysis (figure 4.9).

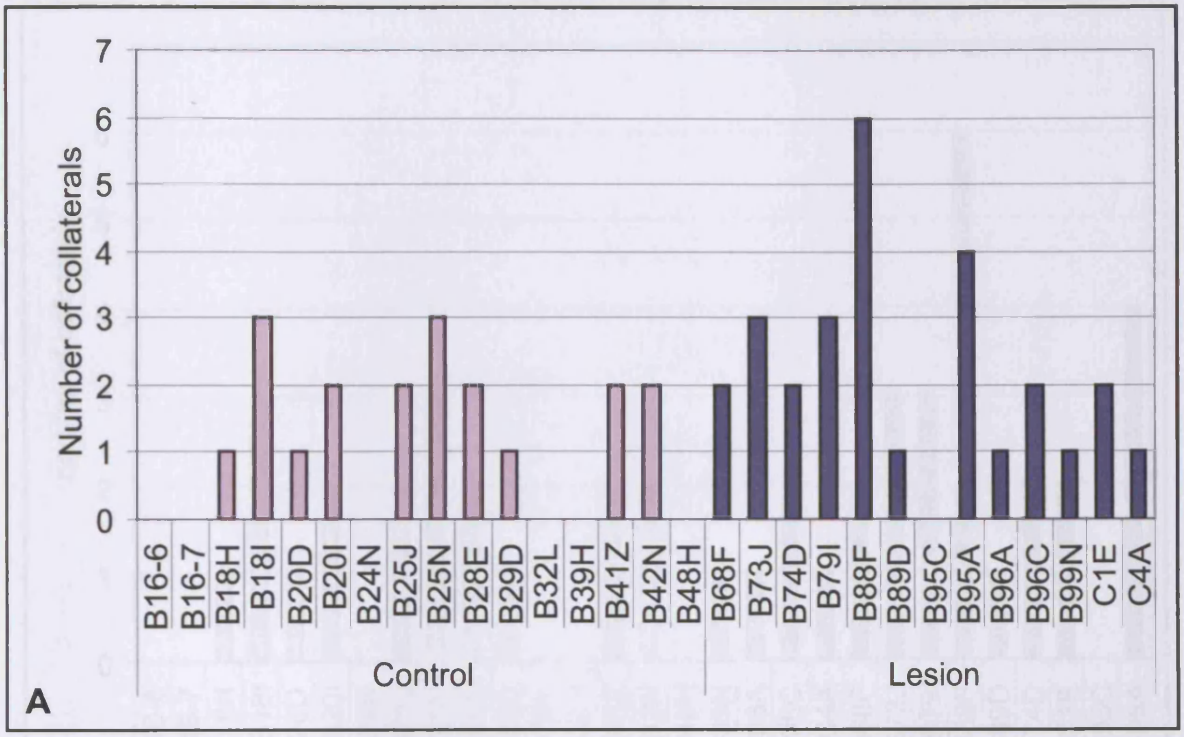

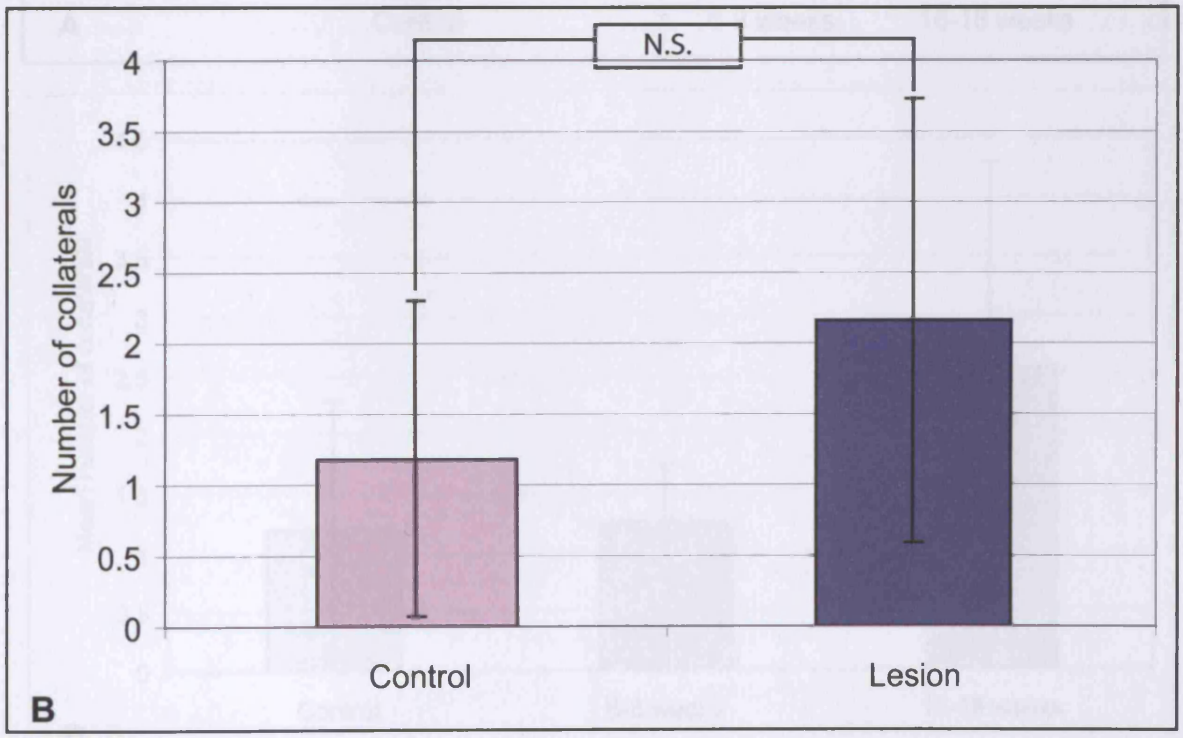

Figure 4.6: Number of collateral branches in the first 3mm of labelled axon of interneurones from the control and the lesion population.
For cells with axons with both ascending and descending branches only the first 1.5 mm of each was used. Cells with less than 3mm labelled axon (B and B) were excluded.
A: Individual cells
B: Means (Note that although there appears to be a difference between the two groups, this is just below the level of significance probably due to the large variations within the groups.)

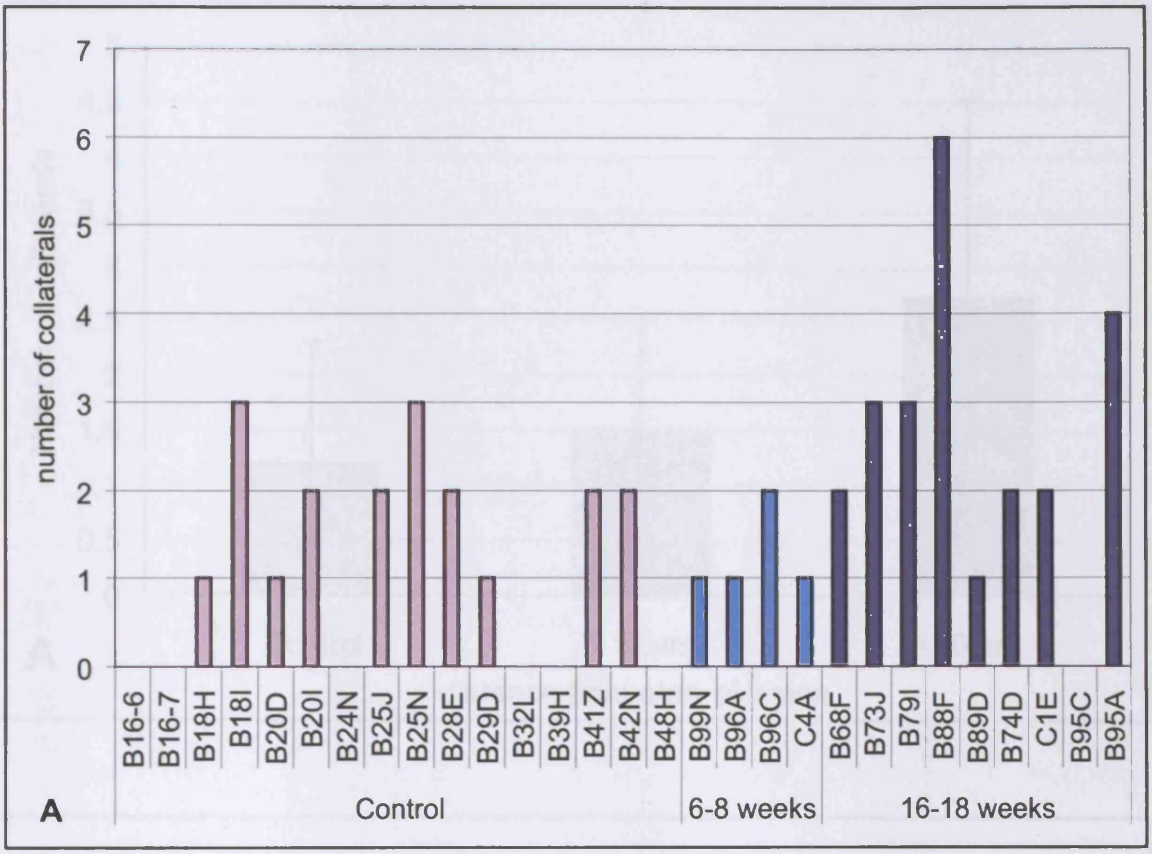

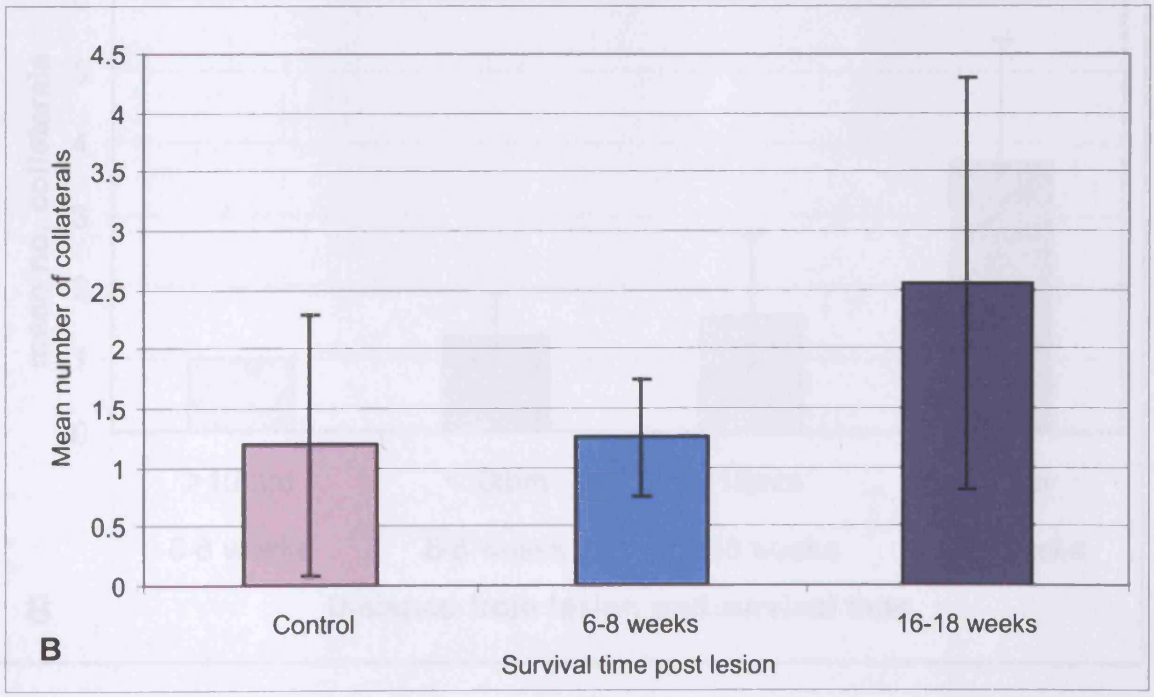

Figure 4.7: Survival time post lesion and number of collateral branches in the first 3mm of labelled axon.
For cells with axons with both ascending and descending branches only the first 1.5 mm of each was used. Cell with less than 3mm labelled axon were excluded.
A: Individual cells
B: Means

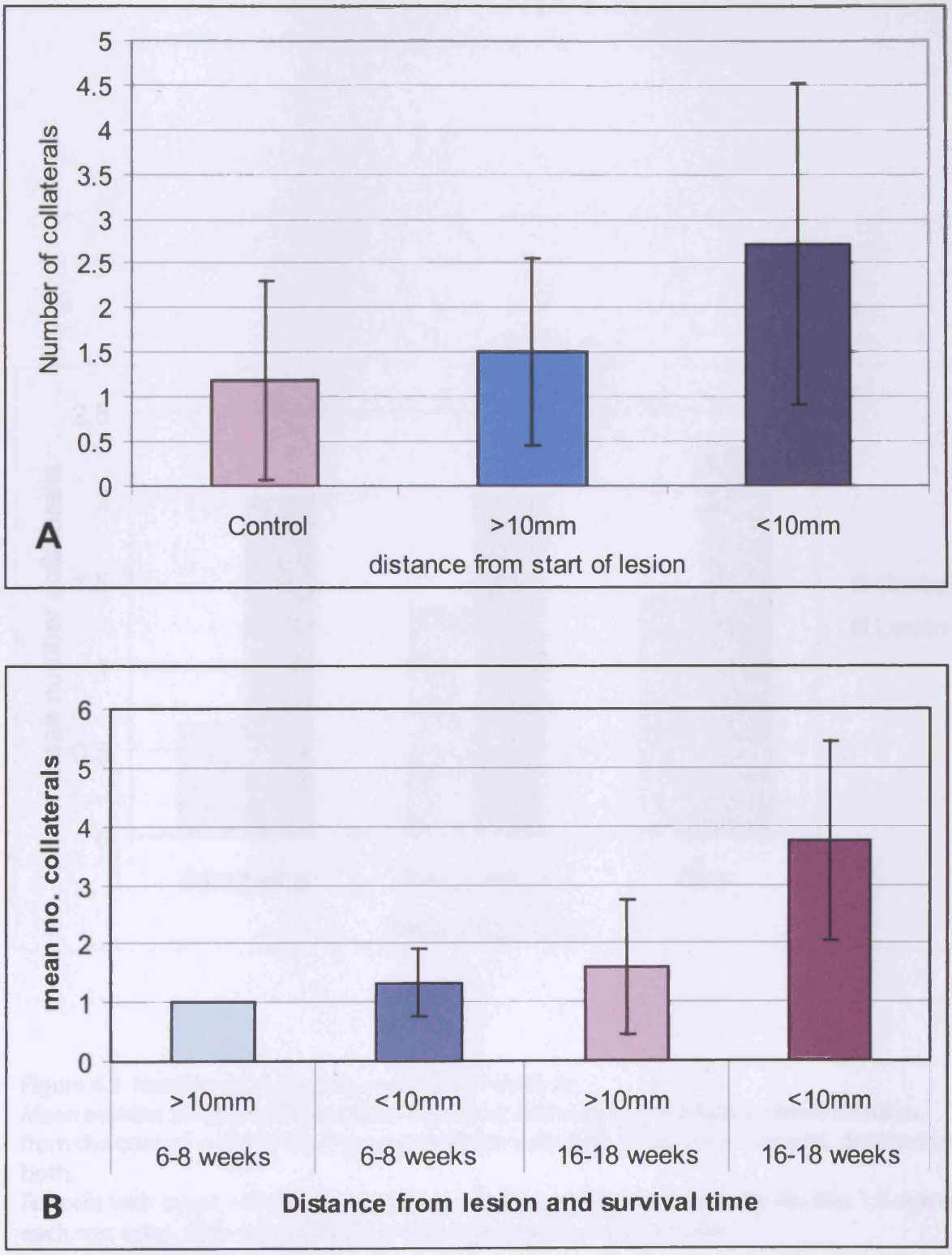

Figure 4.8 Number of Collaterals and Distance from Lesion
Mean number of collateral branches in the first 3mm of labelled axon of interneurones from the control and the lesion population. For cells with axons with both ascending and descending branches only the first 1.5 mm of each was used. Cell with less than 3mm labelled axon were excluded.
A: Distance from lesion only.
B: Distance from lesion and survival time.

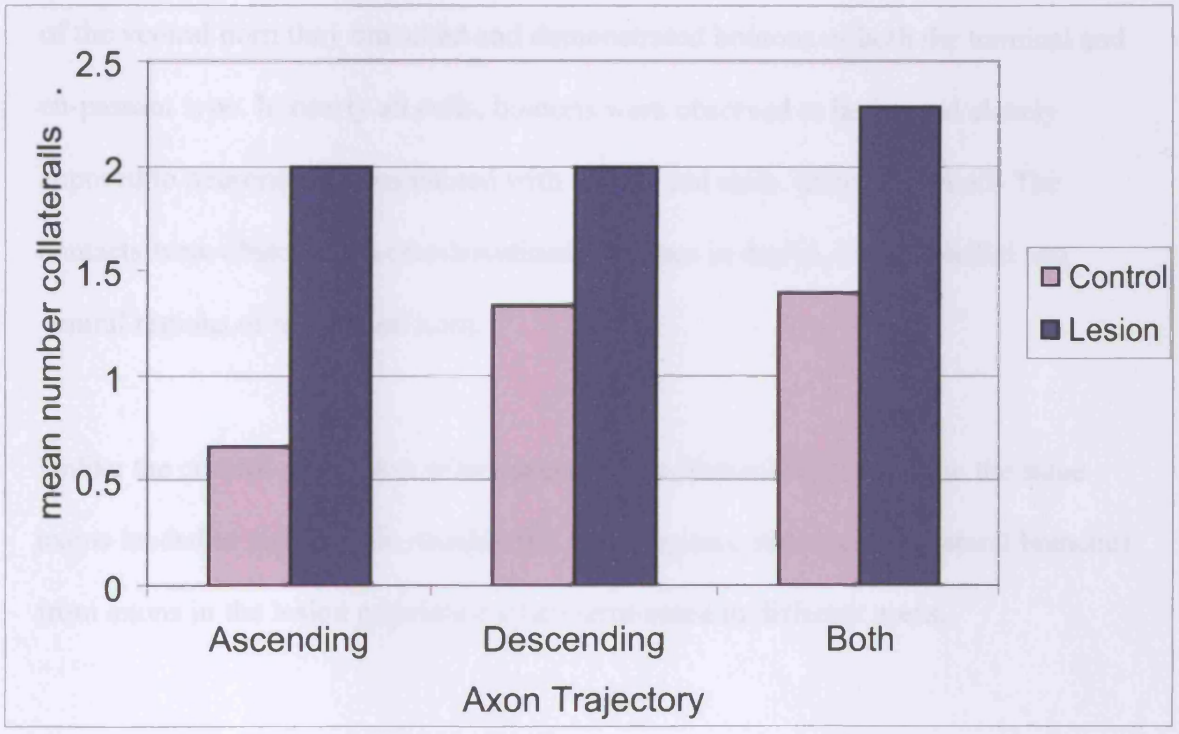

Figure 4.9 Number of Collaterals and Axon Trajectory
Mean number of collateral branches in the first 3mm of labelled axon of interneurones from the control and the lesion populations for cells with axons which ascend, descend and both.
For cells with axons with both ascending and descending branches only the first 1.5 mm of each was used. Cell with less than 3mm labelled axon were excluded.

4.2 Reconstructions of axon collateral branches

Where possible the individual collateral branches were reconstructed. This was possible for 12 axons and these are illustrated in figures 4.10-4.21.

Collaterals branches were finer than the stem axon. Once they reached the grey matter of the ventral horn they branched and demonstrated boutons of both the terminal and en-passant type. In nearly all cells, boutons were observed to be located closely apposed to neurones counterstained with neutral red stain. (shown in pink). The contacts were observed on counterstained neurones in dorsal, lateral, medial and ventral regions of the ventral horn.

Unlike the control population where successive collateral branches from the same axons tended to terminate in roughly the same regions, successive collateral branches from axons in the lesion population often terminated in different areas.

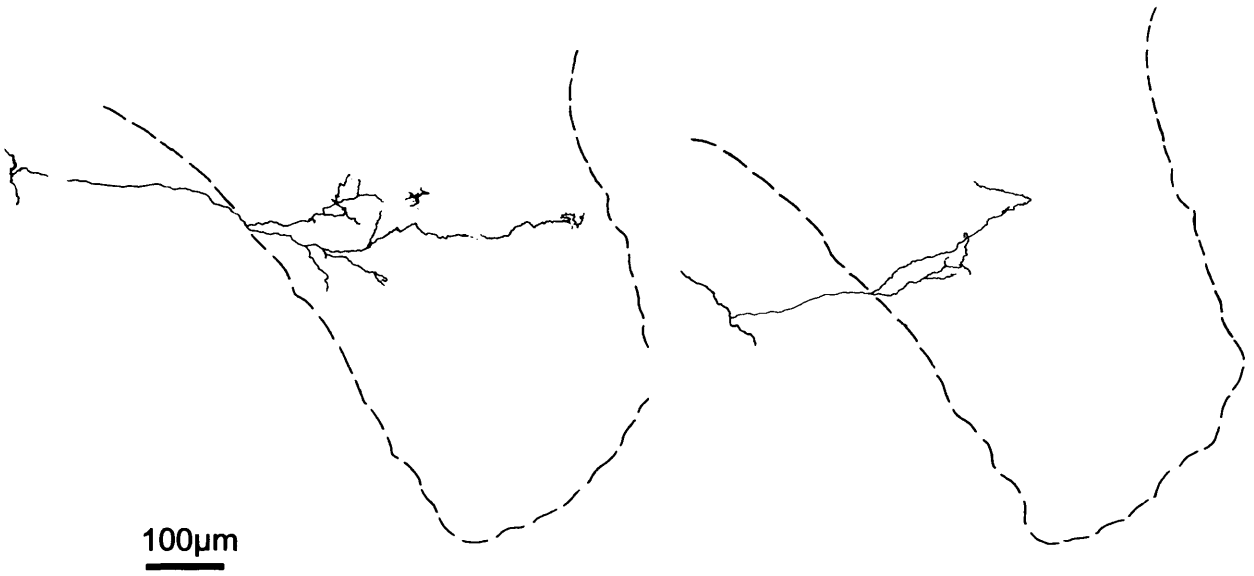

Collateral 1 from rostral branch

Collateral 2 from rostral branch

Collateral 1 from caudal branch

Collateral 2 from caudal branch

Figure 4.10
Reconstructions of axon collateral branches of interneurone B68F

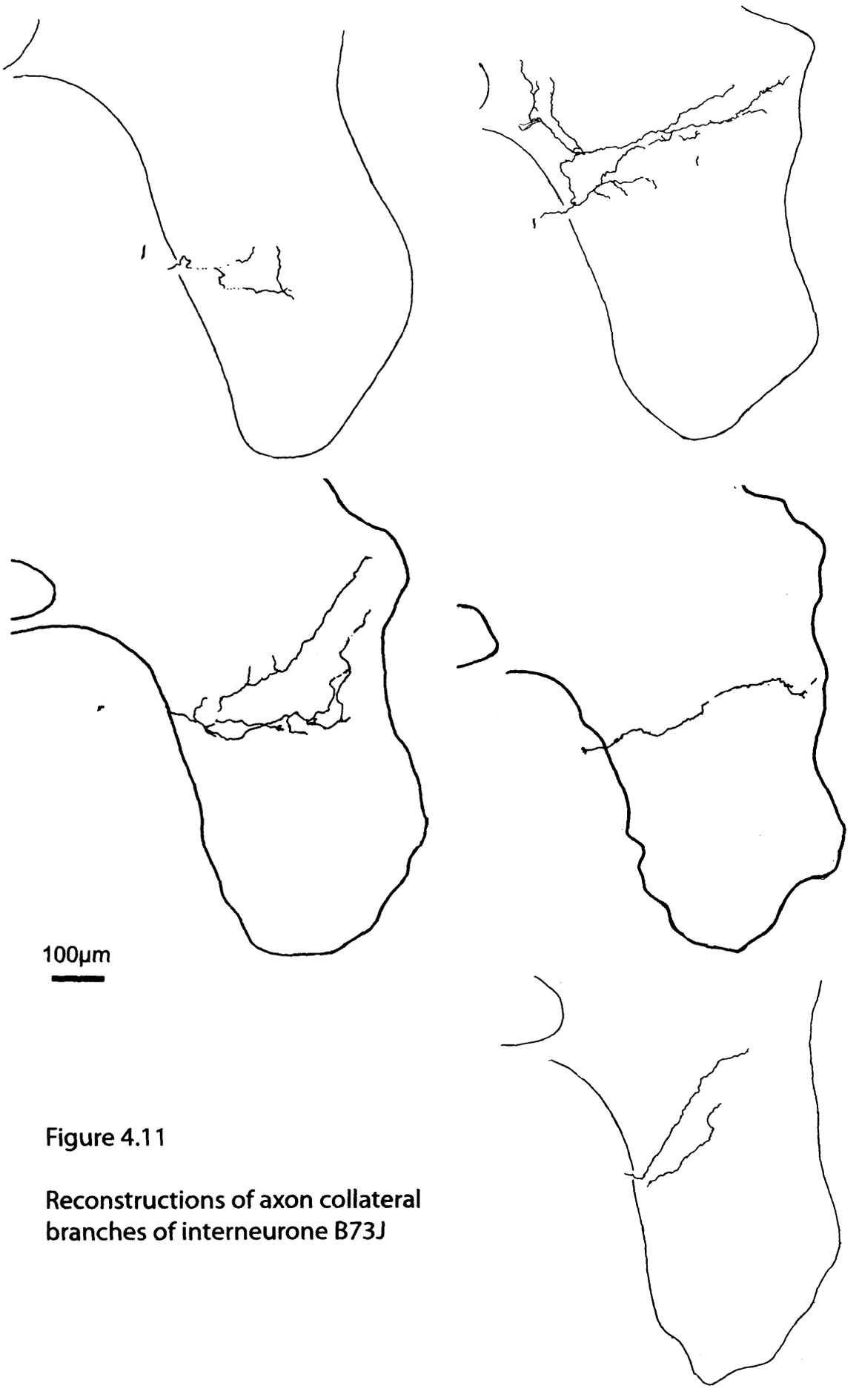

Figure 4.11

Reconstructions of axon collateral branches of interneurone B73J

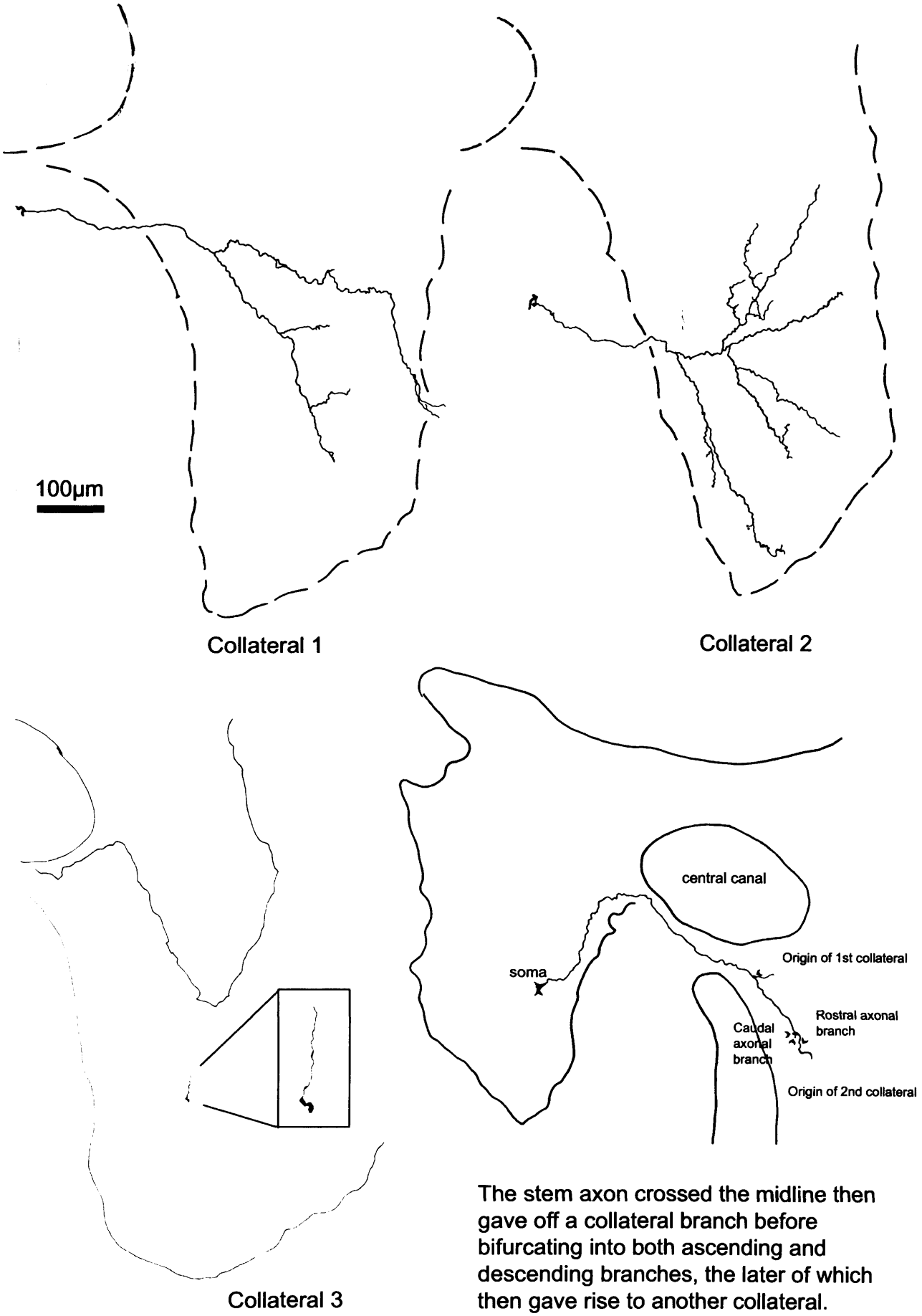

Figure 4.12 Axon collateral branches of interneurone B74D

figure 4.13 - Axon collateral branches of interneurone B79l

Figure 4.14a
Axon collateral branches from the rostral branch of the axon from cell B88F

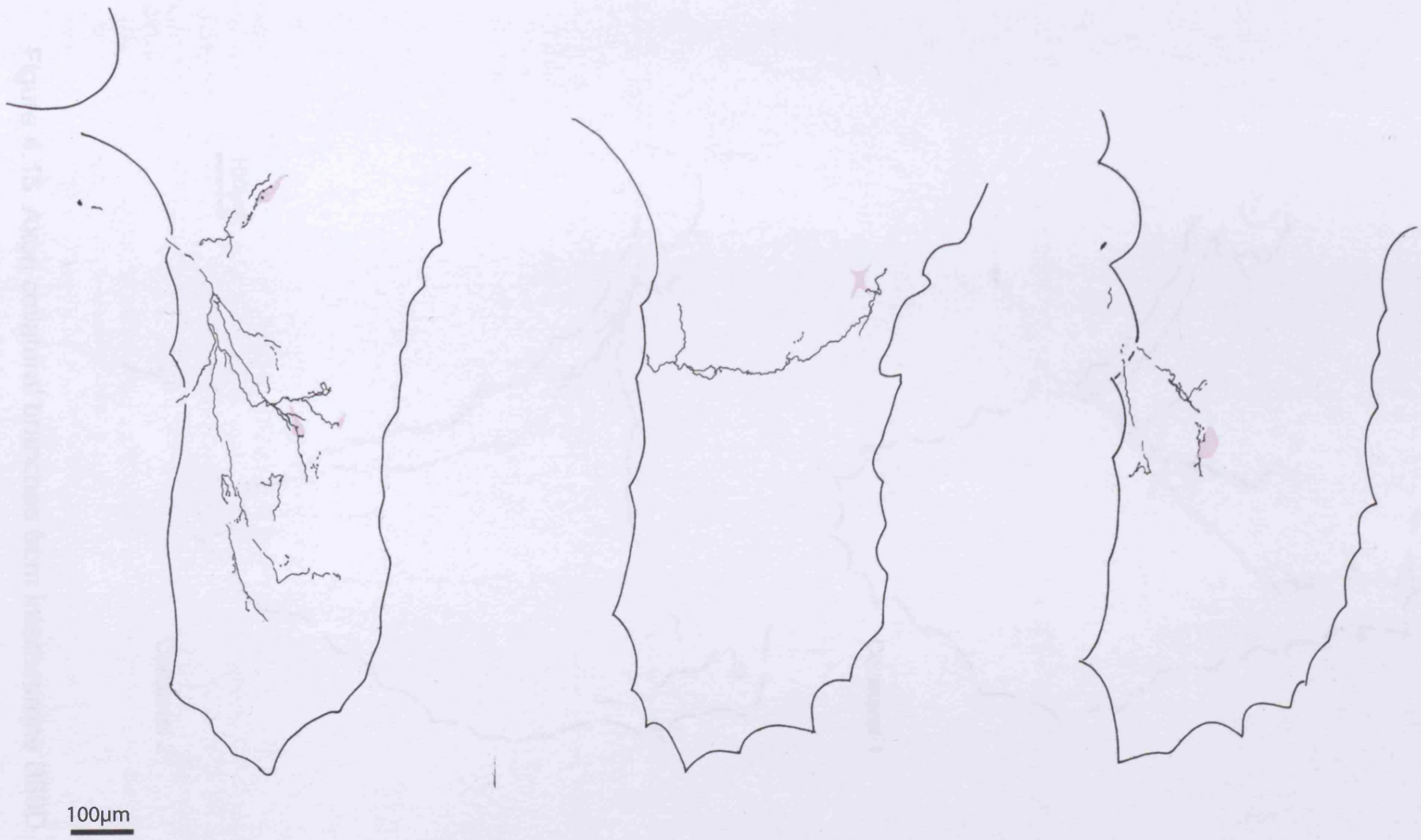

Figure 4.14b : Axon collateral branches from the caudal branch of the axon from interneurone B88F

Figure 4.15 Axon collateral branches from interneurone B89D

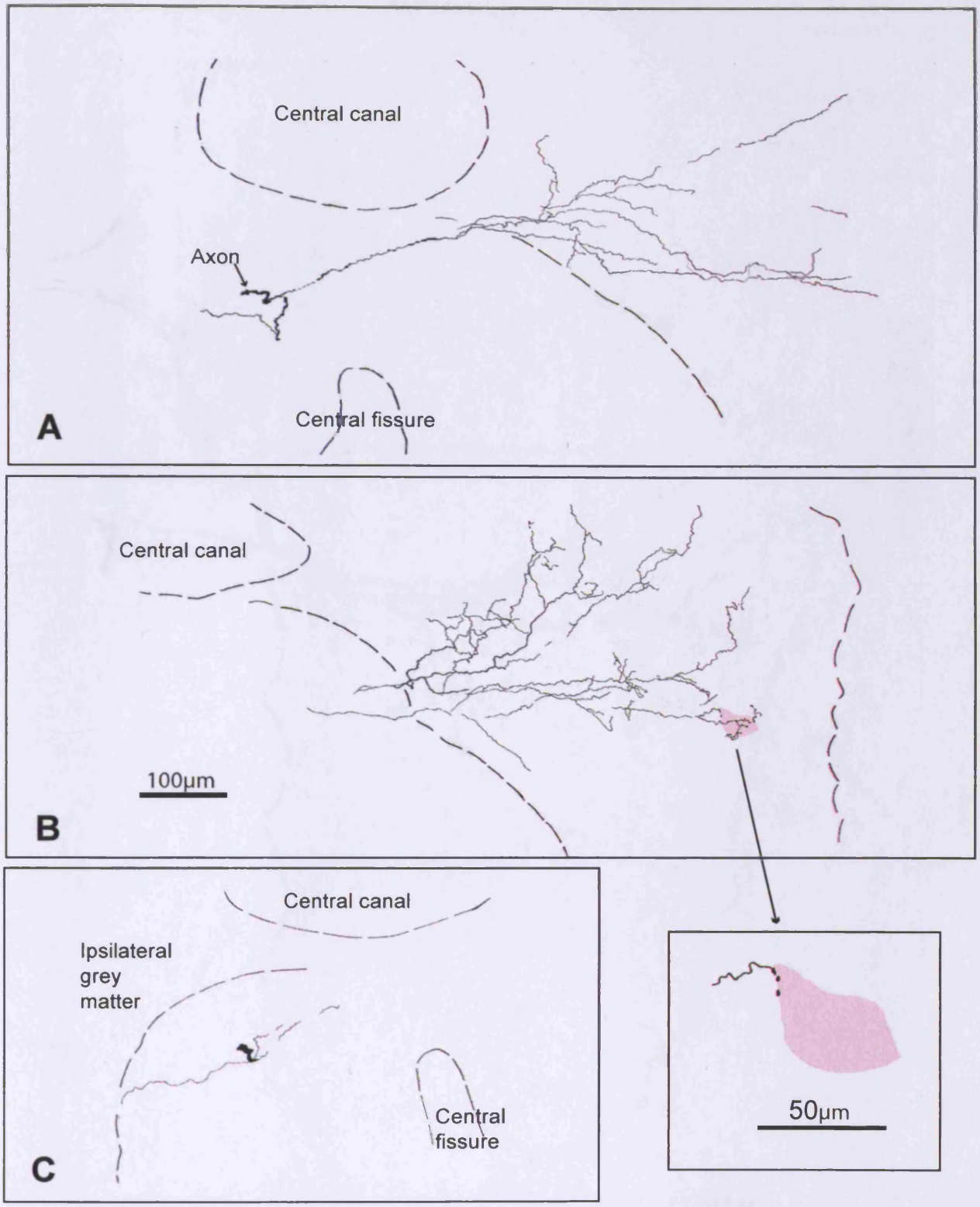

Figure 4.16: Examples of axon collateral branches of cell B95A.
The collaterals for this cell were extremely hard to reconstruct because they showed considerable overlap with each other as well as overlapping with the cells complex dendritic tree. Also some collateral branches occured where the peice of spinal cord was cut into 2 prior to sectioning.
A: Collateral branch originating on the side ipsilateral to the soma crossing to the contralateral side and branching in the contralateral ventral horn
B: Example of a collateral branch in the side contralateral to the soma and stem axon, branching in the contralateral grey matter with boutons opposed on neurones counterstained with neutral red.
C: Main stem axon with the origin of 3 collateral branches at the same point. One branch headed towards the ipsilateral ventral horn, the other two headed towards the contralateral side.

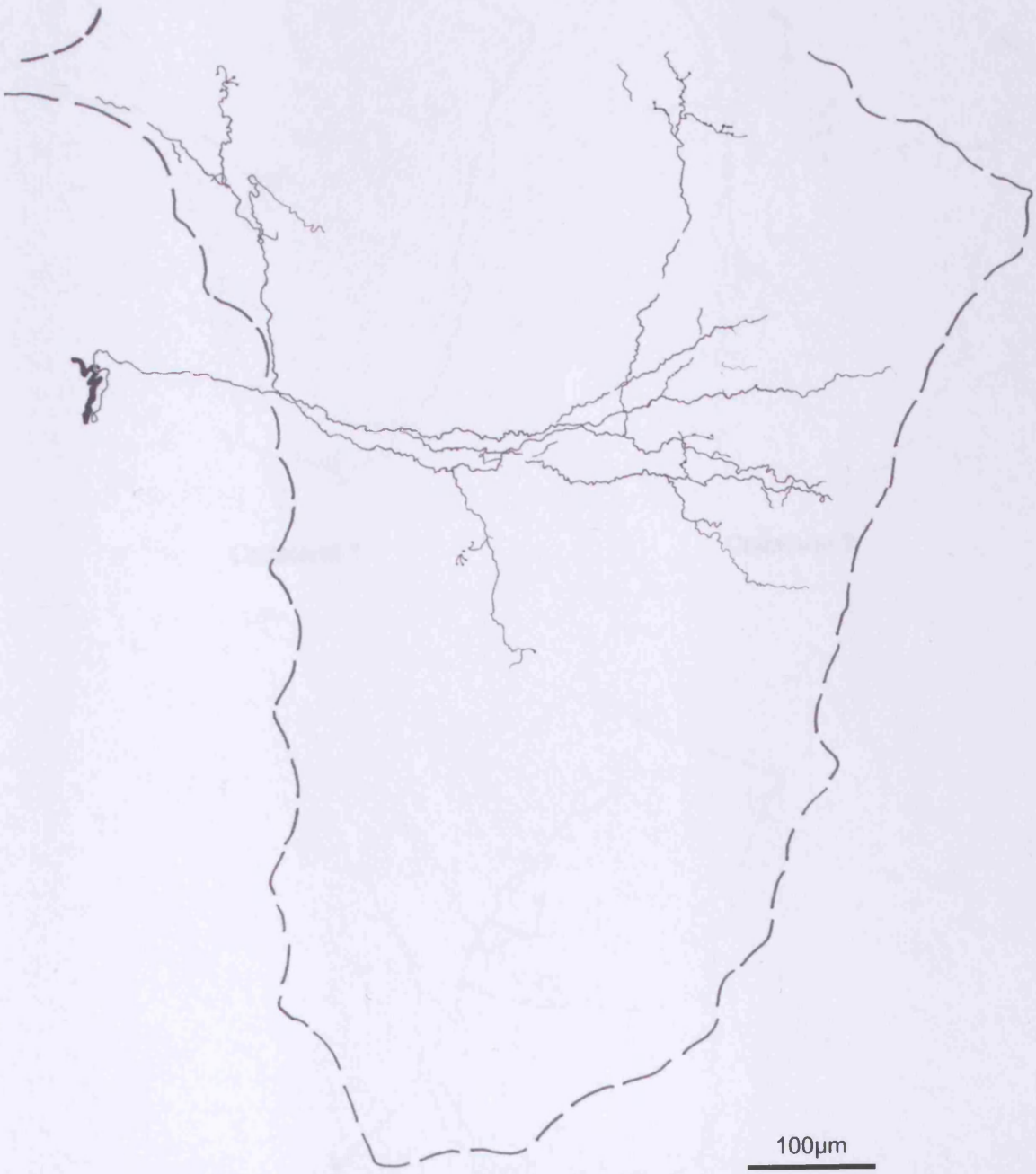

Figure 4.17: Axon collateral branch of interneurone B96A

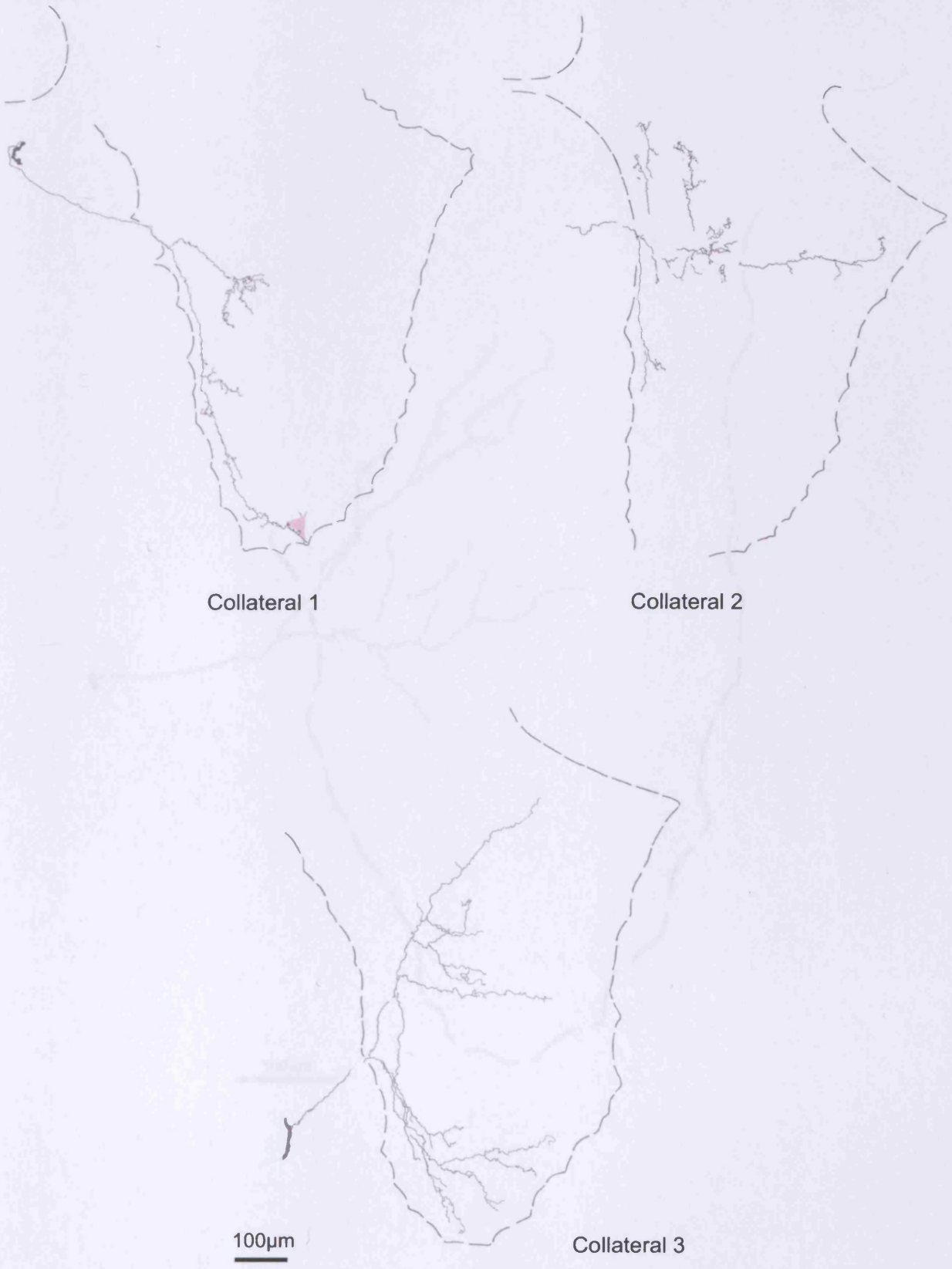

Figure 4.18: Axon collateral branches of interneurone B96F

Figure 4.19: Axon collateral branch from interneurone B99N

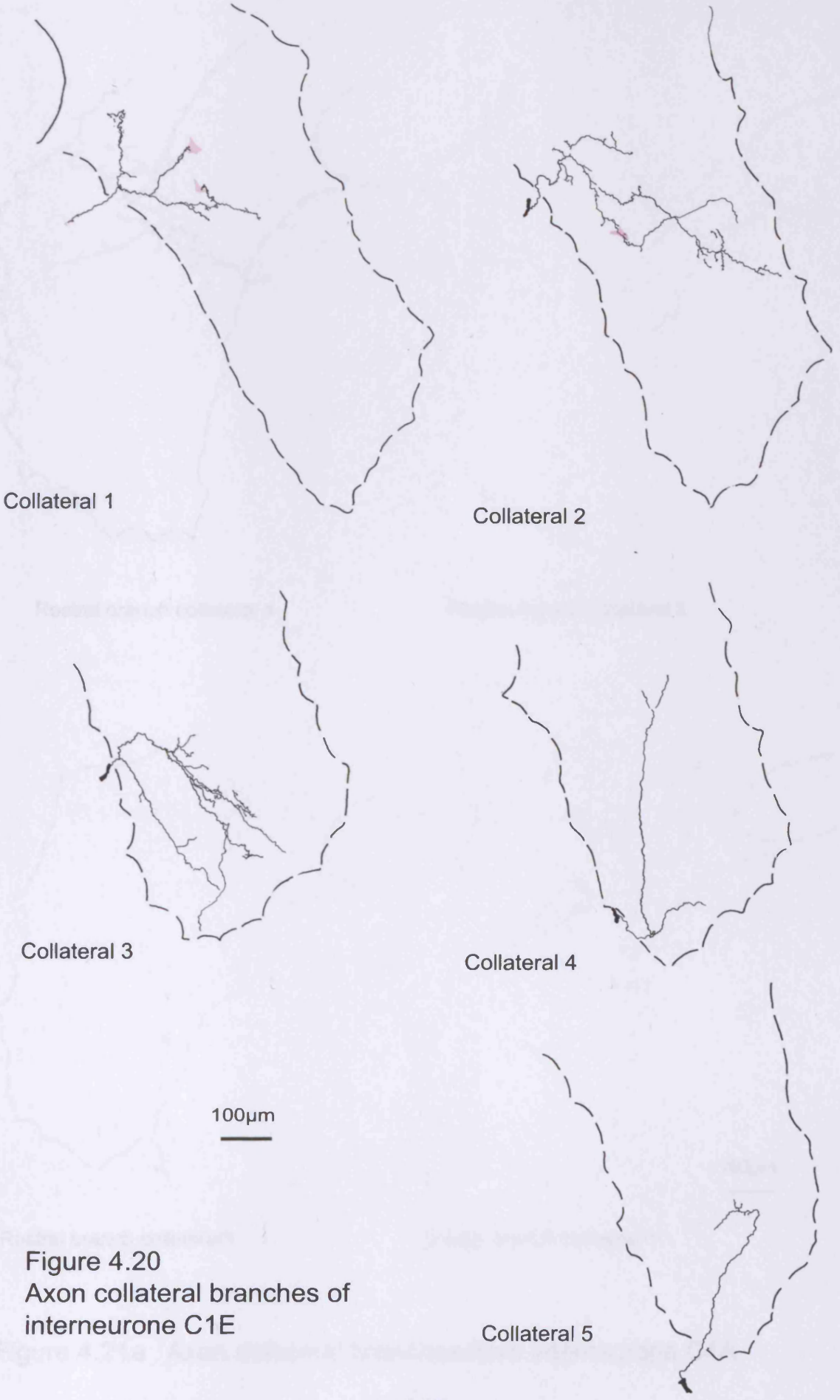

Figure 4.20
Axon collateral branches of interneurone C1E

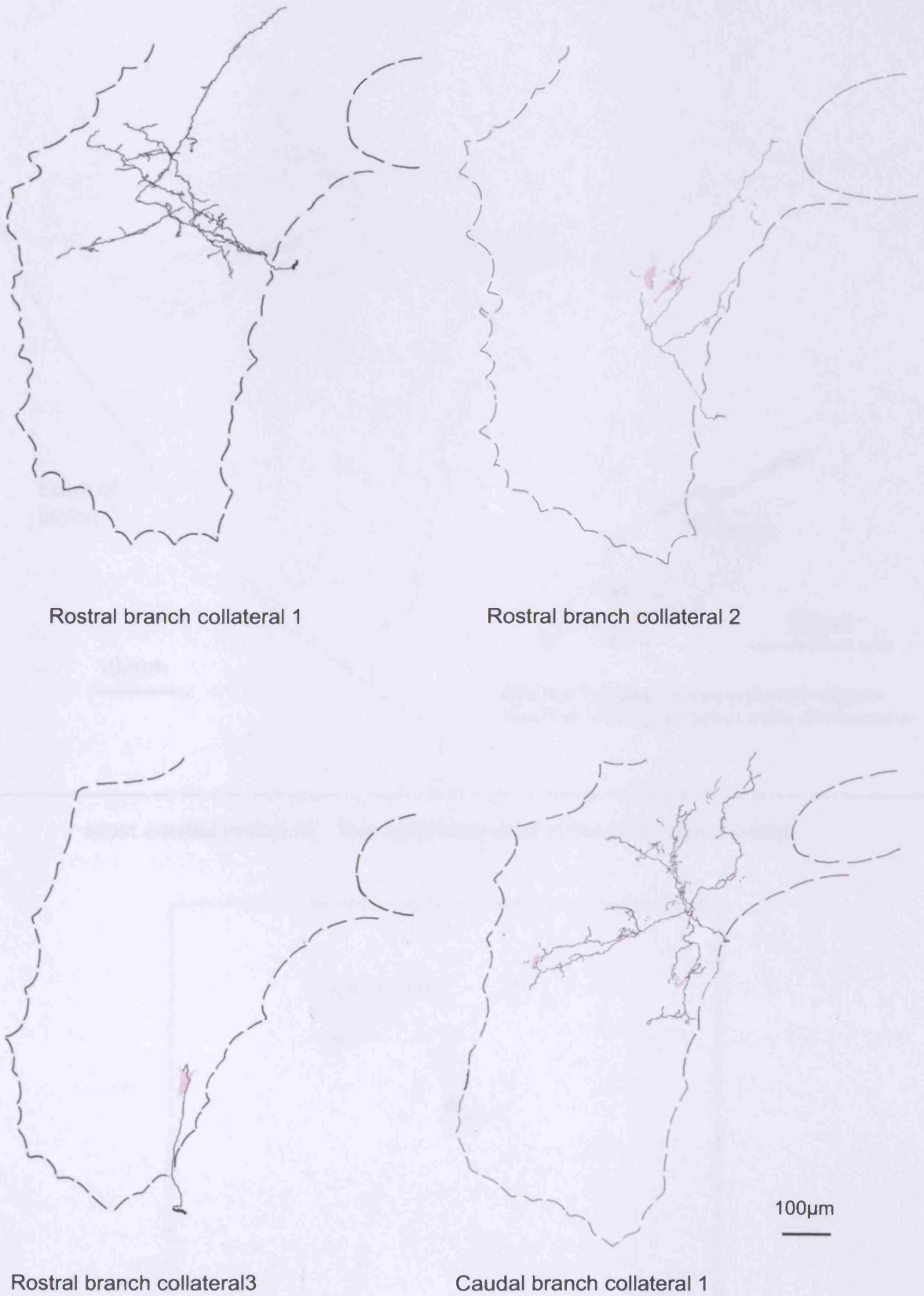

Figure 4.21a Axon collateral branches from interneurone C4A

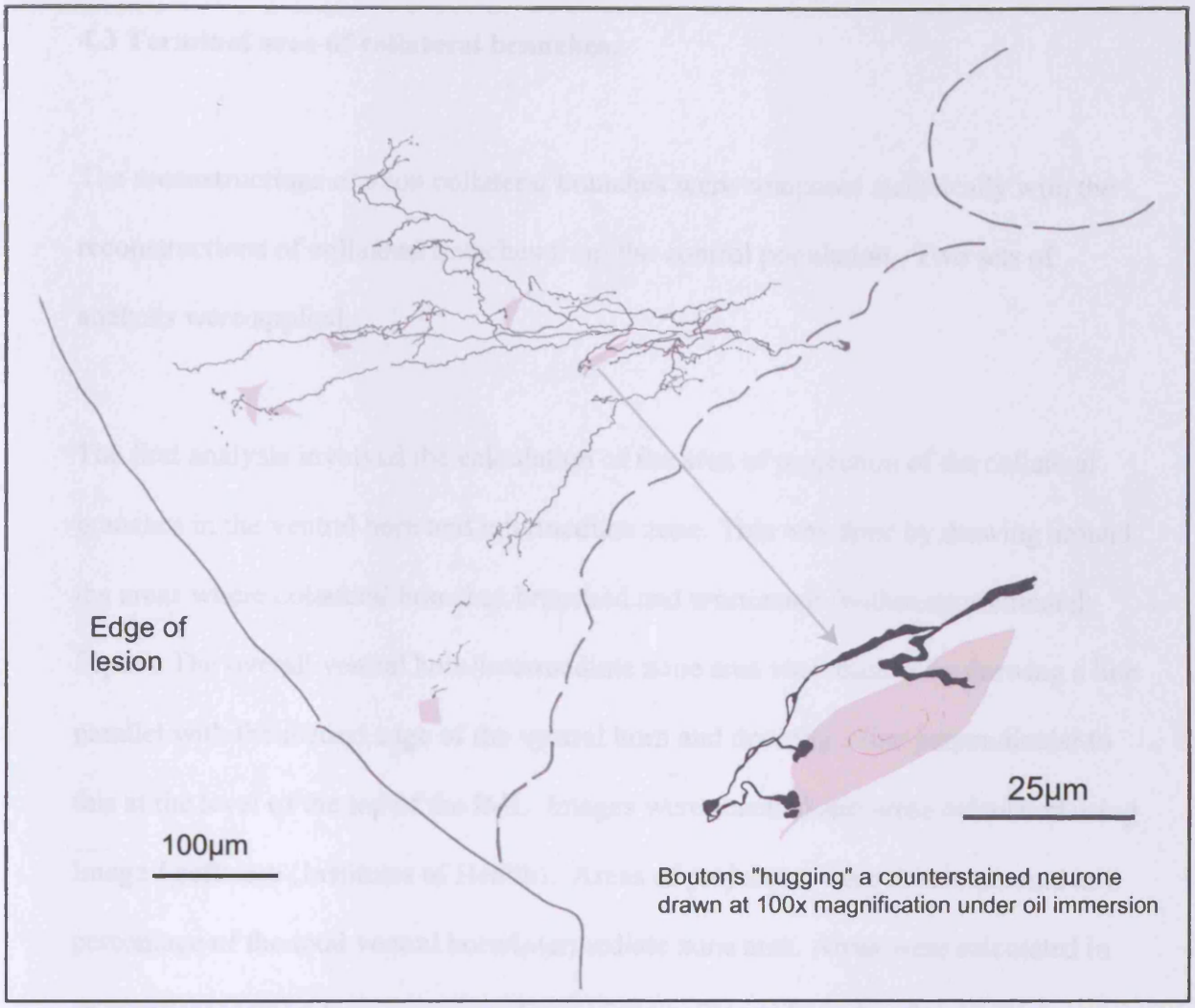

Most caudal collateral. This collateral was at the level of the lesion

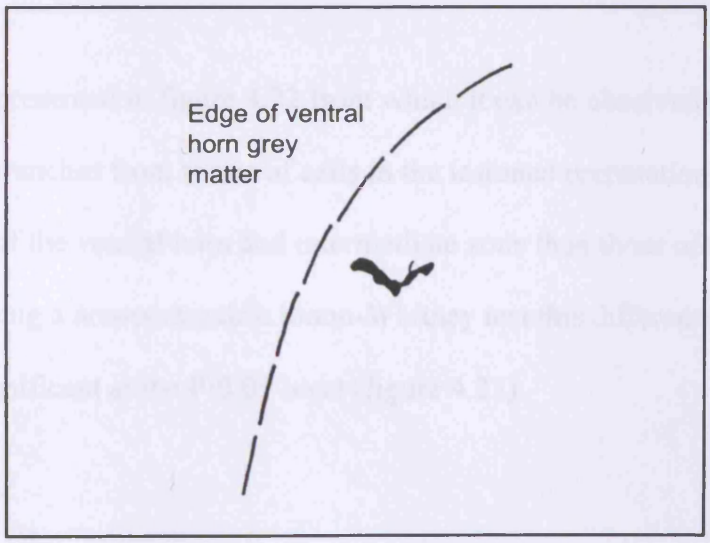

Microcollateral from the stem axon

Figure 4.21b Axon collateral branches of interneurone C4A continued

4.3 Terminal area of collateral branches.

The reconstructions of axon collateral branches were compared statistically with the reconstructions of collateral branches from the control population. Two sets of analysis were applied.

The first analysis involved the calculation of the area of projection of the collateral branches in the ventral horn and intermediate zone. This was done by drawing around the areas where collateral branches branched and terminated (within approximately 50μm). The overall ventral horn/intermediate zone area was reached by drawing a line parallel with the medial edge of the ventral horn and drawing a line perpendicular to this at the level of the top of the IML. Images were scanned and areas calculated using Image J software (Institutes of Health). Areas of projection were then expressed as a percentage of the total ventral horn/intermediate zone area. Areas were calculated in an identical fashion from reconstructions of the collateral branches from cells from the control population.

This data is represented in figure 4.22 from which it can be observed that on average the collateral branches from axons of cells in the lesioned preparation terminated over a greater area of the ventral horn and intermediate zone than those of the control population. Using a non-parametric Mann-Whitney test this difference was statistically significant at the $P<0.05$ level (figure 4.23)

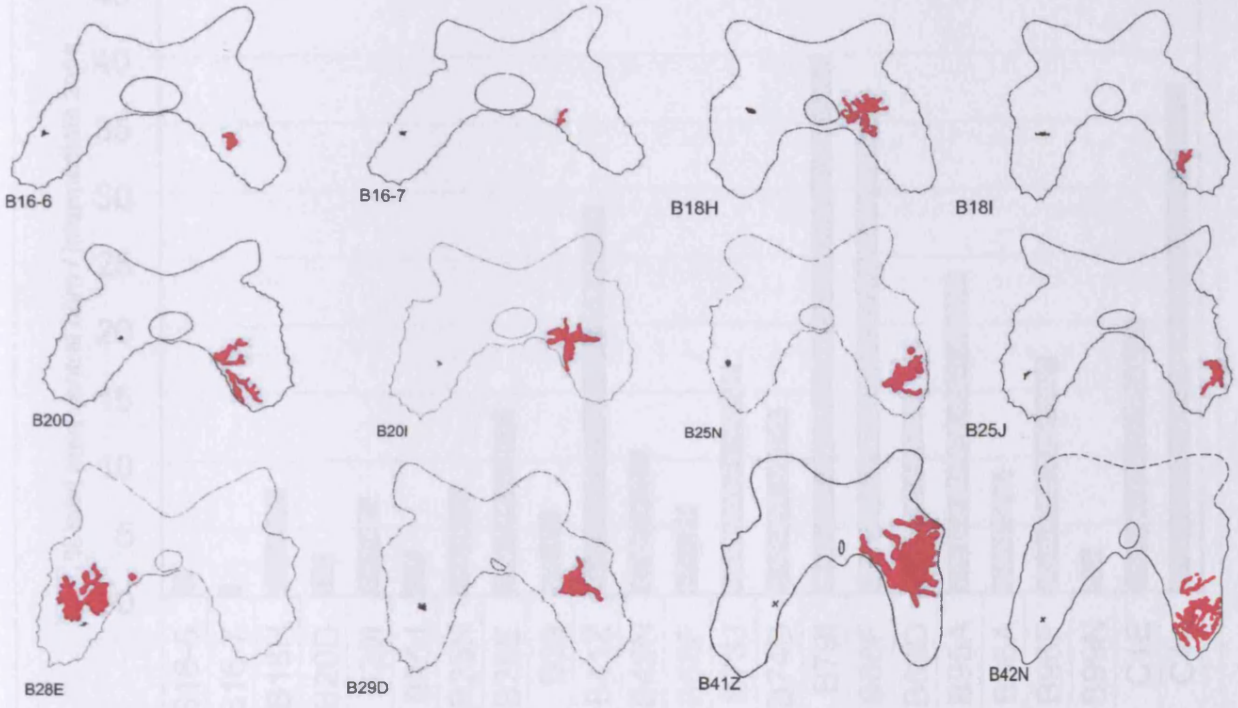

a) Control Population

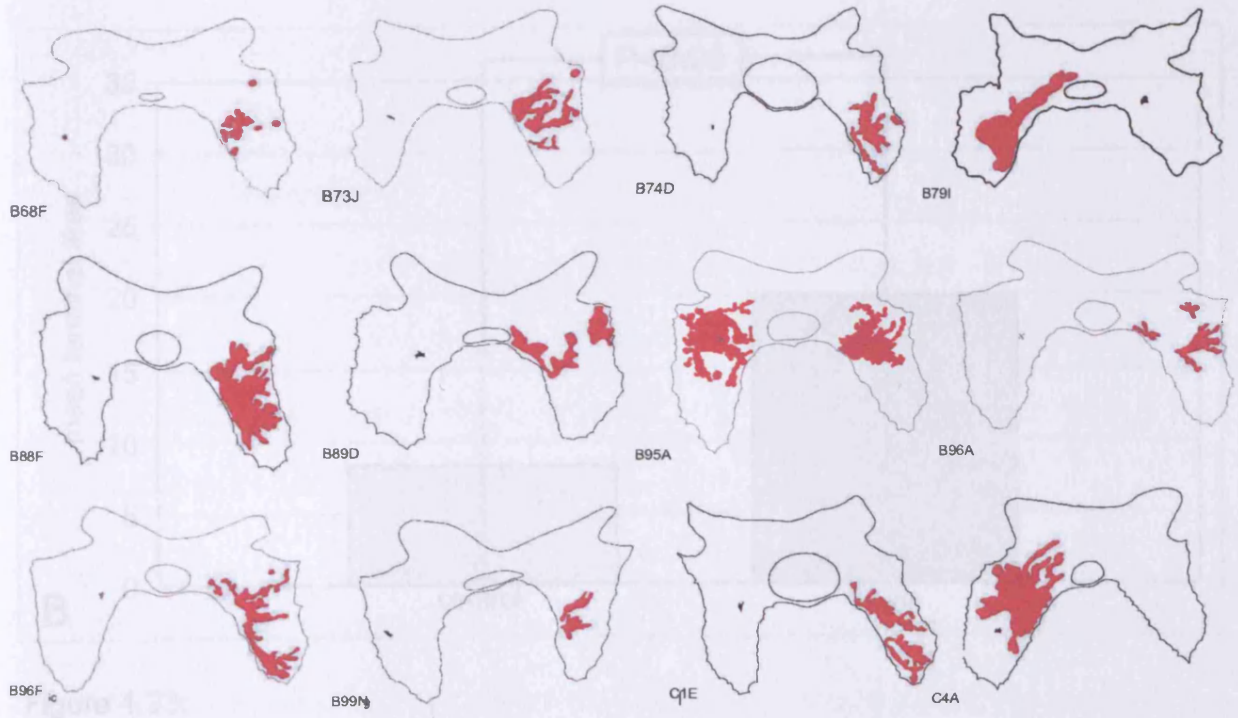

b) Lesion Population

Figure 4.22: Areas of termination of axon collaterals for each interneurone in the control and lesion populations

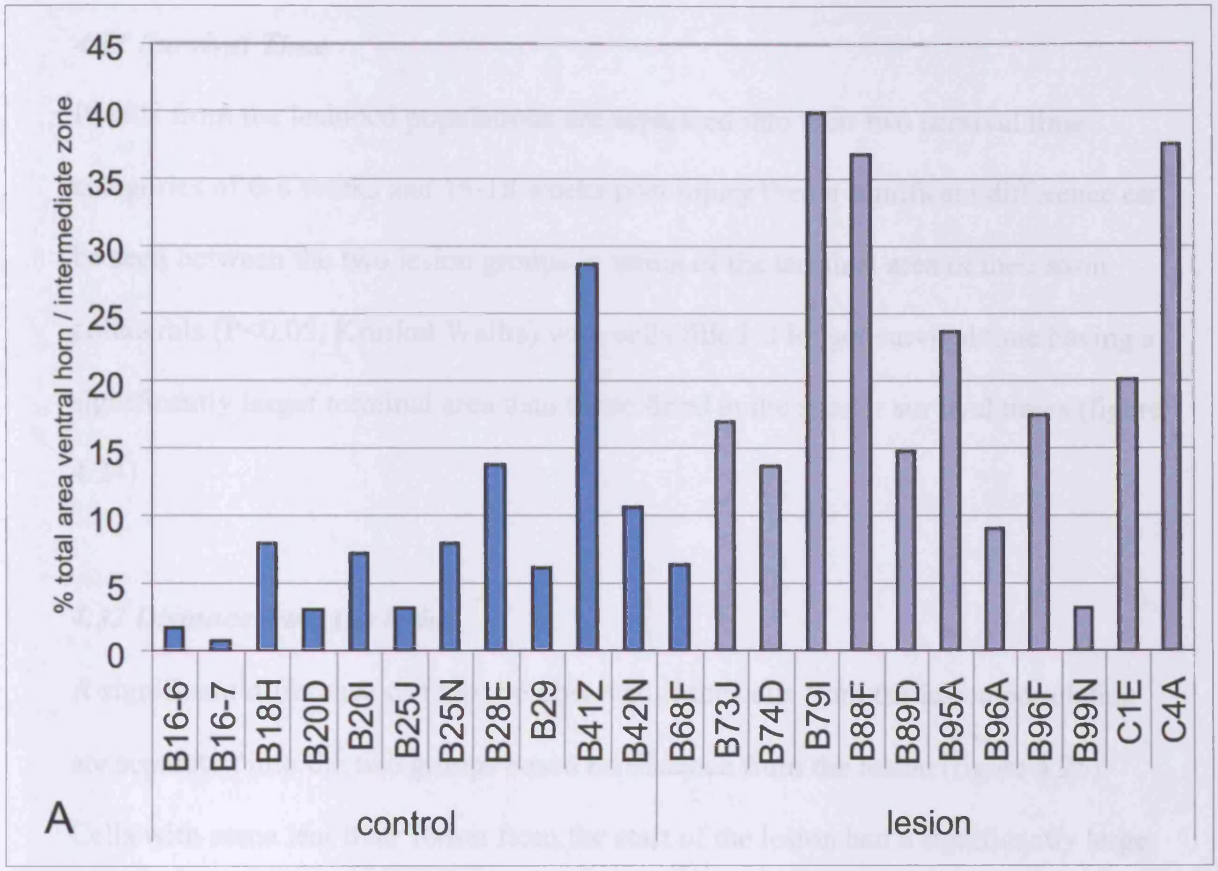

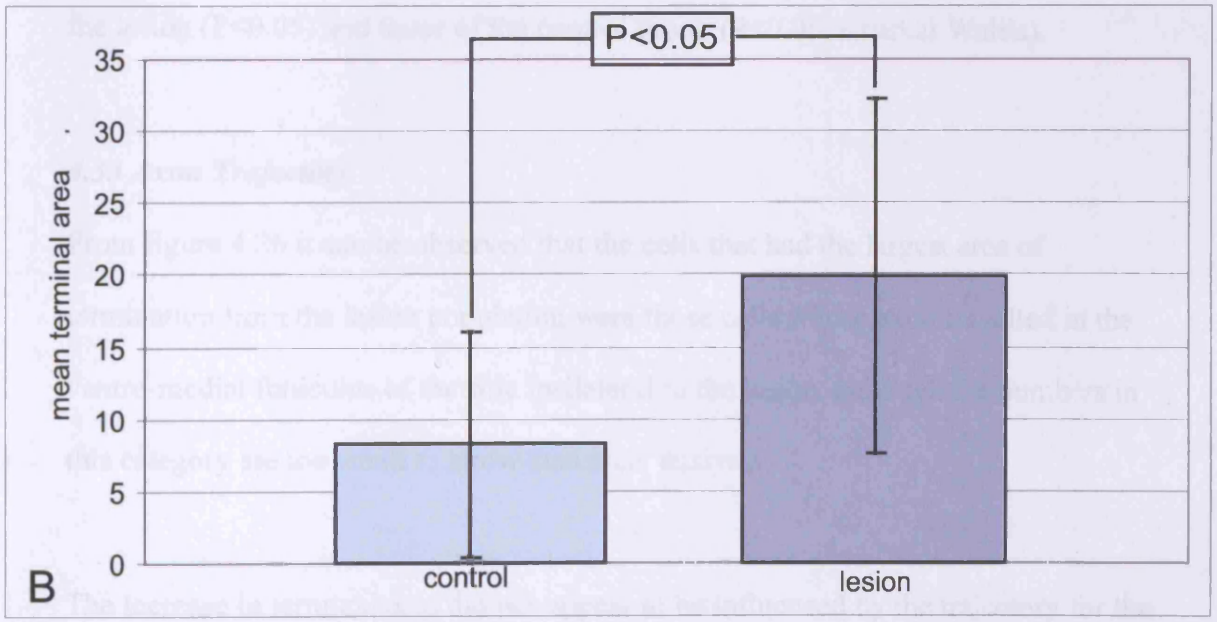

Figure 4.23:
Terminal areas of axon collateral branches of interneurones from control and lesion populations, expressed as the percentage of the total area of the ventral horn / intermediate zone,

A: Individual cells
B: Means

4.31 Survival Time

If cells from the lesioned populations are separated into their two survival time categories of 6-8 weeks and 16-18 weeks post injury then a significant difference can be seen between the two lesion groups in terms of the terminal area of their axon collaterals ($P<0.05$, Kruskal Wallis) with cells filled at longer survival time having a significantly larger terminal area than those filled at the shorter survival times (figure 4.24)

4.32 Distance from the lesion

A significant difference can also be observed if the cells from the lesion population are separated into the two groups based on distance from the lesion (figure 4.25). Cells with soma less than 10mm from the start of the lesion had a significantly larger terminal area than those with soma located more than 10mm away from the start of the lesion ($P<0.05$) and those of the control group ($P<0.05$, Kruskal Wallis).

4.33 Axon Trajectory

From figure 4.26 it can be observed that the cells that had the largest area of termination from the lesion population were those cells whose axon travelled in the ventro-medial funiculus of the side ipsilateral to the lesion, although the numbers in this category are too small to allow statistical analysis.

The increase in terminal area did not appear to be influenced by the trajectory for the axon in the rostro-caudal axis (figure 4.27) with no differences between those cells with ascending axons, those with descending axons or those with both.

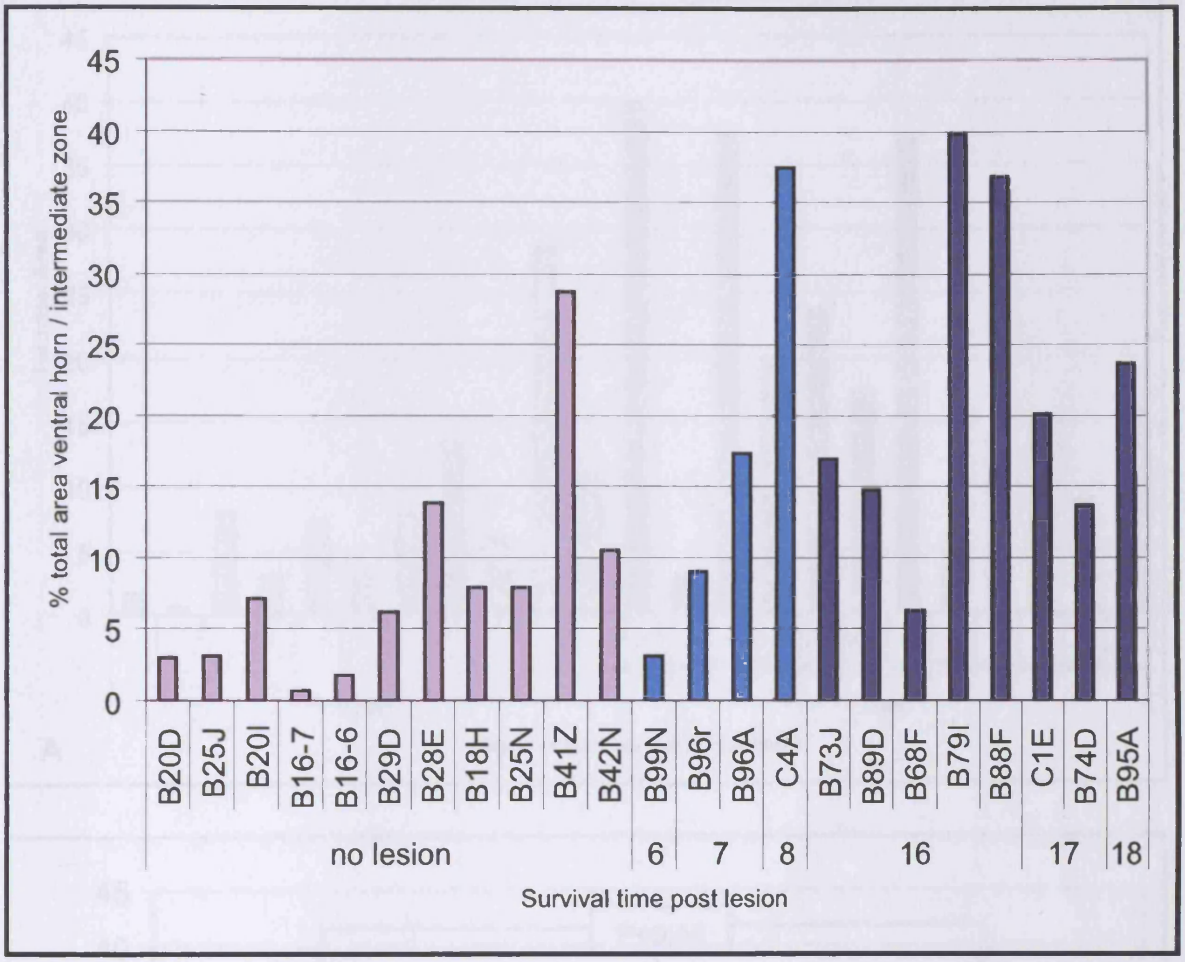

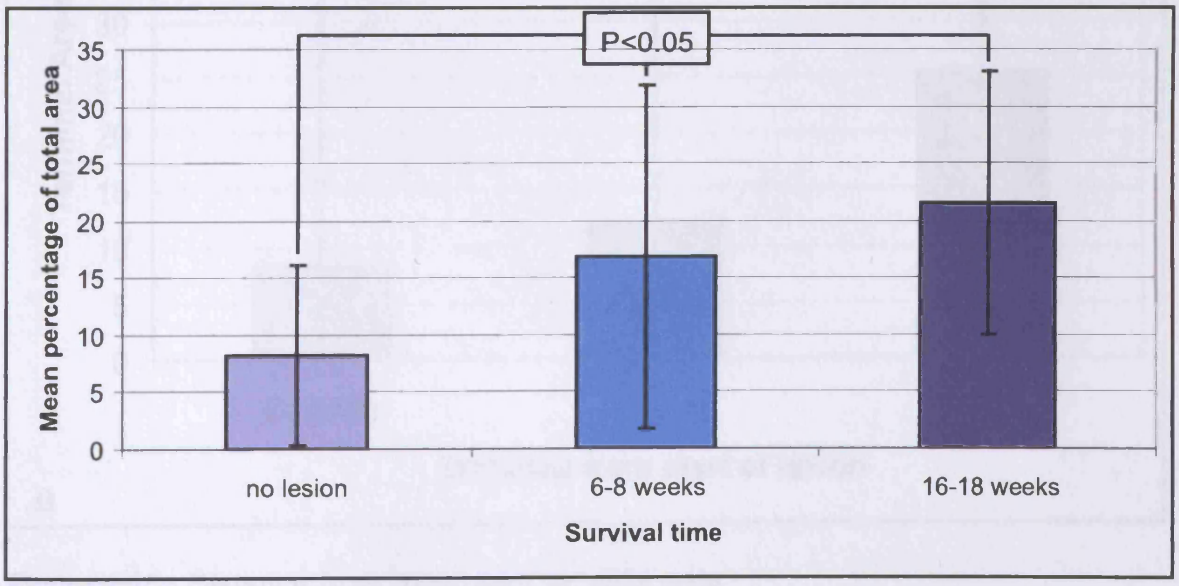

Figure 4.24: Survival time post injury and terminal areas of axon collaterals expressed as a percentage of the total area of the ventral horn and the intermediate zone.

a) Individual cells
B) Means

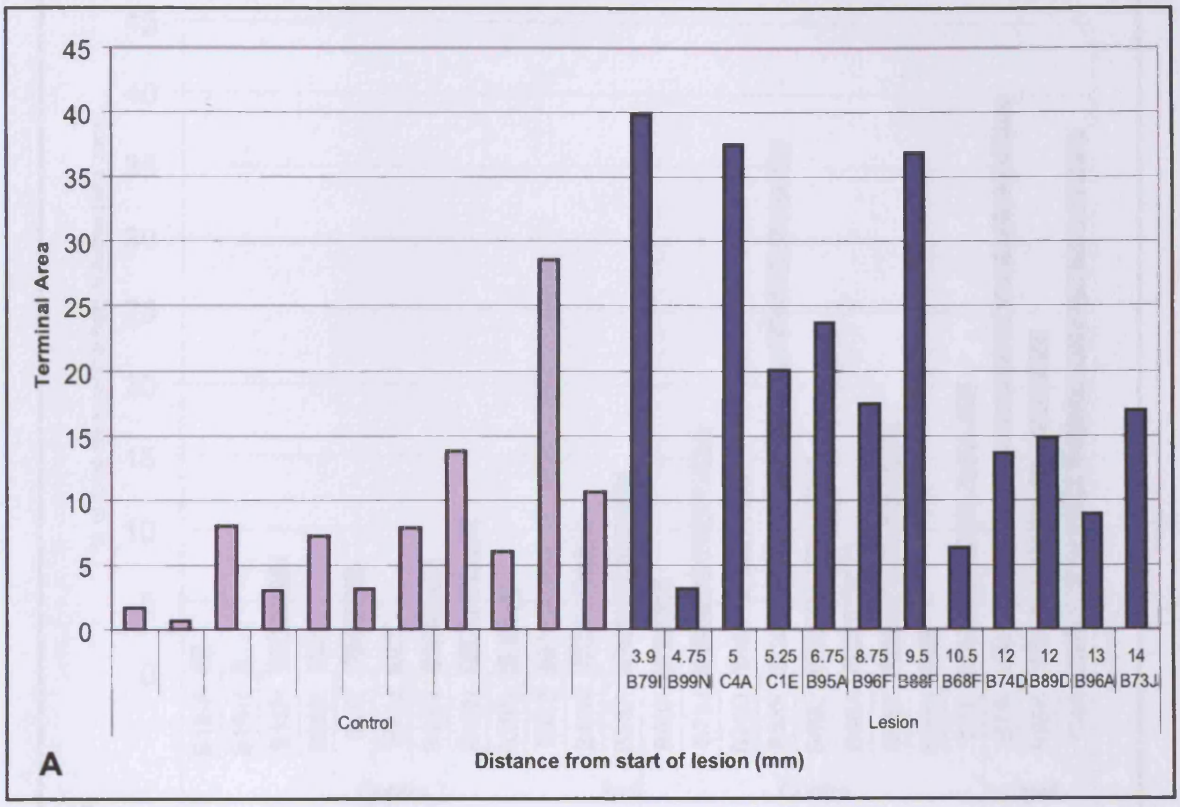

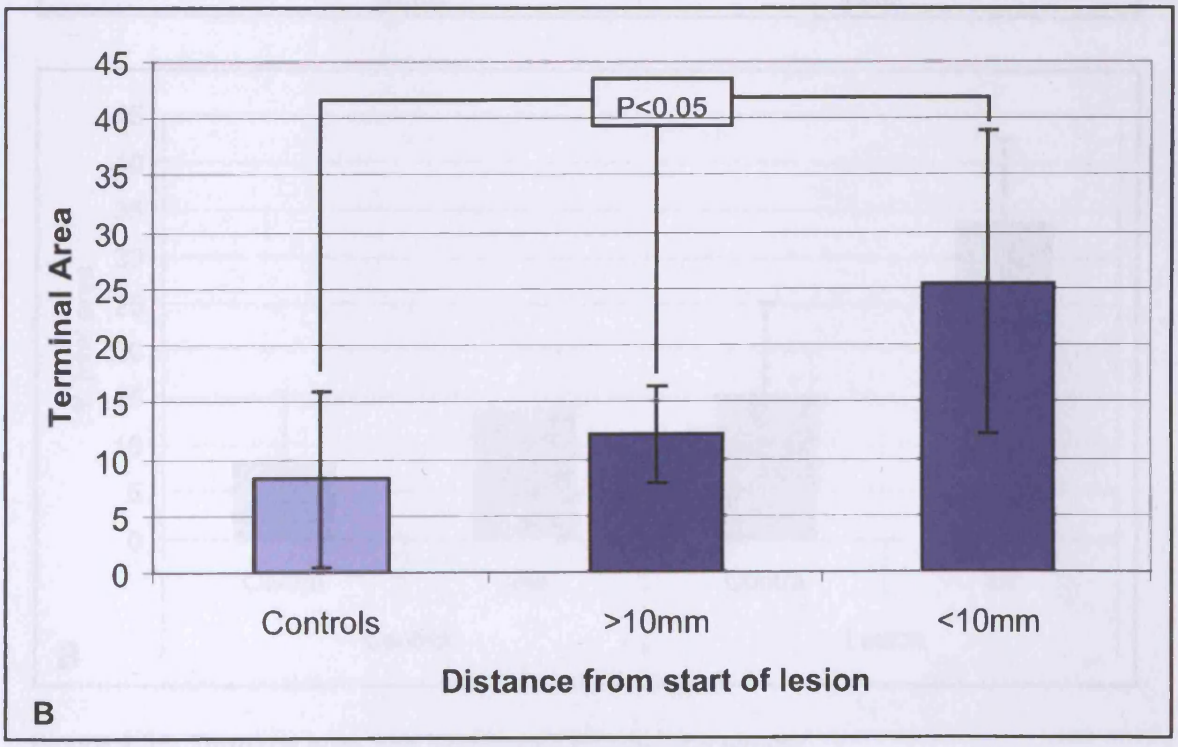

Figure 4.25: Distance from lesion and terminal area
Distance of the interneurone soma from the start of the lesion area and the terminal areas of the axon collateral branches, expressed as the percentage of the total area of the ventral horn / intermediate zone,
A: Individual cells.
B: Means for cells from the control population, those less than 10 mm from the lesion area and those more than 10 mm away from the lesion area.

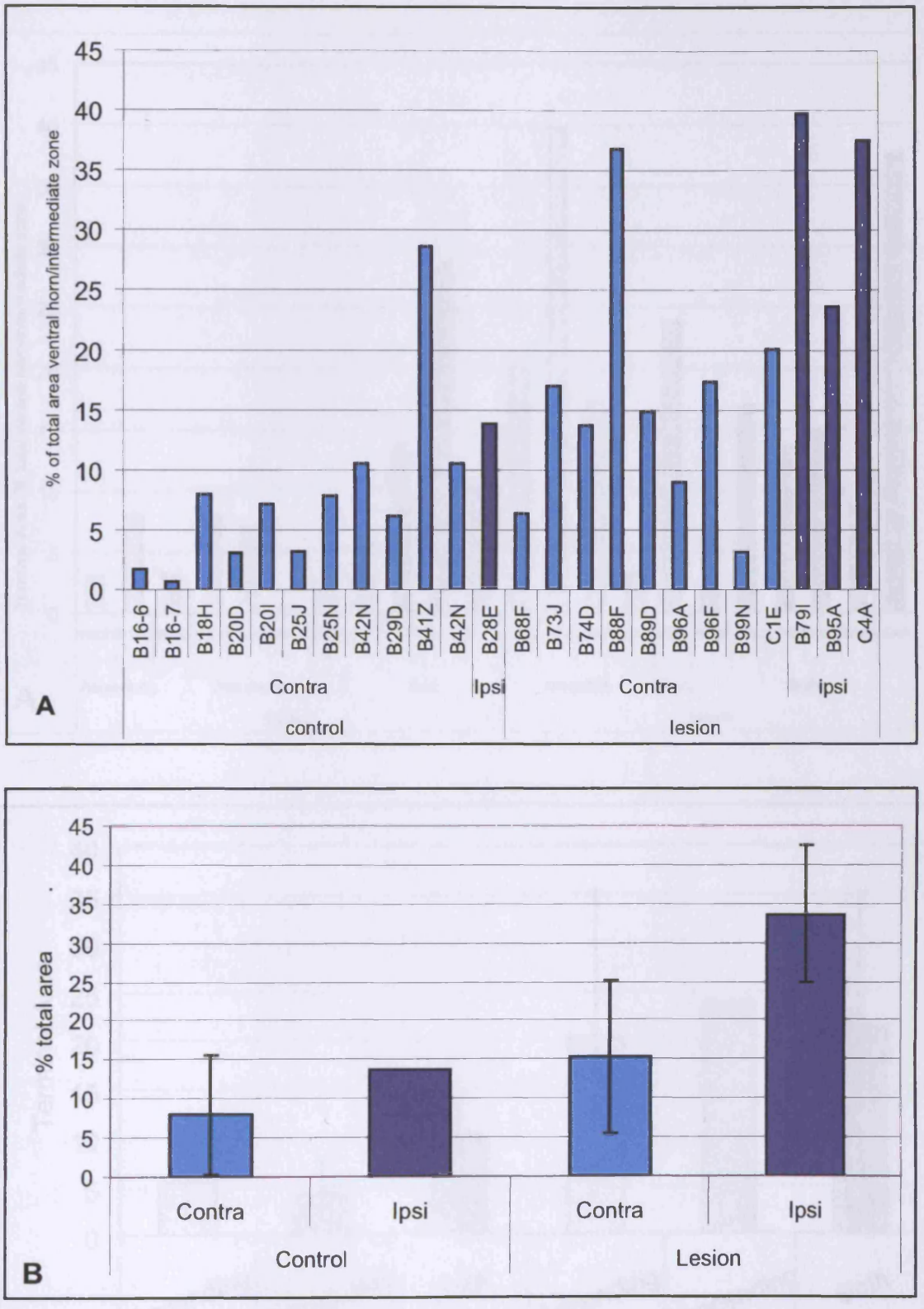

Figure 4.26: Terminal area and ipsilateral/contralateral axons.
Terminal area of axon collaterals expressed as a percentage of the total area of the ventral horn and the intermediate zone for collaterals from axons which travel on the side of the spinal cord ipsilateral to, and contralateral to the lesion (or just the soma for controls)
Note B79I had a contralateral axon but with its soma being on the side contralateral to the lesion this cell is therefore classified as having an axon ipsilateral to the lesion despite being correctly classifed as an contralateral axon in the rest of this thesis.
a) Individual cells
B) Means

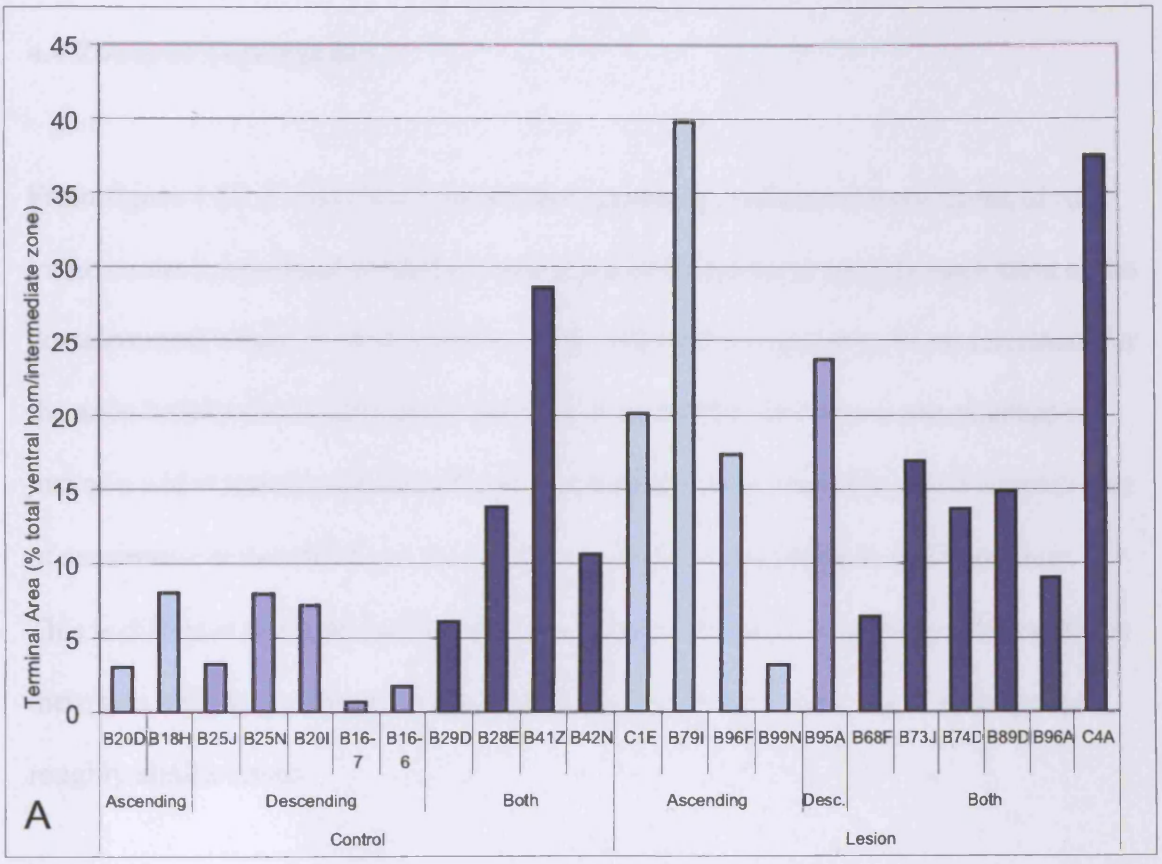

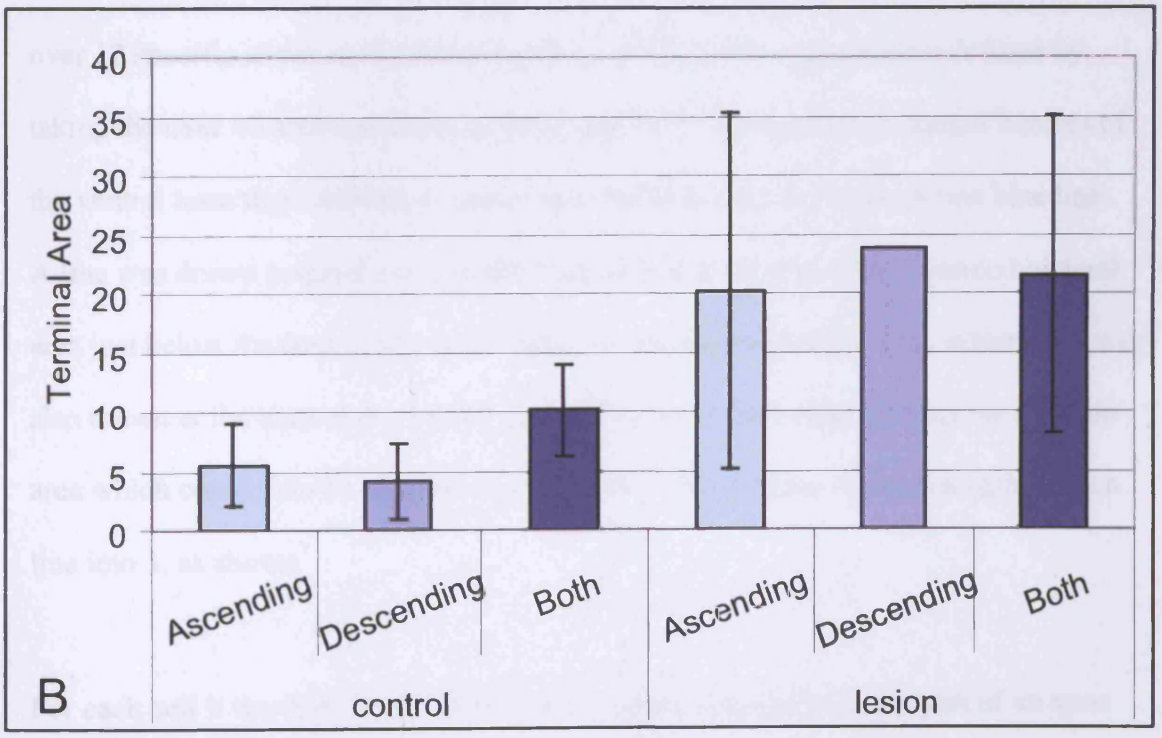

Figure 4.27: Terminal Area and axon trajectory.
Trajectories of axons and the terminal areas of the axon collateral branches, expressed as the percentage of the total area of the ventral horn / intermediate zone.
A: Individual Cells.
B: Means.

4.4 Zones of Termination

From figure 4.22 it could be observed that, generally, collaterals from axons of cells in the control population tended to have areas of termination roughly equivalent to the dorsal/ventral height to their soma location. This did not appear to be so consistent for the axon collaterals of cells in the lesioned preparation. This was a consequence not just of a wider spread of each collateral in the transverse plane but also a consequence of successive collaterals from the lesion population terminating in different areas. This is different from the pattern observed from cells on the control population where there was a tendency for successive collaterals from the same axon to terminate in roughly similar areas.

A second analysis of the termination areas looked at the how the collaterals projected over 12 specific zones as illustrated in figure 4.28. These regions were defined by taking the over all area and drawing lines parallel to the medial and lateral borders of the ventral horn then drawing a central line equidescent from both (dotted blue line). A line was drawn perpendicular to this central line at the top of the intermediolateral area just below the start of the dorsal horn. A line perpendicular to the central line was also drawn at the base of the ventral horn. Thus these four external lines enclosed an area which could then be separated into 12 zones by dividing the total length of each line into 3, as shown.

For each cell it was then noted which of the zones encompassed any part of an axon collateral. For each cell the total numbers of boxes/zones encompassing collaterals was also calculated. This data is illustrated in figures 4.29 and 4.30. From this it can

be seen that on average, collateral branches from cells in the lesioned preparation terminated in a significantly greater number of regions than controls ($P<0.003$ level, Mann Whitney). This is not surprising, being consistent with the previous result of terminal areas.

If we look at specific areas separately we see that there may be certain regions of preference for this innervation (figure 4.31). The biggest difference is that more cells from the lesion population had collaterals terminating in or near the IML region (zone 3). There also appears to be at least 50% more cells in the lesion population which terminated in zones 1 and 6.

Figure 4.28: Grid used to divide the ventral horn and intermediate zone into 12 zones.

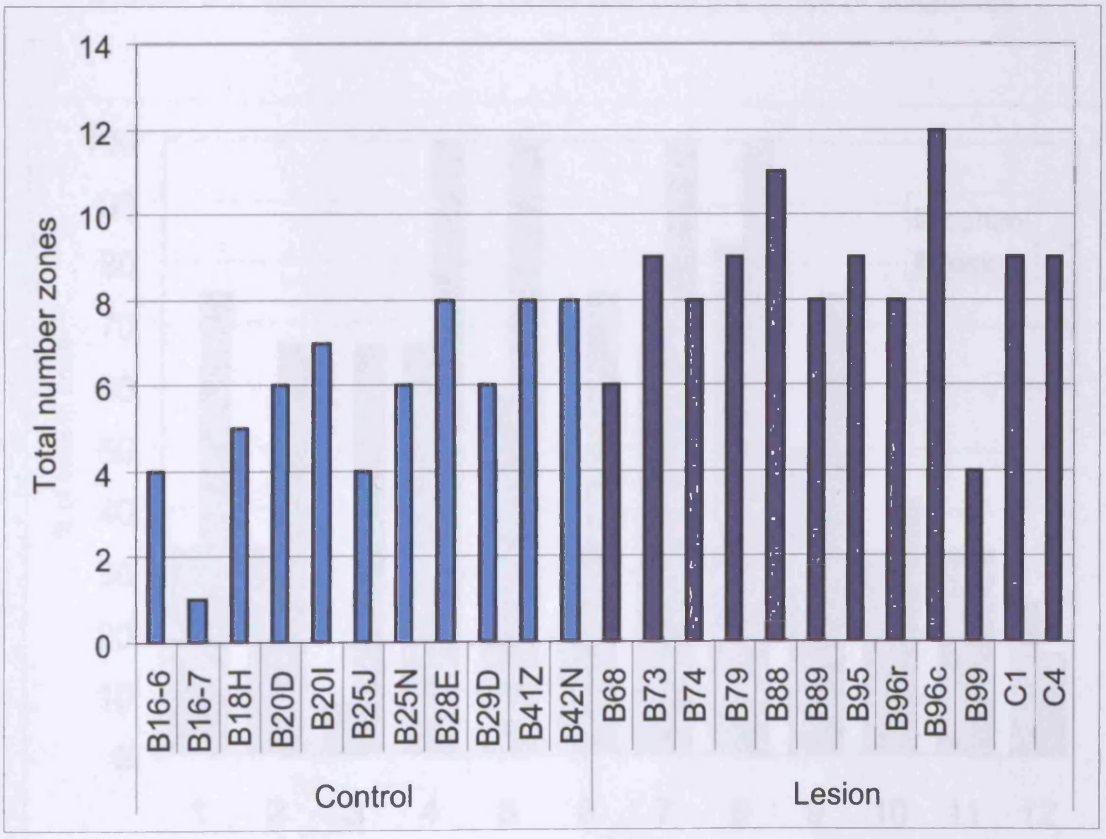

Figure 4.29: Mean number of regions from a possible twelve (see above figure) with the presence of an axon collateral from interneurones in the lesioned and the control spinal cords.

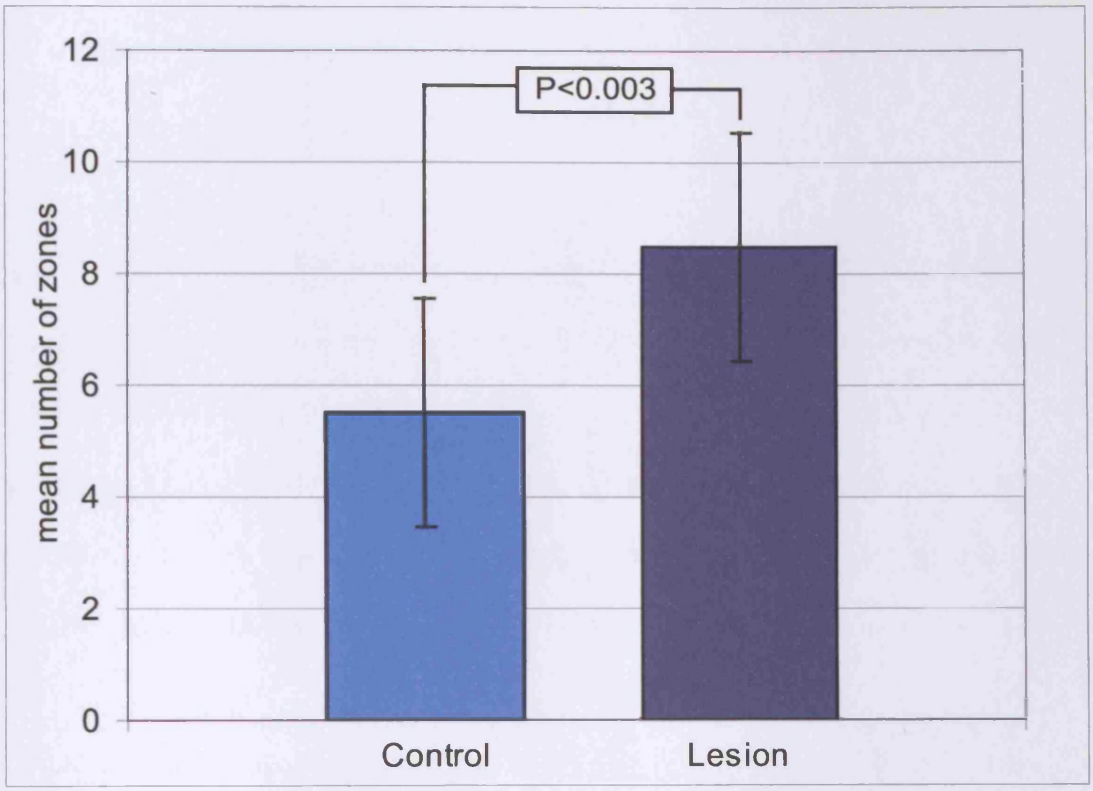

figure 4.30: Mean number of zones with the presence of collaterals.

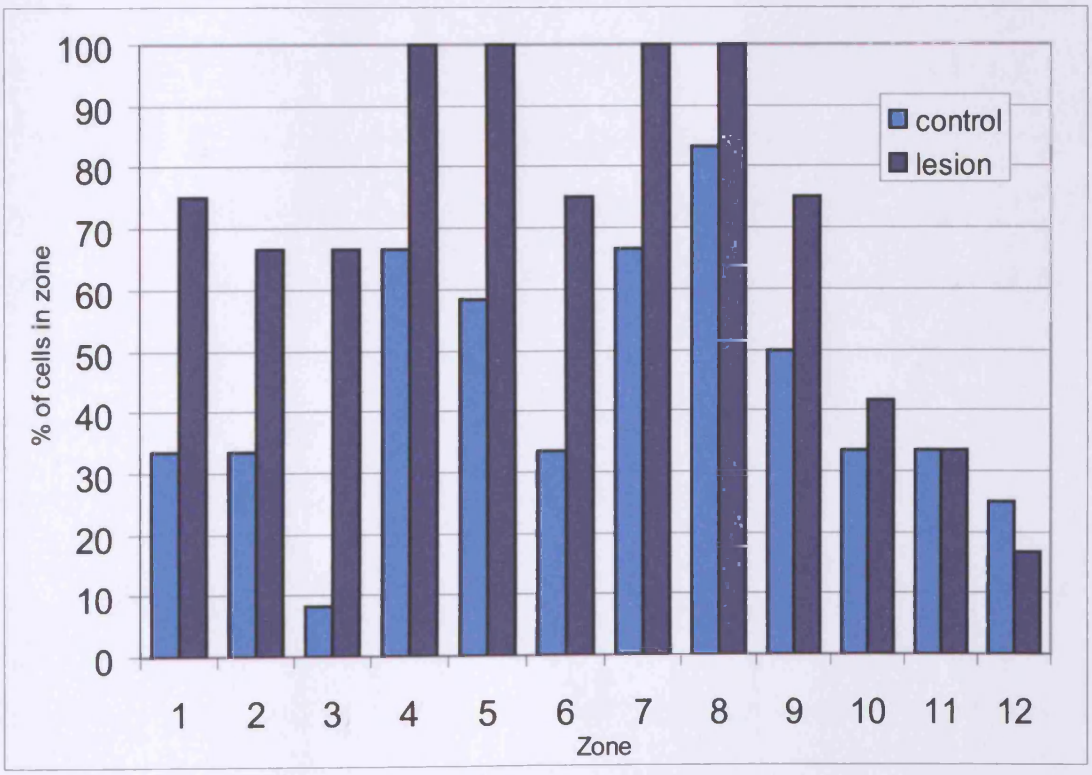

Figure 4.31: Percentage of cells from the control and lesion population which have collaterals branches with terminations or en-passant boutons in each of the 12 zones illustrated in figure 4.28.

Chapter 5

Dendritic Trees

Nine interneurones from the lesioned spinal cord had dendrites sufficiently well labelled to allow full reconstructions of their dendritic trees. Three of these had been labelled at survival time of 6-8 weeks and 6 at survival times of 16-18 weeks. Dendritic trees were reconstructed by hand at 40x magnification (except B77 at 20X). The dendritic trees of these cells can be compared with reconstructions of 8 cells from the control population labelled by S. A. Saywell (2000).

5.1 Rostro-caudal extent of dendrites.

The overall rostro-caudal extent of the dendrites for each cell is illustrated in figure 5.1a (along with the rostral caudal extent of 2 other non-reconstructed cells from the control population). From the means there is only a slight difference between the two populations and a Mann-Whitney statistical comparison confirmed no significant difference between the control and lesion population in terms of overall rostro–caudal extent of dendrites (figure 5.1b). From figure 5.1a it can also be deduced that there appears to be no obvious difference within cells between the rostral extent of the dendritic tree and the caudal extent for both populations.

If interneurones from the two survival time groups are considered separately (figure 5.2a) there is no statistically significant difference between the control group and the 16-18 weeks survival group (numbers in the 6-8 week survival groups are too small to allow statistical analysis).

Similarly, the distance of the soma from the start of the lesion does not appear to influence the overall rostro –caudal extent of the dendritic tree (figure 5.2b).

However the interneurones of the lesioned population showed a number of highly unusual features which marked them out as different from the control group that will be described in the rest of this chapter.

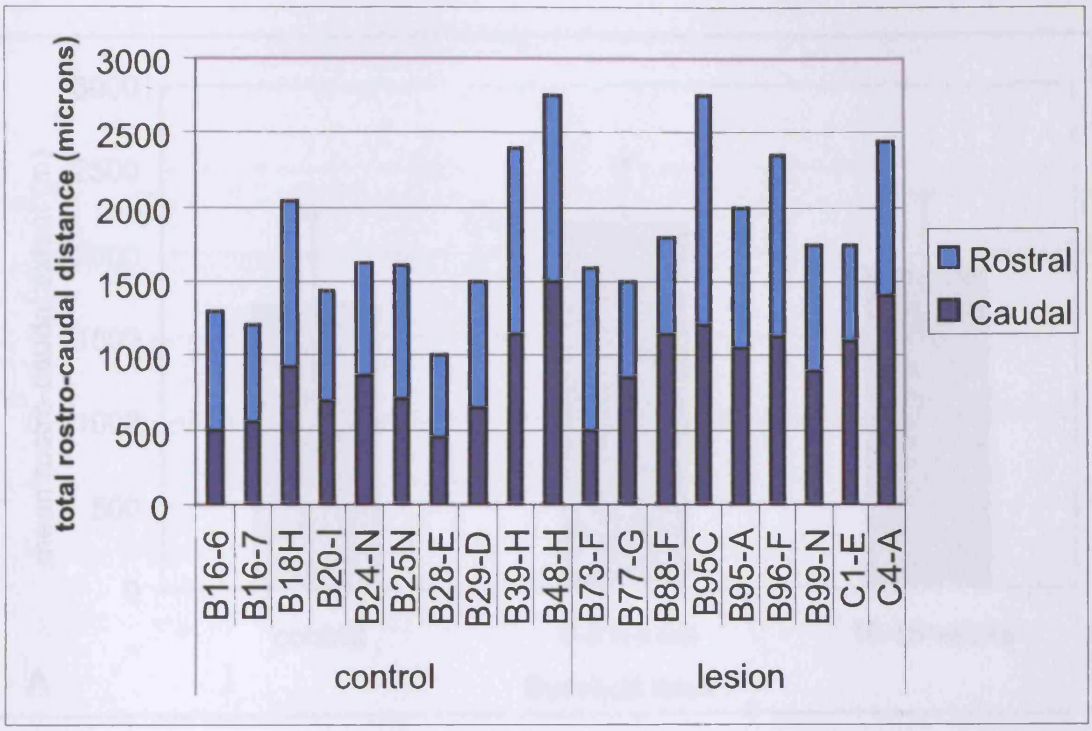

A

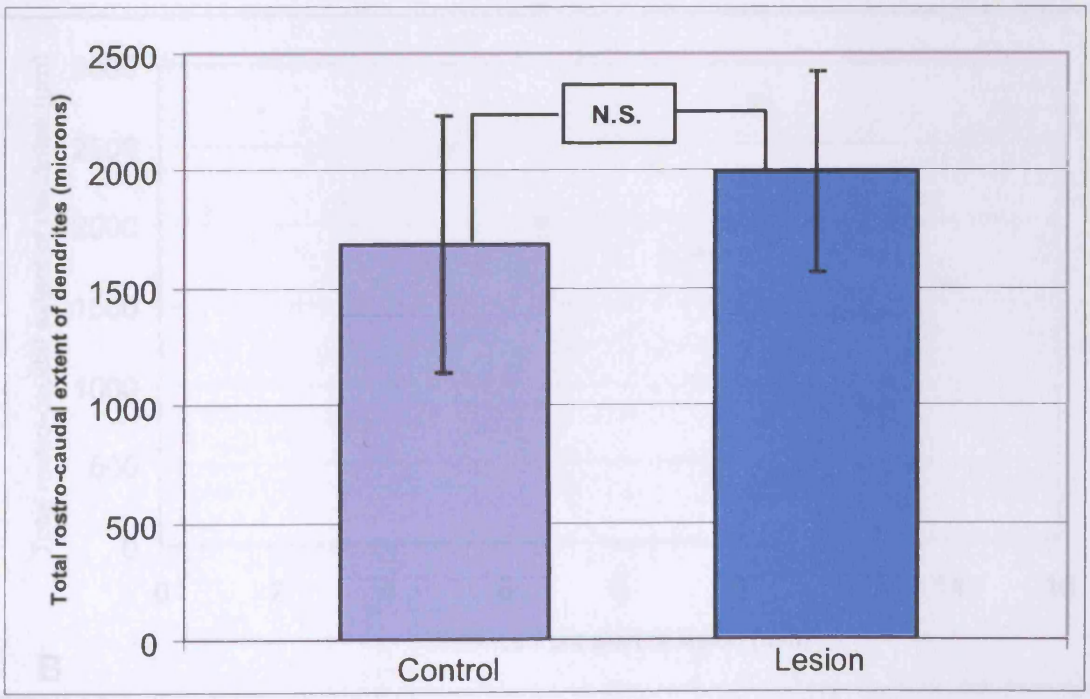

B

Figure 5.1 Total extent of the dendritic trees of interneurones in the rostro-caudal axis.

A: For individual cells, with separate extents for those dendrites rostral to the soma and those caudal to the soma.
B: Mean rostro-caudal extent of dendritic trees for the control and leison populations.

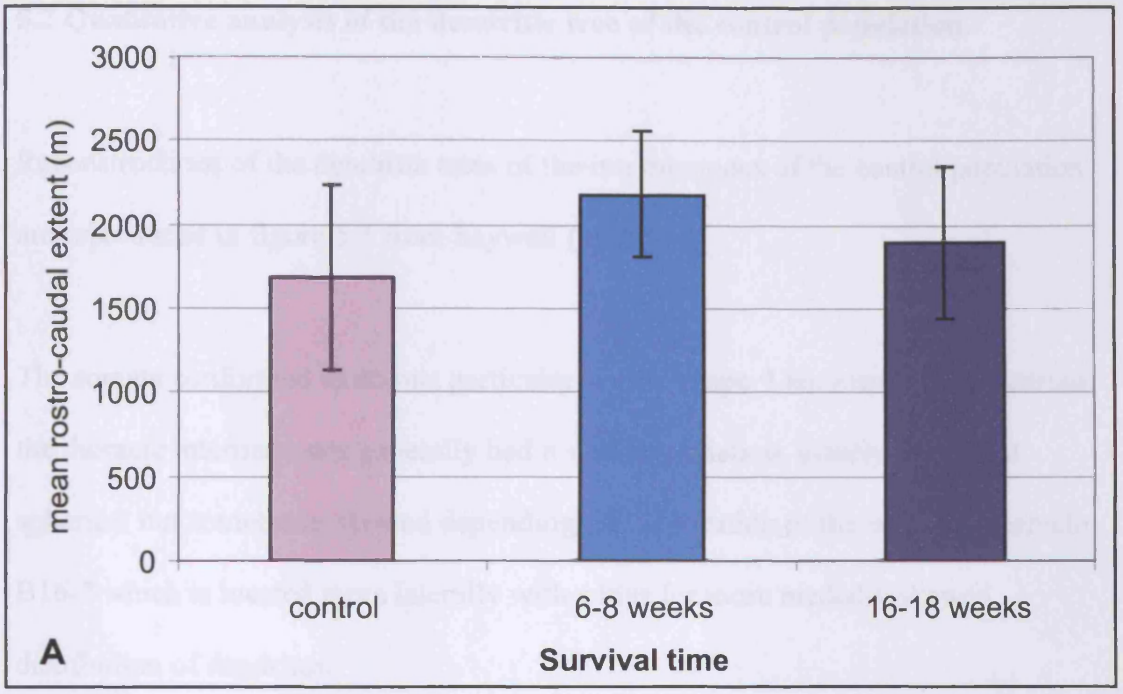

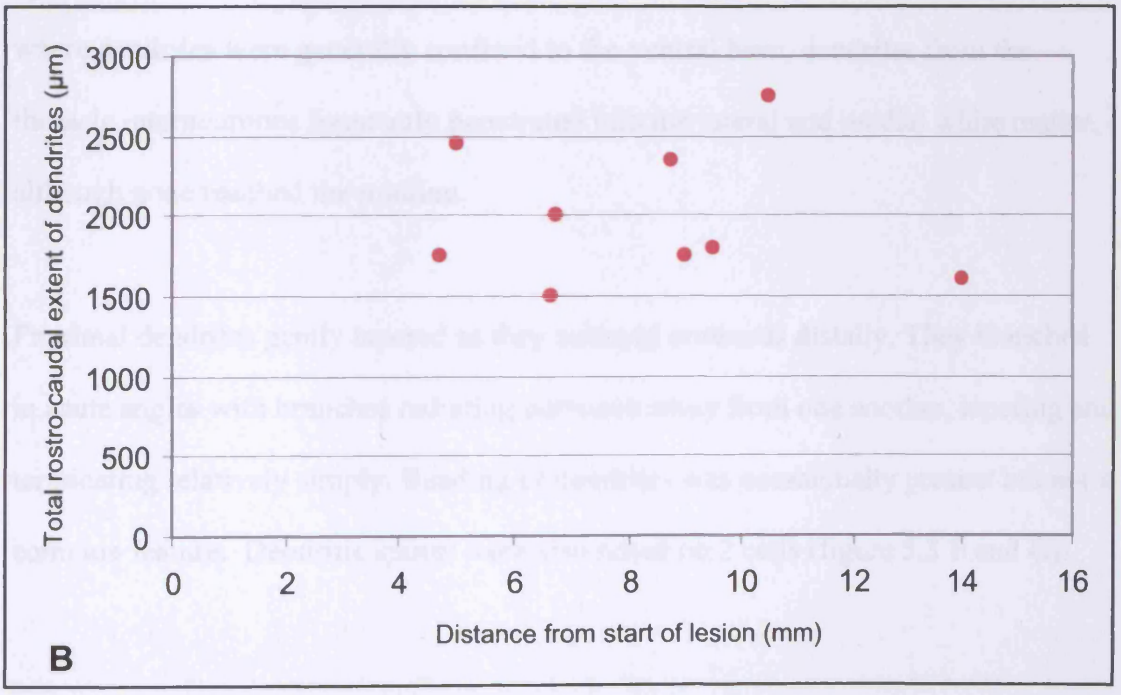

Figure 5.2: Rostro-caudal extent of dendritic trees of the interneurones
A) with respect to survival time post lesion.
B) with respect to the distance of the soma from the start of the lesion (each point represents an interneurone from the lesion population).

5.2 Qualitative analysis of the dendritic tree of the control population.

Reconstructions of the dendritic trees of the interneurones of the control population are reproduced in figure 5.3 from Saywell (2000).

The somata conformed to no one particular size or shape. Like many spinal neurons the thoracic interneurones generally had a stellate radiation, usually somewhat spherical but sometimes skewed depending on the location of the soma for example B16-7 which is located more laterally with a bias for more medially skewed distribution of dendrites.

Unlike the descriptions of thoracic motoneurones of Lipski and Martin-Body (1987) where dendrites were generally confined to the ventral horn, dendrites from the thoracic interneurones frequently penetrated into the lateral and medial white matter, although none reached the midline.

Proximal dendrites gently tapered as they radiated outwards distally. They branched in acute angles with branches radiating outwards away from one another, tapering and terminating relatively simply. Beading of dendrites was occasionally present but not a common feature. Dendritic spines were also noted on 2 cells (figure 5.3 E and G).

Figures 5.3

Reconstructions of the interneurones from the control population

Reproduced with permission from Saywell 2000

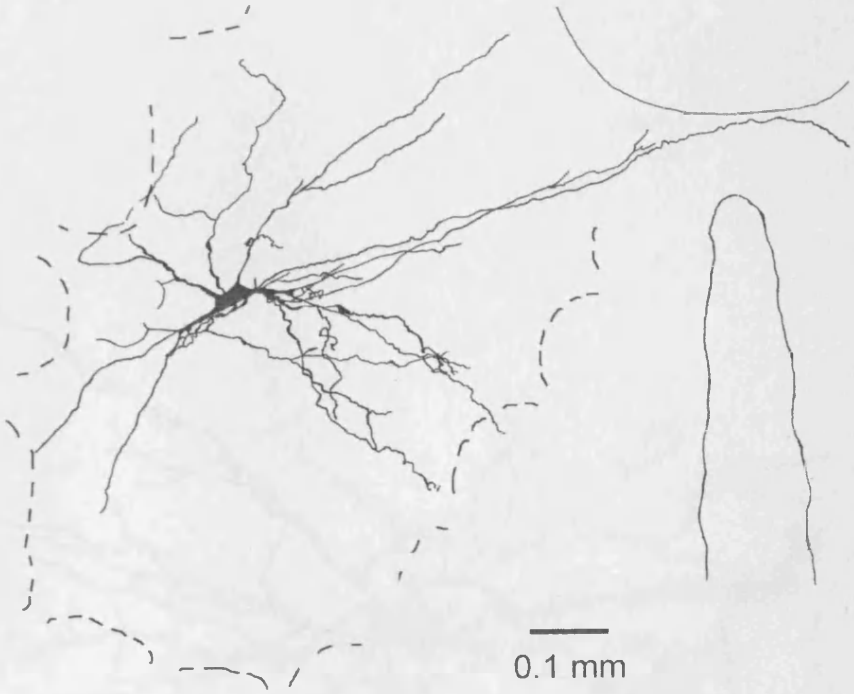

A: Reconstruction of Cell B16-6.

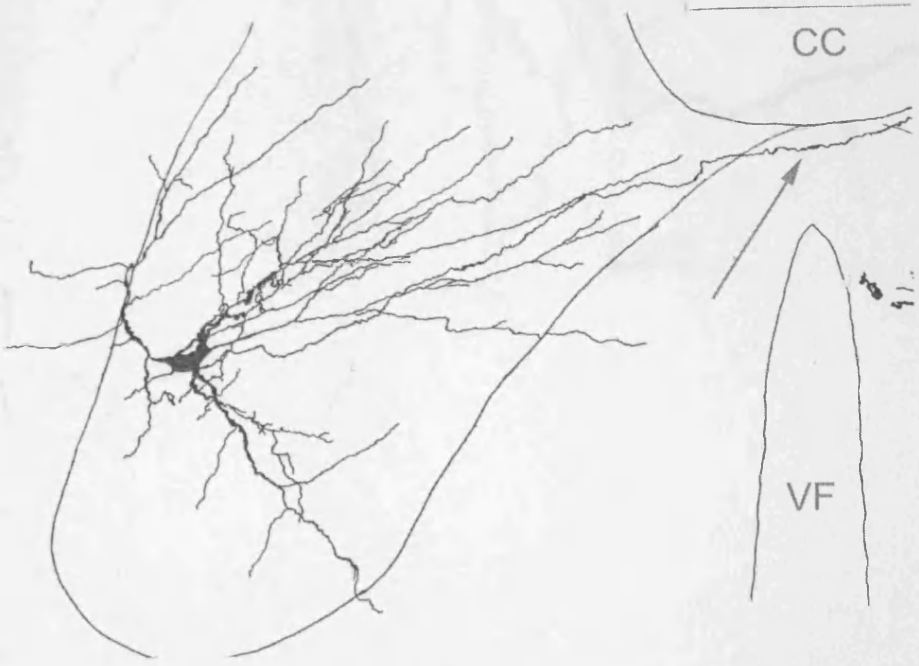

B: Reconstruction of Cell B16-7.

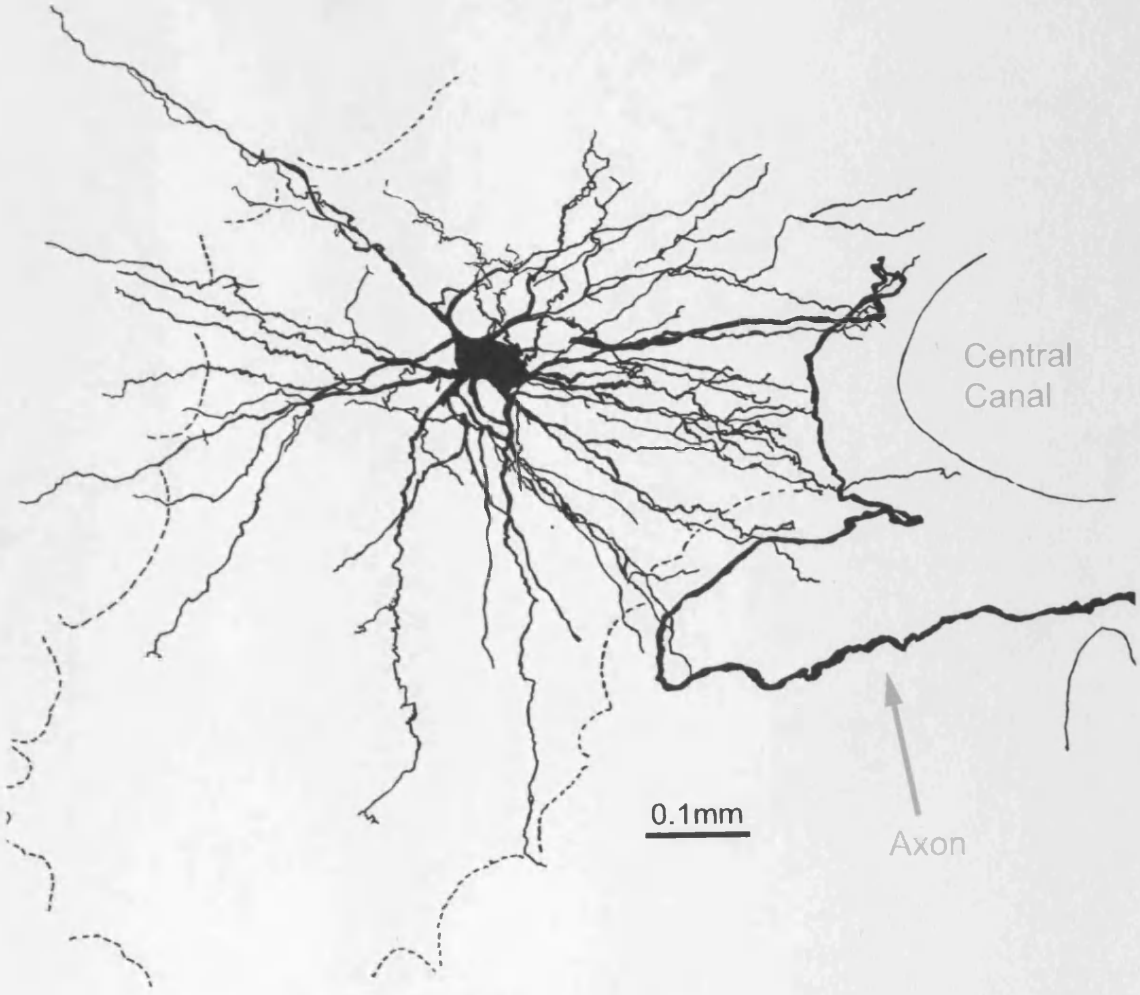

C: Reconstruction of Cell B18-H.

164 →

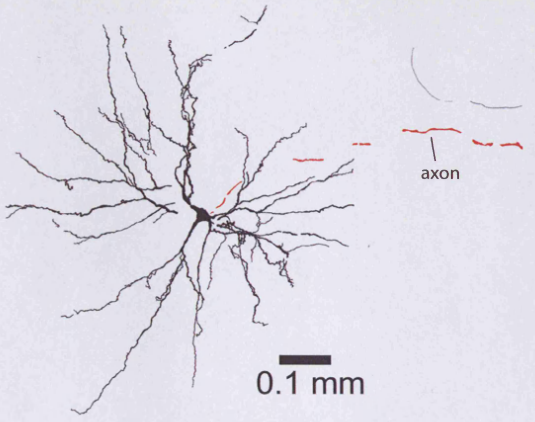

D: Reconstruction of Cell B20l.

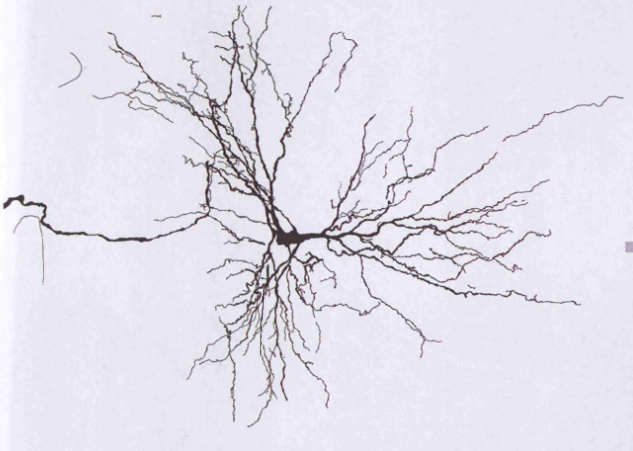

E: Reconstruction of Cell B24N

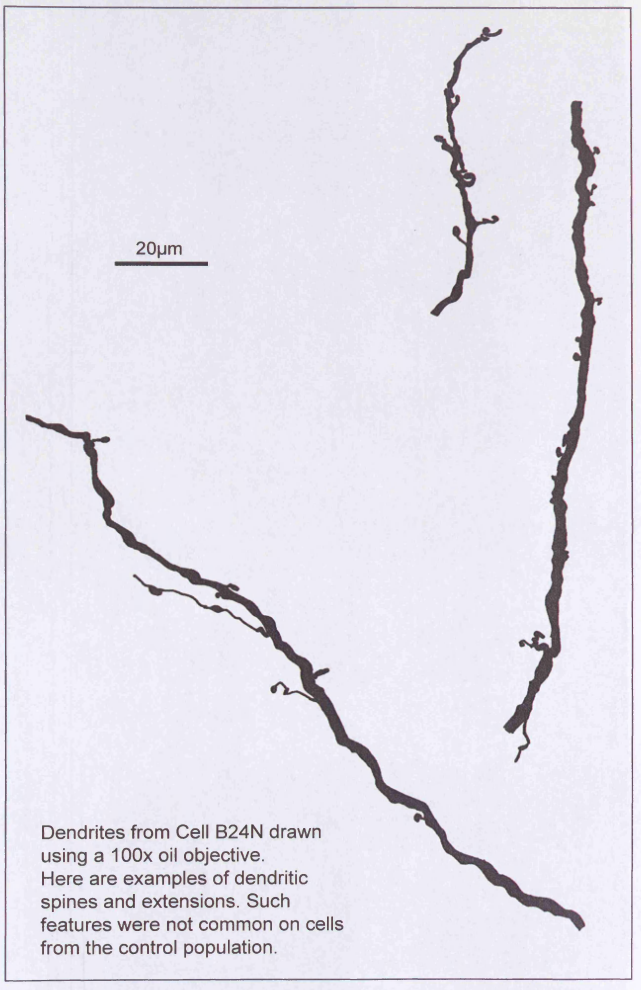

Dendrites from Cell B24N drawn using a 100x oil objective. Here are examples of dendritic spines and extensions. Such features were not common on cells from the control population.

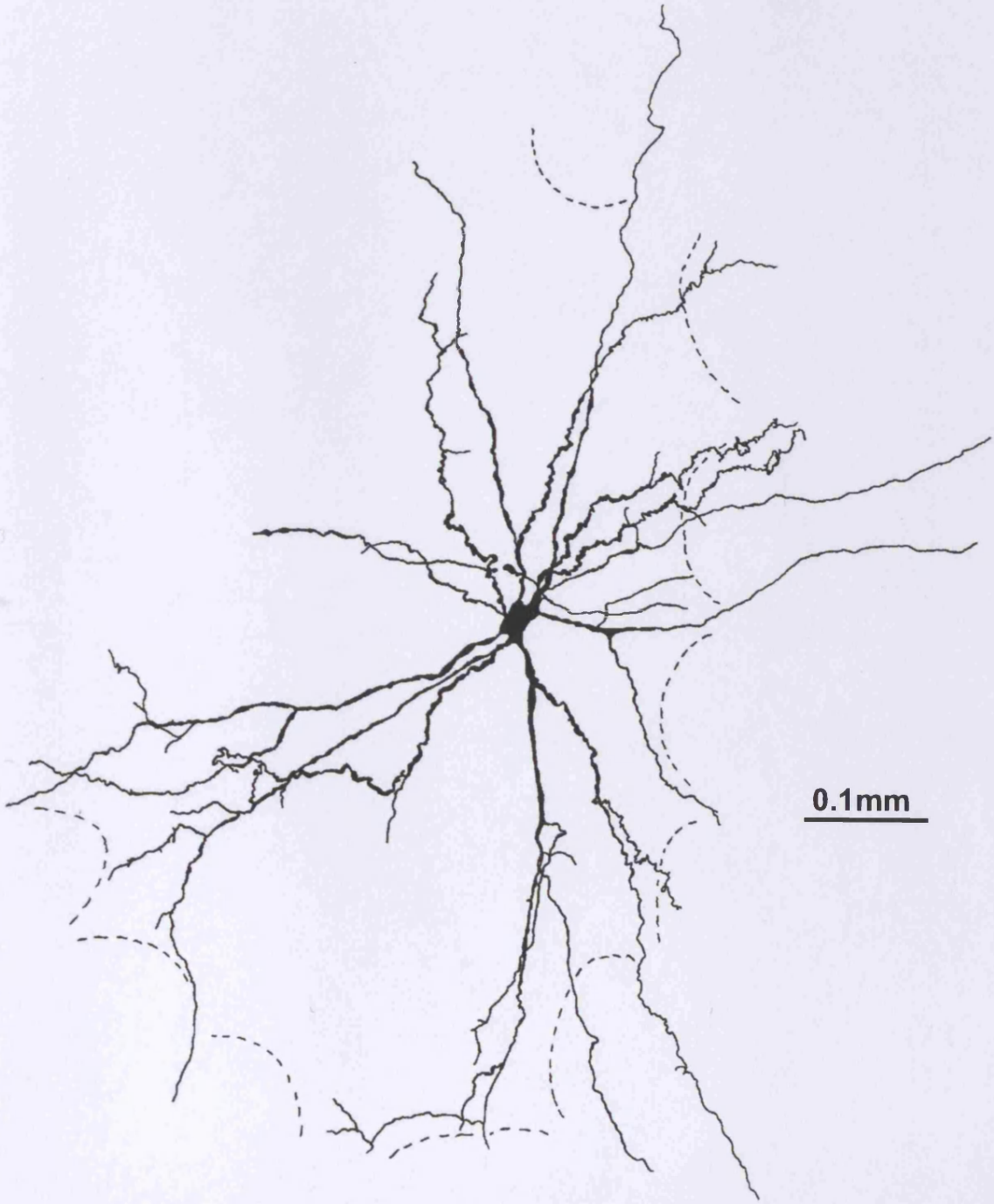

F: Reconstruction of Cell B25N

G: Reconstruction of Cell B28E
Note: Pieces of collateral branches from the axon of this cell, at the level of the dendritic tree, are included on this reconstruction.

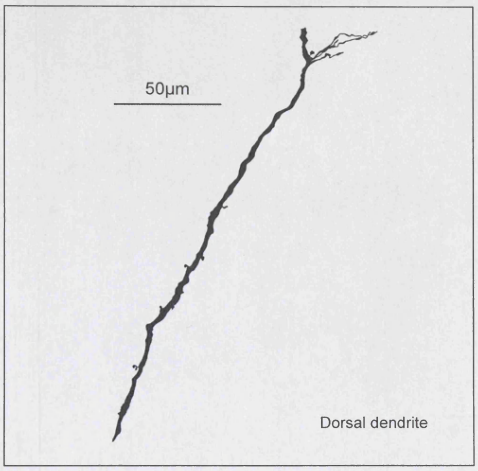

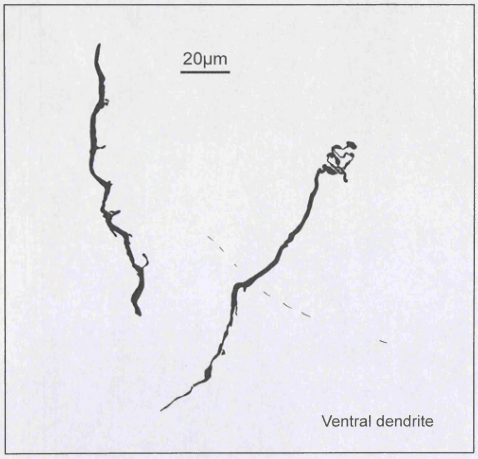

Dendrites from Cell B24N drawn using a 100x oil objective. Here are examples of dendritic spines and extensions. Such features were not common on cells from the control population.

166 →

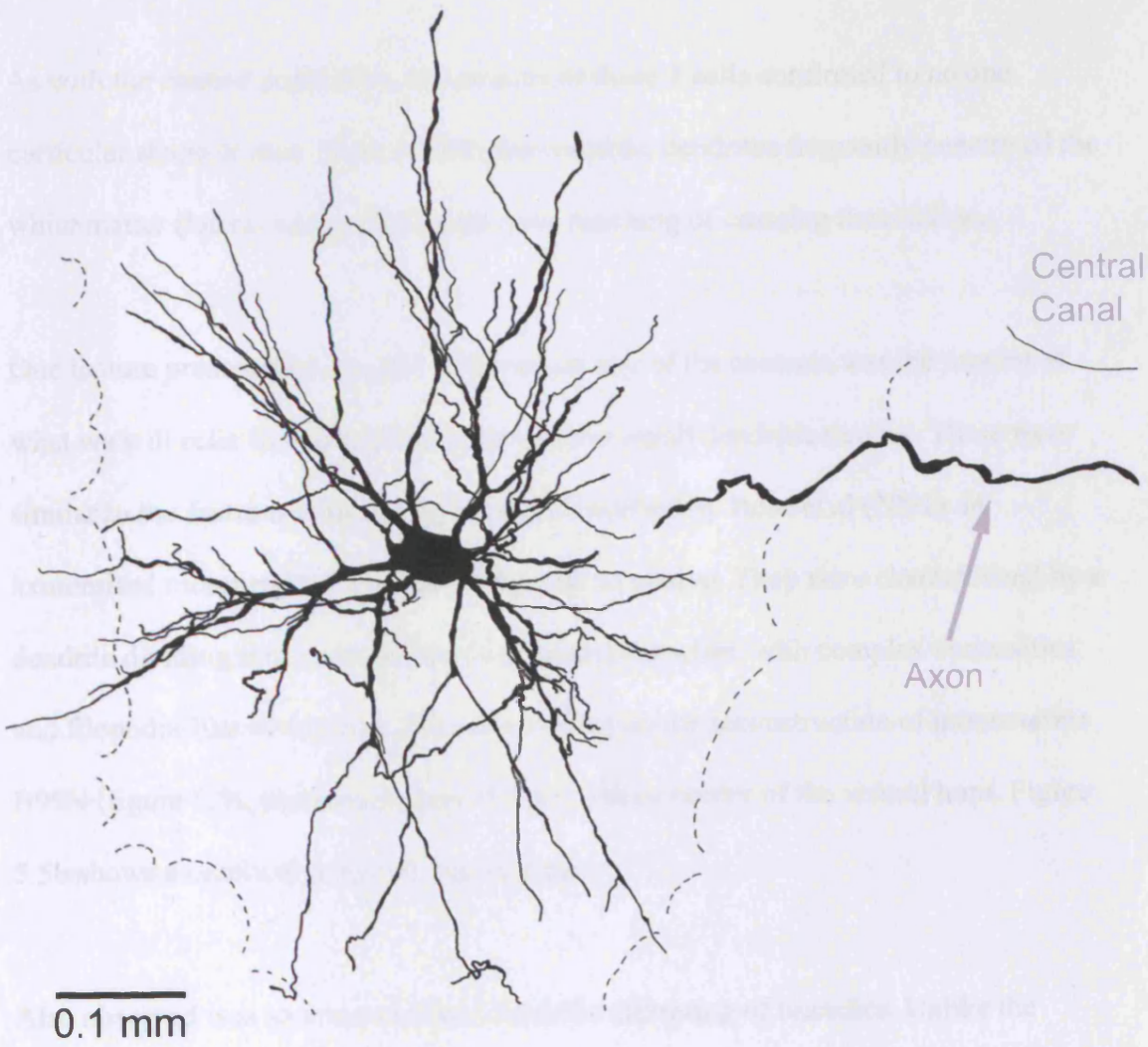

H: Reconstruction of cell B29D

5.3 The 6-8 week survival time interneurones.

Three cells were labeled and reconstructed at survival times of 6-8 weeks. These are illustrated on figures 5.4-5.6

As with the control population, the somata of these 3 cells confirmed to no one particular shape or size. Also, as with the controls, dendrites frequently penetrated the white matter (lateral and medial) with none reaching or crossing the midline.

One feature present that was not observed on any of the controls was the present of what we will refer to as dendritic tortuosities or small dendritic tangles. These were similar to the features with the same name described by Rose et al (2001) in axotomised motoneurones, but generally less extensive. They were characterized by a dendrite dividing into multiple fine intertwined branches, with complex varicosities and filopodia-like extensions. They are evident on the reconstruction of interneurone B99N (figure 5.5), particularly near the grey/white border of the ventral horn. Figure 5.5b shows a confocal image of one of these.

Also observed was an unusual distal dendritic clustering of branches. Unlike the control interneurones, where dendritic branches radiated outwards away from each other, all 3 interneurones from the 6-8 week sample had some dendrites that twisted helically around each other. Examples of these are noted on the illustrations of each of these cells (figure 5.4-5.6). This was never observed in the control population.

Another unusual feature consisted of dendrites branching at right angles. This right angled branching was not a feature of the control population (nor is it regarded as a feature of dendrites in general) and is more commonly associated with axons. This feature is harder to detect in the two-dimensional reconstructions but some examples are indicated in figures 4.5 and 4.6.

Beading is feature of intracellularly filled neurones. Dendritic beading can be described as beads on a string. It was present on some cells of the control group, although not common. Beaded dendrites were also seen on interneurones from the lesioned population. Some conformed to this "beads-on-a-string" description (figure 5.5c) where as others were irregular and best described as dendritic swellings or varicosities, occurring in thicker dendritic processes as well as finer ones and being less regular in shape. The process of sectioning and subsequent reconstruction of the dendrites sometimes gives a swollen appearance to dendrites. Many of the swelling on these dendrites however occurred within the middle of a histological section and thus we can be confident they represent true varicosities. These varicosities were a common feature of these dendrites, although not appearing on all dendrites of a cell. Their occurrence on selected dendrites would suggest they may be more than merely an artifact of the processes of intracellular filling. Given the irregular and varied nature of these swellings on a continuum from those that could be classified as beads those that could be classified as varicosities with hybrids of the two between makes it hard to quantify this abnormality. It can merely be stated that this feature occurred frequently on the dendrites of the cells from the lesioned population, more commonly than that of the control population.

Another feature was processes with multiple small fine protrusions giving the dendrite a hairy appearance. This is illustrated on figure 5.5a and c. As a group these protrusions differ from conventional descriptions of dendritic spines (Falia and Harris (1999). They were very variable on form, often branched, some ending in swellings, some filopodia like, some quite long (up to 20 μm) and they were often seen on association with twisted dendrites (fig 5.5b), varicosities (Fig 5.5A) pr tortuosities (fig5.8). The dendritic spines observed on the two interneurones from the control population were more conventional in appearance.

Some dendrites also showed abnormal tapering and termination such as a thick untapering dendrite that tapered suddenly at the end. In the example noted in figure 5.6 the dendrite suddenly tapered at one point in a tear-drop like shape then became very fine at the very end.

Figures 5.4 – 5.6

Reconstructions of interneurones labelled at survival times of 6 -8 weeks

172 →

Figure 5.4
Reconstruction of thoracic interneurone B96F .
This interneurone was 8.75mm rostral to the start of the lesion and labelled at 7 weeks survival time. The rostral and the caudal dendrites of this cell were assymetric.

73 →

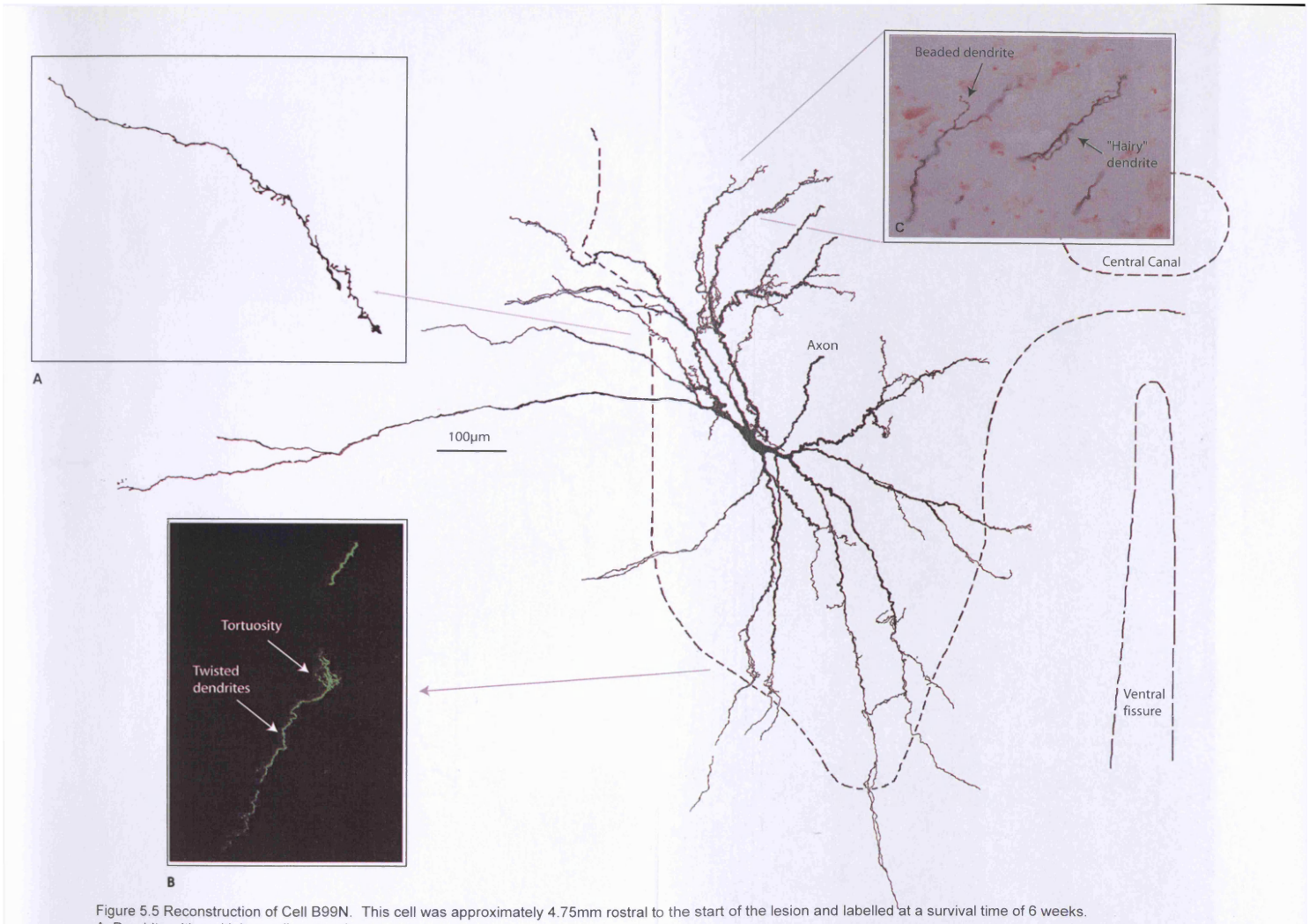

Figure 5.5 Reconstruction of Cell B99N. This cell was approximately 4.75mm rostral to the start of the lesion and labelled at a survival time of 6 weeks.
A: Dendrite with multiple small protrustions.
B: Confocal image of a dendritic tortuosity at the border of the ventral horn with twisted dendrites emanating from the tangle.
C: Photomicrograph of a beaded dendrite and a "hairy" dendrite with multiple small fine protrusions.

174 →

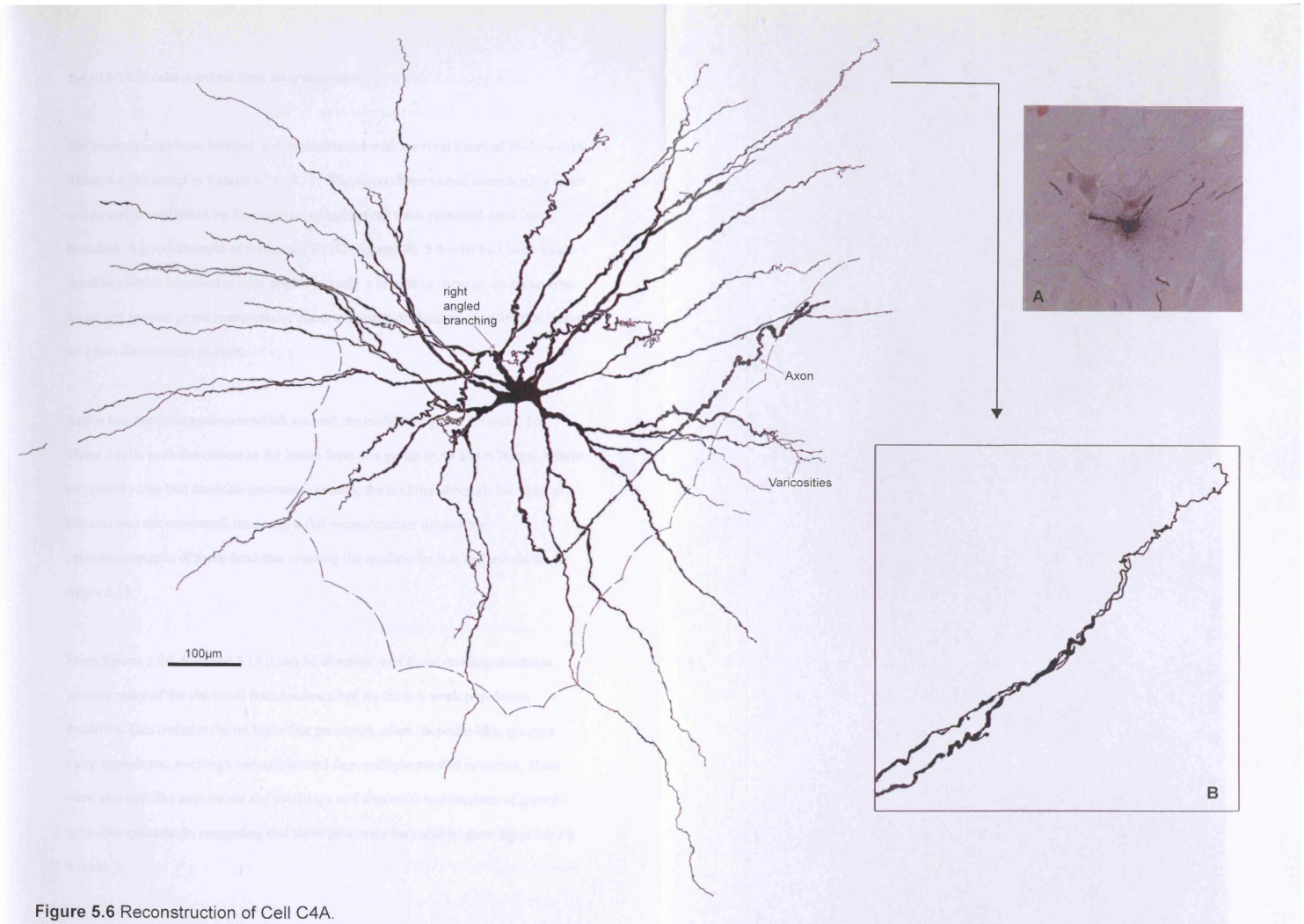

Figure 5.6 Reconstruction of Cell C4A.
This cell was approximately 5mm from the start of the lesion an was labelled at a survival time of 8 weeks. This cell was respiratory modulated, showing a reduction in discharge during inspiration.
Inset: A, Soma, B, twisted dendrites.

abnormal feature was that of an un-even distribution of dendrites rostral to the soma compared with those caudal to the soma. Figure 5.14 (B88F) shows a perfect example of this, with dendrites rostral to the soma laying lateral to the soma and dendrites caudal to the soma directed medially towards the midline. This asymmetry was the case for 7/9 of the cells from the lesioned group (6-8 and 16-18 weeks survival times). This usually consisted of the caudal dendrites favouring the medial/dorsomedial regions. No asymmetrical cases like this were reported for the control population by Saywell (2000). The only cells from the lesioned population not showing this asymmetry were the 2 furthest away from the lesion (B73F: 14mm and B95C: 10.5mm). The remaining, asymmetrical cells were all within 10mm of the start of the lesion.

Figures 5.7 – 5.12

Reconstructions of interneurones labelled at survival times of 16 -18 weeks

179 ⟶

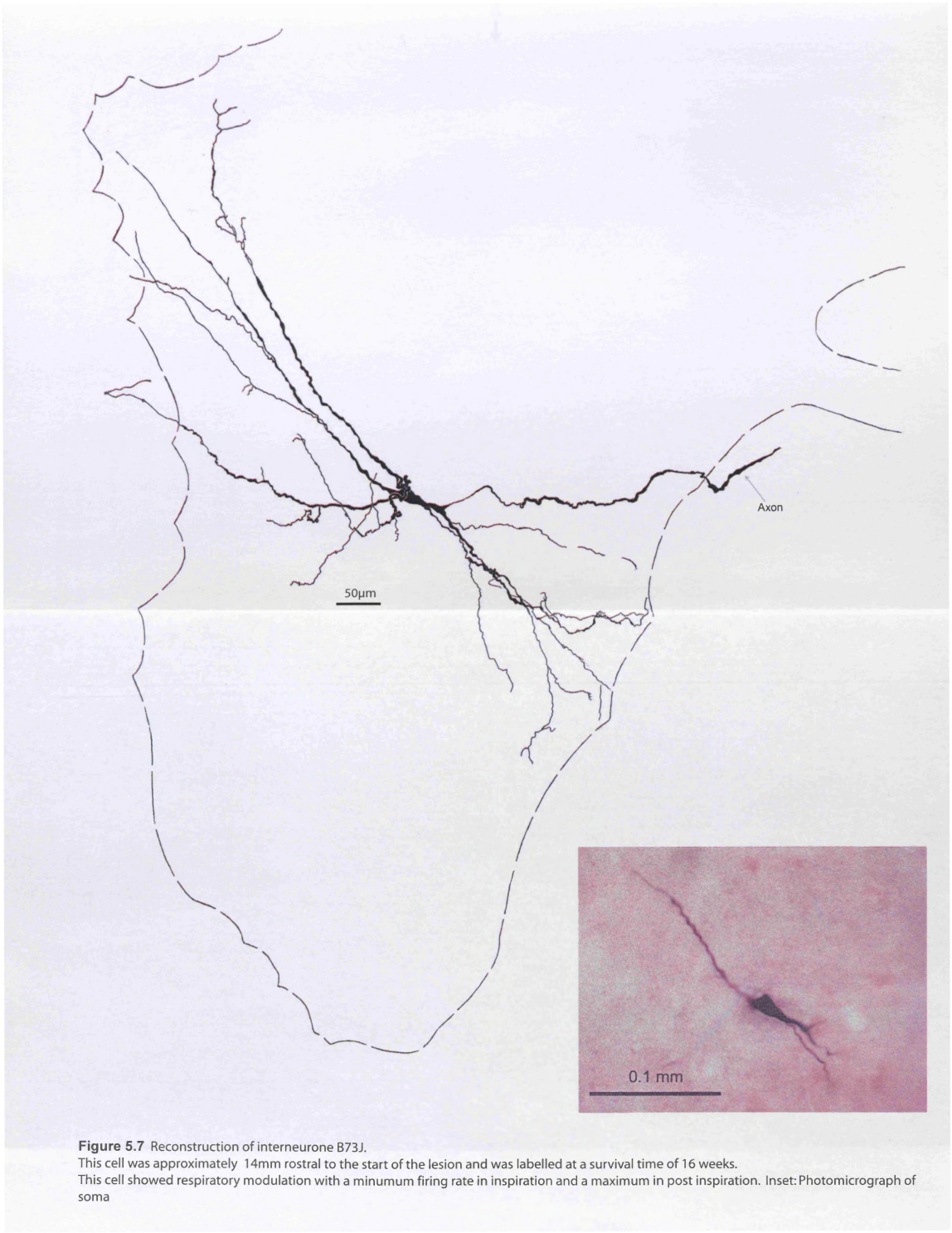

Figure 5.7 Reconstruction of interneurone B73J.
This cell was approximately 14mm rostral to the start of the lesion and was labelled at a survival time of 16 weeks.
This cell showed respiratory modulation with a minumum firing rate in inspiration and a maximum in post inspiration. Inset: Photomicrograph of soma

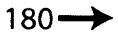
180

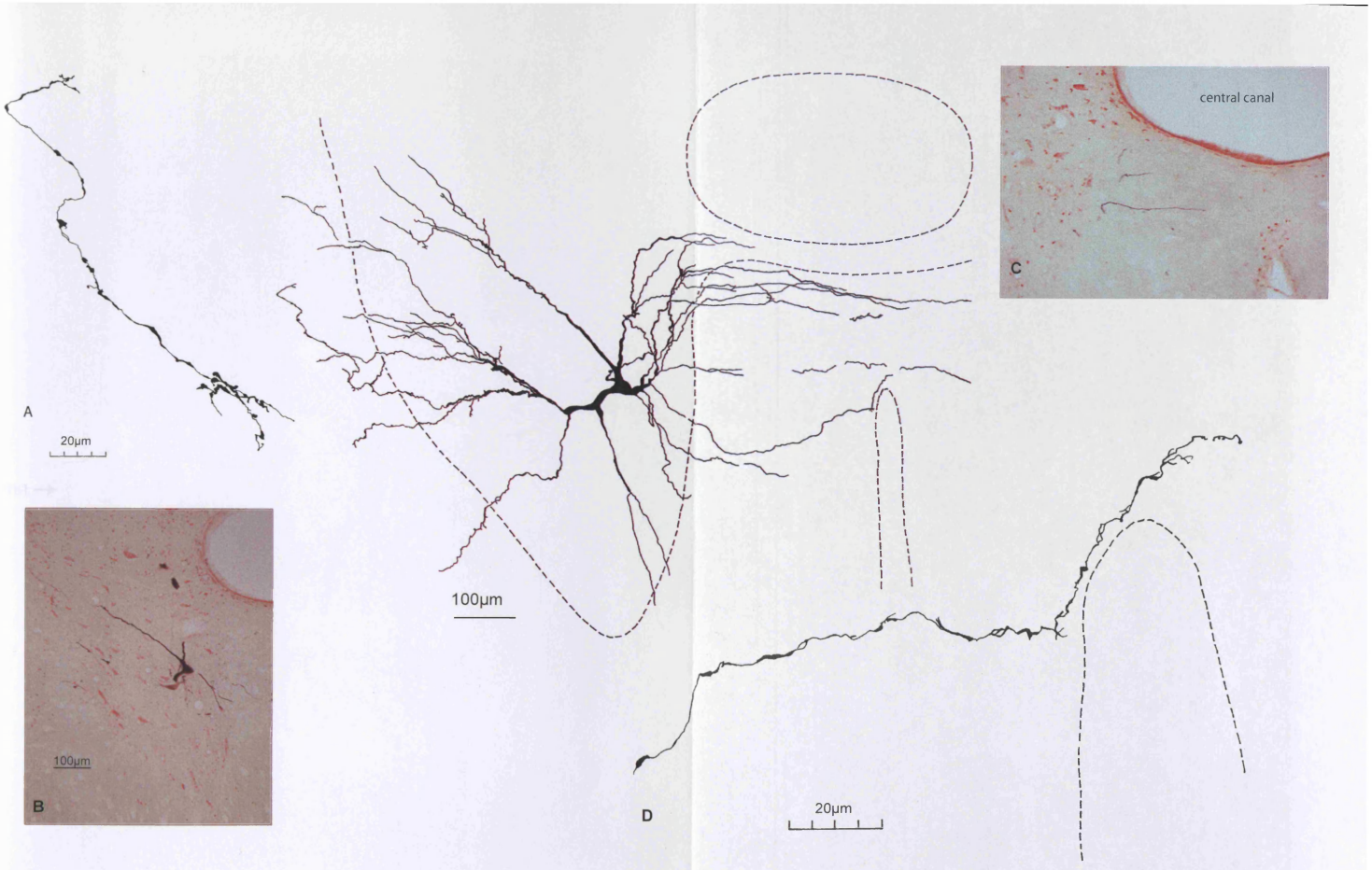

Figure 5.8 Reconstruction of Cell B77G.
This cell was 6.65mm rostral to the start of the lesion and was labelled at a survival time of 16 weeks.
This cell showed respiratory modulation, firing spikes in inspiration.
A: White matter dendrite with beading/varicosites drawn at 100x magnification.
B: Photomicrograph of the soma.
C: Photomicrograph of dendrites which, after having travelled together in the rostro-caudal direction, suddenly turned at the same rostro-caudal level to head towards the midline
D: Dendritic process crossing the midline with multiple small fine protrusions (drawn at 100x magnification)

181 →

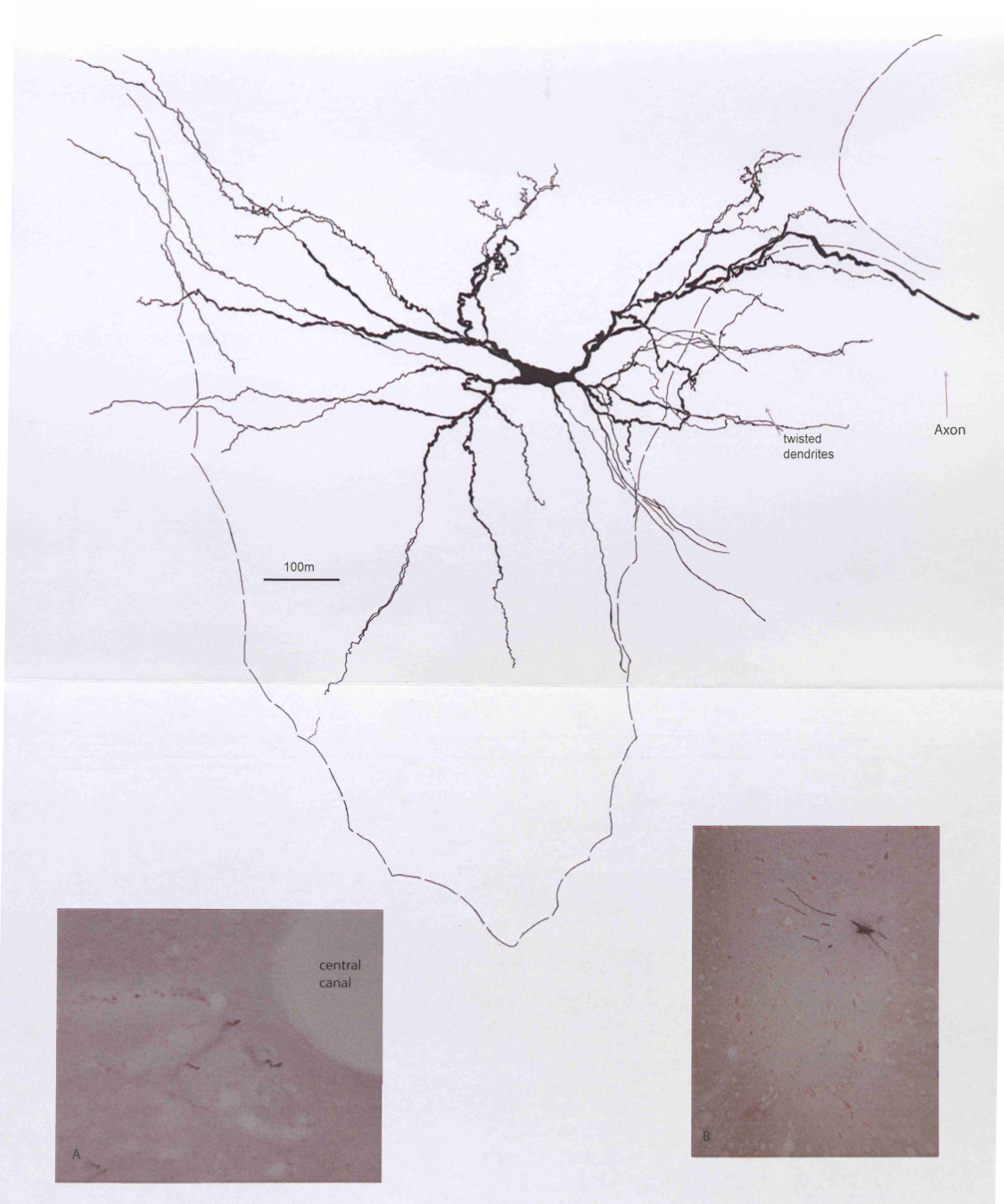

Figure 5.9 Reconstruction of a thoracic interneurone B88F
This cell was approximately 9.5mm fom the start of the lesion aand was labelled at a survival tme of 16 weeks. This cell was assymetric in the sagittal plane with rostral dendrites laying lateral to the soma, caudal dendrites laying medial to the soma towards the midline.
A: Rostro-caudally running dendrites suddenly turning to head towards the midlines on the same plane as the axon.
B: the soma

182 →

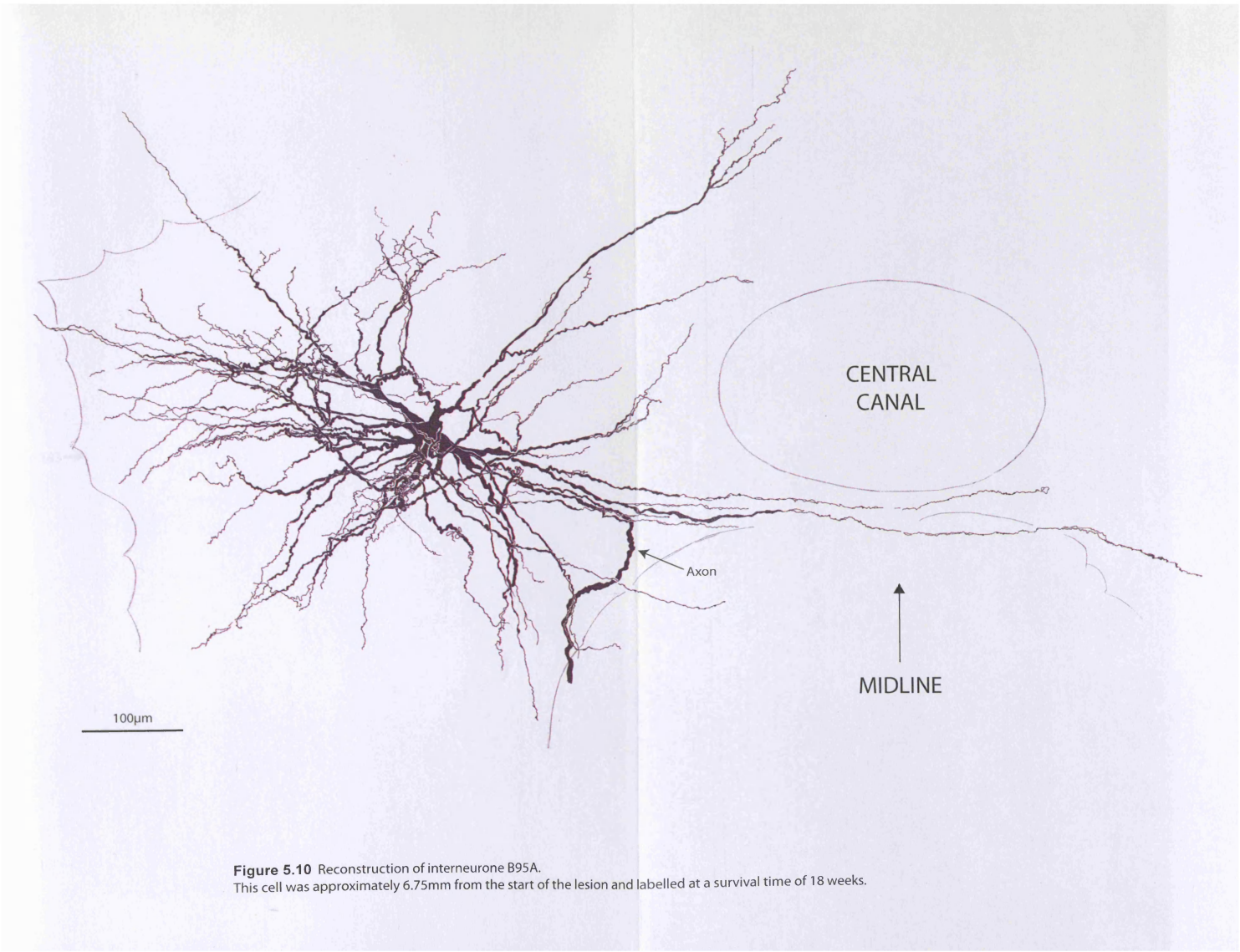

Figure 5.10 Reconstruction of interneurone B95A.
This cell was approximately 6.75mm from the start of the lesion and labelled at a survival time of 18 weeks.

183 →

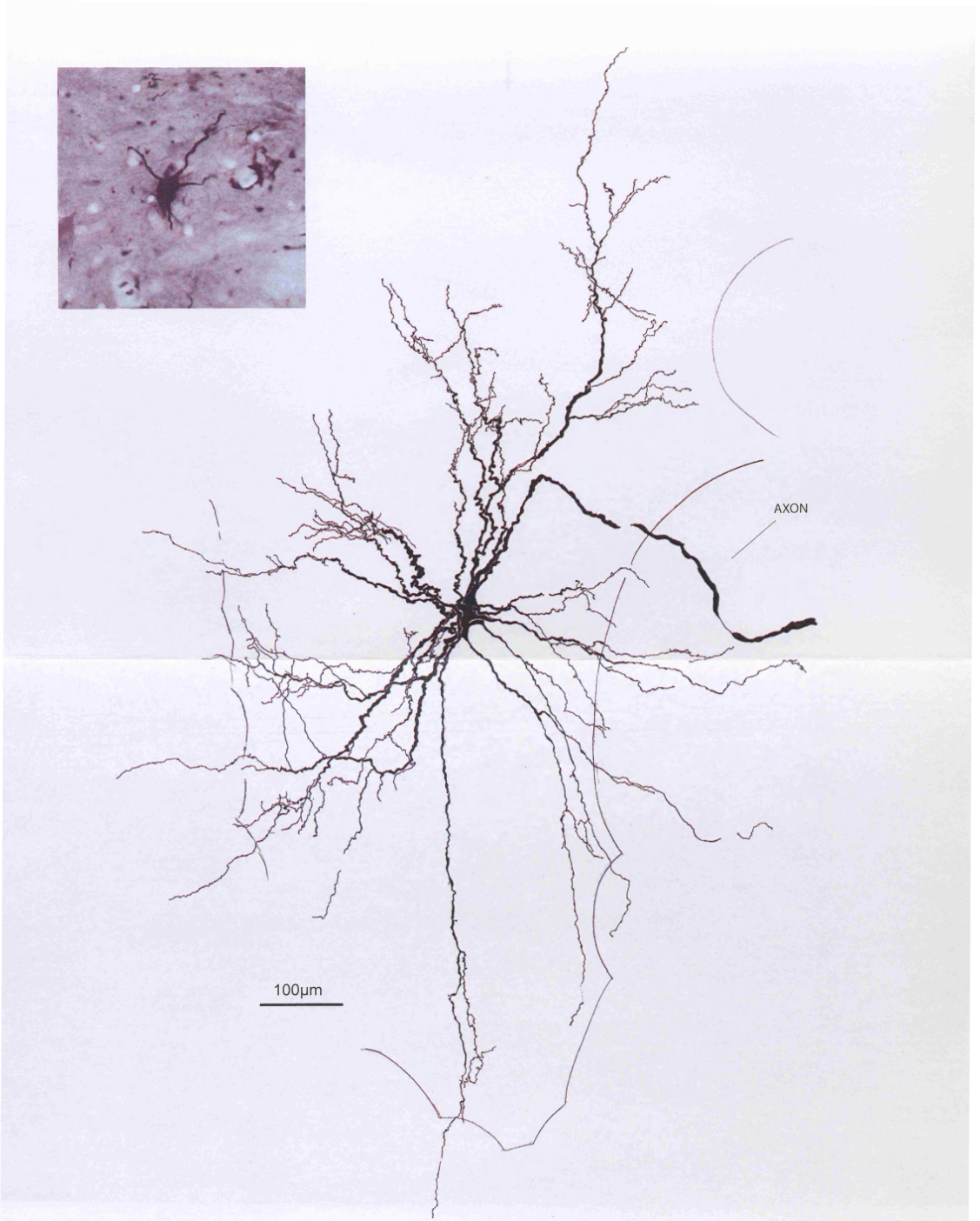

Figure 5.11 Reconstruction of interneurone B95C
This cell was approximately 10.5mm rostral to the start of the lesion and was labelled at a survival time of 18 weeks.
Inset: photomicrograph of soma

184 →

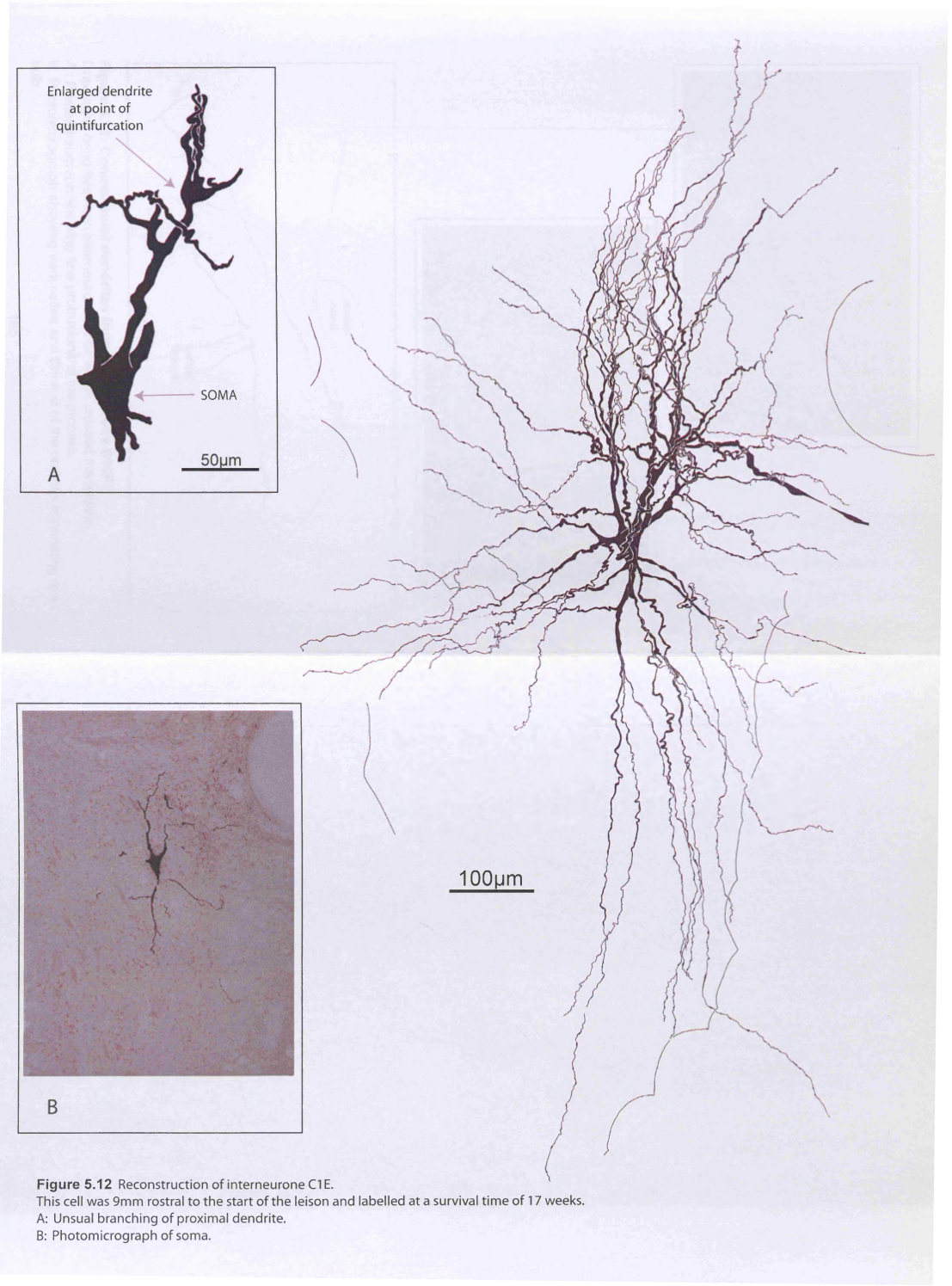

Figure 5.12 Reconstruction of interneurone C1E.
This cell was 9mm rostral to the start of the leison and labelled at a survival time of 17 weeks.
A: Unsual branching of proximal dendrite.
B: Photomicrograph of soma.

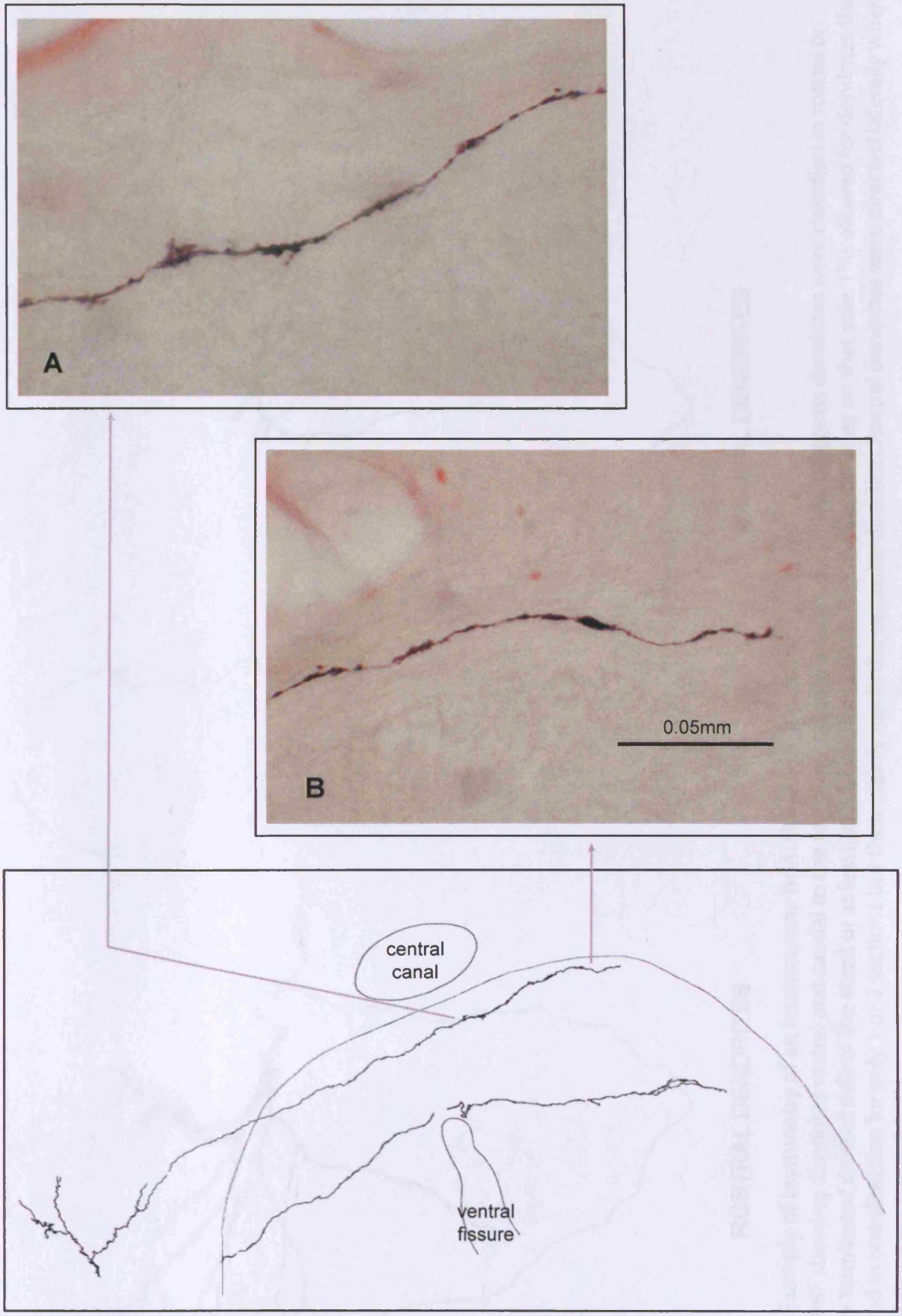

Figure 5.13: Commissural dendrites from interneurone B68F
Drawing of dendrites from interneurone B68F which crossed the midline.
A : Photomicrograph showing fine protrusions of the process.
B: Photomicrograph showing varicosites and the end of the process terminating in a bulb.

Figure 5.14 : Example of asymmetry of an interneurone from the lesion population.
This is Cell B88F showing dendrites rostral and caudal to the soma on separate images. For these diagrams dendrites were classified as rostral or caudal if they terminated on that side of the soma or at least 80% of sections containing the dendrite lay on that side. This allowed for dendrites that initially looped in one direction for only 1 or 2 sections but then mainly run in the opposite direction. Rostral dendrites were directed laterally where as the caudal dendrites run medially.

	Survival time	6-8 Weeks			16- 18 Weeks					
	Cell	B99N	C4A	B96F	C1A	B77G	B95A	B88F	B95C	B73J
	Distance from soma	4.75mm	5mm	8.75mm	5.25mm	6.65mm	6.75mm	9.5mm	10.5mm	14mm
Abnormalities	Enlarged proximal dendrites				*	*	*	*		
	Tortuosities/Tangles	*	*			*	*		*	
	"Hairy" dendrites	*	*		*	*	*	*	*	
	Non- tapering dendrites	*	*		*	*	*	*	*	
	Right angle branching	*	*	*	*	*	*	*	*	
	Twisted dendrites	*	*	*	*	*	*	*	*	
	Commissural dendrites					*	*	*		
	Asymmetrical Dendritic tree	*	*	*	*	*	*	*		
	Swelling/varicosities	*	*	*	*	*	*	*	*	

Table 5.1: Unusual features on dendritic trees of thoracic interneurones from the lesion population.

5.5 MAP2a/b Immunohistochemistry

Alternate sections from some cells were immunohistochemically labelled for MAP2a/b. Staining quality varied from experiment to experiment, although in some experiments it was possible to confirm MAP2 a/b negative dendrites. This identification was initially done using a Ziess microscope with epi-fluorescent illumination. The processes identified as positive or negative for MAP2a/b labelling were then confirmed using a confocal microscope. The process followed through the stack of images, so that the quality of MAP2a/b staining could be checked at each level.

Figure 5.15 illustrates a complete reconstruction of Cell C4 (from the lesioned population) with alternate sections showing either co-localization or lack of co-localization of the avidin and anti-MAP2a/b associated flourophores (confirmed using a confocal microscope). For this experiment, staining was exceptionally good, with good penetration though the tissue. Thus we can be confident that the identification of MAP2a/b negative processes was reliable.

From this it can be seen that many distal dendrites lacked immunoreactivity for MAP2a/b, particularly the distal lateral white matter dendrites. Note also that the abnormal parts of the dendrites (twisted or hairy) were all either negative or not tested for MAP2a/b. It could always be argued that the lack of labelling by itself does not prove the absence of MAP2a/b and may have been a result of bad staining etc. However, further evidence obtained by a general observation of overall MAP2/a/b staining of the spinal cord at this level adds weight to the argument that this lack of

staining of distal dendrites may represent a loss of the protein in these processes in the lesioned spinal cord.

Figure 5.16a (left) shows the MAP2a/b staining (one segment above the lesion, at the level of the cell) of all dendrites in the grey matter and extending into the lateral white matter of the lesioned side. It can be observed that the MAP2a/b positive processes do not extend further than the point at which the dendrites of cell C4E also stopped being MAP2a/b positive. To confirm that this is not merely the result of unreliable staining of thin distal processes one can examine the non-lesioned side of the spinal cord and we observe that the MAP2a/b labelled processes do indeed extend out further (figure 5.16, right). Further, the general labelling of immunoreactive MAP2a/b processes on the lesioned side is denser than on the un-lesioned side. This could suggest that either dendrites on the lesioned side are retracting, a hypothesis which is refuted by the lack of significant difference between overall rostral-caudal distance and by the presence of neurobiotin labelled distal dendrites lacking immunoreactivity for MAP2a/b or that that this could represent sprouting of by MAP2a/b positive processes on the non-lesioned side, a hypothesis questionable given comparable Map2a/b staining in control tissue (figure 5.16b). Thus it would appear that this lack of MAP2a/b immunoreactivity of distal dendrites in this experiment is a reliable indicator of an absence of MAP2a/b.

This difference between the MAP2a/b labelling of lesioned and non-lesioned side was consistent across all sections analysed at the level of the soma for this cell (C4E). This difference was also confirmed in another 2 animals, in which overall MAP2a/b staining had been considered and such a difference consistently noted. In experiment

C4 sections were selected as close to the lesion as possible and both above and below the lesion and immuno-labelled for MAP2/a/b with similar results.

191 ⟶

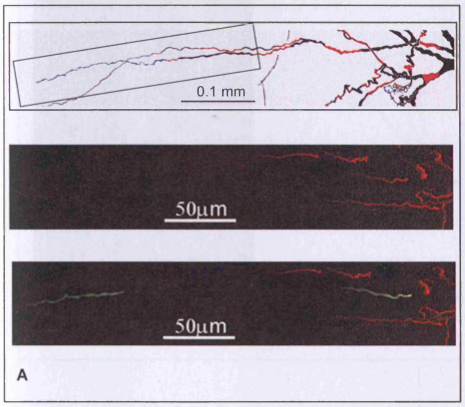

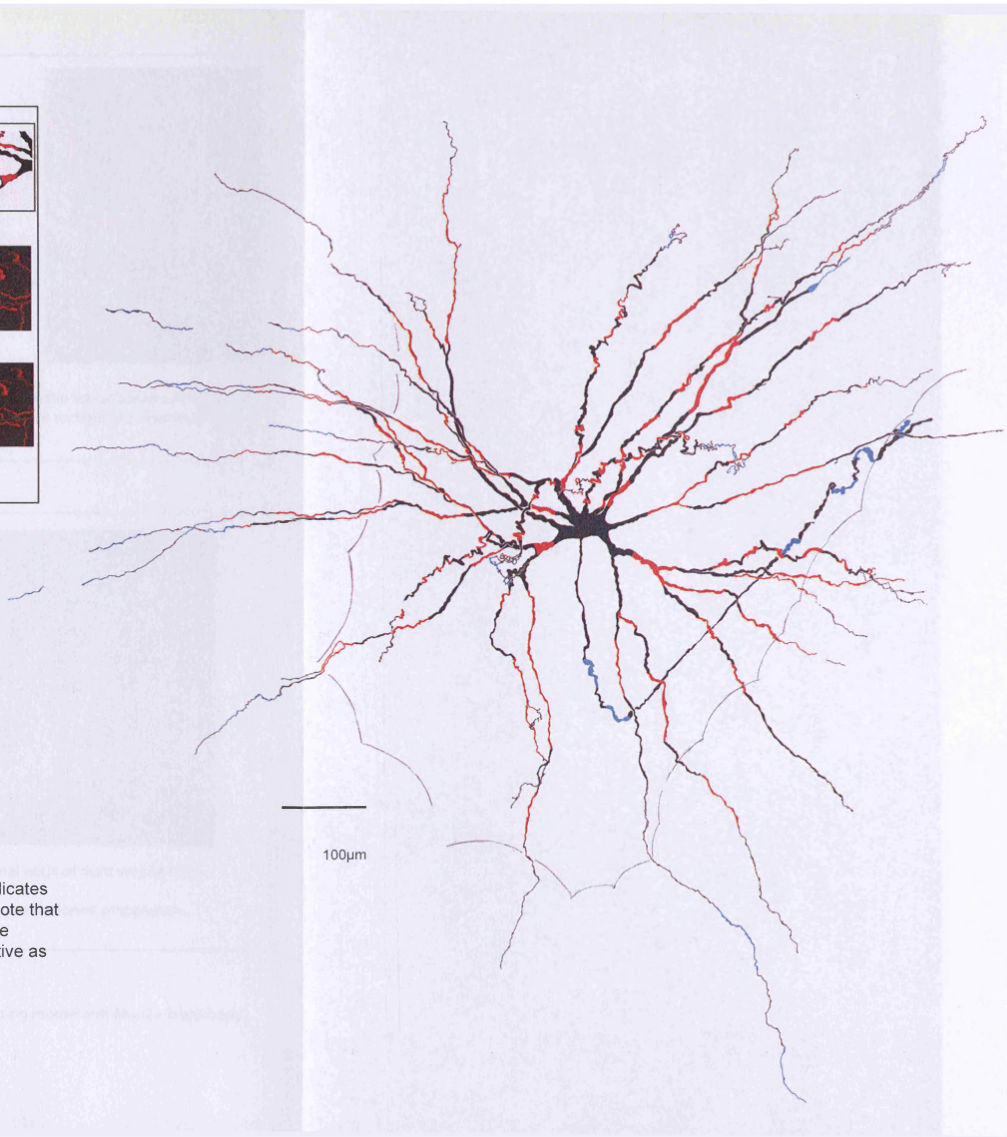

Figure 5.15: Reconstructions of Cell C4A with immunohistochemial data for Map2a/b labelling. Alternate sections were labelled for MAP2a/b. Red indicates co-localisation and blue indicates no co-localisation (note that the axon is blue, hence MAP2a/b negative as would be expected). Some distal processes are MAP2a/b negative as confirmed by the confocal microscope (inset)

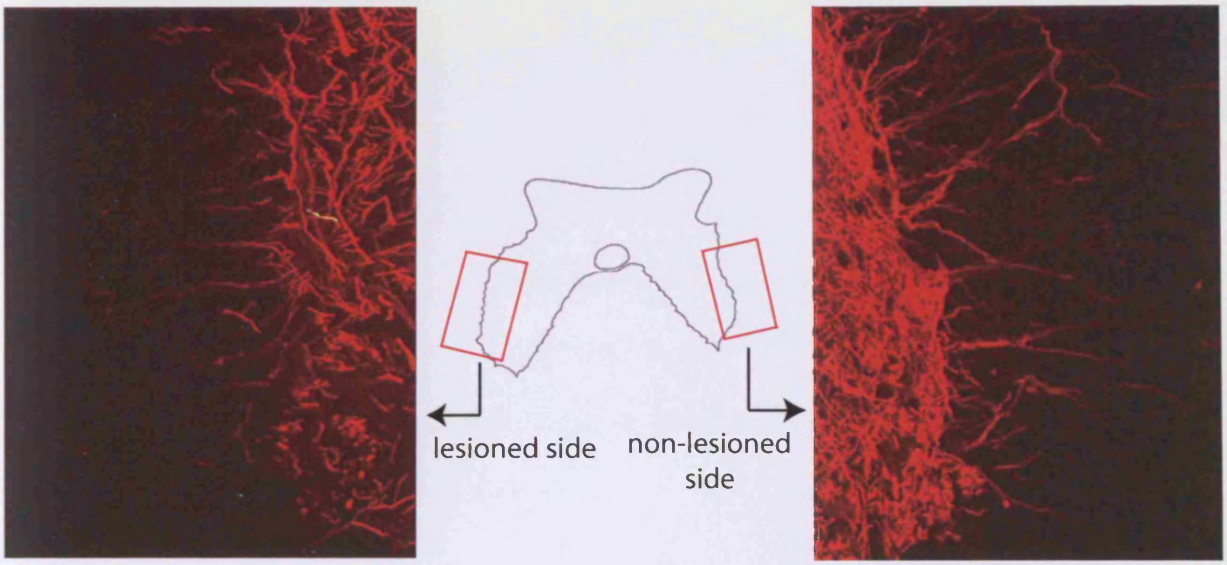

A: Confocal images of MAP2a/b labelled processes extending from the lateral borders of the ventral horns into the lateral white matter. The images were obtained from sections one segment rostral to the injury at the same level as cell C4A (figure 5.15)

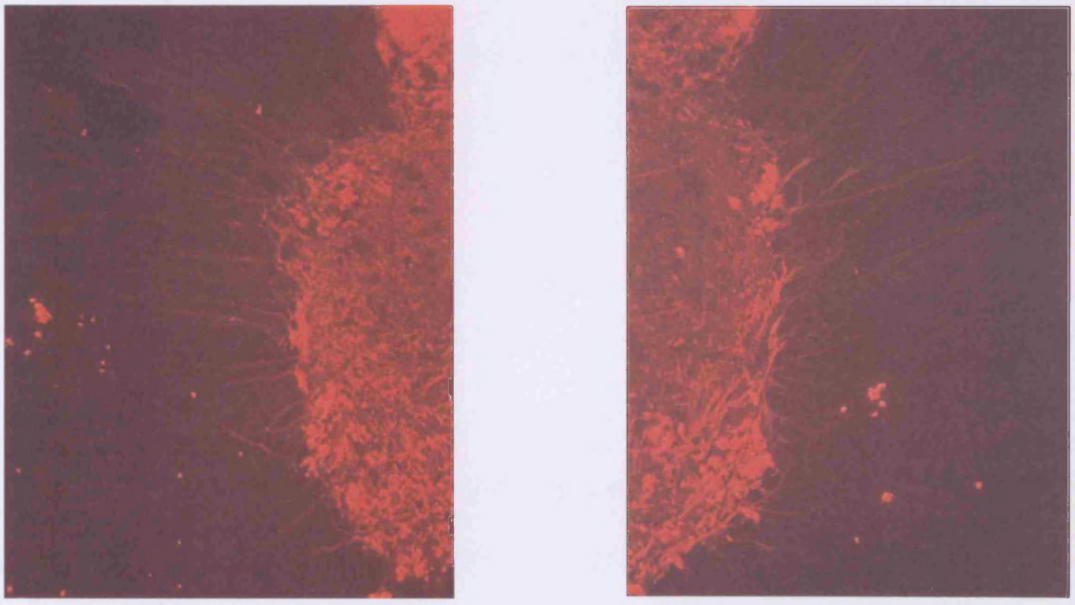

lateral edge of left ventral horn

lateral edge of right ventral horn

B: MAP 2a/b staining of control tissue obtained from a non lesioned preparation. (note these images were not taken with a confocal)

Figure 5.16
MAP 2a/b labelling in control and lesioned preparations using mouse anti-Map2a/b antibody and a secondary congugated to Texas Red

5.6 Motoneurone Dendrites.

During the course of this study 7 motoneurones were also intracellularly labelled at survival times of 6-33 weeks. These motoneurones had been identified and confirmed not to have been axotomised by antidromic stimulation of the dissected peripheral nerves. Their analysis is beyond the scope of this thesis, but one is of particular interest (B91D) and should be mentioned.

The only available description of the morphology of intracellularly labelled thoracic motoneurones has been published by Lipski and Martin-Body (1987). From 60 thoracic motoneurones few had dendrites that penetrated the white matter and in the sagittal plane dendrites were commonly seen to turn at the grey/white border. The authored reported that no dendrites crossed the midline commissures (with the exception of one process which they confess being unable to connect to any cell).

From the motoneurones labelled during the course of this thesis neither of those labelled at survival times of 6 and 8 weeks possessed dendrites which crossed the midline. A motoneurone labelled at 17 weeks had one process which crossed the midline. Of the four motoneurones labelled at the longer survival times, one had no crossing dendrites (29 weeks), two had dendritic processes which reached the midline (33 weeks) and one (B91D) had multiple processes which not only crossed the midline but also branched and terminated in the contralateral ventral horn (30 weeks).

Interestingly the 2 cells which possessed dendrites which crossed the midline were the closet to the lesion (approximately 1750μm and 3150 μm) out of the group.

Although not seen in the Lipski and Martin-Body sample of thoracic motoneurones crossing dendrites are not themselves abnormal to motoneurones, indeed dendritic labelling of control spinal cords revealed many MAP2a/b positive processes which reach or cross the midline. The apparent asymmetry of the dendrites of this cell however is definitely abnormal for dendritic trees of spinal motoneurones. Dendrites extending rostrally from the soma extended rostrally as normal the motor neurons for 1950μm distance. Dendrites caudal to the soma however turned to travel transversely across the midline where they reached and branched in the contralateral ventral horn. Examples of the caudal commissural dendrites are shown in figure 5.17. Figure 5.18 shows examples of commissural dendritic processes from this cell co-localising with immuno-histochemical labelling of the dendritic protein MAP 2a/b labelled.

Figure 5.17 : Motoneurone with commissural dendrites.

Motoneurone B91D, approximately 3150µm from the start of the lesion. Dendrites of this cell, rostral to the soma, ran tightly paced in the rostro-caudal direction, whereas many dendrites caudal to the soma crossed the midline resulting in an asymmetric dendritic tree.

A: Soma, B-E: caudal dendrites travelling to midline, crossing the midline and reaching, then branching in the contralateral ventral horn

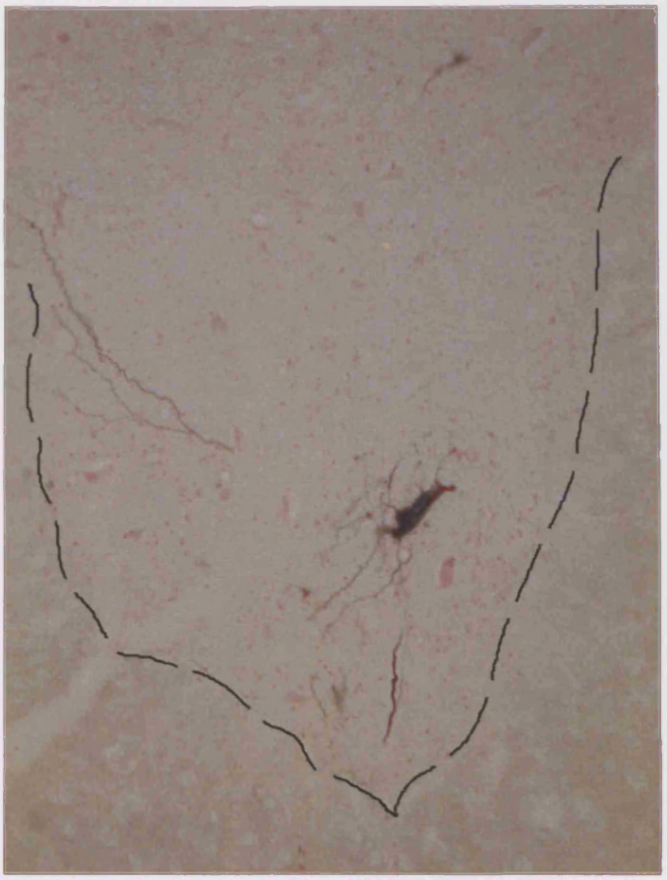

A

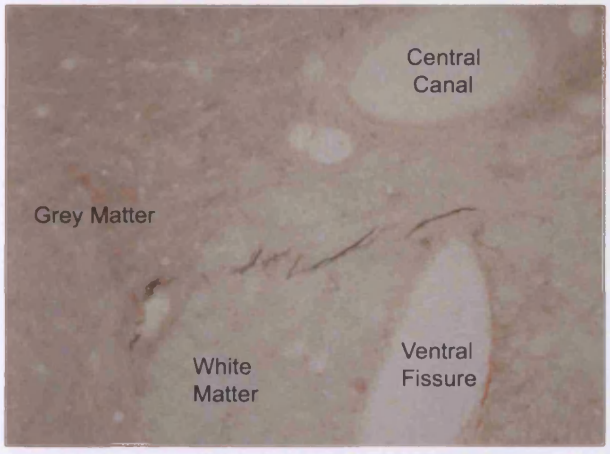

B

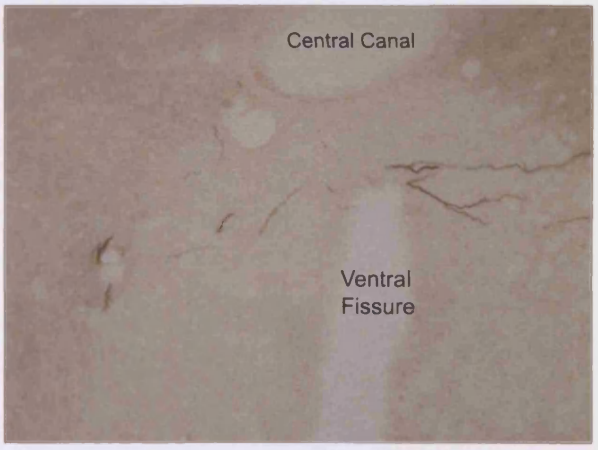

C

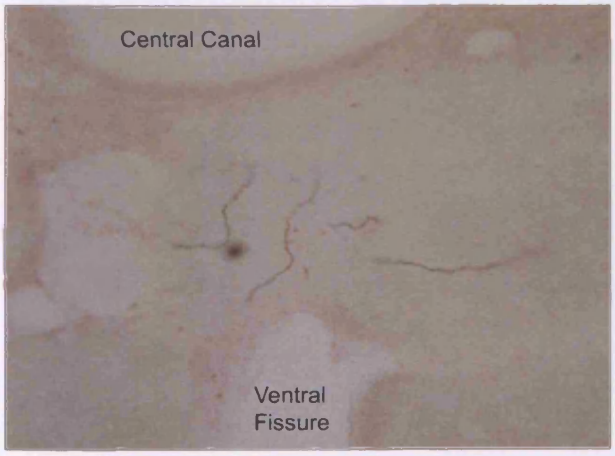

D

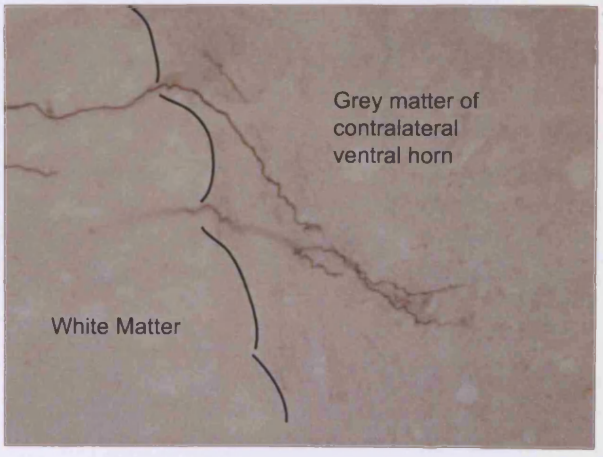

E

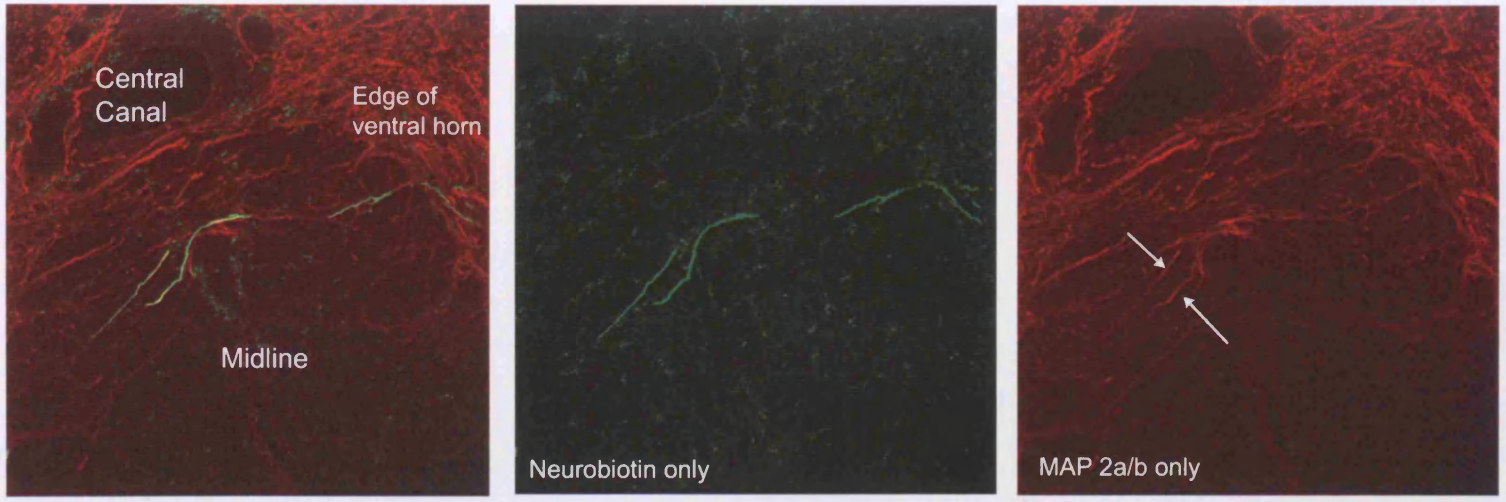

A: At 20 X Magnification

B: Lateral process of above figure but at 40x magnification
The apparent absence of MAP2a/b labelling of the most lateral part of the process was merely a result of the failure of the antibody to penetrate through the whole slice of tissue which was confirmed by analysis of seperate 1.5um stacks obtained by the confocal microscope.

Figure 5.18: MAP2a/b positive commisural dendrites from motoneurone B91D.
Double labelling of neurobiotin with Avidin Fluoroscein (green) and MAP2a/b with Texas red (red) fluorochromes. In this case the neurobiotin is in dendritic processes of the motoneurone B91D which crossed the spinal midline to the contralateral ventral horn. These processes co-localize with the MAP2a/b labeling. These images were overlayed projections of a series of images taken at 1.5μm intervals through a 50μm section using a confocal microscope.

Chapter 6

Discussion

6.1 Summary of results

The aim of this thesis was to test three possible types of sprouting with respect to thoracic interneurones one segment rostral to a spinal hemisection. Sprouting was identified from the axons and the dendrites of the interneurones themselves but this thesis was unable to test the hypothesis of sprouting to the interneurones from the lesioned EBSNs.

When all the interneurone axons labelled in the lesioned cord were considered together, no significant difference was found compared to controls, with respect to the number of axon collateral branches in the first 3mm of labelled axon. This was probably due to the fact that although the means were different there existed a large variation in the lesion population. When the lesion population was examined with respect to time and distance of the soma from the lesion it could be seen that these factors may account for much of this variation. It may be hypothesised that variation shown with each survival time group may be accounted for by differences within that group with respect to distance from start of lesion and vice versa that the variation within the distance from lesion groups may be accounted for differences within that group with respect to survival time. A larger number of cells would be needed however for an analysis of covariance to confirm this. However, when cells with somata within 10mm of the start of the lesion and labelled at survival times of 16-18 week were selected as a single group a significant difference was seen.

Further evidence of sprouting of the thoracic interneurones of this study was obtained by making measurements of areas where the axon collaterals terminated. Axon collateral branches from interneurones one segment rostral to an injury had significantly larger terminal areas than those of controls. Distance of the soma from the start of the lesion and survival times significantly affected this area. Those with somata within 10 mm of the start of the lesion had a significantly greater terminal area than those more than 10mm from the start of the lesion. Those labelled at 16-18 week survival times had significantly larger terminal areas than those labelled at 6-8 week survival times. These observations are consistent with this being a sprouting response.

By using a grid to divide the ventral horn/intermediate zone into 12 regions it was demonstrated that collateral branches from axons in the lesion population terminated in significantly more regions than controls confirming the above. The more dorsal regions showed the largest increases in terms of number of cells with collaterals terminations, in particular the most dorso-lateral zone, which encompassed the IML column.

Intracellular labelling of interneurones in this thesis was often adequate to allow full reconstructions of the entire dendritic trees of the interneurones. No significant difference was found between control interneurones and those from the lesioned spinal cord in terms of the overall rostro-caudal extent of the dendrites. While this provides no direct evidence for sprouting of the dendrites it also therefore provides no evidence of retraction of dendrites.

More obvious evidence of sprouting came from qualitative observations of a number of abnormalities in the dendritic trees of interneurones from the lesion population. These include tortuous structures, thick un-tapered axon like branches with right angle branches, twisted dendrites and asymmetry of the overall dendritic trees.

There were also abnormalities with respect to the distribution of the dendritic cytoskeletal protein MAP2a/b. Some distal dendrites lacked immunolabelling for MAP2a/b as did the axotomised motoneurones of MacDermid et al. (2002). We can be confident that this was not simply a consequence of inadequate labelling, as all distal dendrites extending into the lateral white matter on every section labelled over 3 experiments consistently lacked labelling of MAP2a/b on the side of the lesion where as on the non-lesioned side the labelling was comparable to controls.

The results of this thesis are therefore consistent with a hypothesis of sprouting of axons and dendrites of non-injured thoracic interneurones one segment rostral to a spinal hemisection.

6.2 Alternative explanations:

6.21 Axonal sprouting

Although the apparent increases in collateral branches at longer time intervals and the larger terminal areas of collateral branches of interneurones in the lesion population suggest axonal sprouting of this population, they do not provide conclusive proof. It could be argued that these differences could arise from the selective survival of cells with larger collaterals following a local injury, perhaps due to more trophic support

received from these collaterals. Such a hypothesis would also be consistent with the observations with respect to the effects of distance from the lesion on these statistics.

Tracking for cells gave the impression of a general loss of cells, although no attempt was made at cell counting to confirm or refute this hypothesis. A small number of experiments at longer survival times of 32 weeks proved unsuccessful.

Although for a hypothesis of selective survival to be consistent with the results of this project with respect to survival time differences cell death would have to be occurring at time spans later than 8 weeks. As yet there is no reliable evidence that this occurs. Significant necrosis and apoptosis do occur following spinal cord injury although the most extensive cell death in experimental spinal cord injury models is seen within hours of injury (Schwab and Bartholdi 1996).

Much of the literature focuses on the loss of spinal motoneurones following spinal cord injury. Although there is a significant loss of motoneurones at the lesion site and both rostral and caudal to it, this is mostly during the first 24 hours with no significant loss seen at longer time intervals (Grossman et al 2001, Lui et al. (1997, Kato et al 1996). Using different techniques others have found little evidence of motoneurone loss at 7, 20 and 50 weeks (Bjugn et al 1997, McBride and Feringa 1991).

Few studies have examined the fate of spinal interneurones following a spinal lesion. Conta and Stelzer (2004) examined intraspinal neuronal systems rostral to a T9-T10 contusion injury created using the NYU IMPACTOR device and Multicentre Animal Spinal Cord Injury Study (MASCI) protocols to produce a reproducible spinal cord

contusion model. Using retrograde labelling from below the injury, a drastic reduction of propriospinal fibres were labelled in the cervical and thoracic cord compared with controls. By pre-labeling the short thoracic propriospinal neurones before the injury, Conta and Stelzner (2004) demonstrated large numbers of reterogradely labelled cells in all the spinal laminae similar to those seen in uninjured controls. Thus the short thoracic propriospinal neurones do not undergo post axotomy cell death and are still alive at 2 weeks post injury. Although this population was not examined at longer time intervals there is still no strong evidence that axotomy would cause cells death after this time.

Using a sagittal lesion of the spinal midline which selectively axotomise commissural neck interneurones, Fenrick et al (2004) demonstrate using large extracellular injections of neurobiotin that large numbers of the interneurones can be labelled at 4/8 weeks. Not only this but many even co-localize with GAP-43 suggesting possible regenerative activity.

Thus although there is no evidence which directly contradicts the possibility of selective survival, the available evidence form somewhat similar circumstances does not make this possibility seem likely.

Moreover, some features of the axons in the lesioned population are particularly suggestive of sprouting. This includes the highly abnormal trajectory of cell B95A, the higher incidence of overlapping collaterals in the lesioned population and the different terminations areas of successive collaterals from the same axons (unlike

controls), suggesting that sprouting of the axon collaterals is an appropriate conclusion.

Although cells were confirmed to have not been axotomised by the lesion by antidromic stimulation of the axon below the lesion, it must be acknowledged that it remains possible that axon collateral branches at the lesion site may have been damaged. The precise consequences of damage to axons of interneurones on spouting is unknown, although for motoneurones at least it is known that damage to their axons leads to a reduction of collaterals branches rather than an increase. Havton and Kellerth (1990) at 12 weeks post axotomy found a 40% decrease in the number of first order collaterals, implying elimination of entire axon collateral trees, along with a decrease in the total number of axon collateral end branches and bouton like axon collateral swellings. This retrograde elimination of intramedullarly motor axon collaterals following a peripheral lesion axotomy was more pronounced among juxta-somatic collaterals than among more distal ones. Therefore it could be argued that if any damage had occurred to the axons of cells in this study it may have been more likely to have had the opposite effect than the increase observed in this study.

The cells with axons travelling in the medial funiculus of the side of the lesion appeared to have the largest terminal areas, although the small numbers did not allow statistical analysis of this. Again it must be acknowledged that although these cells were confirmed not to have been axotomised it is possible that they suffered damage to axon collateral branches. These interneurones are also from a different population than the majority of the control cells making comparison difficult. Most of the interneurones by the level of the lesion had reached the ventral funiculi. Those axons

on the ipsilateral side sampled in his thesis remained fairly dorsal in the medial funiculus (resulting in their not being axotomised by the lesion). This is important when one considers that with 2 different populations of funicular cells in the paper of Bareyre et al (2004) there were differences between short and long propriospinal cells at survival times of 12 weeks with long propriospinal axons retaining significantly more of the contact that had been observed to increase at 3 weeks survival times than the short propriospinal cells. Different populations of thoracic interneurones may respond differently to a local injury. In this thesis the ipsilateral axons ran closer to the lesion than contralateral ones and thus may have picked up more trophic factors.

6.22 Dendrites

Although there was no statistical evidence for sprouting of the dendritic trees of the cells one must be extremely cautious with statistics such as the rostro-caudal extent of dendrites when considering the interneurones as one population. Unlike motoneurones, which can be easily categorised with respect to the muscle they innervate and, as such, can be compared with other motoneurones innervating the same muscle, interneurones are harder to characterise. The interneurones of this thesis have been taken as forming one population. In reality however these interneurones are likely to form a heterogeneous population with different patterns of inputs and outputs. It may be argued therefore that it would be more reliable to focus on the more qualitative observation of abnormalities of the dendrites.

One possibility is that the dendrites of the interneurones of this thesis may have retracted and then re-grown. Other factors can affect dendritic retraction/sprouting following an injury than just deafferentation. There is a wealth of literature for

example emphasising the benefits of exercise on functional recovery following spinal cord injury both in humans (Found and Pearson 2004, Rossignol 2000 reviews) and in cats (Barbeau and Rossignol 1987,1994 review). The effects of exercise were studied on the morphology of the dendritic trees of the lumbar motoneurone population caudal to a thoracic spinal cord injury that had been observed to retract following injury. Rats which received treadmill training, however, had dendritic trees of comparable length/arbour to that of controls (Gazula et al 2004). The cats from this thesis recovered quickly and were extremely active. This may explain why we did not observe a retraction of dendrites post injury.

The small sample of motoneurones obtained in this lesioned preparation allows no real valid statistical conclusions to be made. They were worth mentioning however as a number of similar dendritic abnormalities as the interneurones suggest they may also be sprouting in response to a local injury.

Whether or not the commissural nature of some of the dendrites of the motoneurones represent sprouting or not remains a question. A sample of thoracic motoneurones obtained by Lipski and Martin-Body had no examples of motoneurones with dendrites which crossed the midline (except one dendrite which could not be unequivocally joined up to a soma). This sample however, included only motoneurones from the upper thoracic segments. It may therefore be possible that more caudal segments such as used in this thesis may represent a slightly different population. Motoneurones labelled by injections of cholera toxin subunit B into rectus abdominis in the ferret revealed processes dendrites that crossed the midline (Billig et al 1999). Being a midline muscle it is possible that motoneurones innervating this muscle may be more

probable to have commissural attributes. Cell B91X in this study was identified as a motoneurone with an axon travelling in the internal nerve in which rectus abdominus fibres travel and so it is possible that this may be rectus motoneurones, which would have been unrepresented in more rostral spinal segments. However, the commissural dendrites for rectus motoneurones illustrated by Billig et al (1999) are much less extensive than those observed on cell B91.

Using HRP injections of 40 cervical motoneurones innervating neck muscles of the adult cat, Rose and Richmond (1981) discovered their entire sample to possess white matter dendrites regardless of their spinal location or their innervation target. They cite studies of lumbrosacral and cocygeal motoneurones and conclude that white matter dendrites are a prominent feature of many spinal motoneurones in the adult mammal. The authors describe 2 motoneurones found in the commissural nucleus with dendrites projecting across the ventral commissure into the contralateral spinal cord where they were occasionally traced into the dorsomedial region of the contralateral ventral horn. So in itself the presence of commissural dendrites may not represent an abnormality, although again, these commissural dendrites were less extensive than those of B91.

The commissural dendritic processes from cell B91 co-localised with immuno-histochemical labelling of the dendritic protein MAP 2a/b labelled. Hence, these are dendritic in structure and differ from the MAP 2a/b negative commissural dendraxons of MacDermid et al (2004). This cell did however have some examples of unusual dendritic morphology, such as bulbous endings and an asymmetric arrangement of dendrites.

6.3 Methodological issues.

In this study there was considerable variation with respect to the extent of the lesion. Many descending and ascending tracts had been damaged. In some cases very little grey matter was left intact at the lesion site, especially where cysts formed. Thus changes observed may be a consequence of deafferentation of the cells themselves, removal of targets, responses to deafferentation of other local neurones, or the effect of the lesioned environment (e.g. the extracellular matrix). It would be almost impossible to elucidate the effects of one from the other, except to rule out axotomy of the interneurones as a cause.

Due to the accuracy of notes kept at the time of the terminal experiments it was easy to predict the precise location of the filled cells after histology. These interneurones filled with Neurobiotin when reacted with DAB generally appeared quite darkly stained and were easily identifiable as the filled neurones.

Also noticeable however, were a number of very pale "ghostly" stained cells near to the filled neurone. It is possible that some of these may be the consequence of stray labelling although all efforts were made not to pass current whilst anywhere in the ventral horn other than in a cell which was to be labelled and not to linger with the electrode in any cell unless it was intended to label that cell.

One possibility is that the staining of these cells may result from dye coupling, that is, the passing of the low molecular weight neurobiotin through gap junctions in neurones. There is physiological evidence that gap junctions exist in spinal motoneurones in the neonatal spinal cord and these have been successfully stained via

dye coupling. These have been hypothesised to play a role in the synchronisation of motor neurones in development (Traub and Wong, 1983) and in the respiratory system (Bou-Flores and Berger 2001). Electrical coupling involving spinal interneurones has also been observed in the lamprey (Christensen 1983) and in goldfish (Fetcho 1991) during development.

Whilst there is evidence for the expression of the connexion proteins in the adult mammalian CNS in motoneurones and interneurones (Rash et al 2000, Teubner et al 2001), there has been little conclusive proof of electrical coupling in the motor system in the mammalian adult. Dye coupling following has been used to indicate gap-junction formation in adult spinal motoneurones following axotomy by Chang et al (2000) although this has not been confirmed electrophysiologically.

Care must be taken when drawing conclusions of dye coupling as the example shown in this thesis of interneurone C4A (figure 5.6, page174) is most likely to have resulted merely as a consequence of over-filling a cell and neurobiotin leaking out of the cell, hence the presence of the reaction product outside the cells giving it a hazy appearance. Neurobiotin may leak out of a cell and be taken up by other local neurones and glia, resulting in the faint labelling of these cells. The examples of this in these experiments are similar to examples of over-stained cells surrounded by faintly labelled cells of intact spinal neurones illustrated by Brown and Fyffe (1984). Given the difficulty of judging what is an adequate fill and what will be over fill or whether an electrode has or has not damaged a cell enough to cause leakage then it may be argued that examples of dye coupling my be nothing more than a consequence of leakage die to over-staining or damage to a cell.

Most of the cells recovered had an axon labelled well enough to allow analysis of axon trajectories, numbers of collaterals and terminal areas of axon collaterals. Occasionally there was a section of axon, usually close to the soma where the axon appeared to have broken up, this may have been due to axonal penetrations although according to Brown and Fyffe (1984) it is common to observe a failure of the initial part of an axon to stain.

6.4 Relationship of findings to other work

The axonal sprouting of non-injured interneurones in a partially injured spinal cord is consistent with the observations of axonal sprouting of the non-injured interneurones observed by Bareyre et al (2004) following a mid thoracic dorsal hemisection in adult rats. Although in the experiments of Bareyre et al, an initial large increase in collaterals at 3 weeks survival time was followed by a decrease at 12 weeks suggesting the removal of some newly formed connections. This did not appear to be the case for the interneurones of this thesis (if we assume that the significant differences represent sprouting).

Sprouting from local interneurones following spinal cord injury had been previously hypothesised by Weaver et al. (1997), examining GAP-43 immunoreactivity in the spinal cord before and 7-30 days following a mid thoracic cord transection. GAP-43 is normally found in bulbospinal neurones that supply the spinal sympathetic nuclei as well as being up-regulated in growing or sprouting axons. In the injured rat spinal cord terminals with ultrastructural signs of degeneration (using electron microscopy) were abundant in the IML after 3 days, rare by 7 days and absent by 14 days. The

authors concluded that all supraspinal inputs to sympathetic preganglionic neurones had been eliminated by 8 days post injury. At longer survival time terminals immunoreactive for GAP-43 were therefore assumed to have arisen from intraspinal neurones.

Within 30 days rostral to the injury there was a proliferation of GAP-43 processes around sympathetic preganglionic cells (SPG) of the IML. Caudal to the transection, GAP-43 processes formed a reticular network including the SPG in the IML as well as in intermediate grey matter. These processes included not only growing axons with growth cones but also mature axons that appeared to be forming new synapses on SPN.

There was also immunoreactivity in numerous somata of presumed interneurones throughout the intermediate grey matter after 14 days, which had increased by 30 days. Weaver et al suggest that these may be the source of the GAP-43 in the reticular network, growth cones and synapses and that new synapses on preganglionic neurones may be crucial for the development of autonomic dysreflexia.

In the present study no significant difference was found between control interneurones and those from the lesioned spinal cord in terms of the overall rostro-caudal extent of the dendrites. While this provides no direct evidence for sprouting of the dendrites it also therefore provides no evidence of retraction of dendrites as observed by Gazula et al (2004) on uninjured motoneurones caudal to a spinal injury. Using bulk labelling methods with viral vectors injected into the sciatic nerve of rats 5 days post injury, dendritic trees of labelled motoneurones appeared to have retracted

their dendrites compared to controls (Gazula et al 2004). It may be argued that motoneurones caudal to an injury may suffer more deafferentation than the interneurones in this study. Also, the dendritic trees of the motoneurones were only studied in the transverse plane rather than using full reconstructions and thus ignored rostro-caudal running dendrites.

Gazula et al (2004) make no mention of any structural abnormalities of the dendrites, such as seen on the interneurones in this thesis although it must be noted that these cells are caudal to the lesion at distances far greater than that of our interneurones from the lesion. This is relevant, as the distance from the lesion appears to be an important factor with respect to abnormalities, the critical distance in this thesis appeared to be less than 10mm. Also, although the dendrites of the motoneurones appear to have regenerated to normal length it does not necessarily follow that they are normal healthy functioning dendrites, hence it is possible that they may, for example, be MAP2a/b negative distally as ours.

Another unusual feature of the dendritic tree of the interneurones of this thesis is the asymmetrical nature of their dendritic trees. It is unclear why this asymmetry should occur. One possible hypothesis can be pieced together using the following observations.

Hoy, Nolen and Casaday (1985) observe that in the cricket the auditory afferents from each ear terminate ipsilaterally onto a single identified interneurone (Int-1), each of which is excited only by stimulation of its ipsilateral ear but not its contralateral one. Depriving the interneurone of this ipsilateral input during post-embryonic

development by removing an ear causes the medial dendrites of the deprived interneurone to grow across the ganglionic midline and terminate in the intact auditory neuropile of the contralateral side. Here they formed functional synaptic connection with the contralateral afferents.

In this thesis dendrites of our interneurones are observed crossing the midline at 16-18 week survival times. None were observed on the interneurones labelled at survival times of 6-8 weeks. This suggests that they may be a result of sprouting. This is further reinforced by the appearance of structures reminiscent of growth cones on the ends of some of these, suggesting that at 16-18 weeks they may still be sprouting. It was attempted to label interneurones at longer survival times to assess whether the dendrites branched into the contralateral ventral horn but no interneurones were successfully labelled at this survival time. A small number of motoneurones, however, were labelled at 32 weeks post injury. Here dendrites, caudal to the soma, were observed that not only crossed the midline but that branched in the contralateral ventral horn. This is could be argued that deprived of their normal input the sprouting dendrites seek to replace this input from the intact contralateral ascending/descending tracts.

This does not necessarily explain the asymmetry observed in the direction of the dendrites. This could perhaps be explained if different inputs terminate specifically on different parts of the dendritic tree. There is now evidence that for spinal motoneurones at least this may be the case.

Although in the cricket experiments crickets were lesioned a day after birth the authors claim to observe the same thing deafferenting adults. Interestingly the authors note that "it is our impression that whenever deprivation induces sprouting of the medial dendrites there appears to be a concomitant decrease in the complexity and number of lateral dendrites", Hoy, Nolen and Casaday (1985).

Grande et al (2003) used labelling of neurones forming the vestibulocollic pathway which originates from neurones in the rostral parts of the medial and descending vestibular nuclei. These neurones terminate contralaterally on the motoneurones innervating the dorsal neck muscle splenius. Boutons from the vestibular spinal neurones were labelled using PHA-L and BDA and intracellular labelling techniques used to label splenius motoneurone dendrites. The majority of the vestibulospinal inputs were on dendrites medial to the soma suggesting the axons innervated a specific region of the dendritic tree of the motoneurones.

It could therefore be hypothesised that if the lost inputs to the thoracic neurones were preferentially located on specific regions of the dendritic tress of the cells of this thesis then this could explain the asymmetry.

Although the abnormal dendrites of the interneurones share many features with the dendrites of axotomised motoneurones they differ in other ways. One common feature observed on the interneurones not seen on controls or on axotomised motoneurones are the twisting of dendrites. There is no obvious reason why the dendrites should become twisted around one another. If they have retracted and re-grown then it may

be that the guidance cues that would normally guide developing dendrites are not present and thus dendrites merely follow each other.

Although the presence of axon-like process and the absence of the dendritic marker MAP2a/b in some distal dendrites does not in itself prove that these processes are the same "dendraxons" as observed by MacDermid et al (2002) it does raise the possibility that a similar phenomena may be occurring in local spinal cells following spinal cord injury.

There have recently been a number of proteins discovered to play roles in such transformations. One such is the motor protein CHO/MKLP1. This transports microtubules with their minus ends leading into dendrites by generating forces against the plus end distal microtubules thus creating a drag on the plus end distal microtubules (Yu et al 1997 Ferhat et al 1998, Sharp et al 1997). Depletion of CHO/MKLP1 from cultured neurones causes a rapid redistribution of microtubules within dendrites such that minus end distal microtubules are chased back to the cell body while plus end distal microtubules are redistributed forward. Cell processes grow significantly longer and thinner, loose their taper and acquire a progressively more axon-like organelle composition (Yu et al 2000).

These dendrites share a number of features with those of the interneurones of this thesis. The abnormalities observed on our dendrites may be a consequence of the loss of MAP2a/b that we observe. Alterations in intracellular levels of CHO/MKLP-1 following a local injury may be one mechanism by which this can occur.

Another candidate protein is CRMP-2. Inagaki et al (2001) transfected hippocampal neurons with myc-tagged CRMP-2 and examined their morphology after 10 days in vitro by which time the over-expressed myc-CRMP-2 was expressed four times that of endogenous CRMP-2. 57% of the myc-CRMP expressing neurones had more than one (2-5) long process which exhibited the characteristic morphology of axons. They were long and thin and branched at right angles. They were immuno-stained by the axonal marker anti-tau-antibody but immuno-negative for MAP2a/b. They were also immuno-reactive for synaptophysin raising the possibility that these supernumerary axons can form synaptic contacts. A possible up-regulation of CRMP-2 following local injury is another mechanism could perhaps explain the dendritic abnormalities of the interneurones in this thesis.

While the development of supernumerary axons from dendrites may offer an alternative route of regeneration, such plasticity may be of little or no value if it is not maintained. In Hall and Cohen's larval sea lamprey, for example, the growth of axon-type processes reached a maximum at 14 weeks post injury after which time their length decreased and many terminated on amorphous type swellings by 21-26 weeks, suggesting a general retraction of axon type processes over time (Hall and Cohen 1988, Hall et al 1997). New synaptic contacts that are present 7-10 weeks post-axotomy may be lost at longer times post-axotomy.

For the axotomised motoneurones of MacDermid et al (2004), however a different pattern appears. At 6-8 weeks post axotomy unusual processes were mostly arboreal. At 35 weeks axon-like unusual distal processes were observed crossing the contralateral side of the cord. The preliminary observations of the non-injured

motoneurones rostral to the lesion in this thesis are consistent with this pattern seen in the axotomised cell, with the longer survival times possessing the commissural dendrites. Hence, it may be plausible to suggest that as with the axotomised motoneurones the unusual distal dendritic processes on the interneurone of this study may not only persist at longer survival times but may develop further. The appearance of growth cone type structures on the crossing dendrites of cell B69 (16 week survival time) is consistent with this hypothesis. Thus, if such changes persist, then such a phenomenon may have consequences for strategies aimed at repairing injured spinal cords.

However, the general loss of MAP2a/b on the side of the cord ipsilateral to the lesion compared to the contralateral side is unlikely to represent simply the loss of dendrites as a result of their conversion into axons because most of the thoracic interneurones have crossed axons. Thus, the side contralateral to the lesion would have had more interneurones that would have been axotomised and thus should have been more likely to be affected (assuming axotomy is the strongest stimulus for such a conversion)

General alterations in MAP2 labelling following spinal cord injury have been previously observed by Zhang et al (2000). One hour after spinal cord injury (weight drop) dramatic decreases were observed in dendritic MAP2 immunoreactivity within 3-4mm of the lesion epicentre in both the rostral and caudal direction. Remaining MAP2 dendrites had a beaded appearance. In more distal sections MAP2 immunoreactivity appeared normal in the grey matter but there was a pronounced beading of dendrites in the white matter. One to six hours after spinal cord injury, the

dendritic beading was evident throughout the entire rostral – caudal extent of the spinal cord. The extent of the beading was most severe adjacent to the impact site with the severity gradually diminishing towards the rostral and caudal extremities. The most affected region was the lateral funiculus. Beading could also be observed in the ventral funiculus and dorsal funiculus. By 48 hours beading was diminished in intensity and largely restricted to thoracic and lumbar regions. One week later dendritic beading was more restricted being most prominent close to lesion and after 2 weeks dendritic beading was no longer detected. Similar extensive losses in MAP2 immunoreactivity, at the level of a spinal lesion and in the segment above and below, were observed by Li et al (2000).

Zhang et al (2000) argue that the somatic dendritic localization of MAP2 would be expected to enhance its vulnerability to spinal cord injury and excitotoxic mechanisms. It is hypothesised that following spinal cord injury neurofilament loss occurs due to elevations in intracellular Ca+ levels due to influx through NMDA receptors leading to activation of calpains (calcium-activated neural protease). Springer et al. (1997) show evidence of calpain activity at injury sites as early as one hour post injury. The prevalence of MAP2 in the grey matter is argued to render it more vulnerable to spinal cord injury since the secondary ischemia is particularly severe in the grey matter (Zhang et al, 2000). MAP2 may be especially vulnerable to excitotoxic insult given that the excitatory amino acid receptors are mainly localized to dendrites and neuronal cell bodies (Aicher et al 1997, Petralia et al 1994 a, b). Calpains are also enriched in dendrites (Perlmutter et al 1990; Fukuda et al 1990).

Li et al (2000) and Zhang et al (2000) therefore suggest MAP2 levels may serve as an excellent marker of injury severity. They suggest that as MAP2 is exclusively localized in the grey matter the extent of MAP2 loss may reflect the extent of grey matter damage. MAP2 loss observed following ischemia and traumatic brain injury has been taken to be functionally significant and to reflect the neurone loss contributing to the behavioural deficit.

Of course the existence in the thesis of intracellularly labelled dendritic processes that are MAP2/ab negative warns against such simplistic conclusions, suggesting that loss of MAP2a/b may not simply represent dendritic loss but dendritic abnormalities.

6.5 Importance/implications

The difficulties completing the electrophysiological part of this study have implications for studies using electrophysiology to assess connectivity to populations which it is difficult to obtain a sufficiently high yield. This has implications for experiments designed to assess connectivity following experimental regeneration if the targets for regenerating neurones are likely to be cells such as interneurones, which are extremely hard to obtain intracellular recordings of in the lesioned spinal cord. An alternative approach would be to use anatomical tracing/labelling to examine this particular issue by labelling the expiratory bulbospinal neurones using anterograde tracers such as PHA-L or BDA and look for contacts on the labelled cells such as Bareyre et al (2004). Although using this method it would be impossible to retain the functional specificity of the EBSNs. Also previous attempts at this in this laboratory have proved unsuccessful.

The hypothesised sprouting of the interneurone axons from this study are unlikely to represent the formation of a new circuit re-routing the connections of axotomised tracts to restore function (as in Bareyre et al 2004) as this would have to occur faster than 16-18 weeks for this to explain the rapid functional recovery observed in the first weeks following spinal cord injury. This sprouting appears to be occurring at longer survival times post injury thus the time frame of its development may be more consistent with the development of clinical problems such as spasticity and autonomic dysreflexia than functional recovery. Autonomic dysreflexia is a syndrome characterized by abrupt onset of excessively high blood pressure caused by uncontrolled sympathetic nervous system discharge in persons or animals with spinal cord injury. The fact that sprouting of the collaterals appears to occur in regions, which include the IML, could have important consequences for autonomic dysreflexia. Hence, for any experimental approach attempting to encourage such plasticity to reroute circuits it is important to acknowledge that the sprouting occurring may not always be beneficial.

When discussing the implications that our results may have for the development of clinical features of spinal cord injury such as spasticity, tremor and autonomic dysreflexia it must be acknowledged that none of our animals actually exhibited any of these features (with the exception of one animal who developed a hind limb tremor 14 weeks post operatively). Following a chronic spinal cord hemisection in adult cats, Hultborn and Malmsten (1983) also report very good general motor recovery with no syndromes of spasticity from 2 to 515 days.

It must be emphasised though that the lesions described in this thesis were neat hemisections, using a scalpel and so not representative of the degree of damage that would result from a normal spinal cord injury, thus the lack of clinical symptoms in the animals maybe a result of degree. Larger, more complete lesions may exacerbate sprouting responses to an extent sufficient to produce the clinical symptoms seen. It also may be a question of time. There were significant differences between the 6-8 week survival time groups and the 16-18 weeks. It may be that sprouting would continue to develop over time. The onset of tremors, spasticity and autonomic dysreflexia can occur months or even years after a spinal injury.

The lesions used in this study were designed to axotomise certain populations of descending fibres and so may not be representative of type of damage suffered by patients. Using a standardised weight drop contusion injury of the spinal cord, Conta and Stelzer (2004) argue that the long descending propriospinal neurones from the cervical cord are less vulnerable to core contusion than the short thoracic propriospinal neurones as more of their axons survive due to their location on the ventral white matter. Thus they argue that the long descending propriospinal are good candidates for reconnecting the injured spinal cord following contusion injury. Analysis of the thoracic interneurone axons in this thesis however revealed a tendency for the axon to initially travel fairly dorsal in the medial funiculus after laving the soma but eventually to move ventral, with most axons ending up travelling in the ventral funiculus. As a consequence, the proximity of the lesion to the soma may be more of a risk factor for axon damage and as such these thoracic interneurones may still be good candidates.

It is also important to point out that by pre-labeling the short thoracic propriospinal before the injury Conta and Stelzner (2004) demonstrated large numbers of reterogradely labelled cells in all the spinal laminae similar to those seen in uninjured controls. Thus, the short thoracic propriospinal neurones do not appear to undergo post axotomy cell death and are still alive at least at 2 weeks post injury. Thus, in complete spinal transection these cells may still play an important part in experimental regeneration. Neurones axotomised closer to the soma have a more robust regeneration response than those axotomised distally (Benfry & Aguayo 1982; Doster et al, 1991) and thus may be better candidates to bridge the lesion than the long descending tracts axotomised distally by the lesion which could simply sprout to the interneurones. Following a parasagital midline incision selectively axotomising spinal commissural neck interneurones cells in the correct locations for the interneurones were immunolabelled for GAP-43 at 2 and 4 weeks post injury (Skelton 2002; Fenrich et al 2004).

This thesis also raised the implication that the dendritic trees of local cells that may be targets for regenerating axons may be highly abnormal. Changes in dendritic structure will influence the input-output properties of neurones. The apparently greater complexity of the dendritic tree of these interneurones may reflect changes in inputs to these cells. The size and complexity of a dendritic arbour has been shown to relate directly to the number of synaptic inputs received by the neurone (Hume & Purves 1981; Purves & Hume1981). The lack of important dendritic cytoskeletal proteins however suggest that portions of the dendritic tree may not be able to function as normal. The alterations in MAP2a/b immunoreactivity observed in this study above and below the lesion suggest that similar changes may also occur caudal to an injury

which may have implications for attempts to regenerate damaged axons past a lesion if the target dendrites are abnormal.

Swellings were frequently observed on the dendrites of the interneurones of the lesion population, more so than in controls. What such swellings actually represent is unclear. Beaded dendrites have been observed on many types of dendrites of both injured and normal neurones. It has been suggested that they may be a consequence of inadequate fixation of tissue, although his does not explain why one cell may show this but not another cell in the same vicinity, or indeed why only some dendrites on a cell exhibit these. Injury to the cell as consequence of the intracellular penetration is another possibility, although this does not explain why the cells from the lesion population would be more vulnerable to such damage than the control population. In a large sample of intracellularly labelled motoneurones no link was observed between the reports of the physiological state of the cell immediately prior to withdrawal of the electrode and the subsequent presence of absence of beading/swellings (personal communication, PK Rose). Dendritic beading has however been shown to correspond with impaired excitability (Polishchuk et al 1998). Conversely Isokawa and Mello (1991) associate it with hyper-excitability.

One possibility is that the swelling seen on the injured motoneurones of McDermid et al (2002, 2004) and on the cells of this thesis may be boutons. Alternatively given the lack of MP2a/b labelling of such processes, these may also be accumulations of organelles as a consequence of altered transport due to the loss of this protein, which normally helps to maintain the dominant direction of transport in the dendrite. This may also help explain some of the other features seen on these interneurones, such as

the unsually thick dendrites. Some of the swellings observed on dendritic processes of our interneurones differ from descriptions of normal beading. They appeared at the distal end of unusual processes as a single "blob" having the appearance of a growth-cone.

6.6 Suggestions for future work.

Sprouting from non inured interneurones rostral to an injury raises the question, are injured interneurones also sprouting like the non injured ones of this study, perhaps even in a more robust fashion?. If this is the case then this may partially explain clinical symptoms following more complete transactions, such as autonomic dysreflexia. Or, if the axons of interneurones are axotomised do they develop the same dendraxon type of processes as described by MacDermid et al (2002; 2004).

The observation that the dendrites of the interneurones in this thesis exhibit some features reminiscent of those seen on axotomised motoneurones suggests that a lesioned environment (with accompanying deafferentation) may be sufficient to produce such changes. Thus the precise role of axotomy versus deafferentation on dendritic trees is unclear. Comparisons of axotomised and non-axotomised cells of the same populations in injured and normal environments would be needed to help establish this.

6.7 General Conclusions

This thesis demonstrates dendritic and axonal sprouting from non –injured thoracic interneurones whose soma are located one segment rostral to a partial hemisection of the spinal cord. This sprouting is affected by distance of the cell from the lesion and survival time. Such sprouting however may be maladaptive and may help explain the development of clinical symptomology such as autonomic dysreflexia. Most importantly this thesis highlights the plasticity expressed by neurones near an injury, including abnormalities which may have implication for regenerative treatments relying on such cells to form new circuits.

References

Aicher SA, Sharma S, Cheng PY, Pickel VM. 1997. The N-methyl-D-aspartate (NMDA) receptor is postsynaptic to substance P-containing axon terminals in the rat superficial dorsal horn. Brain Res. 772:71-81.

Anissimova NP, Saywell SA, Ford TW, Kirkwood PA. 2001. Distributions of EPSPs from individual expiratory bulbospinal neurones in the normal and the chronically lesioned thoracic spinal cord. XXXIV Int Congr Physiol Sci, Abstr 1029.

Aoki M, Fujito Y, Satomi H, Kurosawa Y, Kasaba T. 1986. The possible role of collateral sprouting in the functional restitution of corticospinal connections after spinal hemisection. Neurosci Res 3(6): 617-27.

Aoki M, Mori S, Kawahara K, Watanabe H, Ebata N. 1980. Generation of spontaneous respiratory rhythm in high spinal cats. Brain Res 202(1): 51-63.

Aoki M, Watanabe H, Ebata N, Mori S. 1978. Spontaneous respiratory activity in spinal cats. Brain Res 157(2): 376-80.

Arata A, Onimaru H, Homma I. 1990. Respiration-related neurons in the ventral medulla of newborn rats in vitro. Brain Res Bull 24(4):599-604.

Bareyre FM., Kerchensteiner M, Raineteau O, Mettenleiter TC, Weinmann O, Schwab ME. 2004. The injured spinal cord spontaneously forms a new intraspinal circuit in adult rats. Nature Neuroscience 7: 269-277.

Bastmeyer M, Daston MM, Possel H, O'Leary DM. 1998. Collateral branch formation related to cellular structures in the axon tract during corticopontine target recognition. J Comp Neurol 392:1-18.

Bellingham MC, Lipski J. 1990. Respiratory interneurons in the C5 segment of the spinal cord of the cat. Brain Res 533(1): 141-6.

Benfey M, Aguayo AJ. 1982. Extensive elongation of axons from rat brain into peripheral nerve grafts. Nature 296: 150-2.

Berger AJ, Averill DB, Cameron WE. 1984. Morphology of inspiratory neurons located in the ventrolateral nucleus of the tractus solitarius of the cat. J Comp Neurol 224(1): 60-70.

Berger AJ. 1979. Phrenic motoneurons in the cat: subpopulations and nature of respiratory drive potentials. J Neurophysiol 42(1 Pt 1): 76-90.

Bernstein JJ, Bernstein ME. 1973. Neuronal alteration and reinnervation following axonal regeneration and sprouting in mammalian spinal cord. Brain Behav Evol 8(1): 135-61.

Bianchi A, Denavit-Saubie M, Champagnat J. 1995. Central control of breathing in mammals: neuronal circuitry, membrane properties and neurotransmitters. Physiol Rev 75: 1-45.

Bianchi AL, Grelot L, Iscoe S, Remmers JE. 1988. Electrophysiological properties of rostral medullary respiratory neurones in the cat: an intracellular study. J Physiol 407: 293-310.

Bianchi AL. 1974. Modalities of discharge and anatomo-functional properties of medullary respiratory neurons. J Physiol 68(5): 555-87.

Billig I, Foris JM, Card JP, Yates BJ. 1999. Transneuronal tracing of neural pathways controlling an abdominal muscle, rectus abdominis, in the ferret. Brain Res 820(1-2): 31-44.

Blight AR, Young W. 1989. Central axons in injured cat spinal cord recover electrophysiological function following remyelination by Schwann cells. J Neurol Sci 91(1-2): 15-34.

Bou-Flores C, Berger AJ. 2001. Gap junctions and inhibitory synapses modulate inspiratory motoneuron synchronization. J Neurophysiol 85(4): 1543-51.

Bradbury EJ, McMahon SB, Ramer MS. 2000. Keeping in touch: sensory neurone regeneration in the CNS. Trends Pharmacol Sci 21(10): 389-94.

Brannstrom T, Havton L, Kellerth JO. 1992. Changes in size and dendritic arborization patterns of adult cat spinal alpha-motoneurons following permanent axotomy. J Comp Neurol 318(4): 439-51.

Budzinska K, von Euler C, Kao FF, Pantaleo T, Yamamoto Y. 1985. Effects of graded focal cold block in the solitary and para-ambigual regions of the medulla in the cat. Acta Physiol Scand 124(3): 317-28.

Budzinska K, von Euler C, Kao FF, Pantaleo T, Yamamoto Y. 1985. Effects of graded focal cold block in rostral areas of the medulla. Acta Physiol Scand124(3): 329-40.

Caceres A, Dotti C. 1985. Immunocytochemical localization of tubulin and the high molecular weight microtubule-associated protein 2 in Purkinje cell dendrites deprived of climbing fibers. Neuroscience 16(1):133-50.

Calancie B, Molano MR, Broton JG. 2002. Interclimb reflexes and synaptic plasticity become evident months after human spinal cord injury. Brain 125(Pt 5): 1150-61.

Cameron WE, Averill DB, Berger AJ. 1983. Morphology of cat phrenic motoneurons as revealed by intracellular injection of horseradish peroxidase. J Comp Neurol 219(1): 70-80.

Chang Q, Pereda A, Pinter MJ, Balice-Gordon RJ. 2000. Nerve injury induces gap junctional coupling among axotomized adult motor neurons. J Neurosci 32(1): 242-9.

Christensen BN. 1983. Distribution of electrotonic synapses on identified lamprey neurons: a comparison of a model prediction with an electron microscopic analysis. J Neurophysiol 49(3): 705-16.

Chuckowree JA, Vickers JC. 2003. Cytoskeletal and morphological alterations underlying axonal sprouting after localized transection of cortical neuron axons in vitro. J Neurosci 23(9): 3715-3725.

Cohen MI, Feldman JL, Sommer D. 1985. Caudal medullary expiratory neurone and internal intercostal nerve discharges in the cat: effects of lung inflation. J Physiol 368: 147-78.

Cohen MI, Piercey MF, Gootman PM, Wolotsky P. 1974. Synaptic connections between medullary inspiratory neurons and phrenic motoneurons as revealed by cross-correlation. Brain Res 81(2): 319-24.

Conta AC, Stelzner DJ. 2004. Differential vulnerability of propriospinal tract neurons to spinal cord contusion injury. J Comp Neurol 479(4): 347-359.

D'Angelo E, Bellemare F. 1990. Electrical and mechanical output of the inspiratory muscles in anesthetized dogs. Respir Physiol 79(2): 177-93.

Darian-Smith C. 2004. Primary afferent terminal sprouting after a cervical dorsal rootlet section in the Macaque Monkey. J Comp Neurol 470: 134-150.

Davies JG, Kirkwood PA, Sears TA. 1985a. The detection of monosynaptic connexions from inspiratory bulbospinal neurones to inspiratory motoneurones in the cat. J Physiol 368: 33-62.

Davies JG, Kirkwood PA, Sears TA. 1985b. The distribution of monosynaptic connexions from inspiratory bulbospinal neurones to inspiratory motoneurones in the cat. J Physiol 368: 63-87.

De Felipe C, Herrero JF, O'Brien JA, Palmer JA, Doyle CA. 1998. Altered nociception, analgesia and aggression in mice lacking the receptor for substance P. Nature 392: 394-97.

De Troyer A, Heilporn A. 1980. Respiratory mechanics in quadriplegia: the respiratory function of the intercostal muscles. Am Rev Respir Dis 122(4): 591-600.

De Troyer A, Legrand A, Wilson TA. 1999. Respiratory mechanical advantage of the canine external and internal intercostal muscles. J Physiol 518(Pt.1): 283-9.

De Troyer A, Ninane V. 1986. Respiratory function of intercostal muscles in supine dog: an electromyographic study. J Appl Physiol 60(5): 1692-9.

De Troyer A. 2002. Relationship between neural drive and mechanical effect in the respiratory system. Adv Exp Med Biol 508: 507-14.

Dick TE, Jodkowski JS, Viana F, Berger AJ. 1988. Projections and terminations of single respiratory axons in the cervical spinal cord of cat. Brain Res 449(1-2): 201-12.

Dick TE, Viana F, Berger AJ.1988. Electrophysiological determination of the axonal projection of single dorsal respiratory group neurons to the cervical spinal cord of cat. Brain Res 454(1-2): 31-9.

Dobbins E, Feldman J. 1990. Subnuclear organization of the lateral tegmental field of the rat. I: nucleus ambiguus and ventral respiratory group. J Comp Neurol 347: 64-86.

Dobbins EG, Feldman JL. 1994. Brainstem network controlling descending drive to phrenic motoneurons in rat. J Comp Neurol 347: 64-86.

Doster SK, Lozano AM, Aguayo AJ, Willard MB. 1991. Expression of the growth-associated protein GAP-43 in adult rat retinal ganglion cells following axon injury. Neuron 6(4): 635-47.

Doubell TP, Mannion RJ, Woolf CJ. 1997. Intact sciatic myelinated primary afferent terminals collaterally sprout in the adult rat dorsal horn following section of a neighbouring peripheral nerve. J Comp Neurol 380(1): 95-104.

Douse MA, Duffin J. 1993. Axonal projections and synaptic connections of C5 segment expiratory interneurones in the cat. J Physiol 470: 431-44.

Duffin J, Ezure K, Lipski J. 1995. Breathing rhythm generation: focus on the rostral ventrolateral medulla. NIPS 10: 133-140.

Duffin J, Lipski J. 1987. Monosynaptic excitation of thoracic motoneurones by inspiratory neurones of the nucleus tractus solitarius in the cat. J Physiol 390: 415-31.

Eccles RM, Sears TA, Shealy CN. 1962. Intra-cellular recording from respiratory motoneurones of the thoracic spinal cord of the cat. Nature 193: 844-846.

Ellenberger HH, Feldman JL. 1990. Brainstem connections of the rostral ventral respiratory group of the rat. Brain Res 513(1): 35-42.

Ellenberger HH, Feldman JL, Goshgarian HG. 1990. Ventral respiratory group projections to phrenic motoneuron electron microscope evidence for monosynaptic connections. J Comp Neurol. 302(4): 707-14.

Ellenberger HH, Feldman JL. 1988. Monosynaptic transmission of respiratory drive to phrenic motoneurons from brainstem bulbospinal neurons in rats. J Comp Neurol. 269(1): 47-57.

Ellenberger HH, Vera PL, Haselton JR, Haselton CL, Schneiderman. 1990. Brainstem projections to the phrenic nucleus: an anterograde and retrograde HRP study in the rabbit. Brain Res Bull 24(2): 163-74.

Ellenberger HH. 1999. Nucleus ambiguus and bulbospinal ventral respiratory group neurons in the neonatal rat. Brain Res Bull 50(1): 1-13.

Fedorko L, Hoskin RW, Duffin J. 1989. Projections from inspiratory neurons of the nucleus retroambigualis to phrenic motoneurons in the cat. Exp Neurol 105(3): 306-10.

Fedorko L, Merrill EG, Lipski J. 1983. Two descending medullary inspiratory pathways to phrenic motoneurones. Neurosci Lett 43(2-3): 285-91.

Feldman JL, Loewy AD, Speck DF. 1985. Projections from the ventral respiratory group to phrenic and intercostal motoneurons in cat: an autoradiographic study. J Neurosci 5(8): 1993-2000.

Feldman JL, Mitchell GS, Nattie EE. 2003. Breathing: rhythmicity, plasticity, chemosensitivity. Annu Rev Neurosci 26: 239-66.

Feldman JL, Smith JC, Liu G. 1991. Respiratory pattern generation in mammals: in vitro en bloc analyses Curr Opin Neurobiol 1(4): 590-4.

Feldman JL, Speck DF. 1983. Interactions among inspiratory neurons in dorsal and ventral respiratory groups in cat medulla. J Neurophysiol 49(2): 472-90.

Ferhat L, Kuriyama R, Lyons GE, Micales B, Baas PW. 1998 Expression of the mitotic motor protein CHO1/MKLP1 in postmitotic neurons. Eur J Neurosci. 10(4): 1383-93

Fetcho JR. 1991 Spinal network of the Mauthner cell. Brain Behav Evol. 37(5): 298-316

Fishman PS, Kelly JP.1984 Identified central axons differ in their response to spinal cord transection. Brain Res. 305(1): 152-6

Fitzgerald M., Woolf C.J., Shortland P.1990 Collateral sprouting of the central terminals of cutaneous primary afferent neurons in the rat spinal cord: Pattern, morphology, and influence of targets. The journal of comparative neurology. 300: 370-385

Ford TW, Vaughan CW, Kirkwood PA. 2000 Changes in the distribution of synaptic potentials from bulbospinal neurones following axotomy in cat thoracic spinal cord. J. Physiol. 524 Pt 1: 163-78

Fouad IK, Pedersen V, Schwab ME, Brösamle C. 2001 Cervical sprouting of corticospinal fibers after thoracic spinal cord injury accompanies shifts in evoked motor responses. Curr. Biol. 11: 1776-1770

Fukuda T, Adachi E, Kawashima S, Yoshiya I, Hashimoto PH. 1990: Immunohistochemical distribution of calcium-activated neutral proteinases and endogenous CANP inhibitor in the rabbit hippocampus. J Comp Neurol. 302(1): 100-9

Funk G, Smith J, Feldman J. 1993 Generation and transmission of respiratory oscillations in medullary slices: role of excitatory amino acids. J. Neurophysiol. 70: 1497-515

Gazula V., Roberts M., Luzzio C. Jawad AF, Kalb R.G. 2004 Effects of limb exercise after spinal cord injury on motoneurone dendrite structure. The journal of comparative neurology. 476: 130-145

Gledhill RF, McDonald WI. 1977 Morphological characteristics of central demyelination and remyelination: a single-fiber study. Ann Neurol. 1(6) 552-60

Goldberger ME, Murray M. 1974 Restitution of function and collateral sprouting in the cat spinal cord: the deafferented animal. J Comp Neurol. 158(1): 37-53

Golder F.J., Reier P.J., Bolser D.C. 2001 Altered respiratory motor drive after spinal cord injury: supraspinal and bilateral effects of a unilateral lesion. The journal of Neuroscience 21(21): 8680-8689

Gray PA, Janczewski WA, Mellen N, McCrimmon DR, Feldman JL. 2001 Normal breathing requires pre-Bötzinger complex neurokinin-1 receptor-expressing neurons. Nat. Neurosci. 4: 927-30

Gray PA, Recking JC, Bocchiaro CM, Feldman JL. 1999 Modulation of respiratory frequency by peptidergic input to rhythmogenic neurons in the pre-Bötzinger complex. Science 286: 1566-68

Guyenet PG, Wang H. 2001 Pre-Bötzinger neurons with pre-inspiratory discharges "in vivo" express NK1 receptors in the rat. J. Neurophysiol. 86: 438-46

Hall GF, Cohen MJ. 1988 The pattern of dendritic sprouting and retraction induced by axotomy of lamprey central neurons. J Neurosci. 8(10): 3584-97

Hamori J, Jakab RL, Takacs J. 1997 Morphogenetic plasticity of neuronal elements in cerebellar glomeruli during deafferentation-induced synaptic reorganization. J Neural Transplant Plast. 6(1): 11-20

Hamori J. 1990 Morphological plasticity of postsynaptic neurones in reactive synaptogenesis. J Exp Biol. 153: 251-60

Harrison BM, McDonald WI. 1977 Remyelination after transient experimental compression of the spinal cord Ann Neurol. 1(6): 542-51

Havton L., Kellerth J.-O.1987 Regeneration by supernumerary axons with synaptic terminals in spinal motoneurons of cats Nature 325(6106): 711-714

Havton L., Kellerth J.-O. 1990 Elimination of intramedullary axon collaterals of cat spinal α-motoneurons following peripheral nerve injury. Experimental brain research 79: 65-74

Hayashi F, Lipski J. 1992 The role of inhibitory amino acids in control of respiratory motor output in an arterially perfused rat. Respir Physiol. 89(1): 47-63

Hilaire G, Monteau R, Dussardier M.1972 Pattern of recruitment of phrenic motor neurons. J Physiol. 64(5): 457-78

Hilaire G, Monteau R.1976 Connections between inspiratory medullary neurons and phrenic or intercostal motoneurones (author's transl). J Physiol. 72(8):987-1000

Hilaire GG, Nicholls JG, Sears TA.1983. Central and proprioceptive influences on the activity of levator costae motoneurones in the cat. J Physiol 342: 527-48

Hill C.E., Beattie M.S., Bresnahan J.C. 2001 Degeneration and sprouting of identified descending supraspinal axons after contusive spinal cord injury in the rat. Experimental neurology. 171: 153-169

Holstege G, van Neerven J, Evertse F. 1987 Spinal cord location of the motoneurons innervating the abdominal, cutaneous maximus, latissimus dorsi and longissimus dorsi muscles in the cat. Exp Brain Res. 67(1): 179-94

Hoskin RW, Fedorko LM, Duffin J.1988 Projections from upper cervical inspiratory neurons to thoracic and lumbar expiratory motor nuclei in the cat. Exp Neurol. 99(3): 544-55

Hoy RR, Nolen TG, Casaday GC. 1985 Dendritic sprouting and compensatory synaptogenesis in an identified interneuron follow auditory deprivation in a cricket Proc Natl Acad Sci U S A. 82(22): 7772-6

Hultborn H, Malmsten J. (1983) Changes in segmental reflexes following chronic spinal cord hemisection in the cat. I. Increased monosynaptic and polysynaptic ventral root discharges. Acta Physiol Scand. Dec;119(4):405-22.

Hume RI, Purves D. 1981 Geometry of neonatal neurones and the regulation of synapse elimination. Nature 293 469-71

Inagaki N, Chihara K, Arimura N, Menager C, Kawano Y, Matsuo N, Nishimura T, Amano M, Kaibuchi K. 2001 CRMP-2 induces axons in cultured hippocampal neurons. Nat Neurosci. 4(8) 781-2

Isokawa M, Mello LE. 1991 NMDA receptor-mediated excitability in dendritically deformed dentate granule cells in pilocarpine-treated rats. Neurosci Lett. 129(1): 69-73

Janczewski WA, Feldman JL. 2002 μ-opioid receptor agonist suppresses rhythmic inspiratory but neither pre-inspiratory nor expiratory activity in the newborn rat. Soc. Neurosci. Abstr. 28: 221.11

Janczewski WA, Onimaru H, Homma I, Feldman JL. 2002 Opioid-resistant respiratory pathway from the pre-inspiratory neurones to abdominal muscles: in vivo and in vitro study in the newborn rat.. J. Physiol. 545: 1017-26

Jeffery N.D., Fitzgerald M. 2001 Effects of red nucleus ablation and exogenous neurotrophin-3 on cortocospinal axon terminal distribution in the adult rat. Neuroscience 104(2): 513-521

Kalia M, Feldman JL, Cohen MI. 1979. Afferent projections to the inspiratory neuronal region of the ventrolateral nucleus of the tractus solitarius in the cat. Brain Res. 171(1):135-41

Kandler K, Katz LC. 1995. Neuronal coupling and uncoupling in the developing nervous system Curr Opin Neurobiol. 5(1): 98-105

Kirkwood P.A., Sears T.A. 1980. The measurement of synaptic connections in the mammalian central nervous system by means of spike triggered averaging Spinal and supraspinal mechanisms of voluntary motor control and locomotion. Prog. Clin. Neurophysiol, ed. Desmedt J.E. 8: 44-71

Kirkwood PA 1995 Synaptic excitation in the thoracic spinal cord from expiratory bulbospinal neurones in the cat. J. Physiol. 484: 201-225

Kirkwood PA, Munson JB, Sears TA, Westgaard RH.1988 Respiratory interneurones in the thoracic spinal cord of the cat. J. Physiol. 395: 161-92

Kirkwood PA, Schmid K, Sears TA. 1993 Functional identities of thoracic respiratory interneurones in the cat. J. Physiol. 461 667-87

Kirkwood PA, Sears TA, Westgaard RH. 1984 Restoration of function in external intercostal motoneurones of the cat following partial central deafferentation. J. Physiol. 350: 225-251

Kirkwood PA, Sears TA. 1978 The synaptic connexions to intercostal motoneurones as revealed by the average common excitation potential. J Physiol. 275: 103-34

Kirkwood PA, Sears TA. 1973 Proceedings: Monosynaptic excitation of thoracic expiratory motoneurones from lateral respiratory neurones in the medulla of the cat. J Physiol. 234(2): 87P-89P

Koshiya N, Guyenet P. 1996 Tonic sympathetic chemoreflex after blockade of respiratory rhythmogenesis in the rat.J. Physiol. 491: 859-69

Leduc D, De Troyer A. 2003 Mechanical effect of muscle spindles in the canine external intercostal muscles. J. Physiol. 548.1:297-305

Li Y, Raisman G. 1995 Sprouts from cut corticospinal axons persist in the presence of astrocytic scarring in long-term lesions of the adult rat spinal cord. Exp. Neurol. 134: 102-111

Liljestrand G. 1953 The effects of ethyl alcohol and some related substances on baroceptor and chemoceptor activity. Acta Physiol Scand. 29(1): 74-82

Linda H, Risling M, Cullheim S. 1985 Dendraxons' in regenerating motoneurons in the cat: do dendrites generate new axons after central axotomy? Brain Res. 358(1-2): 329-33

Lipski J, Duffin J. 1986 An electrophysiological investigation of propriospinal inspiratory neurons in the upper cervical cord of the cat. Exp Brain Res. 61(3): 625-37

Lipski J, Kubin L, Jodkowski J. 1983 Synaptic action of R beta neurons on phrenic motoneurons studied with spike-triggered averaging. Brain Res. 288(1-2):105-18

Lipski J, Merrill EG. 1980 Electrophysiological demonstration of the projection from expiratory neurones in rostral medulla to contralateral dorsal respiratory group. Brain Res. 197(2): 521-4

Liu CN, Chambers WW. 1958 Intraspinal sprouting of dorsal root axons; development of new collaterals and preterminals following partial denervation of the spinal cord in the cat. AMA Arch Neurol Psychiatry. 79(1): 46-61

Llewellyn-Smith I.J., Weaver L.C. 2001 Changes in synaptic inputs to sympathetic preganglionic neurons after spinal cord injury. The journal of comparative neurology. 435: 226-240

MacDermid V., Neuber-Hess M., Short C., Rose P.K. 2002 Alterations to neronal polarity following permanent axotomy: A quantitative analysis of changes to MAP2a/b and GAP-43 distributions in axotomized motoneurons in the adult cat. The journal of comparative neurology 450: 318-333

MacDermid VE, Neuber-Hess MS, Rose PK 2004 The temporal sequence of morphological and molecular changes in axotomized feline motoneurons leading to the formation of axons from the ends of dendrites. J Comp Neurol. 468(2): 233-250

Mannion RJ, Doubell TP, Coggeshall RE, Woolf CJ 1996 Collateral sprouting of uninjured primary afferent A-fibers into the superficial dorsal horn of the adult rat spinal cord after topical capsaicin treatment to the sciatic nerve. J Neurosci. 16(16): 5189-95

Mannion RJ, Doubell TP, Gill H, Woolf CJ. 1998 Deafferentation is insufficient to induce sprouting of A-fibre central terminals in the rat dorsal horn. J Comp Neurol. 393(2): 135-44

Mattson M.P. 1999 Establishment and plasticity of neuronal polarity. Journal of Neuroscience Research. 57: 577-589

Meehan CF, Ford TW, Road JD, Donga R, Saywell SA, Anissimova NP, Kirkwood PA. 2004 Rostrocaudal distribution of motoneurones and variation in ventral horn area within a segment of the feline thoracic spinal cord. J Comp Neurol.472(3): 281-91

Merrill EG 1974 Finding a respiratory function for the medullary respiratory neurons. Essays on the nervous system, Clarendon Press Oxford, ed. Bellairs R, Gray EG 451-486

Merrill EG 1972 Thoracic motor drives from medullary expiratory neurones in cats. J Physiol. 222(2): 154P-155P

Merrill EG, Fedorko L. 1984 Monosynaptic inhibition of phrenic motoneurons: a long descending projection from Bőtzinger neurons. J Neurosci. 4(9): 2350-3

Merrill EG, Lipski J. 1987 Inputs to intercostal motoneurons from ventrolateral medullary respiratory neurons in the cat. J Neurophysiol. 57(6): 1837-53

Merrill EG. 1974 Proceedings: Antidromic activation of lateral respiratory neurones during their silent periods. J Physiol. 241(2): 118P-119P

Miller AD. 1987 Localization of motoneurons innervating individual abdominal muscles of the cat. J Comp Neurol. 256(4): 600-6

Monteau R, Hilaire G.1991 Spinal respiratory motoneurons. Prog Neurobiol. 37(2) 83-144

Monteau R, Khatib M, Hilaire G. 1985 Central determination of recruitment order: intracellular study of phrenic motoneurons. Neurosci Lett. 56(3): 341-6

Munson JB, Sypert GW. 1979 Properties of single central Ia afferent fibres projecting to motoneurones.J Physiol. 296: 315-27

Novikova LN, Novikov LN, Kellerth JO. 2002 Differential effects of neurotrophins on neuronal survival and axonal regeneration after spinal cord injury in adult rats. J. Comp. Neurol. 452(3): 255-63

Ondarza AB, Ye Z, Hulsebosch CE. 2003 Direct evidence of primary afferent sprouting in distant segments following spinal cord injury in the rat: colocalization of GAP-43 and CGRP. Exp Neurol. 184(1): 373-80

Onimaru H, Arata A, Homma I. 1990 Inhibitory synaptic inputs to the respiratory rhythm generator in the medulla isolated from newborn rats.Pflugers Arch. 417(4) 425-32

Onimaru H, Homma I. 2003 A novel functional neuron group for respiratory rhythm generation in the ventral medulla. J. Neurosci. 23(4): 1478-1486

Otake K, Sasaki H, Ezure K, Manabe M. 1989 Axonal trajectory and terminal distribution of inspiratory neurons of the dorsal respiratory group in the cat's medulla. J Comp Neurol. 286(2): 218-30

Otake K, Sasaki H, Mannen H, Ezure K. 1987 Morphology of expiratory neurons of the Bőtzinger complex: an HRP study in the cat.J Comp Neurol. 258(4): 565-79

Paintal AS. 1959 Facilitation and depression of muscle stretch receptors by repetitive antidromic stimulation, adrenaline and asphyxia. J Physiol. 148: 252-66

Palisses R, Persegol L, Viala D, Viala G. 1988 Reflex modulation of phrenic activity through hindlimb passive motion in decorticate and spinal rabbit preparation. Neuroscience 24(2): 719-28

Palisses R, Persegol L, Viala D. 1989 Evidence for respiratory interneurones in the C3-C5 cervical spinal cord in the decorticate rabbit. Exp. Brain Res. 78(3): 624-32

Paton J, Ramirez J, Richter D. 1994 Mechanisms of respiratory rhythm generation change profoundly during early life in mice and rats. Neurosci. Lett. 170: 167-70

Paton JF. 1997 Rhythmic bursting of pre- and post-inspiratory neurones during central apnoea in mature mice. J Physiol. 502 (Pt 3): 623-39

Perlmutter LS, Gall C, Baudry M, Lynch G. 1990 Distribution of calcium-activated protease calpain in the rat brain. J Comp Neurol. 296(2): 269-76

Petralia RS, Wang YX, Wenthold RJ. 1994 Histological and ultrastructural localization of the kainate receptor subunits, KA2 and GluR6/7, in the rat nervous system using selective antipeptide antibodies. J Comp Neurol. 349: 85-110

Petralia RS, Wang YX, Wenthold RJ. 1994 The NMDA receptor subunits NR2A and NR2B show histological and ultrastructural localization patterns similar to those of NR1. J Neurosci. 14(10): 6102-20

Petralia RS, Yokotani N, Wenthold RJ. 1994 Light and electron microscope distribution of the NMDA receptor subunit NMDAR1 in the rat nervous system using a selective anti-peptide antibody. J Neurosci. 14(2): 667-96

Polischuk TM, Jarvis CR, Andrew RD. 1998 Intrinsic optical signaling denoting neuronal damage in response to acute excitotoxic insult by domoic acid in the hippocampal slice. Neurobiol Dis. 4(6): 423-37

Ptak K, Hilaire G. 1999 Central respiratory effects of substance P in neonatal mice: an in vitro study. Neurosci. Lett. 266: 189-92

Purves D, Hume RI. 1981 The relation of postsynaptic geometry to the number of presynaptic axons that innervate autonomic ganglion cells. J Neurosci. 1(5): 441-52

Raineteau O., Fouad K;, Bareyre F.M., Schwab M.E. 2002 Reorganization of descending motor tracts in the rat spinal cord. European Journal of Neuroscience 16: 1761-1771

Ramirez J, Pierrefiche O, Schwarzacher S, Filloux F, McIntosh J, et al. 1994 The influence of N-type calcium channel blockers on the respiratory network of adult cats. Soc. Neurosci. Abstr. 20: 73.12430556

Ramirez JM, Schwarzacher SW, Pierrefiche O, Olivera BM, Richter DW. 1998 Selective lesioning of the cat pre-Botzinger complex in vivo eliminates breathing but not gasping. J Physiol. 507(Pt 3): 895-907

Ramirez JM, Zuperku EJ, Alheid GF, Lieske SP, Ptak K, McCrimmon DR. 2002. Respiratory rhythm generation: converging concepts from in vitro and in vivo approaches. Respir Physiol Neurobiol. 131(1-2): 43-56

Ramon y Cajal 1928 Degeneration and Regeneration of the Nervous System. New York, Hafner.

Reckling JC, Feldman JL. 1998 Pre-Bötzinger complex and pacemaker neurons: hypothesized site and kernel for respiratory rhythm generation. Annu. Rev. Physiol. 60: 385-405

Richter DW, Ballanyi K, Schwarzacher S. 1992 Mechanisms of respiratory rhythm generation. Curr Opin Neurobiol. 2(6): 788-93

Richter DW, Spyer KM. 2001 Studying rhythmogenesis of breathing: comparison of in vivo and in vitro models. Trends Neurosci. 24: 464-72

Rose D, Larnicol N, Duron B. 1984 An HRP study of the cat's spinal respiratory motoneurones during postnatal development Exp Brain Res. 56(3): 458-67

Rose P.K., MacDermid V., Joshi M., Neuber-Hess M. 2001 Emergence of axons from distal dendrites of adult mammalian neurons following a permanent axotomy. European journal of Neuroscience. 13: 1166-1176

Rose P.K., Odlozinski M. 1998 Expansion of the dendritic tree of motoneurons innervating neck muscles of the adult cat after permanent axotomy. The journal of comparative neurology. 390: 392-411

Rose P.K., Richmond F.J.R. 1981 White-matter dendrites in the upper cervical spinal cord of the adult cat: a light and electron microscopic study. The journal of comparative neurology 199: 191-203

Rose PK, MacDermid V, Neuber-Hess M. 2001 Motor Neurobiology of the Spinal Cord, CRC Press, ed. Cope T.

Saywell SA. 2000 Unpublished thesis, University College London

Schmid K, Kirkwood PA, Munson JB, Shen E, Sears TA. 1993 Contralateral projections of thoracic respiratory interneurones in the cat. J. Physiol. 461: 647-65

Schwab M.E., Bartholdi D. 1996 Degeneration and regeneration of axons in the lesioned spinal cord. Physiological Reviews. 76: 319-370

Sears TA. 1964 The fibre calibre spectra of sensory and motor fibres in the intercostal nerves of the cat. J. Physiol. 172a: 150-161

Sears TA. 1964 Efferent discharges in alpha and fusimotor fibres of intercostal nerves of the cat. J. Physiol. 174: 295-315 J. Physiol. 174b: 295-315

Sears TA. 1964 Some properties and reflex connexions of respiratory motoneurones of the cat's thoracic spinal cord J. Physiol. 175c: 386-403

Sears TA. 1964 The slow potentials of thoracic respiratory motorneurones and their relation to breathing. J. Physiol. 175d: 404-424

Sharp DJ, Yu W, Ferhat L, Kuriyama R, Rueger DC, Baas PW. 1997 Identification of a microtubule-associated motor protein essential for dendritic differentiation. J Cell Biol. 138(4): 833-43

Shaw G, Winialski D, Reier P. 1988 The effect of axotomy and deafferentation on phosphorylation dependent antigenicity of neurofilaments in rat superior cervical ganglion neurons. Brain Res. 460(2): 227-34

Sheean G. 2002 The pathophysiology of spasticity. European journal of Neurology. Suppl 1:3-9 dicussion 53-61

Smith J, Ellenberger H, Ballanyi K, Richter D, Feldman J. 1991 Pre-Bötzinger complex: a brainstem region that may generate respiratory rhythm in mammals. Science 254: 726-29

Smith J, Feldman J. 1987 In vitro brainstem-spinal cord preparations for study of motor systems for mammalian respiration and locomotion. J. Neurosci. Methods 21: 321-33

Springer JE, Azbill RD, Kennedy SE, George J, Geddes JW. 1997 Rapid calpain I activation and cytoskeletal protein degradation following traumatic spinal cord injury: attenuation with riluzole pretreatment. J Neurochem. 69(4): 1592-600

St John W. 1996 Medullary regions for neurogenesis of gasping: noeud vital or noeuds vitals. J. Appl. Physiol. 81: 1865-77

Steward O., Zheng B., Ho C., Anderson K., Tessier-Lavigne M. 2004 The dorsolateral corticospinal tract in mice: an alternative route for corticospinal input to causal segments following dorsal column lesions. The journal of comparative neurology. 472: 463-477

Sumner BE, Watson WE. 1971 Retraction and expansion of the dendritic tree of motor neurones of adult rats induced in vivo. Nature 233(5317): 273-5

Suzue T. 1984 Respiratory rhythm generation in the vitro brain stem-spinal cord preparation of the neonatal rat. J. Physiol. 354: 173-83

Telgkamp P, Cao YQ, Basbaum AI, Ramirez JM. 2002 Long-term deprivation of substance P in PPT-A mutant mice alters the anoxic response of the isolated respiratory network. J. Neurophysiol. 88: 206-13

Teubner B, Odermatt B, Guldenagel M, Sohl G, Degen J, Bukauskas F, Kronengold J, Verselis VK, Jung YT, Kozak CA, Schilling K, Willecke K. 2001 Functional expression of the new gap junction gene connexin47 transcribed in mouse brain and spinal cord neurons. J Neurosci. 21(4): 1117-26

Tominaga T, Tominaga Y, Yamada H, Matsumoto G, Ichikawa M. 2000 Quantification of optical signals with electrophysiological signals in neural activities of Di-4-ANEPPS stained rat hippocampal slices. J. Neurosci. Methods. 102: 11-23

Traub RD, Wong RK. 1983 Synaptic mechanisms underlying interictal spike initiation in a hippocampal network. Neurology 33(3): 257-66

van den Pol AN, Collins WF. 1994 Paraventriculospinal tract as a model for axon injury: spinal cord. The journal of comparative neurology 349: 244-258

Waxman SG 1989 Demyelination in spinal cord injury. J Neurol Sci. 91(1-2): 1-14

Weaver LC, Cassam AK, Krassioukov AV. 1997 Changes in immunoreactivity for growth associated protein-43 suggest reorganization of synapses on spinal sympathetic neurons after cord transaction. Neuroscience. 81: 535-551

Webber CL Jr, Wurster RD, Chung JM. 1979 Cat phrenic nucleus architecture as revealed by horseradish peroxidase mapping Exp Brain Res. 35(3):395-406

Weidner N, Ner A, Salimi N, Tuszynski MH. 2001 Spontaneous corticospinal axonal plasticity and functional recovery after adult central nervous system injury Proc Natl Acad Sci U S A. 98(6): 3513-8

Wilson TA, Legrand A, Gevenois PA, De Troyer A. 2001 Respiratory effects of the external and internal intercostal muscles in humans. J Physiol. 530(Pt 2): 319-30

Wong S.T., Atkinson B.A., Weaver L.C. 2000 Confocal microscopic analysis reveals sprouting of primary afferent fibres in rat dorsal horn after spinal cord injury. Neuroscience letters 296: 65-68

Yu W, Cook C, Sauter C, Kuriyama R, Kaplan PL, Baas PW. 2000 Depletion of a microtubule-associated motor protein induces the loss of dendritic identity. J Neurosci. 20(15): 5782-91

Yu W, Sharp DJ, Kuriyama R, Mallik P, Baas PW. 1997 Inhibition of a mitotic motor compromises the formation of dendrite-like processes from neuroblastoma cells J Cell Biol. 136(3): 659-68

Zhang F, Wu Z, Li Y. 1991 Effect of blocking medial area of nucleus retrofacialis on respiratory rhythm. Respir. Physiol. 85: 73-81

Zhang S, Underwood M, Landfield A, Huang F, Gibson S, Geddes JW. 2000 Cytoskeletal disruption following contusion injury to the rat spinal cord J. of Neuropathology and Experimental Neurol. 59(4) 287-296